T.C.
ISTANBUL GEDİK UNIVERSITY
INSTITUTE OF GRADUATE STUDIES

EXPERIMENTAL STUDY ON ADDING DIFFERENT SCREEN WALLS TO THE PIANO KEY WEIR (PKWs) HYDRAULIC STRUCTURE AND ITS EFFECT ON HYDRAULIC PERFORMANCE

MASTER THESIS

Anas Saeed Mohammed Ali AL-NEAMA

Civil Engineering Department

Master in Civil Engineering English Program

FEBRUARY 2024
ISTANBUL

T.C.
ISTANBUL GEDİK UNIVERSITY
INSTITUTE OF GRADUATE STUDIES

EXPERIMENTAL STUDY ON ADDING DIFFERENT SCREEN WALLS TO THE PIANO KEY WEIR (PKWs) HYDRAULIC STRUCTURE AND ITS EFFECT ON HYDRAULIC PERFORMANCE

MASTER THESIS

Anas Saeed Mohammed Ali AL-NEAMA
(211291015)

Civil Engineering Department

Master in Civil Engineering English Program

Thesis Advisor: Assoc. Prof. Dr. Redvan GHASMLOUNIA

Second Supervisor : Lect. Dr. Nashwan K. Al-Deen Mohammed ALOMARI

Istanbul 2024

T.C.

İSTANBUL GEDİK ÜNİVERSİTESİ

Lisansüstü Eğitim Enstitüsü Müdürlüğü

Jüri Tez Onay Formu

05.02.2024

LİSANSÜSTÜ EĞİTİM ENSTİTÜSÜ MÜDÜRLÜĞÜ

Bu çalışma 05.02.2024 tarihinde aşağıdaki jüri tarafından İnşaat Mühendisliği Anabilim Dalı, İnşaat Mühendisliği (Tezli Yüksek Lisans) Programı Yüksek Lisans Tezi olarak kabul edilmiştir.

TEZ JÜRİSİ

Dr. Öğr. Üyesi Redvan GHASEMLOUNIA
Danışman
İstanbul Gedik Üniversitesi

Dr. Öğr. Üyesi Hasan Bozkurt NAZİLLİ
Üye (İmza)
İstanbul Gedik Üniversitesi

Dr. Öğr. Üyesi Mert TOLON
Üye (İmza)
İstanbul Maltepe Üniversitesi

DECLARATION

I Anas Saeed Mohammed Ali Al-Neama as a result of this declare that this thesis titled " Experimental Study on Adding Different Screen Walls To the Piano Key Weir (PKWs) Hydraulic Structure and Its Effect on Hydraulic Performance" is original work I did for the award of the master's degree in the faculty of Civil Engineering Program I also declare that this thesis or any part of it has not been submitted and presented for any other degree or research paper in any other university or institution. (5/2/2024)

Anas Saeed Mohammed Ali AL-NEAMA

DEDICATION

My dear mother (may Allah have mercy on her) and my dear father...

The Best Persons who are dearest and closest to my heart …

They were my help and support, and their blessed supplication had the most significant impact on managing the research ship until it docked in this way.

My dear wife …

Who supported me, guided my steps, and eased my difficulties... She endured and suffered a lot to bring me to this position.

My dear children...

The adornment of this worldly life and the pleasure of my life, With whom the search shared tenderness and kindness.

My teachers and people who credit me...

Who showered me with love, appreciation, advice, and direction.

To all of them, I dedicate this humble work, Asking Allah the Most High and Almighty Lord, to benefit and provide us with success from Him, for He is the best Lord and the best Helper.

PREFACE

Praise be to Allah, Lord of the worlds, and thanks and praise be to Allah Almighty for blessing me with patience and strength.

I extend my sincere thanks and great gratitude to my colleagues at Istanbul Gedik University and the postgraduate staff in the Department of Civil Engineering.

I thank Dr Redvan Ghasemlounia, the supervisor of this research, for the information, the support, and assistance he provided me throughout the research period. and also, I thank Dr Nashwan Kamal Al-Deen Mohammed Alomari the Second supervisor for the effort and the Tips he gave me to develop this thesis, and thanks to everyone who urged me and instilled in me the will and to all of us who gave me a helping hand throughout the research period.

February 2024 Anas Saeed Mohammed Ali AL-NEAMA

TABLE OF CONTENT

Page

ABBREVIATION

PKW : Piano Key Weir
(k- ε) : The turbulent model
ρ : Mass density of water … kg/m
μ : Dynamic viscosity of water … kg/ms
σ : the surface tension force of water … kg/s^2
Q_a : actual flow discharge lt/s … lt/s
g : Ground acceleration …m/s^2
h_1 : upstream flow depth over crest … m
h_2 : depth of tail water at the downstream … m
H_1 : the total upstream hydraulic head $H_1=h_1 + V_1^2/2g$… m
C_d : discharge coefficient of PKW … _
V_1 : The velocity of flow in the channel at the upstream… m/s
V_2 : the velocity for flow in the channel at the downstream … m/s
P : height of piano key weir ... m
L : Total developed length along the overflowing crest axis of piano key weir... m
W : Total width of the PKW ... m
W_i : The inlet key width of PKW ... m
W_o : The outlet key width of PKW ... m
B : Upstream-downstream length of the PKW, $B=B_b+B_i+B_o$ ... m
B_i : Downstream inlet key overhang crest length of PKW ....m
B_o : Upstream outlet key overhang crest length of PKW ... m
B_b : Base length of PKW... m
S_i : Slope of the inlet key … _
S_o : Slope of the outlet key … _
Nu : Number of PKW units constituting the structure …. _
T_s : Sidewall thickness ... m
α : Sidewall angle … ^{o}
Φ : Diameter of the hole inside the screen wall … cm
A_s : The area of the opening shape inside the wall as a function of the shape of the opening … m^2
A_p : The area of the total voids inside the screen wall as a function of porosity … m^2
T_{sw} : Screen wall thickness … m
E_1 : the specific energy of flow at the upstream $E_1=P+h_1+V_1^2/2g$ …. m
E_2 : the specific energy of flow at downstream $E_2=h_2+V_2^2/2g$ … m
$\Delta E/E_1$: the relative energy dissipation $(E_1-E_2)/E_1$ … _
E_2/E_1 : the residual energy … _
Fr : Froude number …. _
Re : Reynolds number …. _ -
We : Weber number …. _
& : and.

LIST OF TABLES

Page

LIST OF FIGURES

Page

EXPERIMENTAL STUDY ON ADDING DIFFERENT SCREEN WALLS TO THE PIANO KEY WEIR (PKWs) HYDRAULIC STRUCTURE AND ITS EFFECT ON HYDRAULIC PERFORMANCE

ABSTRACT

Piano Key Weirs are hydraulic structures that can be used for flood release systems on dams or to increase the discharge capacity when placed in the Watercourse. They also have the ability to pass large discharges for lesser upstream-head values when compared with other weirs types. Where the meandering length of the edge of PKW is greater than the width of the Watercourse itself, this leads to a reduction in the depth of water present in the Watercourse at the discharge itself.

The Piano Key Weir is a special type of labyrinth weir developed as a solution to the problem of traditional labyrinth weirs, which is the inadequacy of dam construction due to the large base area, where PKW is distinguished by a small structural footprint.

PKW geometry consists of successive repetitions of cycles, with new features introduced to form the particular shape of PKW, like a rectangular layout, sloped floors, overhangs and reduced footprint area. These features make the PKW more economical and enable its construction on gravity dam sections, as well as the ability of its hydraulic structure to dissipate energy.

Piano key weir type-A is one of the best types of PKW in terms of performance due to the length of its crest edge, which is considered the longest among the types of PKW, which allows for larger amounts of flow to be released. Also, prefer the usage of Type-A PKW for dam restoration and dam rising projects because they are balanced structures in a static force analysis, where the force resultant is placed inside the base of the structure and is hence typically safe from overturning.

In this research, the addition of different screen walls in terms of diameters of holes, porosity of screen wall, and shapes of holes to the side walls of the piano key weir was studied to determine the extent of their effect on the discharge coefficient, energy dissipation, and residual energy.

The different screen walls applied to five main models of the piano key weir type-A, with a rectangular shape (PKW1, PKW2, PKW3, PKW4, and PKW5) which Different geometric parameters and each model has four heights P=30, 28, 26, 24 cm and addition 13 model of screen walls with different holes and divided into three groups; the group of diameters it includes type-A, type-B, type-c, type-D, type-E, and the group of porosity it includes type-B, type-F, type-G, type-H and the group of shapes it includes type-D (circular), type-I (astral), type-J (hexagonal), type-K(triangular), type-M (square).

The experiments laboratory was conducted in the hydraulics laboratory of the College of Engineering, University of Mosul, where 400 Experiment conducted by passing four flow discharges 37,47,57,67 lt/s through a horizontal concrete channel

with a length of 24.64 m, width of 0.81 m and depth of 0.6 m, with concrete walls 0.2 m thick. And The case of flow was free flow and clear water, and the model of PKW was not immersed.

It was shown that the effect of adding screen walls to the models led to a good and noticeable increase in the discharge coefficient, and this increase appears more evident as the diameter of the holes of the screen walls increases or their porosity increases, as the group of screen walls according to diameter, type-E gave the highest discharge coefficient and type-A The lowest discharge coefficient, and the group of the porosity gave the type-H the highest discharge coefficient and the type-B the lowest discharge, and the group of the shapes of the holes gave very close values for the discharge coefficients, and the discrepancy between them was small, as the type-K gave the highest discharge coefficient, then TYPE-J, TYPE-M, TPYE-D, TYPE-I respectively.

It was also shown that the effect of the screen walls on energy dissipation was inverse, as the rate of energy dissipation decreased with the addition of screen walls, but this decrease in energy dissipation was very small, and the larger the diameter of the holes of the screen walls or the greater their porosity, the more this causes a reduction in energy dissipation.

The research also dealt with a hydraulic study of the transfer of flow from the upstream of the PKW to the downstream through the screen walls and its effect on the head of flow at the upstream and the depth of the tailwater downstream.

The study also addressed the effect of adding different screen walls to PKW while changing the geometric parameters of PKW and their role in affecting the discharge coefficient, energy dissipation, and residual energy. It was found that the high value of (L/W), (W_i/W_o), and (B/P),gives the highest discharge coefficient and the lowest energy dissipation when using the same screen walls.

The research also addressed the effect of (H_1/P) which represents the height of the flow head upstream to the height of the PKW model, which has a role in increasing the discharge coefficient and increasing energy dissipation whenever this percentage decreases. This ratio is also linked to changes in the geometric parameters of PKW and by adding different screen walls to PKW.

The research also included extracting the advantages and Disadvantages of adding screen walls and their effects on the performance of the PKW's work, increasing the stability of the structure, reducing the area of erosion below the dam, and many other benefits.

The research also included developing recommendations related to the topic and ways to develop it.

PİYANO TUŞU SAVAĞI (PKW) HİDROLİK YAPISINA FARKLI PERDE DUVARLARININ EKLENMESİ VE HİDROLİK PERFORMANSA ETKİSİ ÜZERİNE DENEYSEL ÇALIŞMA

ÖZET

Piyano anahtarlı çarklar, barajlarda taşkın tahliye sistemlerinde veya su yoluna konulduğunda deşarj kapasitesini arttırmak amacıyla kullanılabilecek, aynı zamanda diğer savak tiplerine göre daha düşük memba düşü değerleri için büyük debileri geçirebilme özelliğine sahip hidrolik yapılardır. PKW'nin kenarının kıvrımlı uzunluğunun Su Yolunun genişliğinden daha büyük olması durumunda, bu, çıkışta su yolunda mevcut olan suyun derinliğinin azalmasıyla sonuçlanır.

Piyano Tuşlu Savak, geleneksel labirent savak sorunu olan, barajların taban alanının geniş olması nedeniyle baraj üzerine yapılaşmanın yetersizliği sorununa çözüm olarak geliştirilmiş özel tip bir labirent savaktır. PKW'nin küçük bir yapısal ayak izi ile ayırt edildiği yer.

PKW geometrisi, dikdörtgen düzen, eğimli zeminler, çıkıntılar ve azaltılmış ayak izi alanı gibi PKW'nin spesifik şeklini şekillendirmek için sunulan yeni özelliklerle birlikte döngülerin ardışık tekrarlarından oluşur. Bu özellikler PKW'yi daha ekonomik hale getirerek, ağırlık barajı bölümlerinde yapımına ve hidrolik yapısının enerjiyi dağıtma kabiliyetine sahip olmasını sağlar.

Piyano tuşu seti A tipi, daha büyük miktarda akışın serbest bırakılmasına izin veren PKW türleri arasında en uzun olduğu düşünülen tepe kenarının uzunluğu nedeniyle performans açısından en iyi PKW türlerinden biridir. ve aynı zamanda baraj onarımı ve baraj yükseltme projeleri için A Tipi PKW'nin kullanımını tercih etmektedir çünkü bunlar, kuvvetin bileşkesinin yapının tabanına yerleştirildiği ve dolayısıyla tipik olarak devrilmeye karşı güvenli olduğu statik kuvvet analizinde dengeli yapılardır.

Bu araştırmada, piyano tuş duvarının yan duvarlarına delik çapı, ekran duvarının gözenekliliği ve deliklerin şekli açısından farklı ekran duvarlarının eklenmesinin deşarj katsayısı ve enerji üzerindeki etkisinin kapsamı araştırılmıştır. dağılma ve kalan enerji.

A tipi piyano tuş duvarının dikdörtgen şekilli beş ana modeline (PKW1, PKW2, PKW3, PKW4 ve PKW5) farklı geometrik parametrelere sahip ve her modelin dört yüksekliği P=30, 28, 26 olan beş ana modeline farklı perde duvarları uygulanmıştır. , 24 cm ve ilave 13 farklı delikli perde duvar modeli üç gruba ayrılmıştır; çap grubu, A tipi (Φ=0,35 cm), B tipi (Φ=0,5 cm), c tipi (Φ=0,7cm), D tipi (Φ=1,0 cm), E tipi (Φ=1,4 cm) ve içerdiği gözeneklilik grubu; B tipi (gözeneklilik=%3,9), F tipi (gözeneklilik=7,18), G tipi (gözeneklilik=%9,7), H tipi (gözeneklilik=%17,44)) ve içerdiği şekil grubu, D tipi (dairesel), I tipi (astral), J tipi (altıgen), K tipi (üçgen), M tipi (kare) içerir.

Deney laboratuvarı, Musul Üniversitesi Mühendislik Fakültesi Hidrolik Laboratuvarı'nda 24 metre uzunluğunda yatay bir beton kanaldan 37,47,57,67 lt/s'lik

4 adet debi ile 400 deney gerçekleştirilmiştir. ,64 m, genişlik 0,81 m ve derinlik 0,6 m, beton duvarlar 0,2 m kalınlığındadır. ve akış durumu serbest akış, temiz su idi ve PKW modeli suya batmamıştı.

Modellere elek duvarları eklemenin etkisinin, deşarj katsayısında iyi ve gözle görülür bir artışa yol açtığı ve bu artışın, elek duvarlarının deliklerinin çapı arttıkça veya gözeneklilik arttıkça daha belirgin olduğu gösterilmiştir. Çapa göre elek duvarları grubunda E tipi en yüksek deşarj katsayısını, A tipi en düşük deşarj katsayısını, gözeneklilik grubu ise en yüksek deşarj katsayısını Tip-H'ye, B tipi ise en düşük deşarj katsayısını vermiştir. ve delik şekilleri grubu deşarj katsayıları için çok yakın değerler verdi ve aralarındaki fark küçüktü, çünkü K tipi en yüksek deşarj katsayısını verdi, ardından TİP-J, TİP-M, TPYE -D, TİP-I sırasıyla.

Ayrıca, ekran duvarlarının eklenmesiyle enerji yayılım hızının azalması nedeniyle ekran duvarlarının enerji dağıtımı üzerindeki etkisinin tersine döndüğü, ancak enerji dağıtımındaki bu azalmanın çok küçük olduğu ve perde duvarlarının deliklerinin çapı büyüdükçe enerji dağıtımının azaldığı da gösterilmiştir. Ekran duvarları veya gözenekliliği ne kadar büyük olursa, enerji kaybının da o kadar azalmasına neden olur.

Araştırma ayrıca, akışın PKW'nin üst kısmından alt kısmına perde duvarları aracılığıyla aktarılması ve bunun akış yukarı akış yüksekliği ve çıkış suyunun mansap derinliği üzerindeki etkisine ilişkin hidrolik bir çalışmayı da ele aldı.

Çalışma aynı zamanda PKW'nin geometrik parametrelerini değiştirirken PKW'ye farklı ekran duvarları eklemenin etkisini ve bunların deşarj katsayısını, enerji dağılımını ve artık enerjiyi etkilemedeki rolünü de ele aldı. Aynı ekran duvarları kullanıldığında (L/W), (W_i/W_o) ve (B/P)'nin yüksek değerinin en yüksek deşarj katsayısını ve en düşük enerji kaybını sağladığı bulunmuştur.

Araştırmada ayrıca akış yukarısındaki akış yüksekliğinin yüksekliğini temsil eden (H_1/P) değerinin, debi katsayısının arttırılmasında rol oynayan PKW modelinin yüksekliğine olan etkisi de ele alınmıştır.

1. INTRODUCTION

Water is the main nerve of life and the pulsating artery that nourishes it. It is considered one of the most important natural sources that man has known since ancient times and relied on in his daily life. It is an urgent necessity to sustain life and achieve human development.

In order to use and make better use of water as it is a permanent source, sewers and water channels were built, and dams and reservoirs were built to store water and use it when needed, as well as to prevent floods.

Dams, reservoirs, and waterways need water facilities to control and regulate the discharge, and weirs are among the most important hydraulic structures that are usually used to control and regulate the discharge in waterways and rivers.

The weirs have multiple other uses, the most important of which is irrigation and the distribution of water from the main channel to the secondary, and they also it will control floods in narrow valleys (Ribeiro, Pfister, et al., 2012).

In addition, PKWs dissipate energy very efficiently (Farhadi et al., 2023).

The increased need in some waterways for facilities to drain large quantities of water as a result of the increasing demand for electric power generation and irrigation has become a necessity and given the fact that some dams are of low height and the capacity of their waterways is sometimes insufficient to meet all requirements and many of them contain mechanical gates which They are subject to failure or are not properly maintained and operated and are not (Lempérière et al., 2013).

A US Army Corps of Engineers survey states that about 36% of existing dams are currently unsafe due to insufficient capacity of discharge channels (Suprapto, 2013). This deficiency was the cause of one-third of dam failures that resulted in great loss of life and finances (Schleiss, 2011).

As a recent example, in March (2019) the failure of the Spencer Dam in Nebraska due to floods, and another example in May 2020, the Edenville Dam

failure in Michigan, USA, led to the evacuation of thousands of people Figure 1.1, (Association of State Dam Safety Officials, 2020; The Associated Press, 2022).

(a) The Spencer Dam Failure in Nebraska, USA.

(b) The Edenville Dam Failure in Michigan, USA.

Figure 1.1: Examples of dam failure

Source: (a) (Landers, 2021), (b) (Hammel, 2023)

But in the case of waterways of a specific width, the use of a linear weir leads to a rise in the water level in front of the watercourse, and thus leads to submerging the neighbouring lands, and then affects the population of the region and the economic situation as well.

It is possible to reduce the water level provided by using a non-linear weir (Labyrinth weir) whose edge is in the form of zigzag folds from the upper perspective, and it can be in several shapes such as rectangular, trapezoidal, triangular, circular, etc., and given that the length of the edge of the meandering weir is greater than the width of the stream itself, this will lead to reducing the depth of water present in the watercourse at the discharge itself Figure 1.2.

Figure 1.2: Lake Brazos labyrinth weir in Texas, United States.

Source: (Waymark, 2013).

The construction of the Labyrinth weir is the ideal solution to increase discharge, in addition to being less expensive and increasing storage and does not

require maintenance and mechanical operation (Lempérière & Ouamane, 2003).

Increasing the amount of overflow discharge is done in three ways: by increasing the width of the weir, lowering the weir crest elevation, and increase within the existing weir footprint by replacing the existing linear weir with a nonlinear (labyrinth-type) weir (Anderson, 2011).

The use of Labyrinth weirs in the case of concrete dams is not feasible in some cases because the Labyrinth weir needs a larger area to stabilize the vertical walls resulting from the Labyrinth weir in the axis of the edge on the edge of the concrete ebb, which is relatively small (Anderson, 2011).

Therefore, it was resorted to using weirs that are installed above the top of the watercourse and over the entire width of the dam. This type of weir is known as the piano key weir (Erpicum, Laugier, et al., 2013).

Piano Key Weirs (PKWs) are innovative hydraulic structures used in flood control and to enhance the discharge capacity of channels. They consist of a series of rectangular "keys" placed perpendicular to the flow direction, resembling the keys of a piano, hence the name.

PKW solves most problems compared with the original labyrinth and traditional weirs (Anderson & Tullis, 2013).

Such as:

1. Reduced Structural Footprint: Compared to conventional weirs, PKWs require less material and space due to their compact design. This makes them particularly suitable for retrofitting existing structures or implementing flood control measures in constrained areas.
2. Optimized Hydraulic Performance: The geometry of the keys plays a crucial role in achieving optimal hydraulic performance. Through careful design, PKWs can efficiently dissipate energy and control flow rates, reducing the risk of erosion and flooding downstream.
3. Enhanced Discharge Capacity: By increasing the effective length of the weir crest, PKWs can significantly enhance the discharge capacity of channels. This is achieved by increasing the weir's effective length without significantly

increasing the height, allowing for greater control over flow rates and reducing the risk of overflow during periods of high flow.

4. Piano Key Weirs represent a cost-effective and sustainable solution for flood control and hydraulic management, offering improved performance and efficiency while minimizing environmental impact.

According to Anderson and Tullis (2013) the PKW is approximately 20% more efficient than the traditional labyrinth weir.

This type of weir is considered a development of the labyrinth weir, which need more space to stabilize the vertical walls resulting from the meandering at the axis of the weir edge, and it is also used in the case of concrete dams due to the limited width of its base Figure 1.3 (Anderson, 2011).

Figure 1.3: Malarce Dam in France

Source: (Erpicum, Laugier, et al., 2013)

The use of the weir began in the late 1990. early 2000 when the French organization Hydrocoop designed the first weir for a piano key and studied the possibility of establishing it at the University of Biskra in Algeria (Ribeiro, Pfister, et al., 2012), and after a few years of developing concepts elaborated, the first PKW was built by Electricité de France (EDF) at the Goulours Dam in France Figure 1.4, (Laugier, 2007; Schleiss, 2011).

(a) (b)

Figure 1.4: The PKW system at the EDF Goulours dam in France.

Source: (a) (Ribeiro, Bieri, et al., 2012), (b) (Climate-ADAPT, 2019).

Over the last decades, many studies have been carried out in more than 15 institutions in order to comprehend the hydraulic behaviours of PK weir and the influences of several geometrical parameters on PK weir discharge efficiency (Erpicum et al., 2010; Khanh et al., 2011; Laugier, 2007; Ribeiro, Bieri, et al., 2012).

The hydraulic behaviours of the PK weir and the effects of various geometrical parameters on the PK weir discharge efficiency have been the subject of numerous studies conducted over the past few decades in more than 15 institutions (Erpicum et al., 2010; Khanh et al., 2011; Laugier, 2007; Ribeiro, Bieri, et al., 2012).

There are currently over 30 piano key weirs operating or being built in Scotland (Ackers et al., 2014), Sri Lanka (Jayatillake & Perera, 2013), Vietnam (Khanh et al., 2011, 2012), France (Laugier, 2007; Laugier et al., 2009), and Switzerland (Eichenberger, 2013).

With a majority of almost two-thirds being involved with dam repair projects (greater spillway capacity). Certain PK weirs, like the Dakmi 2 and Van Phong Barrage in Vietnam, are multifunctional projects featuring irrigation and hydro features.

The World Register of Piano Key Weirs, which is mentioned in Table 1.1 aims to gather all PK weir projects. Two Algerian labyrinth spillways have also been added to the register as they are similar to the PK weir concept. Some other projects are also being studied in the USA (Crookston et al., 2016).

Table 1.1: The world register of piano key weir

Dam name	Country	Completion year
Bakkhada	Algeria	1938
Beni Bahdel	Algeria	1940
Goulours	France	2006
Saint-Marc	France	2008
Etroit	France	2009
Gloriettes	France	2010
Rattling Lake	Canada	2011
Escouloubre	France	2011
Gouillet	France	2011
Malarce	France	2012
Beaufort	France	2013
Black Esk	United Kingdom	2013
Dak Mi 4B	Vietnam	2013
Dak Rong 3	Vietnam	2013
Giritale	Sri Lanka	2013
Loombah	Australia	2013
Sawra Kuddu	India	2013
Emma	Switzerland	2013
Campauleil	France	2014
Charmines	France	2015
Rambawa Tank	Sri Lanka	2015
Rassisse	France	2015
Raviege	France	2015
Van Phong	Vietnam	2015
Da Dang 3	Vietnam	2016
Dak Mi 3	Vietnam	2016
Record	France	2016
Xuan Minh	Vietnam	2016
Gage	France	2017
Hazelmere	South Africa	2017
Oule	France	2018
Ouljet Mellegue	Algeria	2018
Lewis Creek reservoir	USA	2019

Source: (Tuan & Hiramatsu, 2020).

Regarding the environment, cost, operations and maintenance, and suitability for providing water to people and agricultural areas vulnerable to drought, PKW's creative solution for the Van Phong barrage in Vietnam has been universally

recognized as the best option. April 2015 saw the barrage put into service; Van Phong Barrage is now the world's longest PK weir (475 m) and has the highest discharge capacity among all the weir types (14,400 m3/s). The intake with the irrigation channel is on the left bank, while the powerhouse with two units is on the right bank. Can collect the water from the two turbines and use it to irrigate the lowest land close to the coast Figure 1.5 (Khanh, 2017).

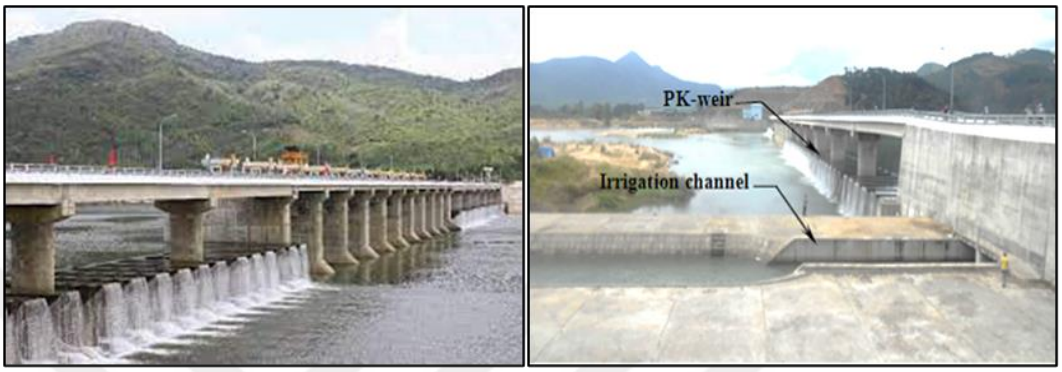

(a) (b)

Figure 1.5: Van Phong Barrage in Vietnam

Source: (a) (Laugier, 2007), (b) (Belaabed et al., 2021)

1.1 General Piano Key Weir Advantages

PW weirs are useful alternatives to dam and river applications because of a number of distinctive design features, which are counted below.

1. **Piano key weir (PKW) is an optimal and special option for boosting the spillway capabilities of existing dams, a relevant solution to many problems, such as emergency spillway operations:**

The piano key weir is a non-linear overflow structure which, because of complex flow patterns in its vicinity, the design aims to provide a much longer overflow length than normal linear weirs; in so doing, an increased flow can be discharged at the upstream head when compared to linear weirs, At the peak efficiency these structures can allow discharges of up to 100 m^3/s/m (Lempérière & Ouamane, 2003), although in practice the maximum discharge values are usually in the order of 20 m^3/s/m for a depth of 2m (Laugier et al., 2017).

This is typically between two to four times higher than that for a linear weir at a similar hydraulic head.

According to a cost comparison study by Paxson et al. (2013) that examined PK weirs, labyrinth weirs, and gated spillways, the piano key weir is a relevant solution to many problems, such as emergency spillway operations (Paxson et al., 2014).

2. **Piano key weir is a relevant solution to many problems, such as water level control and increasing volume storage:**

This is due to the possibility of adding the piano key weir above the top of traditional dams, which increases the height of these dams, and thus, this is reflected in the increase in their storage capacity.

The designers were able to rehabilitate the Hazelmere Dam and raise its level by adding PKW on the Mdloti River, Kwazulu Natal, South Africa. The raising of the Hazelmere Dam wall from 85.98m to 93.00m through the construction of the Piano Key Weir will increase the dam's storage capacity from 23.9 million cubic meters to 43.6 million cubic meters. The project was completed in December 2022 Figure 1.6 (SA News, 2022).

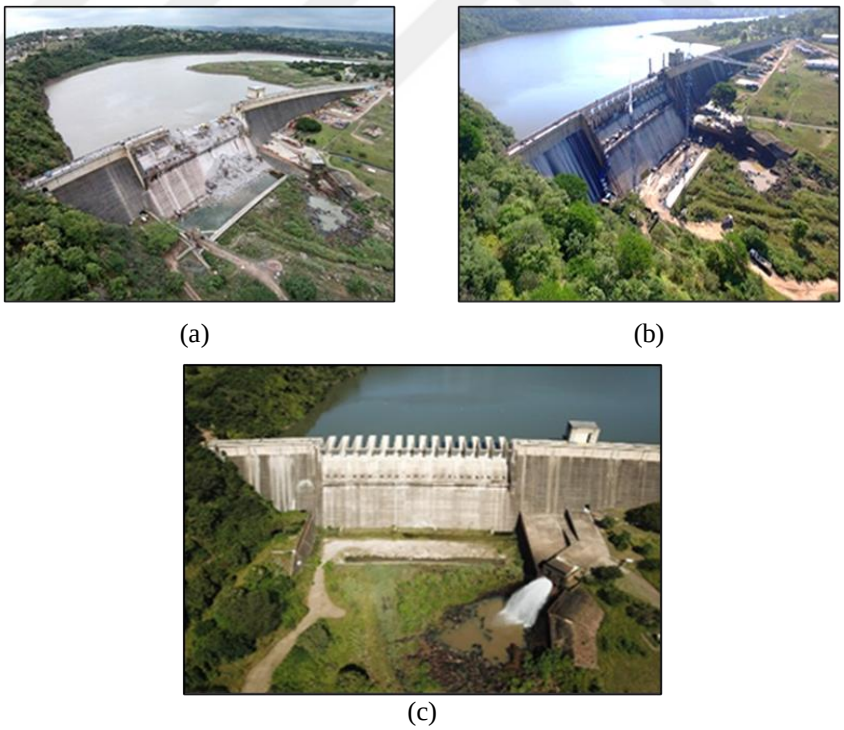

(a) (b)

(c)

Figure 1.6: Stages of raising of the Hazelmere Dam on the Mdloti River, Kwazulu Natal, South Africa.

Source: (a) (Reporter, 2022), (b) (News Detail En, 2017), (c) (SA News, 2022).

3. **Distinctive structure with the ability to reduce the construction footprint:**

When compared to typical labyrinth weirs, a PK weir's comparatively small footprint is one of its key advantages. These structures may now be built on the narrow crests of gravity dams, where labyrinth weirs are not practical because of their wide base widths, which is advantageous from both cost and performance because of the significantly smaller quantities of concrete used.

PKW are an optimal and special option for boosting the spillway capabilities of existing dams, according to a cost comparison study by Paxos et al. in 2013 that examined PK weirs, labyrinth weirs, and gated spillways (Paxson et al., 2014).

4. **Distinctive, easy and modular architectural construction:**

It is feasible to build a conventional PKW off-site in precast modular sections that are subsequently joined on-site due to its thin and repetitive character, as was done at the Black Esko Reservoir in the UK (Ackers et al., 2014).

Because of this, it is possible to produce thin-section steel or concrete components more quickly and with better quality control, resulting in crest profiles that are more precise and level. Cost reductions are another benefit of preproduction. Additionally, most of the PKW may be built off-site and stored before being installed in areas where there are only extremely limited construction windows available (for example, because flooding occurs often).

5. **Ability to work well under submerged conditions:**

The PKW is able to function in submerged circumstances at a better efficiency or a lower upstream head for a given discharge because of its distinctive flow patterns. This is true even if the weir's discharge efficiency at such huge heads is not significantly different from that of a typical linear weir (Belaabed & Ouamane, 2013; Cicero & Delisle, 2013).

Because of this quality, PK weirs are beneficial in riparian settings where developments upstream of the weir could restrict river water levels. In 2016, when the Van Phong Barrage in Vietnam was entirely inundated, this idea was tried successfully.

6. Ability to sweep and drain driftwood and debris:

It has been determined that a PK weir dam spillway is only somewhat sensitive to debris and driftwood. Despite laboratory tests showing that with higher flows, the majority of debris would be swept downstream, the presence of debris on the PK weir did marginally lower the weir's discharge efficiency (Pfister et al., 2013).

The PKW still has around (75–80%) of its discharge capacity if the debris is not washed away. This is because of the structure's particular flow dynamics, which draws flow from below the upstream water level's surface and avoids any potential debris (Laugier et al., 2013).

7. The Financial advantages:

Many studies indicated that the PKW might be a financially viable choice for future dams. The PKW is distinguished by a significant cost reduction for the majority of new dams, a guarantee of their safety, and a potential increase in the storage capacity of many existing reservoirs at a cost in the range of 0.05 USA Dollar per m3 in most developing countries and 0.5 USA Dollar per m3 in industrialized countries (Ouamane, 2011).

PK weirs are thought to be more affordable in many instances and cost-competitive with labyrinth and gated spillways (Paxson et al., 2014).

8. Ability to energy dissipation:

PK weirs offer some energy dissipation similar to labyrinth weirs, which may be useful in new and restoration projects. Low heads experience the highest rates of energy dissipation, which are nonlinear.

Greg Paxson et al. (2014) made a comparison of piano key wheels with the labyrinth and ogee wheels in terms of hydraulics, cost, constructability, and operations. They concluded that PKW present a unique solution to provide significant hydraulic capacity for new dams and for the rehabilitation of existing dams; PKW are considered to be cost-competitive with the labyrinth and gated spillways and may be a more economical solution in many situations; PKW may be a preferable alternative to gated spillways due to their ability to pass large flows

without the operation and maintenance issues and costs related to gates Figure 1.7 & Figure 1.8 (Paxson et al., 2014).

(a) Ogee weir (Shahghasem dam in Iran).

(b) Labyrinth Weir (Lake Townsend Dam in United States).

(c) Piano Key Weir (the Hazelmere Dam in South Africa).

Figure 1.7: Examples of some types of weirs

Source: (a) (Salmasi & Abraham, 2020), (b) (Hammer, 2020), (c) (Phillips, 2023)

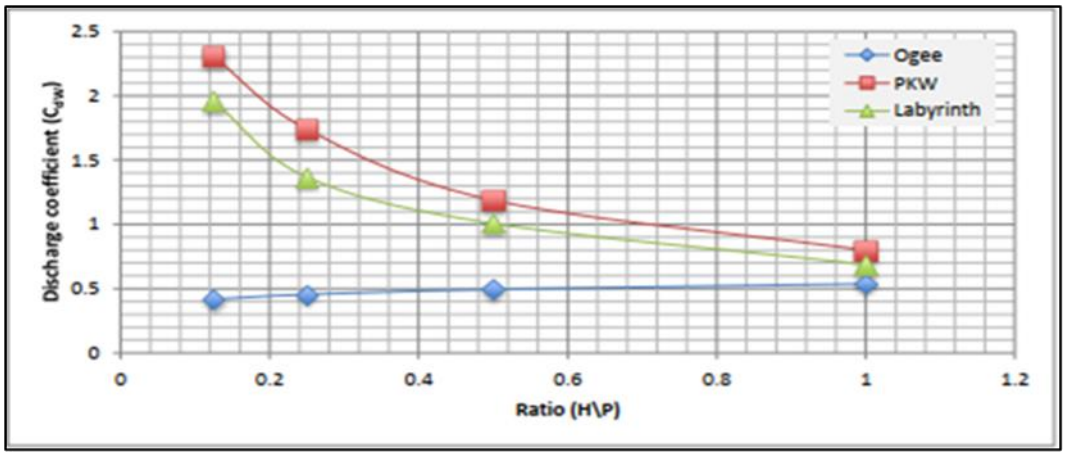

Figure 1.8: A Simple comparison between the piano key weir, the labyrinth weir, and the auger weir in terms of the discharge coefficient and better efficiency in reducing the flow head on the upstream.

Source: (Blancher et al., 2011).

1.2 General Piano Key Weir Disadvantage

1. **Problems related to constructability:**

A PKW's design is heavily influenced by its constructability. Practicality, construction equipment, site accessibility, and worker health and safety issues forced several current prototypes to place restrictions on the length of the overhangs.

The time problem is another constructability problem. Access to a certain building site may be impeded by the occurrence of seasonal or recurring floods. The installation process may be sped up by the use of modular construction, which can help in this respect.

2. **Problems related to Sedimentation:**

As the upstream water body approaches the weir, piano key weirs are known to create secondary flow fields. This flow field has the potential to sweep the region just upstream of the weir under certain circumstances. This self-cleaning behaviour is anticipated to also be seen by piano key weirs; The weir might not function as it would in its normal, sediment-free condition, though, if the impact is too limited (Tiwari & Sharma, 2015).

3. **Problems related to Aeration:**

Higher flows cause the air pocket under the nappe to become isolated, which may lead to circumstances with sub-atmospheric pressure. In trapezoidal labyrinth weirs, Crookston and Tullis (2012) investigated aeration, instability, and nappe interference. They defined several nappe aeration settings and noted that when the nappe adheres to the weir's downstream surface, numerous unwanted situations, such as vibrations, noise, and pressure variations, may happen because of low air pressures beneath the nappe (Crookston & Tullis, 2012).

4. **Problems related to score:**

Jüstrich et al. (2016) investigated the scour hole and ridge formation brought on by PK weirs without any scour protection and came to the conclusion that the entire process is jet-induced scour.

5. **Debris and driftwood:**

Driftwood and Debris affect the performance of the PKW, as floating driftwood sometimes collects under the overhangs of the piano key weir after it comes with the flow coming from the source, in addition to the Debris that moves

from the bottom of the weir and rises through the weir floor slanting with the flow, sometimes causing an obstruction to the flow through (Laugier et al., 2013).

1.3 Types of Piano Key Weir

There are four main types of piano key weirs, depending on the location of the overhang in the body of the weir as the first type (a) has an overhang at the front and back of the weir, the second type (b) has a protrusion in the front of the weir, and the third type (c) has an overhang at the back of the weir and the fourth type (d) does not have any overhang Figure 1.9 & Figure 1.10 (Lemperiere et al., 2011).

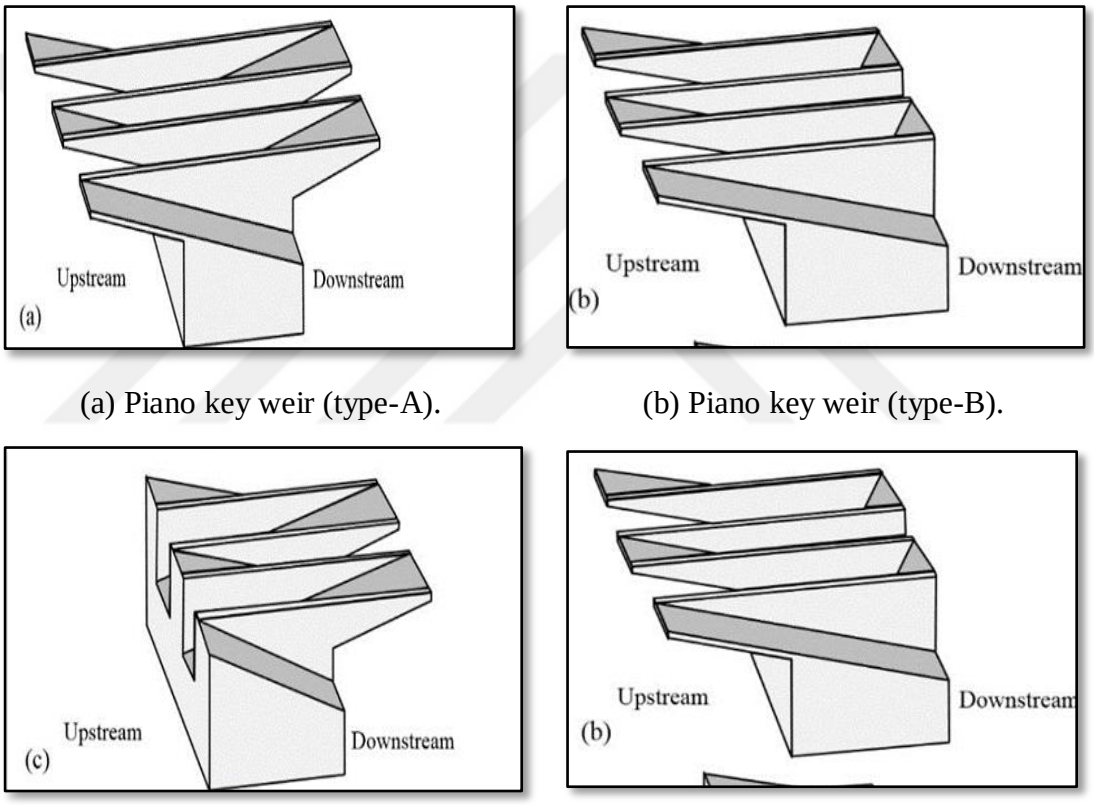

(a) Piano key weir (type-A). (b) Piano key weir (type-B).

(c) Piano key weir (type-C). (d) Piano key weir (type-D).

Figure 1.9: Three-dimensional shapes of the types of piano key weirs.

Source : (Yousif, 2020).

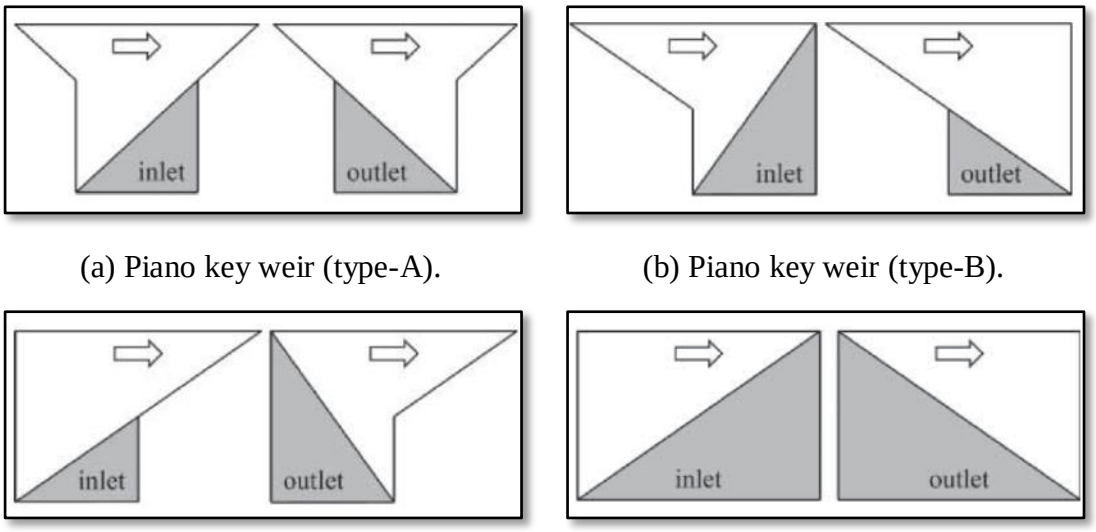

(a) Piano key weir (type-A). (b) Piano key weir (type-B).

(c) Piano key weir (type-C). (d) Piano key weir (type-D)

Figure 1.10: Side sections of types of piano key weirs.

Source: (Ribeiro, Pfister, et al., 2012).

Overhangs have inclinations in their bases that direct the flow away from the edge of the weir and increase the length of the attachment, which leads to an increase in the weir's discharge capacity. Due to the repetition of these rectangles, which overlap with their tendencies, it was called the Piano Key Weir. The keys of this type of weirs take multiple shapes, including rectangular, trapezoidal, and circular.

1.4 Purpose of Research

Some dams need to rehabilitate the spillways due to the increase in the hydrological data records to estimate the maximum discharge of the newly designed flood and the increase in the demand for water or to increase the storage volume of the reservoirs and for the continuity of the safety of the dams.

The construction of a piano weir is the ideal solution to increase discharge; in addition to being less expensive, increasing storage, and not requiring maintenance and mechanical operation, it is also a good dissipator of Energy, which reduces erosion behind dams.

The purpose of this research is to study the effect of adding screen walls with different holes to the lateral walls of the Piano Key weirs type-A on the hydraulic performance:

1. To improve the discharge coefficient and obtain the highest safe discharge of the flow that can be discharged by the weir during floods, ensuring a suitable height for the flow above the weir.
2. To know the behaviour of the flow before, though, and after the piano key weir and to know how Energy is dissipated through it in order to benefit from it in the future in studying cases of erosion and sediment transport before and after the piano key weir, in addition to knowing the amount of dissipated Energy and remaining Energy at the downstream of PKW by using the different screen walls.
3. To demonstrate the extent of the impact of the effect of changing geometric parameters of the Piano Key weirs with adding screen walls with different holes on the hydraulic performance, on the discharge coefficient, on energy dissipation and the amount of the Residual Energy of flow.
4. Reach a conclusion regarding choosing the optimal model of PKW and screen wall from among all the models of this study.
5. To extract the advantages and disadvantages of adding screen walls to PKW and to come up with recommendations about future studies related to this topic.

1.5 Aims of the Study

The laboratory research study aims to demonstrate the effect of adding screen walls to the type-A piano key weir and to demonstrate its effect on (the hydraulic performance of the weir and the extent of its effect on the discharge coefficient as well as its effect on energy dissipation and Residual Energy) by study:

1. Study on the effect of changing the height (P) of the piano key weir while adding screen walls to the weir on the coefficient of discharge and on energy dissipation.
2. Study on the effect of changing (W_i/W_o) on the ratio of the width of the inlet key to the width of the outlet key for piano key weir with the addition of screen walls on the coefficient of discharge and energy dissipation.

3. Study on the effect of changing the edge length (L) of the piano key weir with the addition of screen walls on the coefficient of discharge and on energy dissipation.
4. Study on the effect of changing the length of the inlet keys (B_i) and the length of the outlet keys (B_o) of the piano key weir with the addition of screen walls on the coefficient of discharge and on energy dissipation.
5. Study on the effect of changing the sizes of the diameters of the holes of the screen walls added to the piano key weir on the discharge coefficient and on energy dissipation.
6. Study on the effect of changing the shapes of the holes of the screen walls added to the piano key weir on the coefficient of discharge and on energy dissipation.
7. Study on the effect of changing the porosity ratio of the screen walls added to the piano key weir on the discharge coefficient and on energy dissipation.
8. Study on the effect of changing the discharge with the addition of screen walls to the piano key weir on the discharge coefficient and on energy dissipation.

1.6 Methodology of the Study

This study starts from:

1. Information collection: This study included collecting information from a variety of sources and references, some of which were easy to access and others required a lot of work. This included extensive reading about the hydraulic structure, its types and shapes, the developments made to it, and previous research conducted on it.
2. Creating models: The creation of miniature models of the hydraulic structure included a type A piano key weir with different geometric parameters and different heights, as well as preparing screen walls with different shapes and diameters of holes and different porosity.
3. Laboratory work: It includes preparing the laboratory channel, installing the different models of the piano key weir in it, replacing the different screen wall models and installing them on the weir models, setting up the various

discharges, and measuring the height of the flow at the upstream and downstream.

4. Data analysis and discussion: It includes using the results we obtained from the laboratory work to calculate the discharge coefficients for piano key weir models, and also calculate the amount of Energy dissipated for the flow and the amount of Energy remaining in the channel, and identify and discuss the factors affecting them.
5. Conclusions and decision making: It includes drawing conclusions from analyzing and discussing the results and making a decision regarding them.

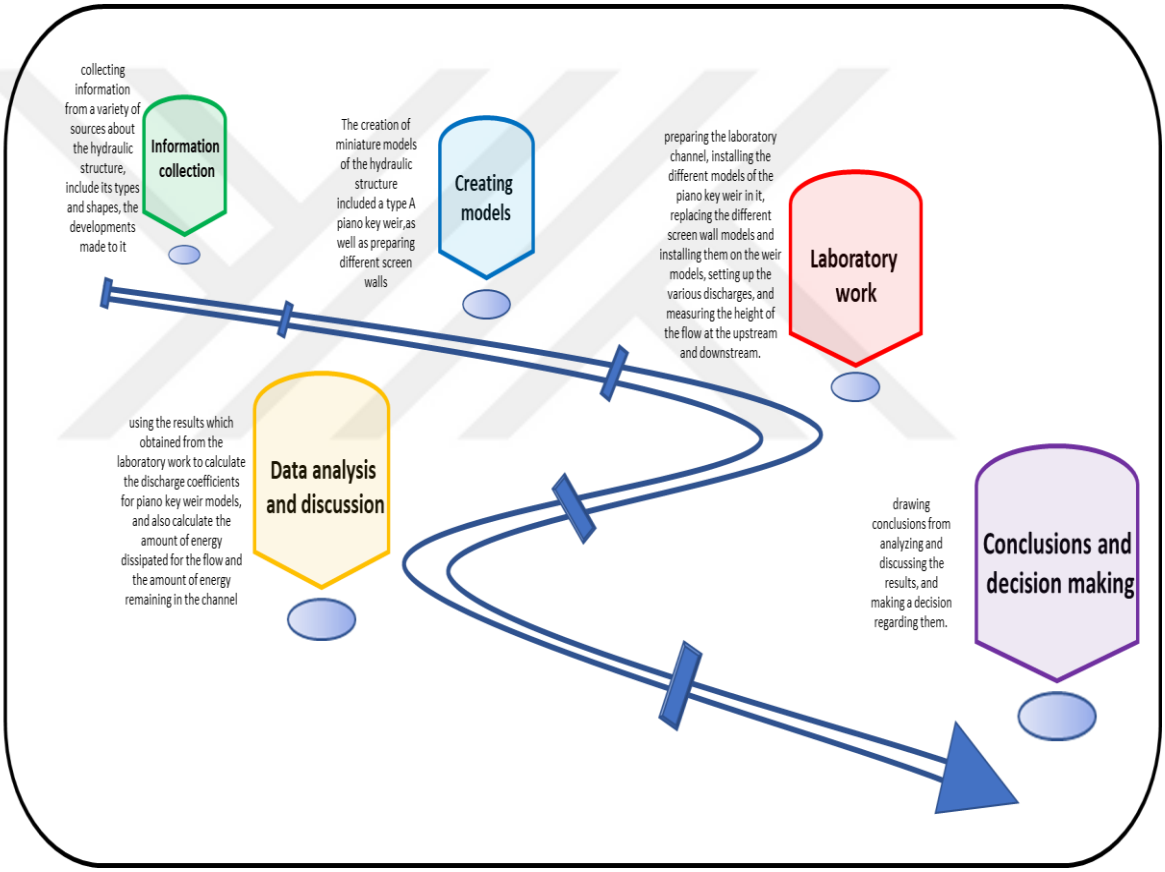

Figure 1.11: The diagram of the methodology of the study

1.7 Scope and Limitation of the Research

Determinants of experimental research:

- Use pure, sediment-free water in all experiments.
- All experiments were conducted under free-flow conditions.
- Neglect of the effect of surface tension, because the flow height over PKW models is more than (3 cm), neglect of the effect of viscosity of the fluid due

to the flow in the flume is turbulent where Reynolds number is large Re > 25,000 (Bhukya et al., 2022; Khassaf et al., 2016; Sangsefidi et al., 2021).

- All 2-units, PKW models were manufactured of 2.5mm thick acrylic glass sheets cut with a CNC (computer numerical controlled) machine (Al-Baghdadi & Khassaf, 2018; Khassaf et al., 2016; Khassaf & Al-Baghdadi, 2015).
- All of the piano key weir models used in the experiments are of type (a) with flat crests (no parapet, no nose).
- Neglect of the effect of the wall thickness of the piano key weir and the thickness of the screen walls in the mathematical calculations; because the effect of thickness 2.5mm on the flow discharge coefficient is very small.
- Four discharges are used for the experimental study, including 67, 57, 47 and 37 lt/s. Because at a discharge that is less than 37 lt/s, the height of the flow above the crest of the weir will be less than 3cm, and this causes tension on the surface, and at a discharge that is more than 67 lt/s, it will cause disturbance and interference to the currents running over the piano key weir which affects the flow system over the weir.
- The percentage of porosity of the screen wall was adopted as equal to the ratio of the sum of the areas of the holes to the area of the screen wall. The holes of the screen walls of different porosities are of a fixed diameter and are equal to 0.5 cm Figure 1.12.

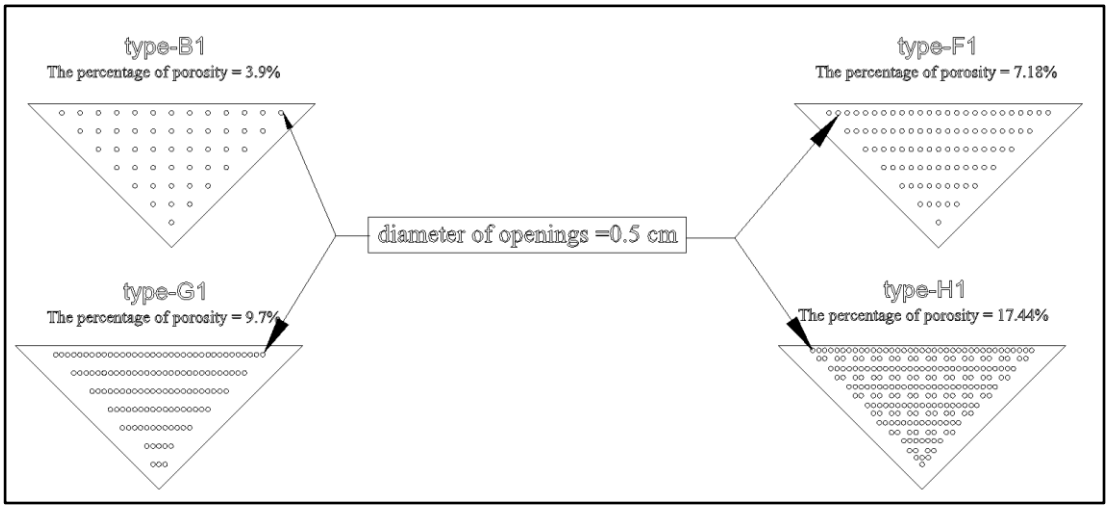

Figure 1.12: Some screen wall models have different percentages of porosity

2. LITERATURE REVIEW

This chapter includes a review of previous research and studies by some of the researchers who contributed to the development of knowledge about the behaviour of weirs and the piano key weir through laboratory experiments of weir models and the change of some influential engineering variables, as well as a comparison between the piano key weir with the rest of the types of piano key weirs and their other forms.

Compared to traditional labyrinth weirs, PKWs offer a more compact design, reducing the required footprint and construction materials. This makes them particularly advantageous for retrofitting existing structures or implementing flood control measures in constrained areas. Additionally, PKWs have been shown to achieve higher discharge capacities and better flow control, attributed to their unique geometry and flow patterns.

However, despite their benefits, the construction of PKWs on dams presents certain challenges. These include the need for precise design and construction techniques to ensure structural integrity and hydraulic performance. Additionally, the incorporation of PKWs into existing dam structures may require modifications to the dam crest and spillway, adding complexity to the construction process.

In evaluating the effectiveness of PKWs, several key parameters are considered, including the discharge coefficient, energy dissipation, and residual energy. The discharge coefficient reflects the ratio of actual discharge to theoretical discharge and is crucial for accurately predicting flow rates and performance. Energy dissipation refers to the ability of the PKW to dissipate kinetic energy from flowing water, reducing the risk of erosion and downstream flooding. Residual energy, on the other hand, represents the remaining energy in the flow after passing over the PKW and is important for assessing potential downstream impacts.

Previous studies have also explored the use of screen walls to further enhance hydraulic performance. The Screen walls are vertical barriers placed downstream of

the Hydraulic structures, serving to guide and control flow patterns. These studies have demonstrated the potential benefits of screen walls in improving flow efficiency, reducing turbulence, and enhancing sediment transport processes.

Previous studies of screen walls included porosity, shapes of screens, numbers, locations, thickness, degree of inclination, size of holes inside them, and the shape of these holes and the effect of these screens on the hydraulic performance of the flow in terms of reducing the head of the flow in the upstream and dissipating energy and dispersing it in the downstream.

2.1 Description of PKW Structure

The piano key weir (PKW) is a regular-shaped structure that can be divided into similar representative PKW units. The unit is made up of the entire inlet key with a sidewall and half of the outlet key on both sides, Figure 2.1, PKW unit is significant since it may be used to reconstruct the entire structure when placed next to one another Figure2.2 (Pralong et al., 2011).

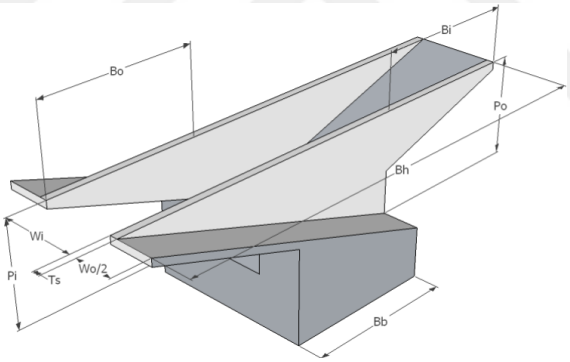

Figure 2.1: One unit of piano key weir.

Source: (Erpicum et al., 2014).

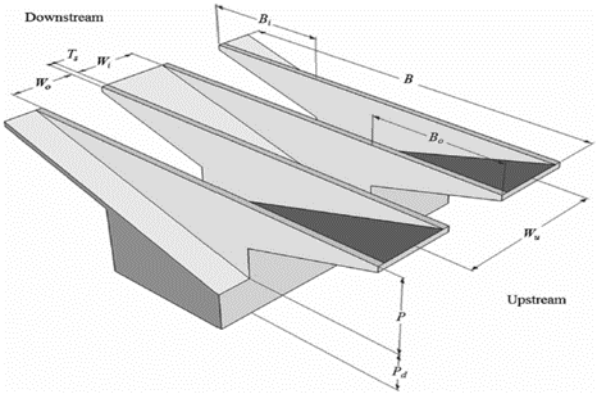

Figure 2.2: Two units of piano key weir.

Source: (Denys, 2017).

The inlet keys, outlet keys and sidewalls compose the main parts of the structure Figure 2.3 while noses and parapet walls are both optional in the PKW design Figure 2.4 (Pralong et al., 2011).

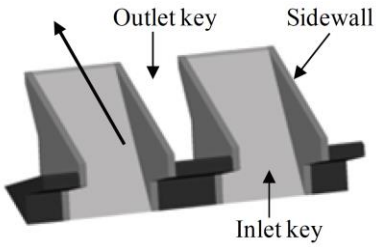

Figure 2.3: The main parts of PKW design.

Source: (Pralong et al., 2011).

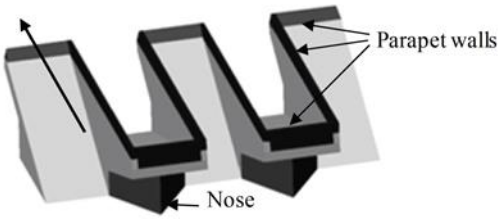

Figure 2.4: The optional parts of PKW design.

Source: (Pralong et al., 2011).

2.2 Naming the Geometric Parameters of the Piano Key Weir

A workgroup gathering EDF – Hydro Engineering Center in cooperation with the Laboratory of Hydraulic Constructions (LCH), Ecole Polytechnique Fédérale de Lausanne and the Laboratory of Hydrology, Applied Hydrodynamics and Hydraulic Constructions (HACH), University of Liege developed a specific vocabulary. The naming convention aims to propose a uniform description to designers while keeping the number of parameters to a reasonable amount. The goal is to use a set number of geometrical inputs to describe the overall shape of PKW, where PKW geometry has a lot of parameters, which makes describing its configuration difficult (Pralong et al., 2011).

Pralong et al. (2011) supplied the definitions and notations of the different geometrical parameters of the Piano Key weir and also gave a description of the global naming system, 22 parameters make up the description of the piano key Weir

which uses several geometrical parameters Figure 2.5, Table 2.1(Pralong et al., 2011).

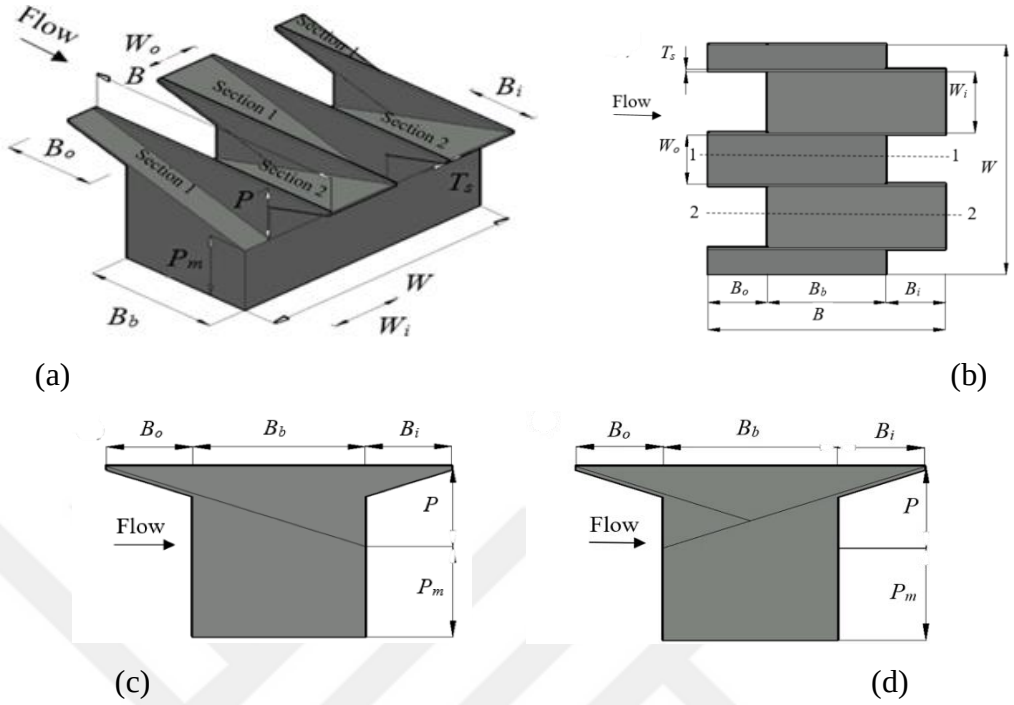

Figure 2.5: The main geometric parameters of type-A piano key weir.
(a) 3D view, (b) plan view, (c) section (1-1), (d) section (2-2).
Source: (Bhukya et al., 2022).

Table 2.1: Nomenclature of the foundational parameters of piano key weir geometry.

Parameter symbol	Meaning
B	Upstream-downstream length of the PKW $B = B_b + B_i + B_o$
B_o	Upstream (outlet key) overhang crest length
B_i	Downstream (inlet key) overhang crest length
B_b	Base length
B_h	Sidewall overflowing crest length measured from the outlet key crest axis to the inlet key crest axis
P_i	Height of the inlet entrance measured from the PKW crest (including possible parapet walls)
P_o	Height of the outlet entrance measured from the PKW crest (including possible parapet walls)
P_b	Height of the apron level at inlet key and outlet key intersection
P_m	Difference between P_i and P_b
S_i	Slope of the inlet key apron (length over height)
S_o	Slope of the outlet key apron (length over height)

Table 2.1: (Cont.) Nomenclature of the foundational parameters of piano key weir geometry.

Parameter symbol	Meaning
W	Total width of the PKW
W_u	Width of a PKW unit
W_i	Inlet key width (sidewall to sidewall)
W_o	Outlet key width (sidewall to sidewall)
T_s	Sidewall thickness
T_i	Horizontal crest thickness at inlet key extremity (measured at the basis of possible parapet walls)
T_o	Horizontal crest thickness at outlet key extremity (measured at the basis of possible parapet walls)
L	Total developed length along the overflowing crest axis
L_u	Developed length of the PKW unit along the overflowing crest axis $L_u = W_i + W_o + 2Bh + 2T_s$
N_u	Number of PKW units constituting the structure
n	Developed length ratio of the PKW: $n = \frac{L}{W}$
n_u	Developed length ratio of a PKW unit: $n_u = \frac{L_u}{W_u}$

Source: (Pralong et al., 2011).

The naming conventions also require the addition of a few physical parameters (Pralong et al., 2011).

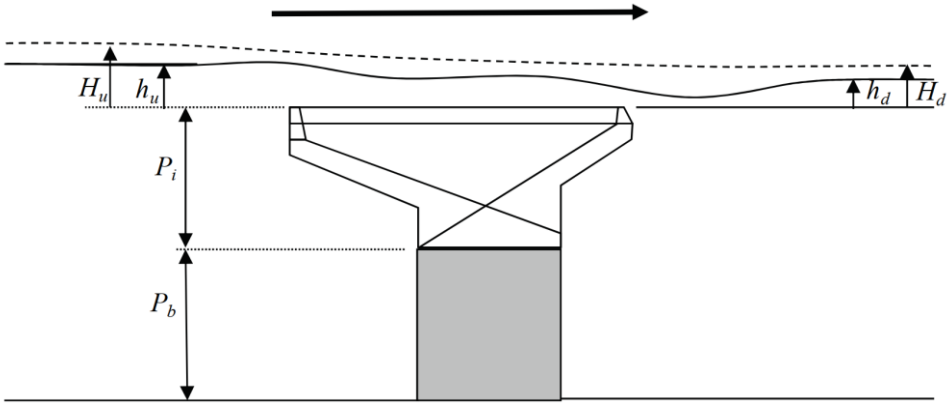

Figure 2.6: Cross section of the physical parameters nomenclature.

Source: (Pralong et al., 2011).

Table 2.2: Physical parameters nomenclature.

Parameter symbol	Meaning
P_d	Dam height
H_u	Total head over crest upstream from weir
h_u	Upstream flow depth over crest
H_d	Total head over crest downstream from weir (can be negative)
H_d	Downstream flow depth over crest (can be negative)
Q	Flow discharge
q_{sw}	Specific discharge referred to total width of the PKW Type equation here. $qsW = \frac{Q}{W}$
C_{dw}	Discharge coefficient related to PKW total width as $Q = C_{dw}.W.\sqrt{2g}.H^{3}/_{2}$
q_{sL}	Specific discharge referred to developed length of the PKW $q_{sL} = \frac{Q}{L}$
C_{dL}	Discharge coefficient related to PKW developed length as $Q = C_{dL}.L.\sqrt{2g}.H^{3}/_{2}$

Source: (Pralong et al., 2011).

2.3 Previous Studies on the Piano Key Weir (PKW)

2.3.1 Comparison studies between different types of piano key weir (PKW)

Ouamane and Lempriere (2006) carried out laboratory tests on 23 different models in order to perform economic research to develop a weir with a novel shape that may provide the highest efficiency. The study used a laboratory channel with a length of 4.3 m, a width of 0.75 m, and a height of 0.75 m connected to a basin with a length of 3 m, 3 m wide, and 1.1 m high. Another channel is connected to the basin, 2 m long, 1 m wide, and 1 m high. The studied models were placed at the front of the second channel. Two models of Algerian cities were among those that were studied: the first was a model of the Zit Amba oil dam that used the Piano key weir type -A to increase storage capacity, and the second was the Ain Zada model that used the Piano key weir type-B to increase storage and discharge capacity. the study determined that the piano key weir It may be used on various types of dams, streams,

and rivers to enhance discharge at a certain depth. Prefabricated pieces with basic geometric shapes were utilized to manufacture it. Despite being more effective, it functions similarly to free flow weirs; up to 100 (m/s) of discharge can be produced, it lowers the cost of dams and guarantees their security; because the water depth before the weir is reduced, the stock is increased (Ouamane & Lempérière, 2006).

Cicera et al. (2010) conducted a laboratory study to rehabilitate the Malarce gravity spillway in France. The dam was designed with a spillway consisting of three gates with a width of 14 m each, with a maximum discharge of 4100 m3/s. When the design discharge was calculated for a return period of 1000 years, the discharge was 4600 m3/s, so it was necessary to create a supplementary drain, a piano key weir, for the purpose of passing the additional amount. Four models of weirs were tested using a piano key: three by hanging from the forward side, type B with changing height and wall thickness, and the fourth by hanging from both sides type A. The models of the dam body, overflow gates, reservoir and weir, were designed in a laboratory at a scale of 1:60. The test was done by changing the level of the edge of the weir, measuring the discharge for each model and measuring the discharge Weir and gates together in the case of maximum flooding, and it was found that when the level of the edge of the weir decreases, the discharge increases as a result of the increase in the hydraulic charge. The best performance was of the type-A weir due to the longer edge length, as the water level was 10 cm less than the maximum level when used, so it was chosen to improve the safety of the dam (Cicero et al., 2010).

Figure 2.7: View of the PKW spillway of Malarce Dam in France during spillage.
Source: (Erpicum, Lempérière, et al., 2013; Sjösten & Vadling, 2020).

Pralong et al. (2011) noted that the Type-A form, which features both upstream and downstream overhangs, is the conventional shape that is typically

utilized. It has been demonstrated that a Type-B piano key weir with just upstream overhangs has a somewhat higher discharge capacity by around 3% than a typical Type-A shape. This is due to the somewhat reduced energy losses in the inlet key made possible by the longer upstream overhangs without downstream overhangs. However, this advantage is quite slight, and using a Type-B PK weir does bring extra structural issues that a Type-A piano key weir does not. Thus, the usage of Type-B PKW should only be taken into account in new dam projects when their unbalanced construction may be included in the primary dam superstructure. The usage of Type-A PKW is preferred for dam restoration and dam rising projects because they are balanced structures, i.e., in a static force analysis, the force resultant is placed inside the base of the structure and is, hence, typically safe from overturning. Type-C PKW with only downstream overhangs has not demonstrated any advantages in terms of discharge efficiency. Nevertheless, depending on site-specific factors like debris control, their usage can be justified (Pralong et al., 2011).

An experimental investigation for type A, B, C, and D Piano Key weirs was carried out by Kabiri-Samani, A.; Javaheri, A. in 2012. The author suggested a formula for estimating the discharge coefficient that would work for all types of PKW, including types A, B, C, and D, under both free-flowing and submerged flow circumstances (Kabiri-samani & Javaheri, 2012).

The discharge characteristics of PK weirs type A, type B and type C were researched by Cicero et al. (2013), who came to the conclusion that type B PK weir offers higher discharge than type A and type C PK weirs (Cicero & Delisle, 2013).

The impact of geometric parameters and piano key weir type on the flow efficiency was examined by Cicero et al. (2016), where Type-B of piano key weir had a flow efficiency that was 5 to 15% greater than Type-A and 15% higher than Type-C under free flow circumstances (Cicero et al., 2016).

Amr A. Bekheete et al. (2022) conducted research evaluating the impact of the design and type of PKW on flow efficiency. Using a CFD model, the investigation is carried out experimentally and numerically. The Type-B PKW demonstrated better efficiency out of the two types of PKW investigated, A and B (Bekheet et al., 2022).

2.3.2 Comparison studies between different Shapes of piano key weir (PKW)

A trapezoidal PKW was the subject of experimental research by Mehboudi et al. (2016). To examine the impact on the discharge coefficient, different flow conditions were applied to the trapezoidal PKW's geometric parameters; the efficiency of the trapezoidal PKW was 22% higher than the rectangular PKW's (Mehboudi et al., 2016).

The hydraulic performance of arced trapezoidal piano key weirs (ATPKW) under various hydraulic and geometric situations was examined by Karimi et al. (2019) using experimental and computational modelling; the numerical flow 3D model was utilized. The hydraulic performance of the weirs was originally lowered when the arc's angle was reduced, but it afterwards saw a great increase (Karimi et al., 2019).

Kumar M et al. (2020) carried out an experimental investigation by using equivalent configurations on trapezoidal and rectangular PKW; the dimensionless geometric parameters were used to determine the discharge coefficient; according to the study, the flow efficiency of trapezoidal PKW is 2-15% higher than that of rectangular PKW (Kumar et al., 2020).

Abhash and Pandey (2020) used Ansys Fluent CFD software to examine two distinct Type-A of PKW plan geometries, rectangular and trapezoidal, with an angle of 9o, Conditions; conditions of partial and complete submergence in flow were examined, at the same discharges. The rectangular PKW had a greater sediment transfer rate than the trapezoidal PKW (Abhash & Pandey, 2022).

Amr A. Bekheet et al. (2022) conducted research evaluating the impact of the form and type of PKW on flow efficiency. Using the Ansys Fluent CFD software model, the investigation is carried out experimentally and numerically on three PKW designs: rectangular, trapezoidal and triangular; the efficiency for the trapezoidal shape was the best and the lowest for the triangle (Bekheet et al., 2022).

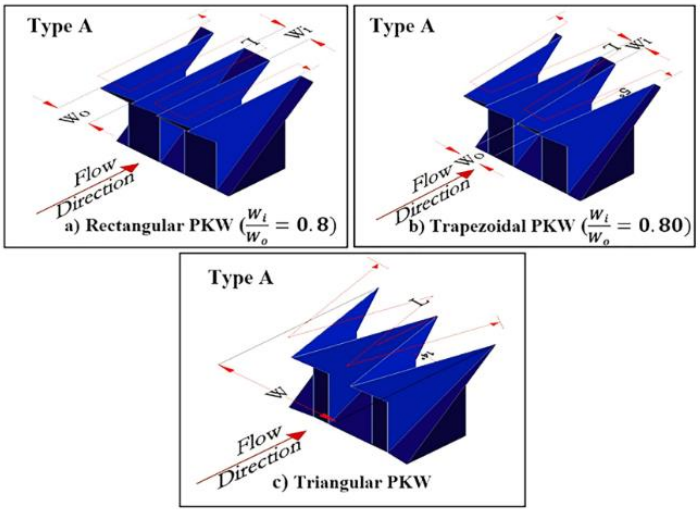

(a) 3D sketch of the studied models.

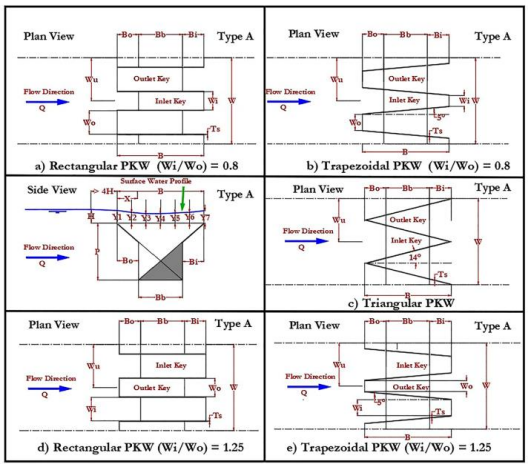

(b) the plan view of the different studied shapes of piano key weir type A

Figure 2.8: Designs of piano key shafts that Amr A. Bekheet et al. (2022.

Source: (Bekheet et al., 2022).

2.3.3 Comparison Studies on the effect of different geometric parameters of the piano key weir (PKW)

The Piano Key Weir geometry involves a large number of geometric parameters. Several experimental studies have been carried out to investigate the main geometric parameters influencing the weir hydraulic efficiency and to define their optimal value to show how the weir height, the keys widths, crest length magnification ratio, and the overhang positions influence the weir discharge capacity.

Lempérière and Jun (2005) examined the impact of (L/W) and found that values in the range of 4 – 7 are advised for design (Lempérière & Jun, 2005).

Similar findings were reported by Hien et al. (2006), who concluded that although an (L/W) number in the range of 5–6 is more efficient and more cost-effective for lower (H/P) ratios, an (L/W)value of 7 is more efficient overall (Hien et al., 2006).

Ouamane A., Lempérière F. (2006) discovered that a value of $(L/W = 8.5)$ provides an increase in the discharge coefficient but only for low values of (H/P), the large (L/W) ratios do not enhance significantly discharge capacity for larger (H/P) values (Ouamane & Lempérière, 2006).

Machiels et al. (2009) conducted a laboratory study of a large model of a type-A piano key weir to determine the flow characteristics at the low head and the effect of the edge thickness and the inclinations of the inlet keys on the discharge capacity. It was concluded that at a low ratio for the height of water above the weir to a height of PKW, $(H/P = 0.05)$ the extrusion remains low; the extrusion becomes free when the ratio (H/P) increases from 0.09 to 0.1 and the ratio for the height of water above the crest weir to the thickness of the edge of weir (H/T) increase 2.4 to 2.6. The flow behaviour differs at the leading edge for the inlet key, where extrusion applies to the edge of the weir walls at $H/P\ 0.16 - 0.17$ and $H/T\ 3.64 - 3.98$ (Machiels et al., 2009).

According to Pralong et al. (2011), the (B_o/B_i) ratio is the parameter that has the least impact on determining the piano key weir discharge capacity. (L/W) and (W_i/W_o) ratios are the most significant parameters for determining the PKW discharge capacity, according to the conclusion that the value of (C_d) rises as (B/P) ,increases (Pralong et al., 2011).

Anderson, (2011) conducted a laboratory study to clarify the effect of some geometric parameters on the discharge efficiency of the piano key weir, tested 13 models for the piano key type-A weir and the labyrinth rectangular weir, using a laboratory channel with a length of 7.4 m, width 0.6 m, and height 0.93 m, The geometric variables included the ratio of the width of the front key to the width of the back key (W_i/W_o). Five values were used for the ratios 0.67, 1.251, 0.8 and 1.5 and the overhang for the inlet key and outlet key and the inclinations of the front and

back keys. The researcher showed that the best discharge efficiency is between 1.5 and 1.25 for (W_i/W_o). The researcher concluded that increasing the overhang of the outlet key and the overhang length of the inlet key increases the discharge efficiency more than the labyrinth weir, where the increases in the overhang of the outlet key at the upstream increase the inlet flow area and wetter perimeter resulting in a reduction of inlet velocities, flow contraction, and energy loss. The researcher also concluded that the effect of slopes on the discharge efficiency is small (Anderson, 2011).

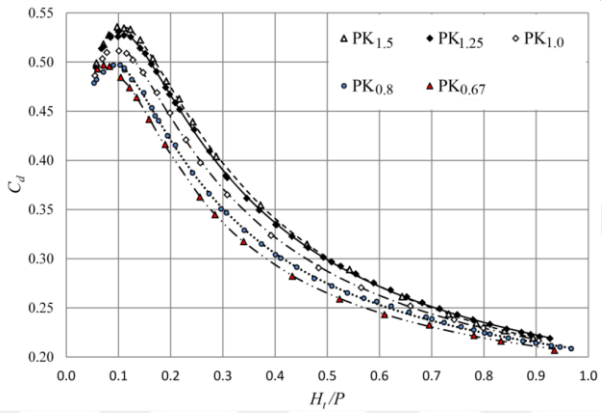

Figure 2.9: Discharge coefficient (C_d) versus H/P data for five inlet key width ratio.
Source: (Anderson, 2011).

The researcher also used the results of the experiments to evaluate the discharge Equation (2.1) that proposed by Lempérière (2009) Which shows the relationship between the discharge and the piezometric head upstream and the relationship between the discharge and the total head upstream as shown in Figure 2.9.

$$q = 4.3h\sqrt{(P-m)} \qquad (2.1)$$

Where (q) is the weir discharge per unit width of spillway channel in cubic meters per second per meter of the weir, and h is the head over the weir crest measured in meters. (No statement is given as to whether this is the piezometric or total head), and Pm, the representative weir height measured in meters.

The researcher concluded that the use of the piezometric head is linear with the performance of the models, which is not generally applicable to PKW, but rather it's specifically applicable to the PKW geometry specified by Lempérière (2009) (e.g., $W_i/W_o = 1.25$, etc.).and concluded that increasing the ratio of the width of the

inlet key to the width of the outlet key (W_i/W_o) increases the weir discharge (Anderson, 2011).

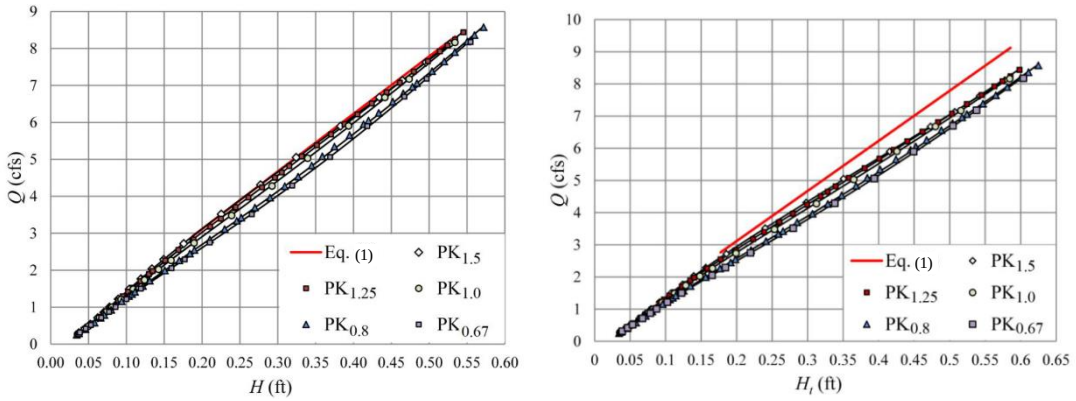

(a) piezometric head (b) total head

Figure 2.10: The relationship between the discharge and the head at upstream.

Source: (Anderson, 2011).

According to Noui and Ouamane, (2011), the discharge coefficient dramatically rises when the (L/W) ratio is increased from 4 -6. For $(Ho/P = 0.2)$ and $(Ho/P = 0.4)$ respectively, this increase is around 15% and 8% (Noui & Ouamane, 2011).

Leite Ribeiro et al. (2011) conducted a study to regulate the effect of the main geometric parameters such as length, width, height, and key flows on the discharge efficiency of the weir of the piano key type -A. He tested 21 models of weir with different dimensions. They concluded that the ratio of the inlet key width to the outlet key width (W_i/W_o) greater than 1 is more efficient, and no significant difference was observed between the values of 1.25, 1.6, and 2. The height of the dam had an important effect on the discharge efficiency. The results showed that the weir with a ratio of (L/W) and a low (Pd/P) rating reduce the discharge efficiency by 15%, found that raising (L/W) from 3 - 7 made a gain of about 50% in discharge coefficient for low heads low (H/P) ratios. But with increasing the ratio of (H/P), this gain tends to decrease (Ribeiro et al., 2011).

Anderson and Tullis (2012) investigated PK weirs and labyrinth weirs with and without slopes. They studied hydraulic behaviour on different weirs, which they categorized into different forms, such as the (PKL, RLRIO, RLRI, RLRO, and RL). The (PKL) model is the piano key weir with both side overhangs, the (RLRIO) model is a rectangular labyrinth weir with a sloped floor in both inlet and outlet key,

the (RLRI) model is a rectangular labyrinth weir with a Sloped floor in the inlet key, the (RLRO) model is a rectangular labyrinth weir with a sloped floor in the outlet key, and the (RL) model is a rectangular labyrinth weir without a sloped floor. The authors concluded that the (PKL) weir shows the highest discharge efficiency compared to others except the (RL) weir, within the range of ($H/P < 0.15$), The highest efficiency of the piano key weir is when (H/P) is between 0.05 – 1 (Anderson et al., 2012b).

Leite Ribeiro, et al. (2012) conducted a study of the hydraulic efficiency of piano key hydraulics. The theoretical data was collected from previous studies of a number of models with the aim of describing the operation of piano key hydraulics. The researchers concluded that the piano key is more efficient with a low head upstream, and its efficiency decreases as the head increases. And the researcher concluded that the ratio of the total length of the edge of the weir to the total width of the weir (L/W) is one of the most influential engineering parameters on the discharge capacity (Ribeiro, Bieri, et al., 2012).

Kabiri-Samani and Javaheri, (2012) conducted a laboratory study to investigate the effect of the geometric parameters of the piano key weir on the discharge coefficient for the case of free and submerged flow for the types of piano key weirs, A, B, C, and D, the geometric parameters included the length, height and width for inlet key and outlet key, upstream and downstream overhang of piano keys, as these parameters were changed for the tested models. The researchers concluded The free flow discharge coefficient (C_d) decreases as the head increases and increases with the increase of the weir height at a fixed head, as the free flow discharge coefficient (C_d) for the total head is affected by the weir height (H/P), and concluded The value of (C_d) increases with increasing (W_i/W_o) and that ($W_i/W_o = 1.22$) gives larger (C_d) values and increasing the ratio does not affect the (C_d) values, also concluded the value of (C_d) increases with the increase in the ratio of the total length edge to the total width of the weir, (L/W), but if the ratio (L/W) is greater than 7, it does not affect the value of, (C_d), concluded (C_d) values by increase an increase the overhang of outlet key more than the overhang of inlet key. The value of (C_d) increases with the increase of the lateral edge length to height ratio (B/P) ,and the influence of large values is small ((Kabiri-samani & Javaheri, 2012).

The Researchers Leite Ribeiro, et al. (2012) conducted a laboratory study on the hydraulics of the piano key weir of a type -A. He used several models of the weir and changed the main geometric parameters such as the length (L), the side length (B), the width of the inlet key (W_i), and the outlet key (W_i/W_o), the height of the inlet key (P_i), the height of the outlet key (P_o), downstream the overhang crest length of the (B_i), upstream the overhang crest length (B_o), and the depth of the channel at the bottom of the weir. The semicircular edge shape and thickness were fixed. Experiments were conducted in a laboratory channel with a length of 40 m, a width of 2 m, a depth of 0.5 m, and a width of the weir of 0.5 m. Parallel longitudinal walls, 3 m long, to limit the flow and make it uniform to the weir. In analyzing the study, the researcher relied on the efficiency of performance (r) discharge the piano key weir into a linear weir discharge with an edge length equal to the weir width at the same head. The researcher found that the main effects of parameters such as the height of the weir (P) and the width of the weir (W) and the small effect of the two leads on the discharge capacity were found. There are also secondary effects of the ratio of the width of the inlet key to the width of the outlet key (W_i/W_o), the ratio of the height of the outlet key to the height of the inlet key (P_o/P_i), the length of the overhang, and the height of the barrier wall on the discharge capacity, although their effect is small, it cannot be neglected (Ribeiro, Bieri, et al., 2012).

Anderson and Tullis (2012) conducted an experimental study to develop an understanding of the effect of geometric parameters on the discharge efficiency of a piano key weir. Nine models of the weir were tested by changing some geometric parameters, such as changing the ratio of the width of the inlet key to the width of the outlet key $(Wi/Wo = 1.5, 1.25, 1, 0.8\ and\ 0.67)$, and the rest of the parameters remained constant. The researcher concluded that it is between 1.25 and 1.5 as it gives the highest value for the discharge efficiency; there is an increase in the discharge efficiency by increasing the height of the piano key weir using the diaphragm wall. This is the result of increasing the size of the inlet and outlet keys (Anderson et al., 2012a).

Erpicum et al. (2021) The ratios of the overhang lengths (B_i/B_o) and key widths are (W_i/W_o) important secondary factors because modifying them results in efficiency increases of around 30% and 20%, respectively (Erpicum et al., 2014).

2.3.4 Studies on the effect of different auxiliary geometric parameters of the piano key weir (PKW)

The impact of auxiliary geometrical factors on the piano key weir's discharge capacity was examined by Li et al. (2020). The Researcher came to the conclusion that the author noticed a 16.8% rise in discharge coefficient (C_d) when the auxiliary geometrical parameters were added compared to when they weren't, and they suggested a discharge coefficient (C_d) equation (Li et al., 2020).

2.3.4.1. Lateral angle slope

In their experimental study of four non-rectangular Type-A piano key weirs, Khassaf and Al-Baghdadi (2015) examined the effects of sidewall angle and sidewall inclination angle on (C_d) and came to the conclusion that raising the sidewall angle from 0 - 5 improves discharge capacity by 4%. However, a sidewall angle increases of more than 10° results in an 18% reduction in discharge capacity (Khassaf & Al-Baghdadi, 2015).

2.3.4.2 Parapet walls

On the crest of the PKW, there is a rather short vertical wall known as a parapet wall. Its existence has been demonstrated to be advantageous because it heightens the weir and enhances the loudness of the individual keys.

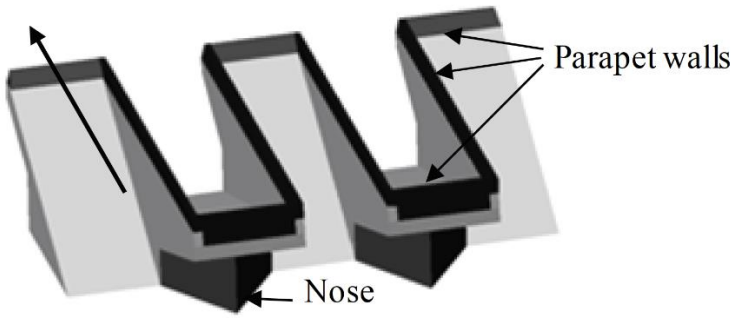

Figure 2.11: Explains the location of parapet walls and nose on PKW.

Source: (Pralong et al., 2011).

As part of a PK weir model study of the Etroit dam, Ribeiro et al. (2009) assessed the effects of adding a parapet wall on top of the standard PK weir crest (i.e., the PK weir height was raised without changing the length of the overhangs). According to the study, compared to the identical PK weir design without the parapet wall, increasing the height of the PK weir by 12.3% with the vertical parapet wall

about 1 m in the prototype boosted discharge efficiency by 15% (Ribeiro et al., 2009).

To further understand the impact of employing the parapet wall, the researcher Machiels et al. (2013) carried out a laboratory study. The height of the weir and the slopes of the keys were altered using models with or without the parapet wall. The study demonstrated that adding a parapet wall increases the weir's overall height, increasing the discharge efficiency by increasing the size of the leading keys, which reduces longitudinal velocity by increasing discharge from the side edges (Machiels et al., 2013).

2.3.4.3 Crest shape

Efficiency of discharge has been demonstrated to be influenced by crest form, in addition to the research done by Barcouda et al., (2006), Riberio et al. (2007) evaluated three different PKW crest geometries: An upstream quarter round, a downstream quarter round, and a flat crest. The results showed that the upstream quarter round is the most effective, but the relative change in discharge efficiency, specific to each crest shape, was not documented (Barcouda et al., 2006; Ribeiro et al., 2007).

The shape of the crest has a fairly significant role to play on the efficiency of any spillway or weir, especially at low water levels. when compared the flat-top crests with improved crest shapes (half-round) significantly boost discharge efficiency at low heads, as (H_t) grows the efficiency advantages rapidly diminish (Anderson et al., 2012a).

2.3.4.4 Noses

The PKW's entrance became more hydraulically effective because of the installation of noses beneath the upstream apex overhangs due to decreased flow contraction, energy loss, and potentially altered critical flow section placement, and discharge efficiency increased as well, as shown in Figure 2.10 (Anderson et al., 2012a).

According to Philips and Lesleighter (2013), an interesting design element is the insertion of a tapered nose beneath the upstream outlet key overhang to direct flow to the inlet keys on either side of it. Its presence results in smoother flow lines,

reduced energy losses, and less vortex shedding, all of which boost the discharge efficiency of the PKW (Philips & Lesleighter, 2013).

The use of Noses beneath upstream overhangs with enhanced hydraulic forms (e.g., rounded, triangular, etc.) results in discharge efficiency gains of 10 and 7%, respectively, according to (Ouamane & Lempérière, 2006).

2.3.4.5 Number of PKW units

Research on the hydraulic behavior of the piano key weir was undertaken by Leite Ribeira et al. (2012) utilizing nine versions of the type-A of PKW and altering the Number of PKW units with fixed (W_i/W_o), (L/W). The researcher came to the conclusion that the number of PKW units had no impact on the discharge from the weir on the piano key (Pfister et al., 2012).

2.4 Available Equations for the Coefficient of Discharge (C_d) for the Piano Key Weir

According to previous studies using scaled physical models, the hydraulics of piano key weir PKW depend on a number of geometrical parameters, including the weir height (P), the total weir crest length (L), the lateral weir crest length (b), the channel or transverse width (W), the upstream and downstream overhang key lengths (B_i) and (B_o), and the up- and downstream key widths (W_i) and (W_o).

According to Ribeiro et al. (2012), both primary and secondary factors have a considerable impact on discharge capacity. The weir height (P) and total weir width (W) are referred to as the important factors. The inlet-to-outlet key width ratio (Wi/Wo) and the height ratio (Pi/Po) are two examples of secondary parameters (Ribeiro, Pfister, et al., 2012).

According to Machiels et al. (2014), the most important affecting factors are the weir heights (P), the ratio of the inlet to outlet key width (W_i/W_o), and the overhang ratio (B_i/B_o) (Machiels et al., 2014).

Kabiri-Samani and Javaheri. (2012) carried out an experimental study on scaled physical model PK weirs types A, B, and C within a particular discharge range of 0.025 to 0.175 m^3/s. A sharply crested PK weir was the subject of the

researcher's proposed free and submerged flow equation (Kabiri-samani & Javaheri, 2012).

The general discharge equation for a rectangular sharp-crested weir is (Kabiri-samani & Javaheri, 2012).

$$\boldsymbol{Q = \frac{2}{3} C_d \sqrt{2g} W H^{3/2}} \qquad \textbf{(2.2)}$$

Where (Q) is the discharge flow and (C_d) the discharge coefficient, (W) is the channel width, (g) is the acceleration due to gravity, and (H) is the upstream head on the weir.

Because the geometry of the piano key weir is complex and due to the large number of geometric parameters in it, other equations were derived, which the researchers concluded and relied on in calculating the discharge coefficient and performance efficiency. The researchers set conditions and limitations for them in terms of geometric parameters and flow conditions (free flow, partially submerged, and completely submerged) and the state of the water (turbulent, undisturbed, the amount of flow, and its speed) and the properties of the fluid (viscosity, surface tension, and mass density), all according to the case being investigated.

Table 2.3 has been prepared for some of these equations which (Bhukya et al., 2022) have included in their review of recent developments.

Table 2.3: The equations mentioned by Bhukya, et al. (2022) for the discharge coefficient in the review of recent developments.

Kabiri-Samani and Javaheri (2012)	$C_d = 0.212\left(\frac{H}{P}\right)^{-0.657}\left(\frac{W_i}{W_o}\right)^{0.426}\left(\frac{B}{P}\right)^{0.306} e^{1.504\left(\frac{B_o}{B}\right)+0.093\left(\frac{B_i}{B}\right)} + 0.606$ Given parameter ranges are $(0.1 \le H/P \le 0.6), (2.5 \le L/W \le 7)$, $(1 \le (B/P), \le 2.5), (0.33 \le W_i/W_o \le 1.22), (0 \le B_i/B \le 0.26), (0 \le Bo/B \le 0.26)$. Free flow over a PK weir
Kabiri-Samani and Javaheri (2012)	$C_s = \left\{1 - 0.858\left(\frac{H_D}{H}\right) + 2.628\left(\frac{H_D}{H}\right)^2 - 2.489\left(\frac{H_D}{H}\right)^3\right\}\left(\frac{L}{Y}\right)^{0.055}$ where Cs is the discharge coefficient for submerged flow. $2.5 \le L/W \le 6, HD/H > 0.6$ (HD is head over the weir crest on the downstream side)
Crookston et al. (2013)	$C_D = \left[\frac{1}{a_1 + b_1\left(\frac{H}{P}\right) + \frac{C_1}{\left(\frac{H}{P}\right)}} + d_1\right]\left(\frac{L}{W}\right)$ where a1, b1, c1, and d1 are constants given by the author for the different inlet to outlet key ratios. For the $(W_i/W_o = 1)$, (a=0.5091, b=10.29, c=0.09712 and d=0.1164).

Table 2.3: (Cont.) The equations mentioned by Bhukya, et al. (2022) for the discharge coefficient in the review of recent developments.

Laugier. (2007)	$C_D = 0.63 \times r$ Where: $r = 1 + 0.24\left(\frac{(L-W)P_i}{WH}\right)^{0.9}(WPW_iW_o)$ $W = \left(\frac{W_i}{W_o}\right)^{0.05}$ and $P = \left(\frac{P_i}{P_o}\right)^{0.25}$ with the free flow condition
Cicero and Delisle. (2013)	$C_D = \frac{3}{2}\left[a_2 + a_3\left(\frac{H}{P}\right)^2 + a_4\left(\frac{H}{P}\right)^2 + a_5\left(\frac{H}{P}\right)^3 + a_6\left(\frac{H}{P}\right)^4\right]$ With the submerged flow. Where: Where (a2), (a3), (a4), (a5), and (a6) are coefficients of Equation, for type A PK weir, ranges of parameters and coefficients are $(0.1 < H/P < 0.72)$ and $(a2 = 1.63), (a3 = 0.590, (a4 = -11.56), (a\ 5 = 21.72)$ and $(a6 = -12.46)$
Al-Baghdadi and Khassaf. (2018)	$C_D = a_7\left(\frac{H}{P}\right)^8$ Where: (a7) and (a8) are the constants, and the values of these constants are given in Table 2.4 with constant values of $(W_i/W_o = 1.25), (B/P = 2.4), (B_i\ /B = 0.25), (B_o\ / B = 0.25)$.
Al-Baghdadi and Khassaf. (2018)	$C_D = 0.6793\left(\frac{H}{P}\right)^{-0.4421}\left(\frac{L}{W}\right)^{0.4354}$ for $(3 \le L/W \le 7)$ and $(0.15 \le H/P \le 1.95)$.
Al-Shukur and Al-Khafaji. (2018)	$C_D = 0.8816\left[\frac{H}{P}\right]^{-0.8539}\left[\frac{\mathrm{L}}{\mathrm{W}}\right]^{0.3619}\left[\frac{W_i}{W_o}\right]^{0.0802} e^{\left(0.0527\left(\frac{\mathrm{B}}{P}\right)-1.2182\left(\frac{P_i}{P_o}\right)\right)} + 0.5346$ For type B PK weir geometry $(3 \le L/W \le 7), (0.5 \le W_i\ /W_o \le 2), (1.5 \le (B/P), \le 5), \&\ (0.7 \le P_i\ /P_o \le 2)$
Li et al. (2020)	$C_D = \left[a_9 + a_{10}\left(\frac{H}{P}\right) + a_{11}\left(\frac{H}{P}\right)^2 + a_{12}\left(\frac{H}{P}\right)^3 + a_{13}\left(\frac{H}{P}\right)^4\right]$ for type A PK weir with auxiliary geometries, such as nose and parapet wall. Where: (a9), (a10), (a11), (a12), and (a13) are the coefficients of corresponding fitting formula values shown in Table 2.5.
Guo et al., (2018)	$C_D = 0.285\left[\frac{H}{P}\right]^{-0.465}\left[\frac{\mathrm{L}}{\mathrm{W}}\right]^{0.45}\left[\frac{W_i}{W_o}\right]^{0.05}\left(\frac{\mathrm{B}}{P}\right)^{0.1} + 0.1$ the geometrical parameters ranges of $(H/P > 0.1), (2.5 < L/W < 8.5), (0 < W_i/W < 2.45), (1 < (B/P), < 6)$
Kumar et al. (2020)	For rectangilar PK weirs: $H/P \le 0.249$ and $L/W \le 5.5$ $C_D = -4.0038\ H/P + 0.338\ L/W + 0.569$ $H/P \le 0.249$ and $L/W \le 5.5$ $C_D = -5.1737\ H/P + 0.285\ L/W + 1.185$ $H/P \le 0.249$ $C_D = -2.4112\ H/P + 0.1944\ L/W + 1.03$ For trapezoidal PK weirs: $H/P \le 0.249$ and $L/W \le 5.5$ $C_D = -4.8713\ H/P + 0.3707\ L/W + 0.653$ $H/P \le 0.249$ and $L/W \le 5.5$ $C_D = -6.3375\ H/P + 0.3114\ L/W + 1.368$ $H/P \le 0.249$ $C_D = -2.7319\ H/P + 0.193\ L/W + 1.98$

Table 2.3: (Cont.) The equations mentioned by Bhukya, et al. (2022) for the discharge coefficient in the review of recent developments.

Kumar et al. (2020)	For rectangilar PK weirs: $H/P \leq 0.249 \; and \; L/W \leq 5.5$ $C_D = -4.0038 \; H/P + 0.338 \; L/W + 0.569$ $H/P \leq 0.249 \; and \; L/W \leq 5.5$ $C_D = -5.1737 \; H/P + 0.285 \; L/W + 1.185$ $H/P \leq 0.249$ $C_D = -2.4112 \; H/P + 0.1944 \; L/W + 1.03$ For trapezoidal PK weirs: $H/P \leq 0.249 \; and \; L/W \leq 5.5$ $C_D = -4.8713 \; H/P + 0.3707 \; L/W + 0.653$ $H/P \leq 0.249 \; and \; L/W \leq 5.5$ $C_D = -6.3375 \; H/P + 0.3114 \; L/W + 1.368$ $H/P \leq 0.249$ $C_D = -2.7319 \; H/P + 0.193 \; L/W + 1.98$
Singhal et al. (2011)	$For \; L/W = 3.56$ $C_D = 0.6858 \left(\frac{H}{P}\right)^{-0.305}$ $For \; L/W = 4.84$ $C_D = 0.667 \left(\frac{H}{P}\right)^{-0.3703}$ $For \; L/W = 7.4$ $C_D = 0.688 \left(\frac{H}{P}\right)^{-0.4673}$ For (type-A) piano key weir.
Khassaf and Al-Baghdadi. (2015)	$C_D = a_{14} \left(\frac{H}{P}\right)^{a_{15}}$ study on the PK weir with a change in sidewall angle (α) and sidewall inclination angle (β). coefficients of equation a14 and a15 which are given in Table 2.6.

Table 2.4: Values of coefficients (a) and (b) for different (L/W) ratios for Equation of Al-Baghdadi and Khassaf. (2018).

L/W	a_7	a_8	R^2
3	1.1197	-0.300	0.9908
4	1.2566	-0.433	0.9982
5	1.3042	-0.479	0.9986
6	1.4088	-0.496	0.9972
7	1.5263	-0.469	0.9883

Source: (Bhukya et al., 2022).

Table 2.5: Coefficients of corresponding fitting formulas for equation of (Li et al., 2020).

a_9	a_{10}	a_{11}	a_{12}	a_{13}	H/P	R^2
2.4	-4.31	4.64	-2.46	0.51	0.15-1.46	0.998

Source: (Bhukya et al., 2022).

Table 2.6: The coefficients for equation of Khassaf and Al-Baghdadi. (2015).

Model	a_{14}	a_{15}	H/P	R^2
M	1.3042	-0.479	0.25-0.71	0.9986
α_5	1.3161	-0.448	0.23-0.63	0.9975
α_{10}	1.1432	-0.458	0.21-0.62	0.9972
β_5	1.3009	-0.499	0.25-0.71	0.9937
β_{10}	1.2213	-0.384	0.25-0.8	0.9768

Source: (Bhukya et al., 2022).

2.5 Piano Key Weir's Hydraulic Conduct

To understand the behaviour of flow through the weir of a piano key. Machiels et al. (2010), have done a combined experimental and numerical analysis at the Laboratory of Structures Hydraulics at the University of Liege. The experiments seek to determine the streamlines above the weir and in the inlets by monitoring the colouring agent. The discharge capacity of the PKW has been connected to the streamlines' subsequent analysis; determining the streamlines on the PKW based on the upstream head was the major goal of the test. To accomplish this, 12 various heads, ranging in (H/P) from 0.05 to 0.45, have been investigated. The streamlines are quite evenly dispersed throughout the whole weir crest at low heads, $(H/P < 0.2)$ as shown in Figure 2.12 & Figure 2.15. The bottom stream mostly supplies the inlet key's downstream crest, and the surface stream supplies the majority of the outlet key's upstream crest of the discharge. The lateral crest is supplied in its downstream part by streams coming in front of the inlet key and in its upstream part by streams coming in front of the outlet key under the crest level (Machiels et al., 2010).

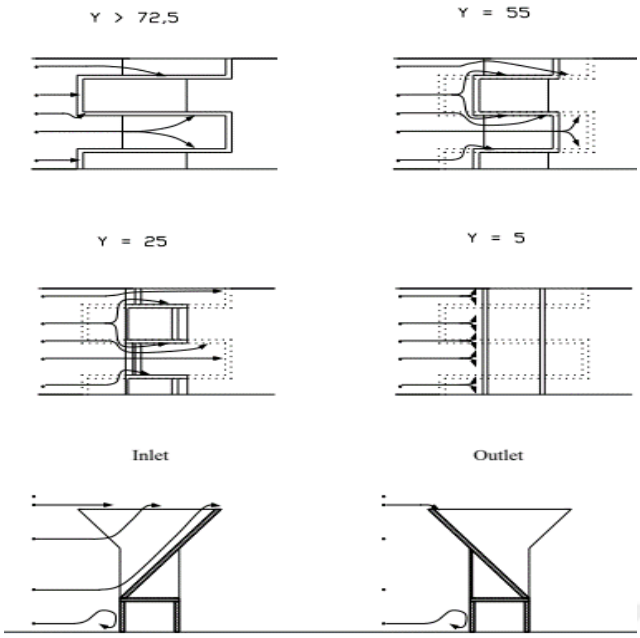

Figure 2.12: Stream lines for low heads (H/P < 0.2).

Source: (Machiels et al., 2010).

The streamline distribution is less suitable, when ($H/P > 0.2$) as shown in Figure 2.13 & Figure 2.15. The bottom stream and streams entering in front of the inlet key with significant velocity always supply a considerable portion of the downstream crest of the inlet key. The surface stream continues to feed the outlet key's upstream crest; streams entering in front of the outlet key and below the crest level do not adequately supply the lateral crest (Machiels et al., 2010).

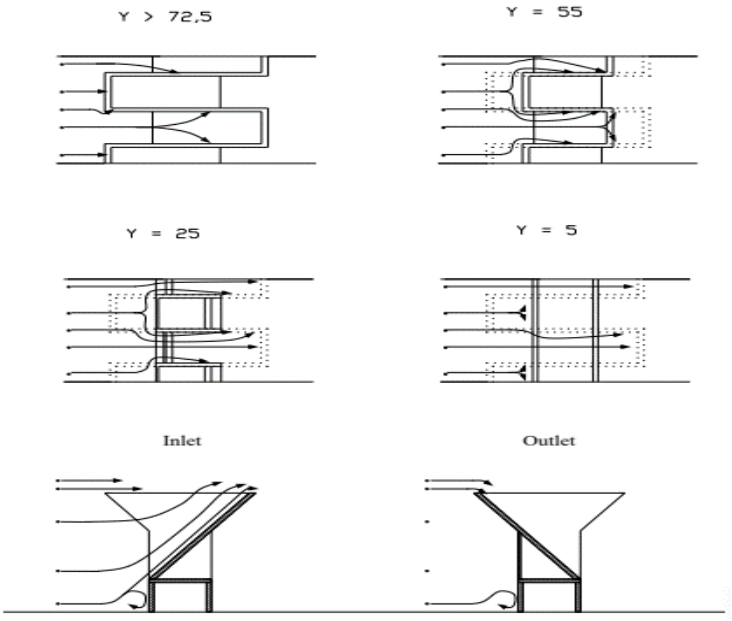

Figure 2.13: Stream lines for high heads ($H/P > 0.2$).

Source: (Machiels et al., 2010).

The transition between the mainstream lines sketch corresponds to the transition between a flat-free surface line to a ripple-free surface line along the PKW, as shown in Figure 2.14.

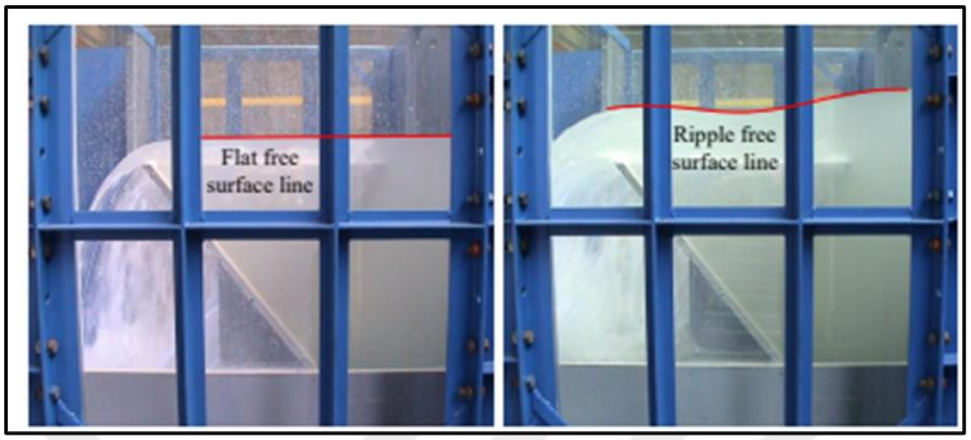

Figure 2.14: Surface line profiles for low and high heads ($H/P = 0.15\ and\ 0.35$).

Source: (Machiels et al., 2010).

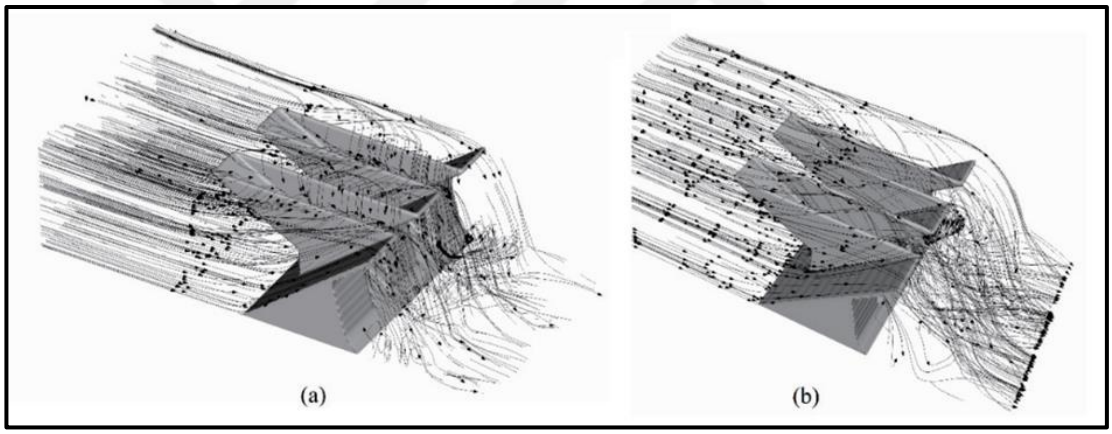

Figure 2.15: 3D sketch of streamlines for (a) low head ($H/P < 0.2$), (b) high head.

Source: (Tuan & Hiramatsu, 2020) .

Analyzing the streamlines distribution for high heads might help to identify a potential reason for this decline in efficiency. Due to the downstream flow's inertia, the downstream crest of the intake is oversupplied for these heads. This portion of the PKW is reached by more streamlines than by low heads.

The same longitudinal flow inertia causes the lateral crest to be undersupplied. Less frequent and more widely spaced streamlines can be found along this crest. The outlet's upstream crest receives the same amount of water for both high and low heads with the same streamlines. The entrance slope and the resulting fluctuations in the water depths cause a critical section to occur when the free surface

ripples. The crucial section along the weir crests shifts upstream with rising heads, reducing the weir's effective length and, thus, and then reducing PKW's discharge coefficient (Machiels et al., 2010).

2.6 Energy Dissipation due the Piano Key Weir

PKWs dissipate energy very efficiently, especially when the relative total upstream head is low, as PK weirs placed above stepped spillways provide quicker effective energy dissipation than ogee weirs for equivalent conditions, the PKW's shape substantially influences relative residual energy or energy dissipation at the weir's base (Singh & Kumar, 2023).

A portion of the energy dissipation comes from flow entering the structure beneath the upstream overhangs, with the front perpendicular faces of the PKW. Also, the nappes are thought of as opposing planar jets that mix, create turbulence, boost aeration, and form jets that travel downstream on a path that resembles the outlet cycle ramps. These jets enlarge and engage with the tailwater after they collided with the PK weir's toe (Eslinger & Crookston, 2020).

Laboratory tests have, however, determined that the residual energy in the flow on the steps downstream of a PKW is actually higher than if it were downstream of a normal ogee crest (i.e. the energy dissipation is less), The suspected reason for this is that the PKW focusses flow into jets which exit the outlet key which does not spread evenly over the whole width of the channel. When PKW is placed on a gravity dam with a stepped discharge chute, a PK weir is able to induce fully aerated flow on the steps much sooner than a standard ogee can (Silvestri et al., 2013).

Also, Despite the positive benefits of piano key weirs, the problems that they may cause cannot be overlooked, and among these problems is the problem of erosion at the back of the weirs, including the piano key weir. An area with a low level leads to the movement of bed materials at the back of the weir away from its original location and then the formation of pits, which in turn affects the stability of the hydraulic installations, causing weakness in the area and may lead in the future to its collapse and complete failure (Al-Hafith & Noori, 2007).

Consequently, Designing and constructing energy-efficient hydraulic structures is essential to preventing scouring at the downstream ends of the structures and maximizing energy dissipation at the base of the weir. Like labyrinth weirs, PK dissipate some energy, which might be advantageous in new and rehabilitation projects because the rate of dissipation is nonlinear and highest at low heads (Eslinger & Crookston, 2020).

Figure 2.16: Treating the downstream of PKW to protect against erosion, (Van Phong Dam) in Vietnam.

Source: (Yazdi et al., 2022).

In terms of scour downstream of a PKW in a riverine setting, physical model studies have shown that the scour depth and scour hole volume are not only related to the sediment characteristics, the discharge, the head differential and the tailwater depth but also to the PKW's downstream overhang length (B_i) (Jüstrich et al., 2016).

2.6.1 Previous studies on energy dissipation

There have been many hydraulic studies regarding discharge capacity for nonlinear weirs but comparatively few studies on the subject of energy dissipation. Hydraulic studies on energy dissipation for the general case of free overfalls and vertical drops include, among others.

The study of energy dissipation and flow characteristics downstream of trapezoidal labyrinth dams began at the National Civil Engineering Laboratory (LNEC) through the work Magalhes, A.P.; Lorena,1994 (Eslinger & Crookston, 2020).

After about ten years, Lopes et al. (2006) and Lopes et al. (2011) analyzed their own experimental data of Magalhes, A.P.; Lorena (1994). and estimated the relative residual energy $(H_i\ /H_o)$ downstream of trapezoidal labyrinth weirs. (H_o) is

the upstream specific energy, $(H_o = H_i + P)$, (P) is weir height, and (H_i) is the downstream specific energy. In order to forecast (H_i / H_o), an empirical equation was fitted to the data and compared with energy dissipation downstream of vertical dips. The researchers concluded that it grows nonlinearly as (H_o) increases at the base of labyrinth weirs. Labyrinth weirs were also demonstrated to waste more energy than vertical drops for a given (H_o), in part because of the clashing nappes in the downstream cycles. (Lopes et al., 2006, 2011).

Six models were developed and tested by Ho Ta Khanh et al. (2011) to dissipate flow energy, including slab baffle blocks, natural rock protection, shifting ski jumps, and deflector walls, where PKW with stepped spillways and a short stilling basin could be appropriate for medium- to large dams, and PKW with a short stilling basin could be sufficient for small dam projects to dissipate energy (Khanh et al., 2011).

Bier et al., (2011) used a PK weir, a winding stepped channel, and an intermediate stilling basin to accomplish up to (90%) energy dissipation for (Gloriettes dam in the French Pyrenees) (Bieri et al., 2011).

According to Ho Ta Khanh et al. (2011), In general, the piano key weirs put on small gravity dams with short stilling basins able to dissipate energy effectively, but when installed on medium to large gravity dams, PK weirs may work best when combined with a short stilling basin and a stepped spillway (Khanh et al., 2011).

According to Erpicum et al. (2011), given identical circumstances, PK weirs situated above stepped spillways offer faster effective energy dissipation than ogee weirs. They also suggested conducting more testing with a smaller stepped spillway (Erpicum et al., 2011).

In order to aid in the optimization of stilling basin configurations, energy dissipation and flow characteristics downstream of rectangular labyrinth weirs were examined at (Bundesanstalt für Wasserbau (BAW) in Germany, 2018) for and $(0.1 < \frac{H}{P} < 0.21)$ and $(W_i / W_o = 1.0)$ over a constrained range. They observed that the energy dissipation offered by rectangular labyrinth weirs and that of trapezoidal labyrinth weirs are pretty comparable (Merkel et al., 2018).

Al-Shukur and Al-Khafaji (2018) examined how piano key weir slopes affected energy dissipation and found that dissipation decreased with decreasing

slope. The hydraulic jump's distance downstream from the toe of the piano key weir was used to calculate the magnitude of energy dissipation. They made the assumption that as the distance to the hydraulic leap gets longer, energy dissipation gets smaller (Al-Shukur & Al-Khafaji, 2018).

Eslinger and Crookston (2020) conducted a thorough analysis of energy dissipation over type-A PKWs using various relative width ratios. The type-A PKW was found to have a higher energy dissipation than its alternatives for $(H/P \leq 0.28)$ which indicates that it has a higher dissipating efficiency than those alternatives. They suggested two empirical prediction equations for estimating the residual energy of the downstream piano key weir. A PKW's energy dissipation appears to be influenced by the parameter (W_i/W_o) in the following range: $(0.2 \leq H/P \leq 0.8)$. As (W_i/W_o) rises, the hydraulic efficiency rises as well, leading to less energy being dissipated. Energy dissipation appears to be rather consistent, regardless of the (W_i/W_o) parameter, for values of $(H/P \leq 0.2)$ and $(H/P \leq 0.28)$ (Eslinger & Crookston, 2020).

Hooman Farhadi et al. (2022) studied in experimental the influence of the weir's height, arrangement and height of the baffle blocks located on the outlet keys slopes on the energy dissipation were investigated. were used an Arced Piano Key Weir with a 53 degrees central angle (APKW-53) and a Trapezoidal Piano Key Weir TPKW with two height ratios of (P/W_u) equal to 0.9 and 1.2 where Wu the Width of unit of weir, (m), (P) the height of weir, (m), Three height ratios of (h/W_u) equal to 0.06, 0.12 and 0.18 and two A and B-arrangements were selected for the baffle blocks. The most important findings of this study are in all models; the relative energy dissipation decreases when the discharge increases, and the relative energy dissipation at the $(P/W_u = 0.9)$ are lesser than at $(P/W_u = 1.2)$ at a constant (H/P), occurring because of the lesser outlet key slopes of the weir at the $(P/W_u = 0.9)$ (Farhadi et al., 2023).

2.7 Screen Walls

The use of dams, weirs, and other water-powered constructions ranges from irrigation to flood control to electricity production. Since the water is moving at a

high and supercritical velocity downstream of these structures, this might cause the sides and bottom of channels and rivers to be scourged.

Because of this, hydraulics researchers and engineers focused on using hydraulic structures that create hydraulic jumps to reduce and dissipate the kinetic intensity of the flow downstream of the facilities and make the flow velocity subcritical. This is in contrast to other methods for dissipating Stream Energy, such as stilling basins, Slanted and stepped walls, roller buckets, free jets, and hydraulic jumps (Chow, 1959).

In recent years, a different technique for releasing excess energy in water downstream of small hydraulic structures has been developed, and it involves the use of screen walls.

Screen walls are porous vertical baffles that are used to distribute flow energy downstream of tiny hydraulic structures that are close to the flow domain in order to lessen the scour caused by the high flow rates (Balkiş, 2004).

These walls are more advantageous when the bed materials are soft since they are more susceptible to scouring. Different forms, including round, square, hexagonal, and others, are present. Additionally, the distances between them and the wall vary.

2.7.1 Previous studies on screen wall

Previous studies of screen walls included porosity, shapes of screens, numbers, locations, thickness, degree of inclination, size of holes inside them, and the shape of these holes and the effect of these screens on the hydraulic performance of the flow in terms of reducing the head of the flow in the upstream and dissipating energy and dispersing it in the downstream.

Bozkus et al. (2006) conducted a laboratory analysis to find the effect of vertical and inclined triangular screen walls below small hydraulic structures on energy dissipation. The important variables were identified, including the depth of flow, the thickness of the screen wall, the location of the screen wall based from the hydraulic design, and the Froude number which was measured upstream of the flow. The Froude number had values between 7.5 and 25.5. The results of each test conducted on the triangular screen demonstrated that for a given Froude number,

energy dissipation is always significantly greater than that of a classical full jump. In the range studied, the relative screen thickness (t/d) has no significant effect on the system performance, screen performance, and system efficiency. The system's efficiency and performance are not significantly impacted by the relative screen position (X/d), and the analysis's findings demonstrated that, for the same Froude number values, the vertical and angled triangular screen walls greatly lower flow energy when compared to the traditional hydraulic jump. There is a general trend that as the Froude number increases, system performance rises, and system efficiency falls. All screen configurations examined showed that for the screen walls' ability to dissipate energy, none of them significantly outperformed the others, and none of them significantly outperformed the others. Because it is less expensive and simpler to construct, it is advised that the vertical screen be used in actual practice (Bozkuş et al., 2006).

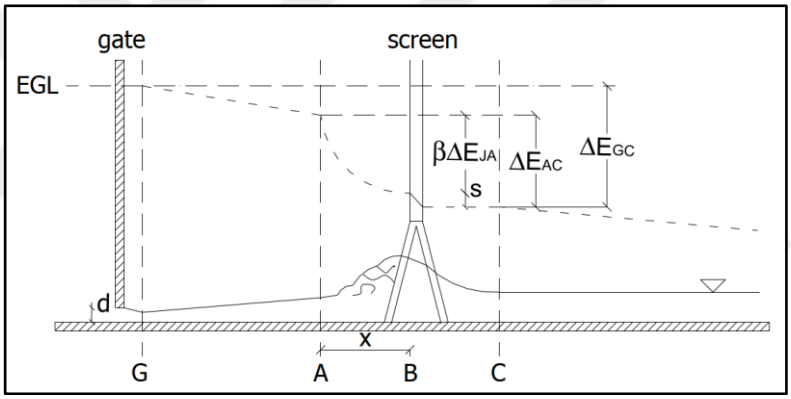

Figure 2.17: Energy Dissipation by Triangular Screens.

Source: (Bozkuş et al., 2006).

V. Aslankara (2007) conducted an experimental study and analysis to determine the impacts of tailwater depth and the use of numerous screen walls on the effectiveness of the screen walls in terms of energy dissipation. The trials use one double screen wall and two double screen configurations with vertically positioned double screen walls with a porosity of 40%. The study's Froude number coverage ranges from 5.0 to 22.5. The gate opening, which simulates a hydraulic structure, is modified at heights of 2 cm and 3 cm in line with the dimensional analysis and (h_t/d) relationships. This research study showed the triangle screen's ability to dissipate energy more efficiently than a traditional complete leap for the same Froude number in every test. However, triangular displays do not outperform previously researched inclined or vertically positioned screens. The system

performance and efficiency are not significantly impacted by the relative screen location, (X/d) There is no discernible difference between the system performance, screen performance, and system efficiency depending on the relative screen thickness. (t/d). Additionally, considering that it is less expensive and simpler to construct, it is advised that the vertical screen be employed in practice as shown in Figure 2.17& Figure 2.18 (Aslankara, 2007).

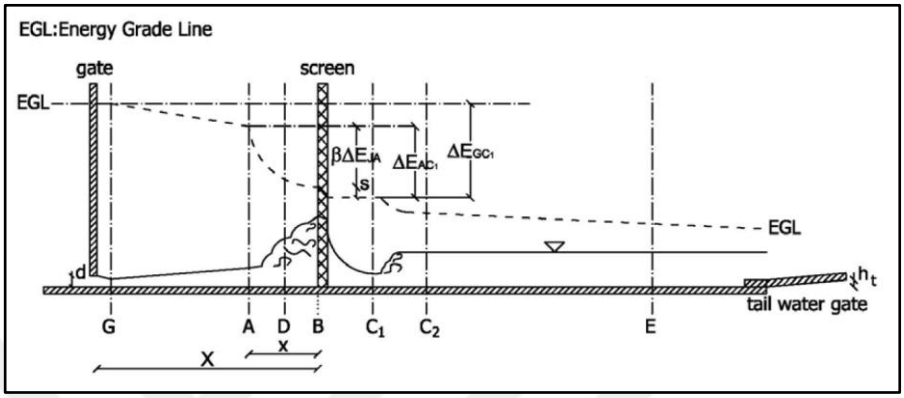

Figure 2.18: General sketch to increase energy loss of one double arrangement screen

Source: (Aslankara, 2007).

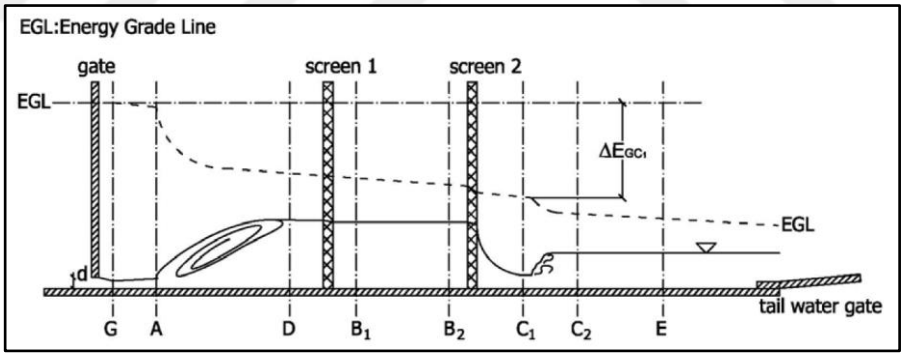

Figure 2.19: General illustration to increase energy loss of tow arrangement dual screen.

Source: (Aslankara, 2007).

Bozkus, P. Akir, and A. M. (2007) conducted a series of tests in a horizontal rectangular laboratory channel measuring 7.5 m in length, 29 cm in width, and 70 cm in depth was used to analyze the energy dissipation of the flow downstream of small water-powered facilities. Under the channel, a sluice gate directs the water toward a screen wall that is positioned perpendicular to the direction of the flow. The studies encompassed a range of screen sites up to 100 times the undisturbed upstream depth, porosities between 20% and 60%, and Froude values between 5.0 and 18.0. The

results of the data analysis led to the following conclusions: a main characteristic of screen walls as energy dissipators is that their energy dissipation performance improves with an increase in Froude number. The investigations revealed that 40% porosity offers typically stronger energy dissipation. Double screens are preferred over single screens because they could be structurally stronger. The efficiency of the system declines as the Froude number rises. Double screens dissipate somewhat more energy than single screens, as shown in Figure 2.20 (Bozkus et al., 2007).

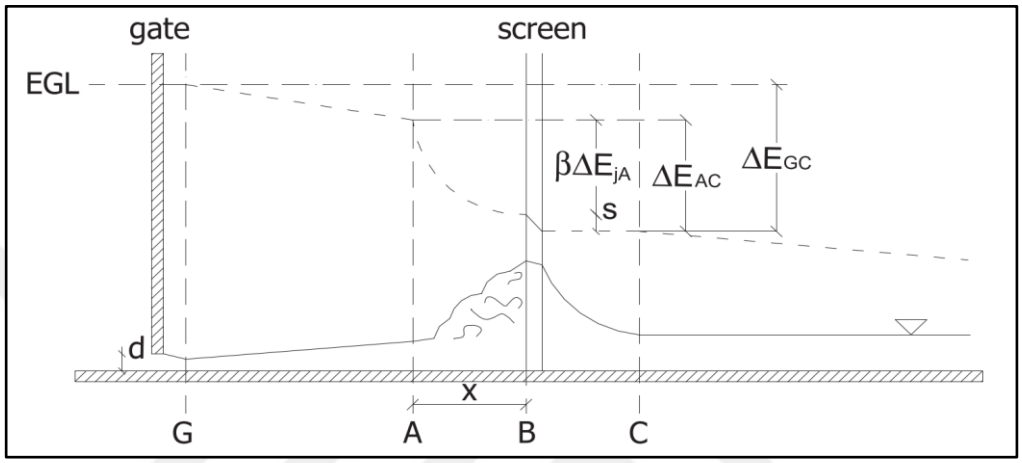

Figure 2.20: General sketch showing the flow pattern and energy-loss definitions. EGL, energy grade line.

Source: (Bozkus et al., 2007).

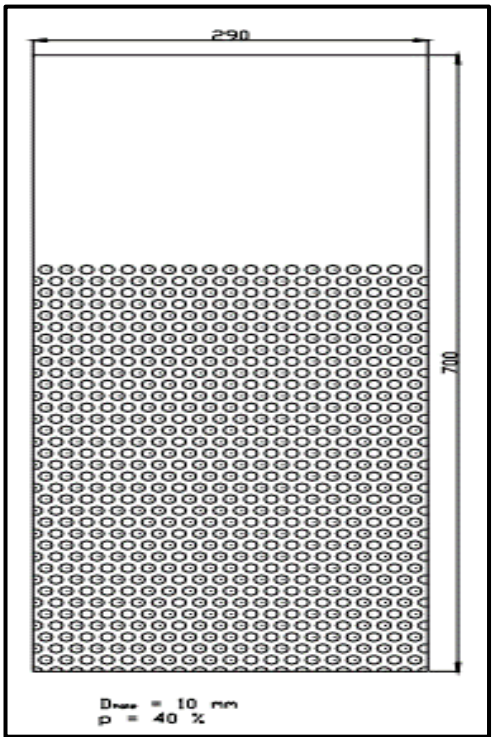

Figure 2.21: Screen wall with a porosity of 40%.

Source: (Bozkus et al., 2007).

R. Ghufran (2011) conducted a laboratory experiment to investigate the scour downstream screen walls, which once served as energy dissipators. It comprises research on the impact of screen wall thickness (t) and hole diameter φ on scour operation. A concrete tube was used to conduct 60 trials with one type of crushed stone. Five different discharges were employed, two different gate opening heights of 4 and 5 cm, three different screen opening diameters of 0.8, 1.2, and 1.6 cm, two different screen wall thicknesses of 0.4 and 0.8 cm, and a fixed 40% porosity. The results revealed that, in contrast to other sizes, screen wall holes with a diameter of 1.2 cm offer the smallest depth of scour holes. This was particularly evident when the thickness of the screen wall was 0.8 cm (Alrahhawi & Hayawi, 2011).

Sh. Jalil, A. Yaseen, and H. Mahmoud (2013) investigated the impact of hole shapes in the screen wall on the effectiveness of energy dissipation in an experimental investigation conducted in a laboratory flume. On-screen walls are circular, square, and hexagonal, with a set porosity of 40%. Three holes of various shapes were employed for each model, and the screen walls were fastened at a distance that was 80 and 120 times the opening of the gate. It was discovered that Fr is the main dimensionless parameter significantly affecting energy dissipated, with the other dimensionless parameters having less impact. Screens can be used to stop extremely critical flows, and some kinetic energy is lost when the flow passes through the gaps in the screens. The study came to the conclusion that three screens with various aperture shapes and dimensions waste more energy than traditional hydraulic systems. With the Froude number upstream rises, a part of energy dissipation increases. The proportion of energy dissipation is too tiny to be affected by relative distance (X/D), opening shape, and dimensions. The proportion of energy dissipation decreases as the length of the hexagonal aperture h in the screen increases (Jalil et al., 2013).

M. Zayed et al. (2018) used a triangle V-shaped screen wall with various angles, blockage ratios, and circular bars in the research's laboratory study to improve the performance of standard screen walls, which are susceptible to blockage opening difficulties and have negative economic and environmental effects. Blockage ratios and costs that are verified using a physical model were also used in the research. The analysis's findings demonstrated that, as compared to a conventional screen, a triangular screen with a 90° angle and circular bars reduces

the head loss coefficient. Using a low-angle screen reduces the head loss coefficient. As the blockage ratio and flow discharge rise, the head loss coefficient of screen walls does as well (Zayed et al., 2018).

S. Elaswad and colleagues (2021) conducted a study of the effect varying screen widths on the properties of submerged hydraulic jumps in a 0.30-meter-wide, 0.468-meter-deep, and 15.6-meter-long channel. The effect of passing flow over changing screen area on the hydraulic jump performance was investigated using screens with a 22 cm width and a 3 cm depth. The screen walls had 24 holes with respective relative hole areas of 0.046, 0.103, 0.183, 0.285, and 0.411 m2 and diameters of 0.4, 0.6, 0.8, 1.00, and 1.2 cm. The results showed that the screens with different relative widths improved the characteristics of the submerged hydraulic jump. In order to maximize relative energy loss while reducing the depth and length of the submerged hydraulic jump, the screen wall's relative diameter should be roughly 1 cm (Elaswad et al., 2021).

3. LABORATORY WORKS

3.1 General

This chapter includes a detailed explanation of the laboratory experiments conducted in the Hydraulics Laboratory at the College of Engineering University of Mosul in Iraq, where (400) experiments were conducted.

Figure 3.1: Hydraulics laboratory at the college of engineering university of Mosul in Iraq.

The experiments included the use of 20 models of type-A piano key weirs. These models differ from each other in terms of geometric parameters, so that each model has its own geometric parameters in terms of width of the inlet keys (W_i) and width of the outlet keys (W_o), length of the inlet keys (B_i)and length of the out keys (B_o), slope of the inlet keys (S_i) and slope of the outlet

keys (S_o), the length of the top edge of the weir model (L), the heights of the weir model (P).

The experiments also included the use of 13 models of screen walls. These walls differ from each other in terms of the holes within them. Each model has its own characteristic of holes in terms of diameters, shapes, and percentage of porosity, as shown in Table 3.1.

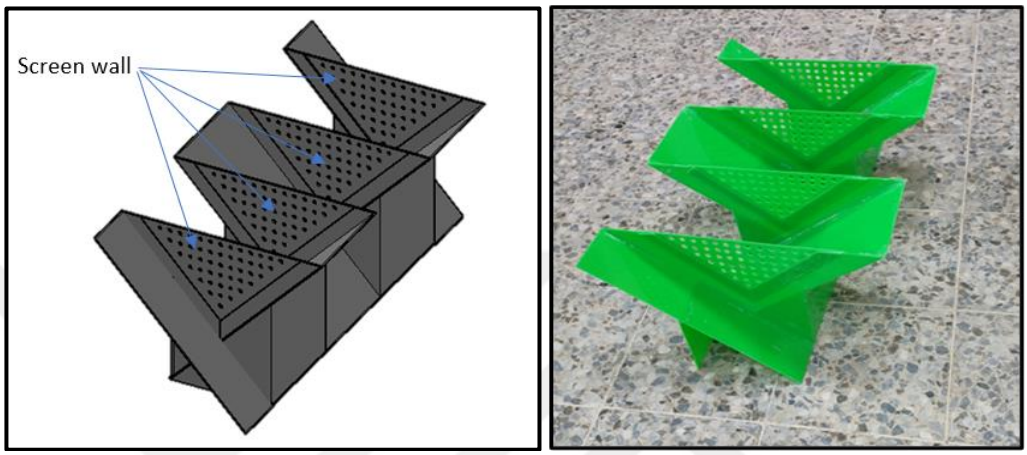

Figure 3.2: Shows the position of the screen walls on the piano key weir structure.

The piano key weir models used are designed in a way that allows the screen wall model to be installed on them and the possibility of replacing it with other models. The experiments included launching four discharges and conducting experiments on them. The flow inside the channels is below the free flow conditions. Experiments were carried out to obtain information about the hydraulic performance of the piano key weir after adding different screen walls to it and their effect on the discharge coefficient as well as their effect on energy dissipation.

This chapter also includes a description of the laboratory channel and laboratory models, a description of the mechanism for conducting experiments, and the necessary measurements.

3.2 Piano Key Weir Models Used in the Experiments

Experiments were conducted using models of a type A piano key with a width of 81 cm, and inlet keys and outlet are rectangular in shape.

- All models are made of acrylic glass sheets 2.5 mm thick.

- The model consists of two units: two complete keys for the inlet key and two outlet keys (a complete key in the middle and two halves of a key on both ends).
- The piano key weir model contains three overhangs upstream of the weir and two overhangs downstream of the weir.

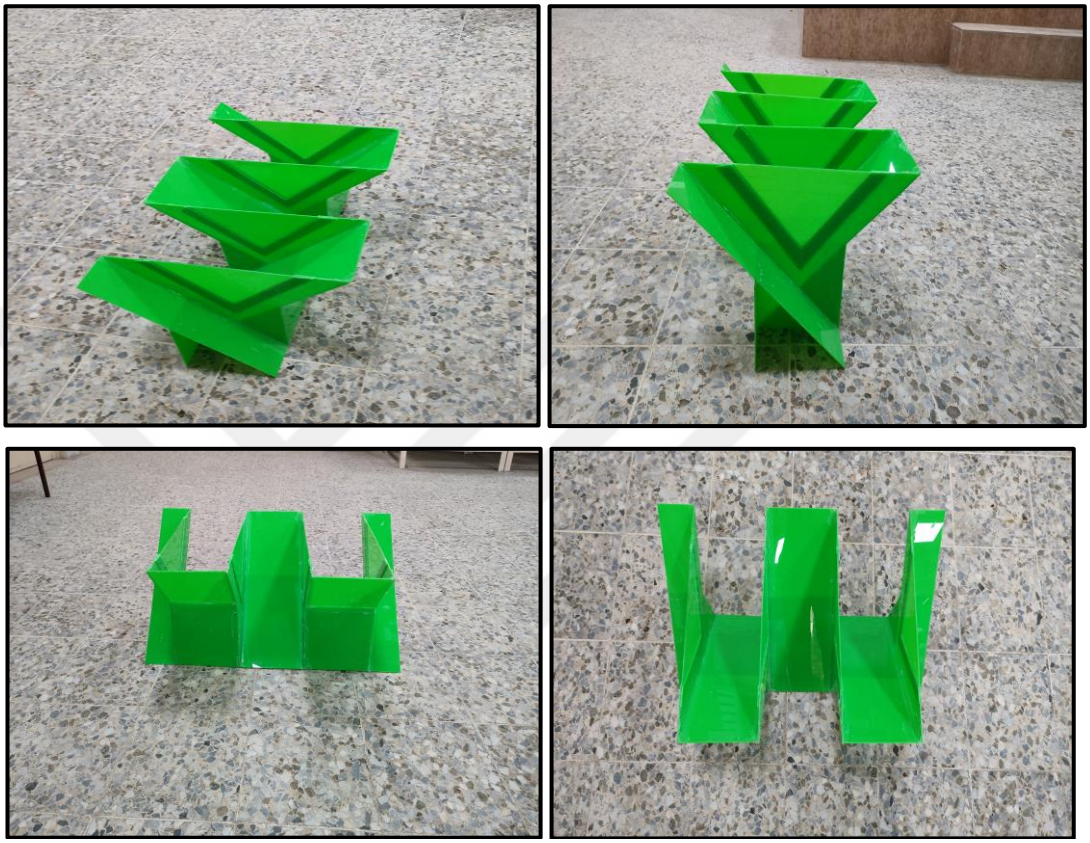

Figure 3.3: Model of piano key weir with screen wall without holes.

- 20 models of piano key weirs were used, and these weirs differ among themselves in their geometric parameters. Each model has its own geometric parameters. Note that the geometric parameters of the piano key weir models used in conducting the experiments are within the limits set by Kabiri-Samani and Leite Ribeiro in applying their equations to calculate the discharge factor (Pfister et al., 2012).

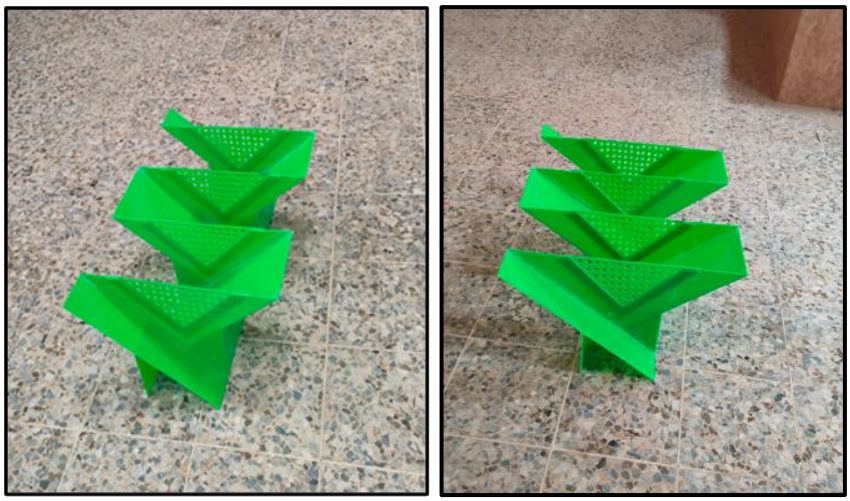

Figure 3.4: Models of piano key weir with screen wall containing holes.

A layer of acrylic glass sheet with a length of 81cm, width of 70 cm and thickness of 0.25 cm is added below the model to become a base on which the model is fixed, and then it is easy to install the model well on the concrete channel floor.

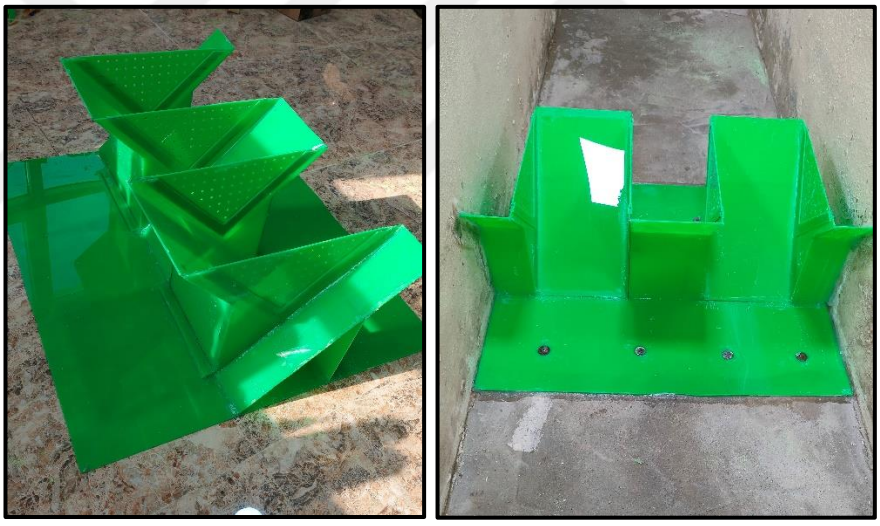

Figure 3.5: The additional acrylic glass sheet below PKW model.

The piano key weir models used in the experiments differ in terms of geometric parameters, as they include differences in:

- Width of the inlet keys Wi and width of the outlet keys (W_o), where the ratio of the width of the inlet key to the outlet key (W_i/W_o) ranged between 0.81, 1, and 1.22, as shown in Figure 3.6.

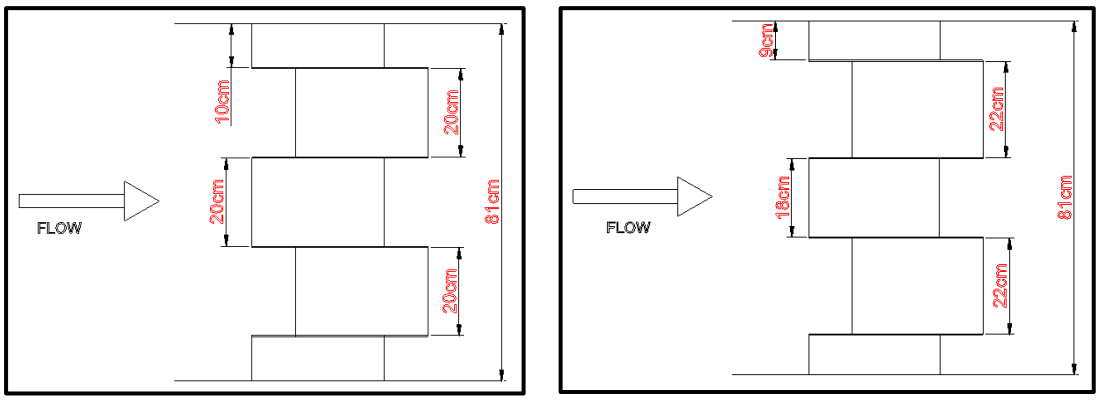

(a) $W_i/W_o = 1$. (b) $W_i/W_o = 1.22$.

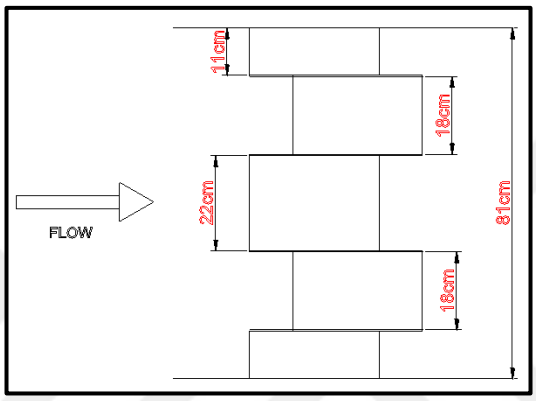

(c) $W_i/W_o = 0.81$.

Figure 3.6: The ratio of the width of the inlet key to the outlet key (W_i/W_o).

- The lengths of the inlet key are (B_i) and the lengths of the outlet key are(B_o). The lengths range from 10, 15, and 20 cm. as shown in Figure 3.7.
- The length of the crest edge of model (L) ranged from 320, 298.6, 280, 277.33, 261, 265, 242.67, 240, 224, 208, and 192 cm.
- The slope of the inlet key is (S_i) and the slope of the outlet key is (S_o), where the slope ranged between 1, 0.86, and 0.75, as shown in Figure 3.7.

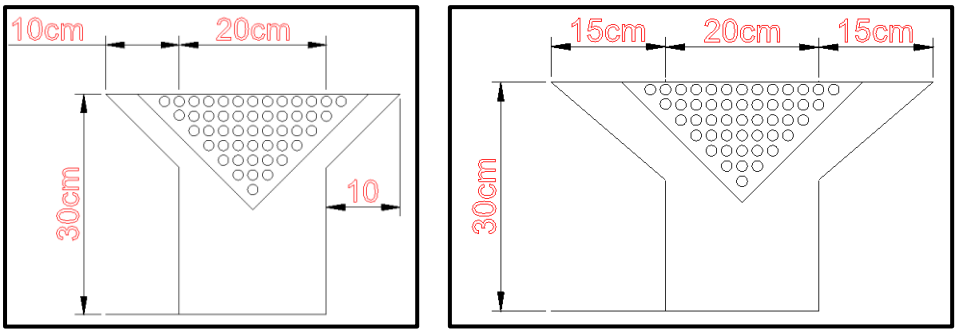

(a) B_i=10, B_o=10, S_i=1, S_o=1. (b) B_i=15, B_o=15, S_i=0.86, S_o=0.85.

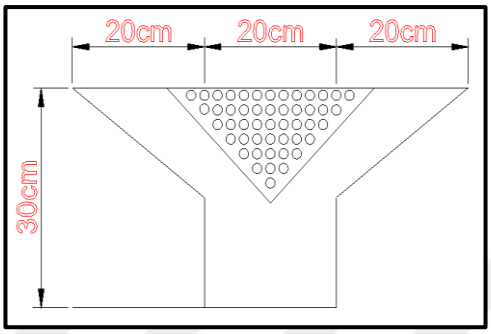

(c) B_i=20, B_o=20, S_i=0.75, S_o=0.75

Figure 3.7: Side section of piano key weir.

- The heights of the Piano key weir (P) models range between 30, 28, 26, and 24 cm, as shown in Figure 3.8.

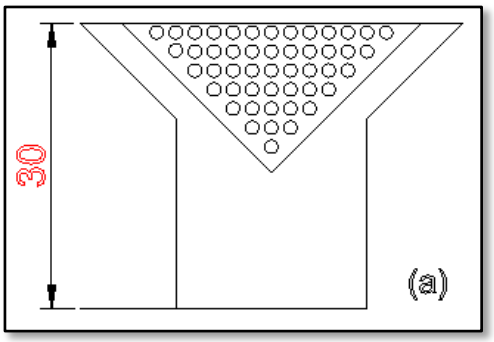

(a) P = 30 cm.

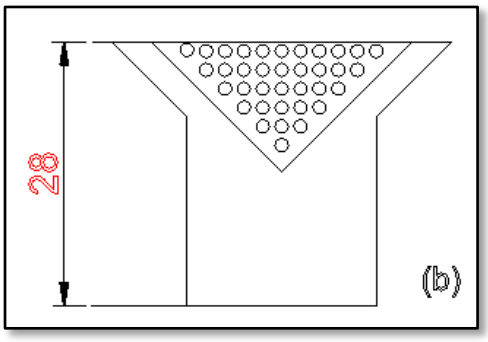

(b) (P = 28 cm).

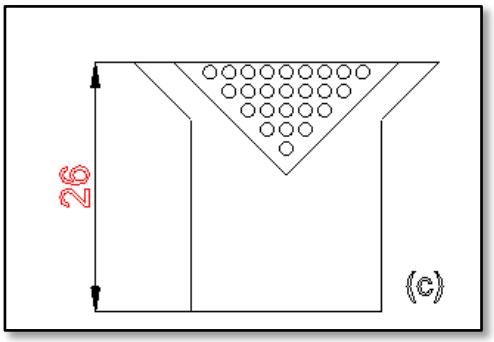

(c) (P = 26 cm).

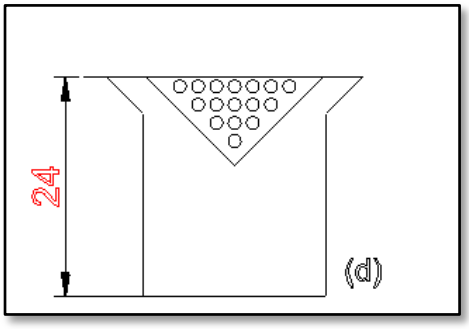

(d) (P = 24 cm).

Figure 3.8: The heights of the piano key weir models.

Table 3.1: The geometric parameters of the piano key weir models used in conducting the experiments.

	Name of (PKW) Model	P (cm)	B (cm)	L (cm)	B_i (cm)	B_o (cm)	W_i (cm)	W_o (cm)	S_i	S_o
1	PKW1 L1	30	40	241	10	10	20	20	1	1
2	PKW1 L2	28	36	225	8	8	20	20	1	1
3	PKW1 L3	26	32	209	6	6	20	20	1	1
4	PKW1 L4	24	28	1.93	4	4	20	20	1	1
5	PKW2 L1	30	40	241	10	10	22	18	1	1
6	PKW2 L2	28	36	225	8	8	22	18	1	1
7	PKW2 L3	26	32	209	6	6	22	18	1	1
8	PKW2 L4	24	28	1.93	4	4	22	18	1	1
9	PKW3 L1	30	40	241	10	10	18	22	1	1
10	PKW3 L2	28	36	225	8	8	18	22	1	1
11	PKW3 L3	26	32	209	6	6	18	22	1	1
12	PKW3 L4	24	28	193	4	4	18	22	1	1
13	PKW4 L1	30	60	321	20	20	20	20	0.75	0.75
14	PKW4 L2	28	54.6	300	17.3	17.3	20	20	0.75	0.75
15	PKW4 L3	26	49.4	278	14.7	14.7	20	20	0.75	0.75
16	PKW4 L4	24	44	257	12	12	20	20	0.75	0.75
17	PKW5 L1	30	50	281	15	15	20	20	0.85	0.85
18	PKW5 L2	28	45.4	262	12.7	12.7	20	20	0.85	0.85
19	PKW5 L3	26	40.6	243	10.3	10.3	20	20	0.85	0.85
20	PKW5 L4	24	36	225	8	8	20	20	0.85	0.85

- All these models were designed with a special design that allows the possibility of installing screen wall models on them, as large holes were made in their side walls in the shape of a triangle in which the screen wall is placed.

3.3 Screen Wall Models Used in the Experiments

- There are 13 types of screen wall models, all of which are in the shape of an isosceles and a right-angled triangle, as shown in Figure 3.9.

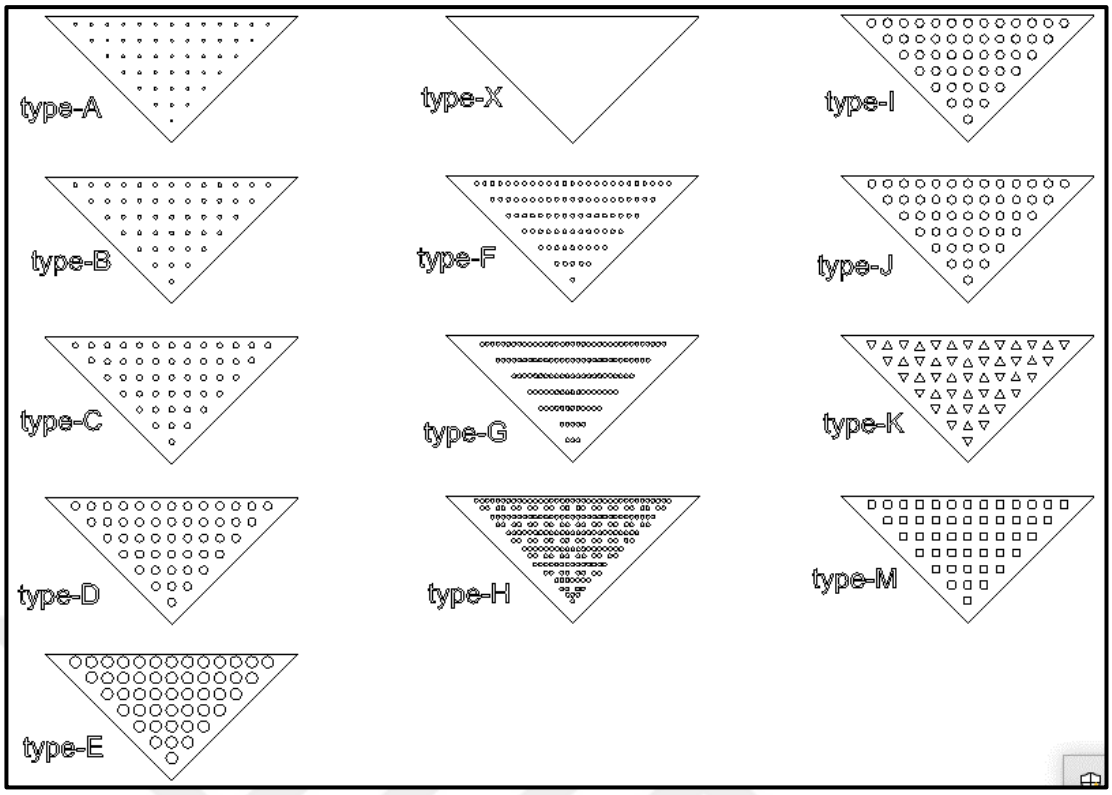

Figure 3.9: Screen wall models

The screen wall models have areas of 248.3, 189.2, 138.2, and 95.2 cm^2 distributed according to the heights of the piano key weir models, as shown in TableA.1.

- Screen wall models vary according to the shapes of the holes, the diameters of the holes within them, and according to the percentage of porosity in them, as shown in Table A.1.
- The screen wall models were made of 2.5 mm thick acrylic glass sheets.
- All screen wall models can be installed on the walls of the piano key wall models, each according to the height of the screen for which it was designed.
- Four copies were made for each type of screen wall model so that when the experiment was carried out, these four copies of the screen wall model were distributed on the four walls of the piano key weir model.
- Each 13 types of screen walls were divided into four groups as follows:

❖ **A closed group that does not contain any holes:**

This type of screen wall model is placed in weir models to obtain the setting that the piano key weir model does not contain a screen wall with holes.

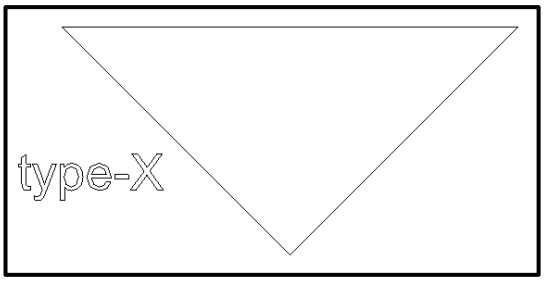

Figure 3.10: Model of a screen wall that does not have holes.

❖ **Group by hole diameters:**

- This collection includes five types of screen wall models, as shown in Figure 3.11 & Figure 3.12.
- This group includes models of screen walls containing circular holes of different diameters.
- The diameters of the holes for these models range between 0.35, 0.5, 0.7, 1.0, and 1.4 cm. Each type of screen wall model has a specific diameter as shown in Table A.11 & Figure 3.11.
- Each type of screen wall model contains a group of holes, ranging in number from 49, 36, 25, and 16 holes, depending on each level of the height of the piano key weir model (L1), (L2), (L3), and (L4), respectively, as shown in Table A.11 & Figure 3.13.

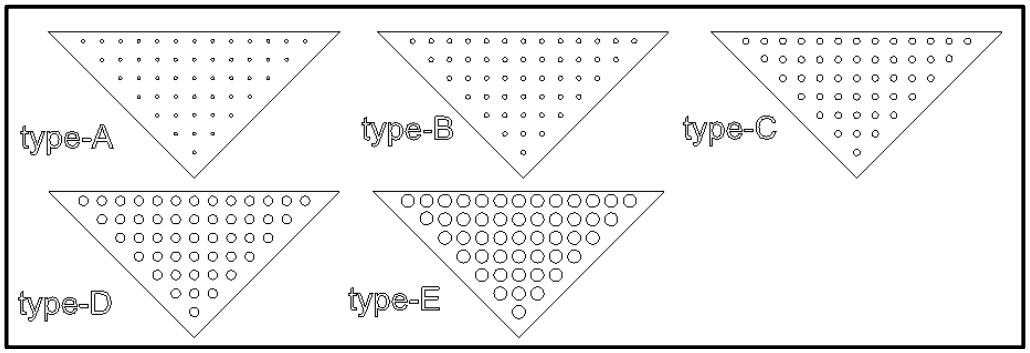

Figure 3.11: Models of a screen wall containing circular holes of different diameters, for [type-A (Φ=0.35cm), type-B (Φ=0.5cm), type-c (Φ=0.7cm), type-D (Φ=1.0cm), type-E (Φ=1.4cm)].

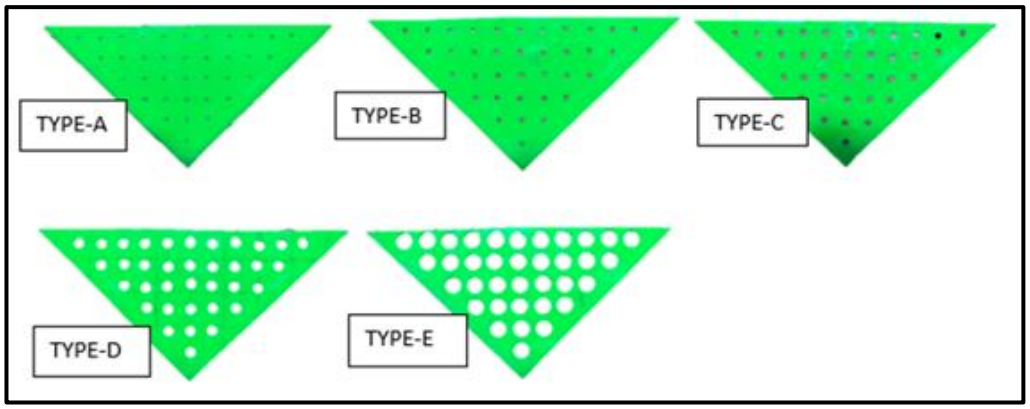

Figure 3.12: Models of a screen wall containing circular holes of different diameters.

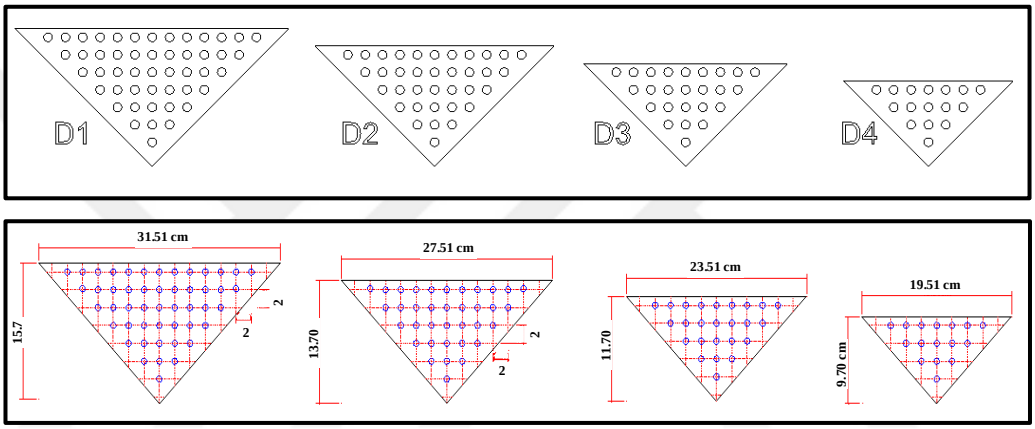

Figure 3.13: Models of screen wall type-d ranging in number from 49, 36, 25 and 16 holes, as an example.

❖ **Group by hole shapes:**

- This collection includes five types of screen wall models, as shown in **Hata! Başvuru kaynağı bulunamadı.**.
- This group includes screen wall models containing different shaped holes: circular, square, hexagonal, triangular, and star. Each type of wall model has a specific shape of holes.
- The holes of these models for screen walls are equal in area, with the area of one opening being 0.785 cm^2.
- Each type of screen wall model contains a group of holes whose numbers range from 49, 36, 25, and 16 holes, depending on each level of the height of the piano key weir model (L1), (L2), (L3), and (L4) respectively as shown in Figure3.15.

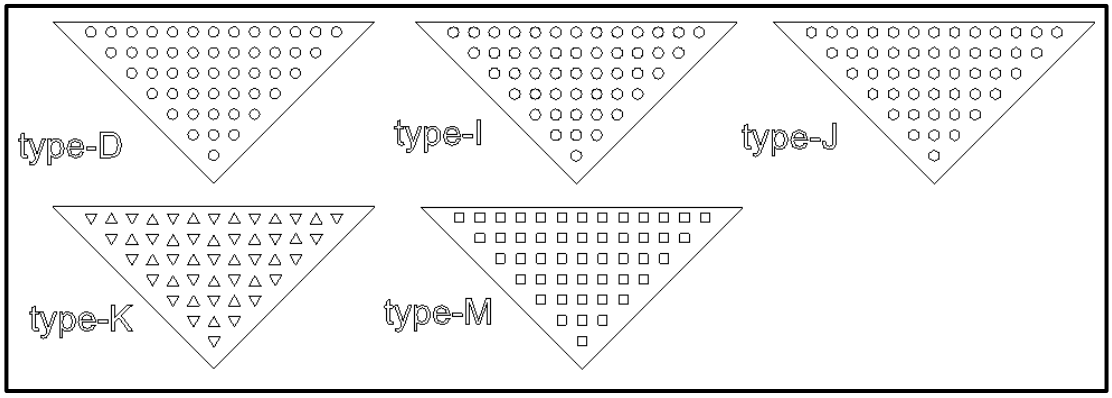

Figure 3.14: Models of screen walls that contain different shaped holes, for [type-d (circular), type-i (astral), type-j (hexagonal), type-k(triangular), type-

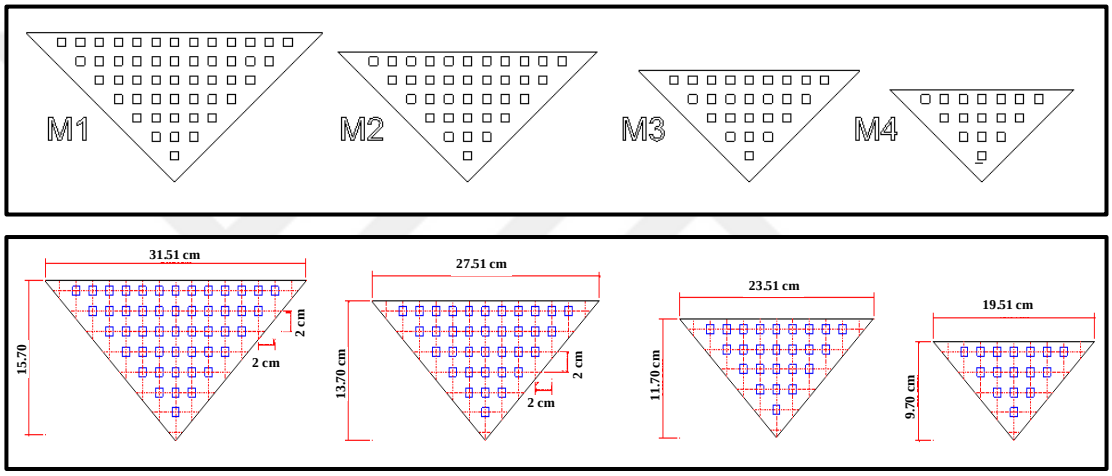

Figure 3.15: Models of screen wall type-m ranging in number from 49, 36, 25, and 16 holes as an example.

❖ **Group according to porosity.**

- This group includes four types of screen wall models, as shown in Figure3.16.
- This group includes models of screen walls that contain holes that are different in terms of their porosity.
- Each model of a screen wall in this group has its own porosity ratio.
- The percentage of porosity for the models of this group ranges between 3.9% - 17.44% according to each type and according to each level of the height of the piano key head model, as shown in Table A.1 & Figure 3.17.
- The diameters of these holes are uniform for this group, which is 0.5 cm.

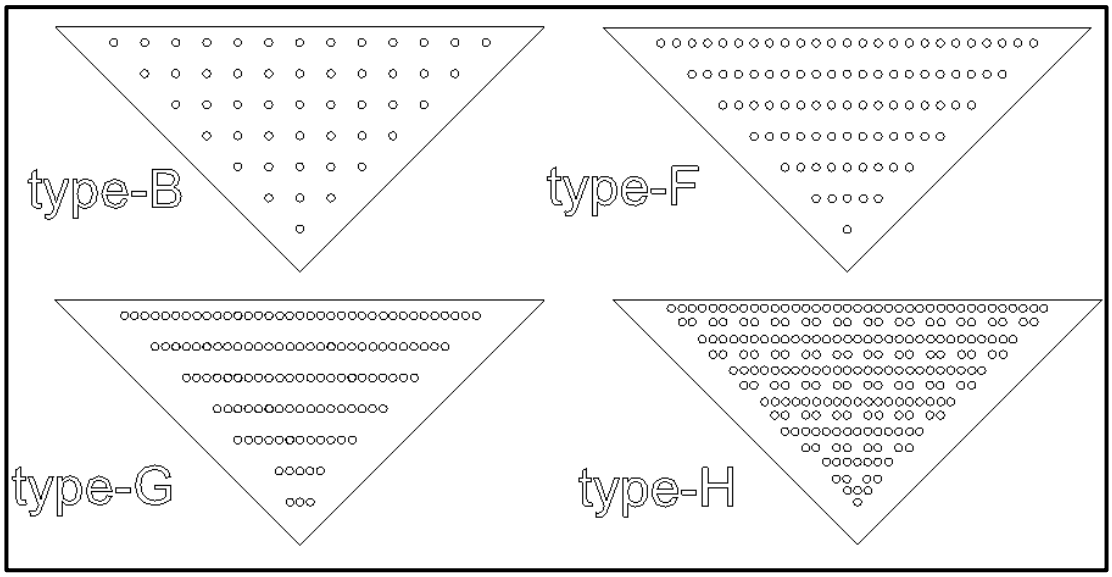

Figure 3.16: Models of screen walls that contain holes that different in terms of their porosity.

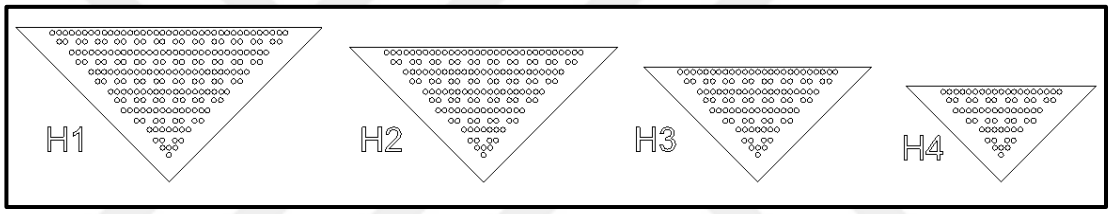

Figure 3.17: An example models of screen wall type-h ranging in the percentage of porosity from 17.44 %, 16.57 %, 15.46 %, and 14.0% holes.

3.4 Laboratory Measurements

3.4.1 Discharge measurement

The discharge was measured by means of the iron weir installed at the end of the discharge basin, as it was based on the weir equation adopted by the researcher Al-Saidi, (2020), which links the relationship between the discharge passing through the channel and the depth of the water above the edge of the iron weir and with a coefficient of determination ($R^{\wedge 2} = 0.999$) as shown by Equation (3.1) (Hayawi, 2006).

$$\boldsymbol{Q = 0.9558 \times h_o^{105}} \qquad \textbf{(3.1)}$$

Where (Q) is the discharge passing through the channel in (m^3/sec), h_1 is the height of water above the top edge of the iron weir (m).

The four discharges, 37,47,57, and 67 lt/s, were adopted in all experiments for this research because in this research, at a discharge that is less than 37 lt/s, the

height of the flow above the crest of the weir will be less than 3cm and this causes to appearing the surface tension phenomena, and the discharge that is more than 37 lt/s the height of the flow above the crest of the weir will be more than 3 cm and this causes no tension on the surface. Therefore, the surface tension associated with the Weber number can be cancelled (Bhukya et al., 2022; Khassaf et al., 2016; Sangsefidi et al., 2021).

A discharge that is more than 67 lt/s, will cause disturbance and interference to the currents running over the piano key weir, which affects the flow system over the weir. Therefore, it will affect the accuracy of the results.

3.4.2 Measuring water depth

A vertical point gauge, which has an accuracy of ±0.1 mm, was used to measure the water surface level and the depth of flow along the center line of the inlet keys and the center line of the outlet keys upstream, at a distance of (2P) from the piano key weir model and continuing up to a distance of (8P) From the middle of the piano key weir model downstream, at intervals of every 10 cm, for all experiments.

Figure 3.18: Point Gauge

3.4.3 Measuring water temperature

The temperature was measured by a mercury thermometer with an accuracy of 0.5 Celsius degree, as the water temperature was between 25-27 Celsius during the study experiments in May, June and July.

Figure 3.19: Mercury Thermometer.

3.4.4 Construction level

The construction level is used to determine the vertical and horizontal level of the weir model inside the canal, especially since the canal is concrete and its walls are made of concrete, which requires ensuring that the weir model is placed at the level. After placing the model in the appropriate location in the canal and ensuring its level is good, the model is installed with a roller bolt and silicone. To ensure that the model does not move and that water does not leak through it.

Figure 3.20: Construction level

3.4.5 Measuring tape

The measuring tape is used to measure some of the necessary dimensions and distances, such as the dimensions of the channel, the dimensions of the geometric parameters of the weir model, the location of the piano key weir models in the channel, as well as the distances at which the point scale is placed at the source and downstream of the piano key weir.

Figure 3.21: Measuring tape

3.5 Laboratory Channel

The experiments were conducted in a horizontal concrete channel with a length of 33.5 m, a width of 0.81 m and a depth of 0.6 m, with concrete with a thickness of 0.2 m.

For concrete channels, Manning's roughness coefficient n value can vary depending on surface conditions and the specific properties of the concrete used in construction. Since the concrete channel has slight roughness, a Manning coefficient (n) equal to (0.013) was adopted, where the Manning roughness coefficient represents the resistance to flow in the open channel, including concrete channels.

On both sides of the s, a right-angled rail Dixon is installed horizontally along the channel to facilitate the movement of depth measuring devices point gauge along the channel, which moves easily on this rail and along the channel.

The beginning of the channel is connected to the supply basin, with dimensions of 2.25 m×1.25 m and a depth of 1.2 m.

Water reaches the supply basin through a pipe with a diameter of 15.24 cm.

Water is pushed through this pipe by a water pump that gives a discharge of up to 100 lt/s. The pump draws water from a ground tank under the floor of the laboratory. The water passes from the supply basin to the concrete channel, from there to the discharge basin, and then to the ground tank, thus completing the cycle.

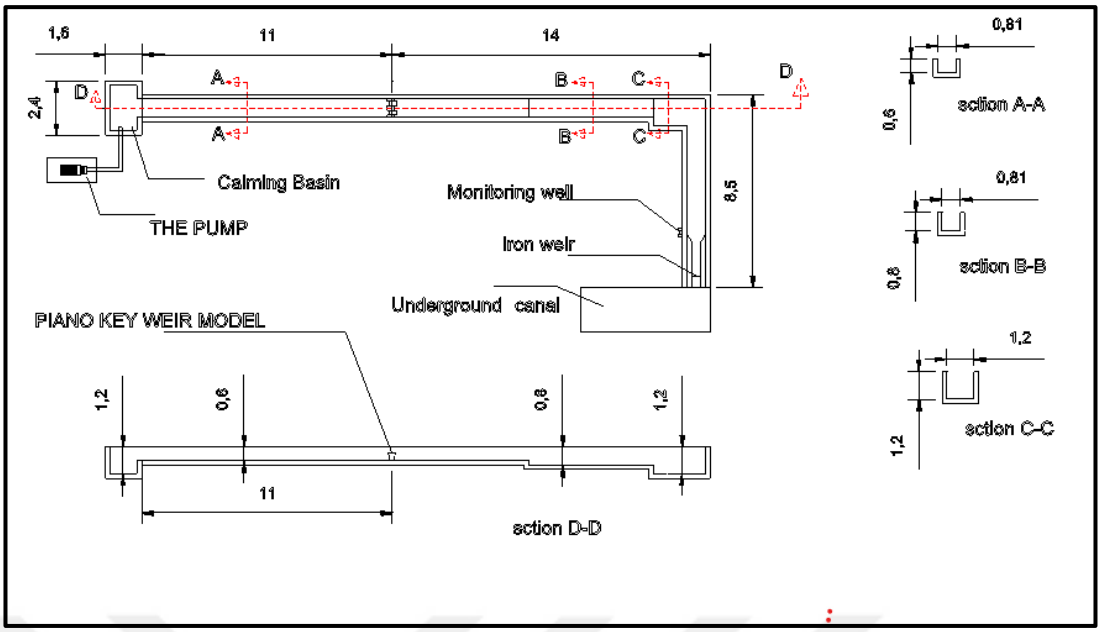

Figure 3.22: Plan, Cross-sections, and longitudinal section of the laboratory channel

The discharge basin Connected to the end of the channel, the discharge basin has a length of 8.5m, a width 0.81m, and a depth of of 1.2 m. At its end there, is a waist with a length of 2.0 m and a height of 0.5m. An iron weir with dimensions of 0.17 m × 0.5 m and a thickness of 0.5 cm is attached to its end to measure the discharge of the water passing through the channel, and this iron weir shall be fixed at a level through which guarantees the occurrence of free flow in the channel.

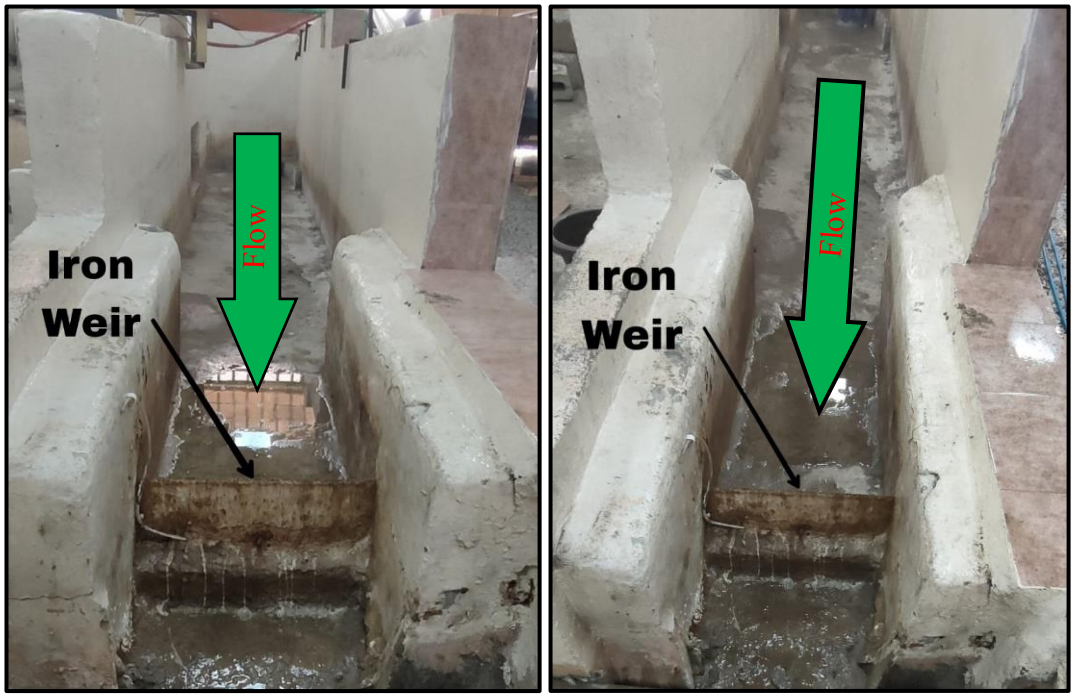

Figure 3.23: Iron Weir at the End of Channel.

On the left side of the basin, at a distance of 1.75 m in front of the iron weir, there is a concrete calming well with dimensions 15 cm×15 cm and a depth of 0.6 m. One of its sides is glass. It can be through it to observe and measure the depth of the water in the calming well with a ruler fixed to it. The depth of the water in the calming well represents the depth of the water above the edge of the iron weir.

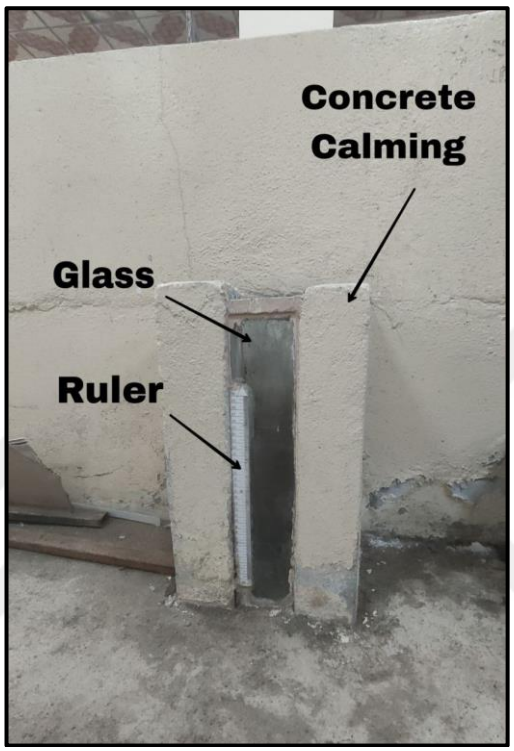

Figure 3.24: The Calming Well.

The use of a calming well is to ensure a stable and calm water level to read the water height more clearly and accurately.

The 5 PKW models were installed inside the channel and at a distance of 11 m from the end of the supply basin to obtain good water stability at the source of the weir. The level was used to ensure that the piano key weir model was placed flat and horizontally, and mounting screws and silicone adhesive was used to attach the models to the walls and bed of the channel and fill any small and precise gaps.

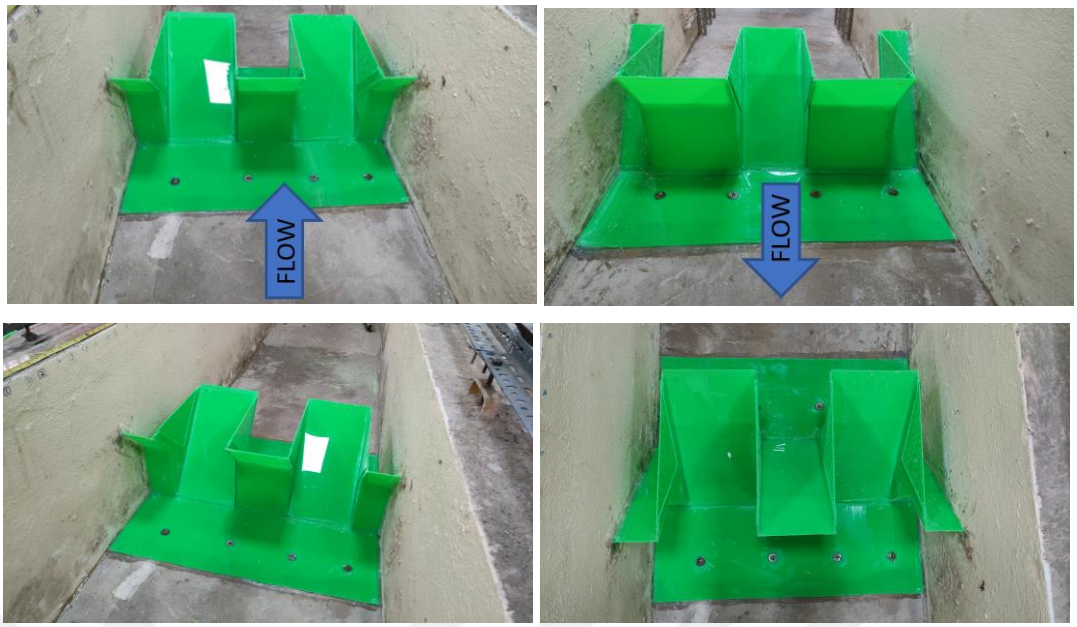

Figure 3.25: Piano key weir models were installed inside the channel.

3.6 Steps for Conducting Laboratory Experiments

1. The first model of piano key weir PKW1 L1, which contains the screen wall type- X, is placed in the channel at a distance of 11 meters from the supply basin, with a sufficient distance to ensure a stable and subcritical water level. After ensuring that the model is placed well in the channel, vertically and horizontally, by using a construction level, the model is then fixed with silicone adhesive to the floor and walls of the channel, making sure to fill all the soft spaces between the model and the concrete surface to ensure that water does not leak through them.
2. The point gauge is zeroed at the Channel bottom level at upstream. Then, start measuring the water level
3. Turn on the water pump and open the control valve according to the required discharge.
4. It is necessary to wait for a certain period between 5 to 10 min to obtain a stable discharge above the weir model of the piano key in order to reach the state of stable flow upstream.
5. Discharge is measured using an iron weir installed at the end of the discharge basin.

6. The water surface levels are taken at the distance 2P from the center of the PKW model at the upstream side to ensure that the flow surface level is constant before it is affected by the weir, and the water surface levels at the distance 8P from the center of PKW model at the downstream side. The distance 8P was chosen based on the distance downstream needed until the flow surface returns to a nearly constant level.

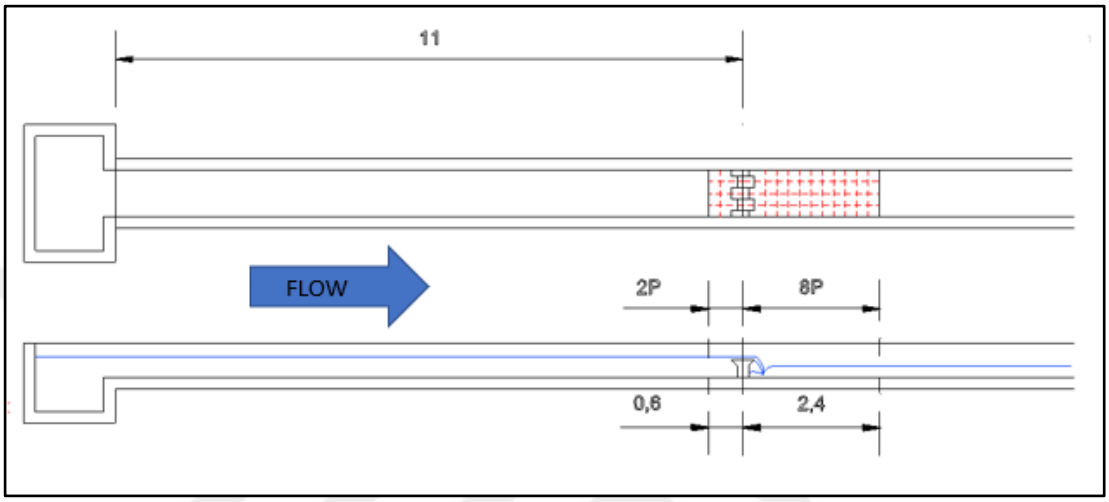

Figure 3.26: The Water Surface Levels are taken at the Center Line of the Inlet and Outlet Keys of PKW

7. After that, the first screen wall type-X is replaced with a second screen wall type-B and installed on a piano key weir model.
8. Steps 3-7 are repeated. Then, a replacement screen wall type-D is applied.
9. The first model of the piano key weir PKW1 L1 is replaced with the piano key weir model PKW1 L2, and steps 1-8 are repeated.
10. Repeat step 10 with the remaining 18 piano key weir models.
11. The piano key weir models PKW1 L1, PKW1 L2, PKW1 L3 and PKW1 L4 is excluded, including the installation of all models of screen walls A, C, E, F, G, H, I, J, K, and L on it and performing all the steps 1-9 before it.
12. By applying the laboratory work steps, laboratory results were obtained (flow height upstream and downstream) for the piano key weir, as shown in Table A.2, and it is possible to observe the steps of the laboratory experiment program from Figure 3 27.

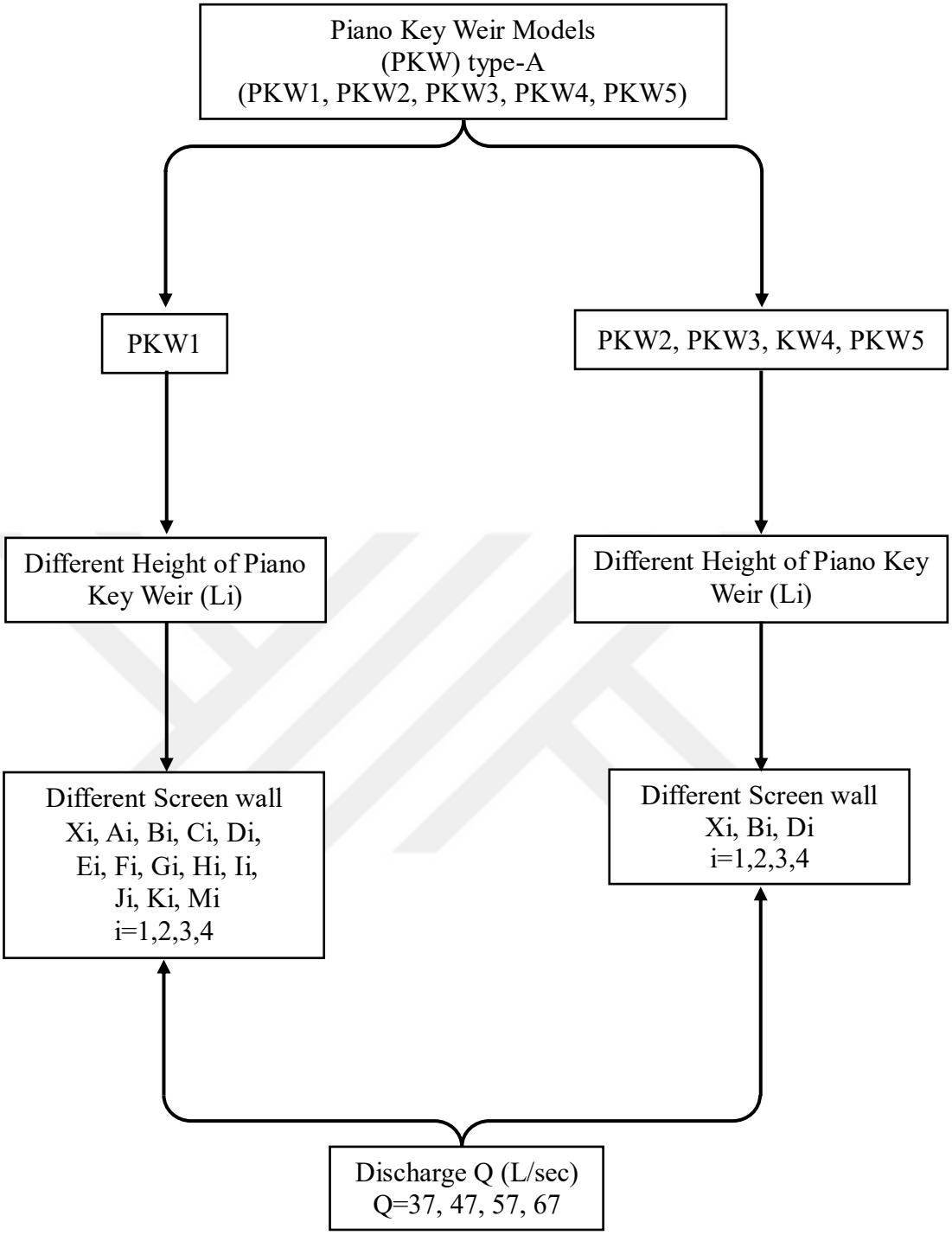

Figure 3.27: Laboratory Experiment Program using Different Models of Piano Key Weir Type-A with Different Heights and using Different Screen Walls.

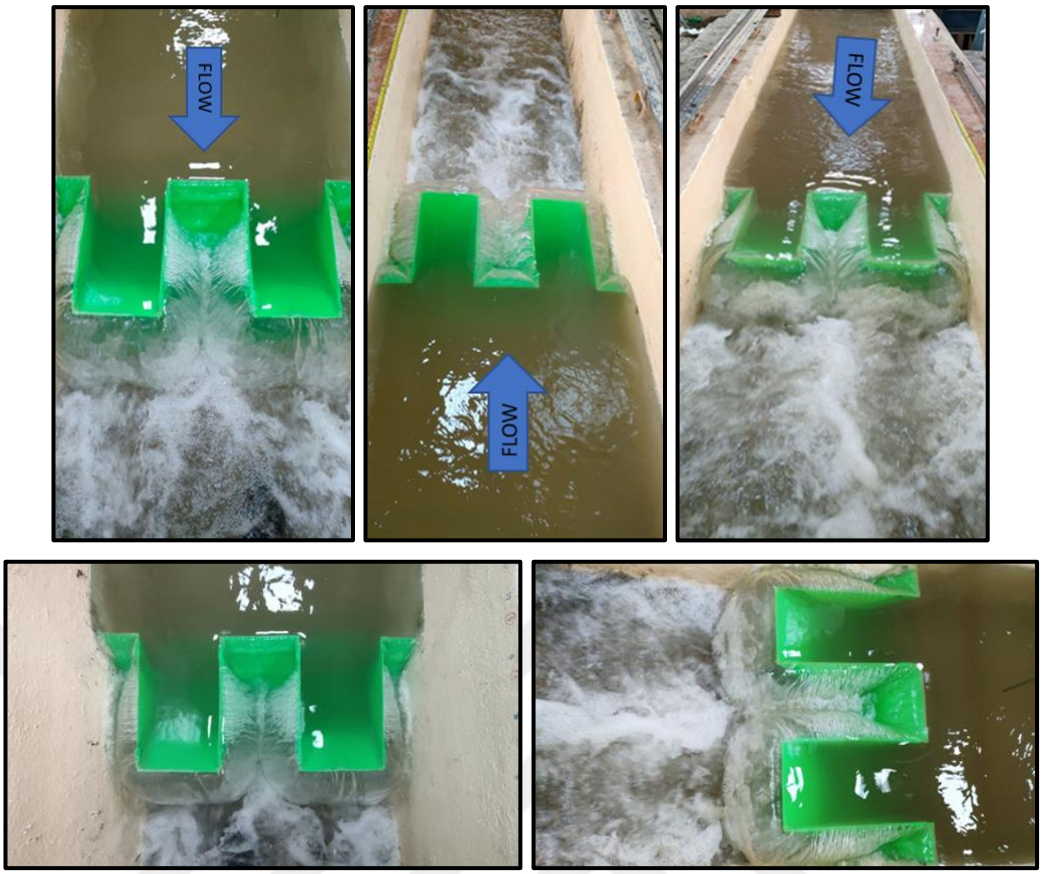

Figure 3.28: Water flow over the piano key weir and through the added screen wall

3.7 Dimensional Analysis

3.7.1 Dimensional analysis for Discharge coefficient flow(C_d)

The general discharge equation for a rectangular sharp-crested weir is (Kabiri-samani & Javaheri, 2012):

$$\boldsymbol{Q = \frac{2}{3} C_d \sqrt{2g} W H^{3/2}} \qquad \textbf{(3.2)}$$

Where (Q) is the discharge passing through the channel (lt/s), (C_d) the discharge coefficient, g the gravity acceleration (m/s^2), W the channel width m, and (H_1) is the total upstream hydraulic head (m), which is calculated from Equation (3.3).

$$\boldsymbol{H_1 = h_1 + V_1^2/2g} \qquad \textbf{(3.3)}$$

Where (H_1) the head over the piano key weir, (V_1) represents the main velocity upstream (m/s), Figure 3.27 clarifies the flow over PKW, which (V_1) is calculated through Equation (3.4).

$$V_1 = \frac{Q_a}{[(P+h_1)\times W]} \quad (3.4)$$

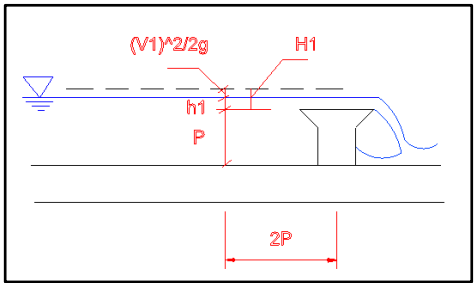

Figure 3.29: Flow condition over PKW type-A

For the purpose of studying and improving the performance efficiency of the flow discharge coefficient of the PKW type-A weir, the variables affecting the values of the flow discharge coefficient were identified in order to conduct a dimensional analysis of these variables; these variables are listed in Table 3.2.

Table 3.2: The variables affecting on the values of the discharge coefficient

Fluid variables	ρ	Mass density of water … ML^{-3}
	μ	Dynamic viscosity of water … $ML^{-1}T^{-1}$
	σ	The surface tension force of water … MT^{-2}
Variables related to flow	Q	The discharge passing through the channel …L^3T^{-1}.
	g	Ground acceleration … LT^{-2}.
	H_1	Is the total upstream hydraulic head … $H_1 = h_1 + {V_1^2}/{2g}$ … L.
	V_1	The flow velocity in the channel … ${L}/{T}$.
Variables related to the piano key weir model type-A	P	Weir height ... L.
	L	Total developed length along the overflowing crest axis ... L.
	W	Total width of the PKW ... L.
	W_i	The inlet key width of PKW ... L.
	W_o	The outlet key width of PKW ... L.
	B	Upstream-downstream length of the PKW $= Bb + B_i + B_0$ ... L.
	B_i	Downstream inlet key overhang crest length of PKW ... L.
	B_o	Upstream outlet key overhang crest length of PKW ... L.
	B_b	Base length of PKW... L.
	T_s	Sidewall thickness ... L.
	α	Sidewall angle.
	S_i	Slope of the inlet key.
	S_o	Slope of the outlet key.

Table 3.2: (Cont.) The variables affecting on the values of the discharge coefficient

Variables related to the screen wall	Φ	Diameter of the hole inside the screen wall … L.
	A_s	The area of the opening shape inside the wall as a function of the shape of the opening … L^2.
	A_p	The area of the total voids inside the screen wall as a function of porosity … L^2.
	T_{sw}	Screen wall thickness … L.

The relationship for the flow discharge coefficient of the weir was formulated so that it is a function of the following variables:

$$\boldsymbol{C_d = f(H_1,\ P,\ W,\ W_i,\ W_o,\ B,\ B_i,\ B_o,\ B_b,\ L,\ S_i,\ S_o,\ T_s,\ \alpha,\ Q,\ V_1,\ g,\ \rho,\ \mu,\ \sigma,\ \Phi,\ A_s,\ A_p,\ T_{sw})} \quad \textbf{(3.5)}$$

The Reynolds number Re describes the effect of the flow viscosity. when Re is high, the flow reaches a state of complete turbulence, the viscosity μ effect is small compared with the gravity effect and then the effect of the viscosity (μ) in open channels disappears, and therefore, it can be neglected from the Equation and since the depth of the water is above the weir More than 3 cm, the effects of surface tension σ on discharge are small, then tensile force (σ) is excluded from the analysis (Bhukya et al., 2022; Khassaf et al., 2016; Sangsefidi et al., 2021).

Since the width of the weir base (B_b)is constant, the thickness of the weir wall (T_s) is constant, the thickness of the screen wall (T_{sw}) is constant, and the weir side wall angle $(\alpha = 0)$, their effect is canceled out.

Therefore, the Equation (3.4) becomes as Equations (3.5) & (3.6):

$$\boldsymbol{C_d = f(H_1, P, W, W_i, W_o, B, B_i, B_o, L, S_i, S_o, Q, V_1, g, \rho, \sigma, \Phi, A_s, A_p)} \quad \textbf{(3.6)}$$

$$\boldsymbol{f(C_d, H_1, P, W, W_i, W_o, B, B_i, B_o, L, S_i, S_o, Q, V_1, g, \rho, \sigma, \Phi, A_s, A_p) = 0} \quad \textbf{(3.7)}$$

Relying on the Buckingham π-theorem in the dimensional analysis of Equation (3.7) which can be formulated with the Equation (3.8):

$$\boldsymbol{f(\pi_1, \pi_2, \pi_3, \pi_4, \pi_5, \pi_6, \pi_7, \pi_8, \pi_9, \pi_{10}, \pi_{11}, \pi_{12}, \pi_{13}, \pi_{14}, \pi_{15}, \pi_{16}) = 0} \quad \textbf{(3.8)}$$

By adopting (V_1), (H_1), and (ρ) as recurrent variables, the relationship of the variables is explained as follows:

$$\pi_1 = \rho V_1 H_1 C_d \qquad \pi_2 = \rho V_1 H_1 \mathrm{P} \qquad \pi_3 = \rho V_1 H_1 W \qquad \pi_4 = \rho V_1 H_1 W_i$$
$$\pi_5 = \rho V_1 H_1 W_o \qquad \pi_6 = \rho V_1 H_1 B \qquad \pi_7 = \rho V_1 H_1 B_i \qquad \pi_8 = \rho V_1 H_1 B_o$$
$$\pi_9 = \rho V_1 H_1 L \qquad \pi_{10} = \rho V_1 H_1 S_i \qquad \pi_{11} = \rho V_1 H_1 S_o \qquad \pi_{12} = \rho V_1 H_1 Q$$
$$\pi_{13} = \rho V_1 H_1 g \qquad \pi_{14} = \rho V_1 H_1 \Phi \qquad \pi_{15} = \rho V_1 H_1 \mathrm{A}_s \qquad \pi_{16} = \rho V_1 H_1 \mathrm{A}_p$$

Then the following dimensional values were obtained:

$$\pi_1 = C_d \qquad \pi_2 = {}^{\mathrm{P}}/_{H_1} \qquad \pi_3 = {}^{W}/_{H_1} \qquad \pi_4 = {}^{W_i}/_{H_1}$$
$$\pi_5 = {}^{W_o}/_{H_1} \qquad \pi_6 = {}^{\mathrm{B}}/_{H_1} \qquad \pi_7 = {}^{B_i}/_{H_1} \qquad \pi_8 = {}^{B_o}/_{H_1}$$
$$\pi_9 = {}^{L}/_{H_1} \qquad \pi_{10} = S_i \qquad \pi_{11} = S_o \qquad \pi_{12} = {}^{\mathrm{Q}}/_{V_1 {H_1}^2}$$
$$\pi_{13} = {}^{H_1 g}/_{V_1^2} \qquad \pi_{14} = {}^{\Phi}/_{H_1} \qquad \pi_{15} = {}^{\mathrm{A}_s}/_{{H_1}^2} \qquad \pi_{16} = {}^{\mathrm{A}_p}/_{{H_1}^2}$$

By substituting the values of (π) into Equation **Hata! Başvuru kaynağı ulunamadı.**, which can be formulated with Equation **Hata! Başvuru kaynağı bulunamadı.**3.9):

$$f\left(\boldsymbol{C_d},\ {}^{\boldsymbol{P}}/_{\boldsymbol{H_1}},\ {}^{\boldsymbol{W}}/_{\boldsymbol{H_1}},\ {}^{\boldsymbol{W_i}}/_{\boldsymbol{H_1}},\ {}^{\boldsymbol{W_o}}/_{\boldsymbol{H_1}},\ {}^{\boldsymbol{B}}/_{\boldsymbol{H_1}},\ {}^{\boldsymbol{B_i}}/_{\boldsymbol{H_1}},\ {}^{\boldsymbol{B_o}}/_{\boldsymbol{H_1}},\ {}^{\boldsymbol{L}}/_{\boldsymbol{H_1}},\ \boldsymbol{S_i},\ \boldsymbol{S_o},\ {}^{\boldsymbol{Q}}/_{\boldsymbol{V_1 {H_1}^2}},\ {}^{\boldsymbol{H_1 g}}/_{\boldsymbol{V_1^2}},\ {}^{\boldsymbol{\Phi}}/_{\boldsymbol{H_1}},\ {}^{\boldsymbol{A_s}}/_{\boldsymbol{{H_1}^2}},\ {}^{\boldsymbol{A_p}}/_{\boldsymbol{{H_1}^2}}\right) = \mathbf{0} \qquad \textbf{(3.9)}$$

by using inverse $\pi_2 = {}^{H_1}/_{P}$.

by using division ${}^{\pi_3}/_{\pi_2} = {}^{W}/_{P}$.

by using division ${}^{\pi_4}/_{\pi_5} = {}^{W_i}/_{W_o}$.

by using division ${}^{\pi_7}/_{\pi_6} = {}^{B_i}/_{B}$.

by using division ${}^{\pi_6}/_{\pi_2} = {}^{\mathrm{B}}/_{P}$.

by using division ${\pi_8}/{\pi_6} = {B_o}/{B}$.

by using division ${\pi_9}/{\pi_3} = {L}/{W}$.

by using division ${\pi_9}/{\pi_2} = {L}/{P}$.

by using division ${\pi_{12}}/{\pi_{13}} = {{Q}/{V_1 {H_1}^2}} \Big/ \left({H_1 g}/{V_1^2}\right)^{0.5} = {{Q}/{{H_1}^{2.5}}} \Big/ {g^{0.5}} = Fr$

The final form of the dimensional analysis equations can be obtained, which can be formulated with Equation (3.10):

$$\boldsymbol{C_d = f\left({H_1}/{P},\ {W}/{P},\ {W_i}/{W_o},\ {B}/{P},\ {B_i}/{B},\ {B_o}/{B},\ {L}/{W},\ S_i,\ S_o,\ Fr,\ {\Phi}/{H_1},\ {A_s}/{{H_1}^2},\ {A_p}/{{H_1}^2} \right)} \quad \textbf{(3.10)}$$

Since the slope of the inlet and outlet key were taken as constant and also the length of the overhang upstream equal to the length of the overhang downstream so (B_i/B_o) and (S_i) & (S_o) can be neglected. Therefore Equation (3.10) becomes:

$$\boldsymbol{C_d = f\left({H_1}/{P}, {W}/{P}, {W_i}/{W_o}, {B}/{P}, {L}/{W}, Fr, {\Phi}/{H_1}, {A_s}/{{H_1}^2}, {A_p}/{{H_1}^2} \right)} \quad \textbf{(3.11)}$$

The values of the non-dimensional variables were obtained for all models of the piano key type-A with the different screen walls and for all experiments, the number of which was 400 experiments, as shown in

3.7.2 Dimensional analysis for flow energy dissipation $(\Delta E/E_1)$

Due to the difficulty of measuring the energy dissipated through the hydraulic jump due to the complex nature of the piano key weir structure, the turbulent and complex nature of the hydraulic flow emerging from it at the toe of the base of the weir, and the difficulty of measuring the energy at the region of the hydraulic jump which ranges from irregular and unstable, energy dissipation was calculated by measuring the energy difference for the upstream flow at distance $(2P)$ from PKW to the downstream flow at distance $(8P)$ from PKW in order to insure stabilize the flow level and transform it into a stable state, and to rely on these measurements as an indicator of energy dissipation.

In this study, tailwater was not artificially controlled for tests that featured a hydraulic jump at the toe of the structure and upstream of flow depth measurements. It should be noted that the amount of energy dissipated by hydraulic jump is negligible compared to energy dissipated by PKW (Eslinger & Crookston, 2020). For this reason, relied on the depth of flow at the source in calculating the energy (E_1), and the depth of the tailwater in calculating (E_2). The upstream and downstream energy across the piano key weir was calculated as Equations (3.12) & (2.13):

$$\boldsymbol{E_1 = P + h_1 + {V_1^2}/{2g}} \qquad \textbf{(3.12)}$$

$$\boldsymbol{E_2 = h_2 + {V_2^2}/{2g}} \qquad \textbf{(3.13)}$$

Where $(E_{1,}\, E_2)$ represent the specific energy upstream and downstream, respectively, as shown in Figure 3.29.

Where P is the height of the piano key weir m, (H_1) is the head over the piano key weir m, h_2 is the depth of tailwater at the downstream m, (V_1) & (V_2) represent the average velocity at upstream and downstream (m/s) respectively, Where (V_1) & (V_2) velocities are calculated using Equations(3.14) & (3.15) respectively:

$$V_1 = {Q}/{[(P + h_1) \times W]} \quad (3.14)$$

$$V_2 = {Q}/{[(h_2) \times W]} \quad (3.15)$$

Where (Q) is the discharge passing through the channel (lt/s), (W) is the total width of the PKW (m).

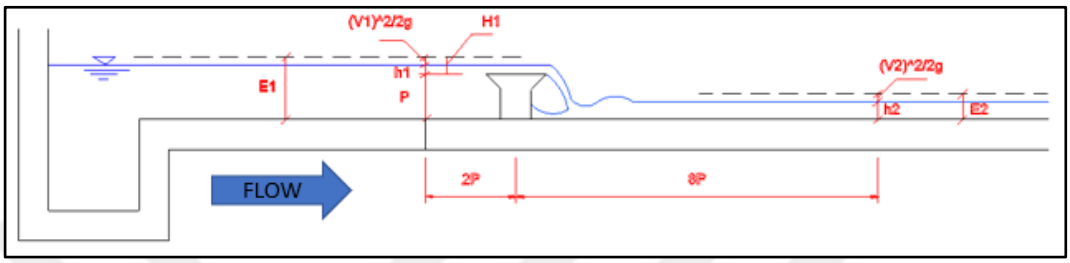

Figure 3.30: Schematic plot for specific energy measurement.

The values of (E_1) and (E_2)were used to determine the relative energy dissipation and residual energy by the Equations (3.16) & (3.17) (Singh & Kumar, 2023):

$$\textbf{relative energy dissipation } {\Delta E}/{E_1} = {(E_1 - E_2)}/{E_1} \quad (3.16)$$

$$\textbf{residual energy} = E_1 - E_2 \quad (3.17)$$

Relative energy dissipation refers to how much energy is lost or dissipated compared to the total energy input. It's a measure that helps in evaluating the efficiency or effectiveness of a system or process, indicating the amount of wasted or unavailable energy in relation to the initial input energy.

Residual energy refers to the remaining energy within a system after a transmission process of flow from upstream to downstream across PKW. It represents the energy that has not been dissipated, utilized, or transferred elsewhere but remains within the system under consideration.

Many variables geometrical and hydraulic parameters influence the energy dissipation across the piano key weir. The following hydraulic and geometrical parameters were considered in the submitted study in order to compute the energy dissipation downstream of the PKW, which are mentioned in Table 3.3:

Table 3.3: The variables affecting on the values of the energy dissipation.

Fluid variables	ρ	Mass density of water … ML^{-3}
	μ	Dynamic viscosity of water … $ML^{-1}T^{-1}$
	σ	The surface tension force of water … MT^{-2}
Variables related to flow	Q	The discharge passing through the channel …L^3T^{-1}.
	g	Ground acceleration … LT^2.
	H_1	Is the total upstream hydraulic head … $H_1 = h_1 + {V_1^2}/{2g}$ … L.
	V	The flow velocity in the channel … LT^2.
	E_1	Specific energy at the upstream of PKW ... L.
	E_2	Specific energy at the downstream of PKW ... L
Variables related to the piano key weir model type-A	P	Weir height ... L.
	L	Total developed length along the overflowing crest axis ... L.
	W	Total width of the PKW ... L.
	W_i	The inlet key width of PKW ... L.
	W_o	The outlet key width of PKW ... L.
	B	Upstream-downstream length of the PKW $= Bb + B_i + B_0$ ... L.
	B_i	Downstream inlet key overhang crest length of PKW ... L.
	B_o	Upstream outlet key overhang crest length of PKW ... L.
	B_b	Base length of PKW... M.
	T_s	Sidewall thickness ... L.
	α	Sidewall angle.
	S_i	Slope of the inlet key.
	S_o	Slope of the outlet key.
Variables related to the screen wall	Φ	Diameter of the hole inside the screen wall … L.
	A_s	The area of the opening shape inside the wall as a function of the shape of the opening … L^2.
	A_p	The area of the total voids inside the screen wall as a function of porosity … L^2.
	T_{sw}	Screen wall thickness … L.

The relationship for the flow discharge coefficient of the weir was formulated so that it is a function of the following variables:

$$\Delta E = f\left(E_1.\ E_2,\ H_1,\ P,\ W,\ W_i,\ W_o,\ B,\ B_i,\ B_o,\ B_b,\ L,\ S_i,\ S_o,\ T_w,\ \alpha,\ Q,\ V,\ g,\ \rho,\ \mu,\ \sigma,\ \Phi,\ A_s,\ A_p,\ T_{sw}\right) \quad \text{.....(3.18)}$$

The Reynolds number (Re) describes the effect of the flow viscosity, when Re is high, the flow reaches a state of complete turbulence, the viscosity (μ) effect is small compared with the gravity effect and then the effect of the viscosity μ in open channels disappears, and therefore it can be neglected from the equation and since the depth of the water is above the weir More than 3 cm, the effects of surface tension σ on discharge are small, then tensile force (σ) is excluded from the analysis (Bhukya et al., 2022; Khassaf et al., 2016; Sangsefidi et al., 2021).

Since the width of the weir base (B_b) is constant, the thickness of the weir wall (T_s) is constant, the thickness of the screen wall (T_{sw}) is constant, and the weir side wall angle ($\alpha = 0$), their effect is canceled out.

Therefore, the Equation (3.18) becomes as follows:

$$\Delta E = f\left(E_1, E_2, H_1, P, W, W_i, W_o, B, B_i, B_o, L, S_i, S_o, Q, V, g, \rho, \Phi, A_s, A_p\right) \quad \textbf{(3.19)}$$

$$f\left(\Delta E, E_1, E_2, H_1, P, W, W_i, W_o, B, B_i, B_o, L, S_i, S_o, Q, V, g, \rho, \Phi, A_s, A_p\right) = 0 \quad \textbf{(3.20)}$$

Relying on the Buckingham π-theorem in the dimensional analysis of the Equation (3.20 which can be formulated with the Equation (3.21)(3.21):

$$f(\pi_1,\ \pi_2,\ \pi_3,\ \pi_4,\ \pi_5,\ \pi_6,\ \pi_7,\ \pi_8,\ \pi_9,\ \pi_{10},\ \pi_{11},\ \pi_{12},\ \pi_{13},\ \pi_{14},\ \pi_{15},\ \pi_{16},\ \pi_{17},\ \pi_{18},\ \pi_{19},\ \pi_{20},\ \pi_{21},\ \pi_{22}) = 0 \quad \textbf{(3.21)}$$

By adopting (V, H_1, ρ) as recurring variables, the relationship of the variables is explained as follows:

$\pi_1 = \rho V H_1 \Delta E$ $\pi_2 = \rho V H_1 E_1$ $\pi_3 = \rho V H_1 E_2$ $\pi_4 = \rho V H_1 P$

$\pi_5 = \rho V H_1 W$ $\pi_6 = \rho V H_1 W_i$ $\pi_7 = \rho V H_1 W_o$ $\pi_8 = \rho V H_1 B$

$\pi_9 = \rho V H_1 B_i$ $\pi_{10} = \rho V H_1 B_o$ $\pi_{11} = \rho V H_1 L$ $\pi_{12} = \rho V H_1 S_i$

$\pi_{13} = \rho V H_1 S_o$ $\pi_{14} = \rho V H_1 Q$ $\pi_{15} = \rho V H_1 g$ $\pi_{16} = \rho V H_1 \Phi$

$\pi_{17} = \rho V H_1 A_s$ $\pi_{18} = \rho V H_1 AP$

Then the following dimensional values were obtained:

$\pi_1 = \Delta E$ $\pi_2 = {E_1}/{H_1}$ $\pi_3 = {E_2}/{H_1}$ $\pi_4 = {P}/{H_1}$

$\pi_5 = {W}/{H_1}$ $\pi_6 = {W_i}/{H_1}$ $\pi_7 = {W_o}/{H_1}$ $\pi_8 = {B}/{H_1}$

$\pi_9 = {B_i}/{H_1}$ $\pi_{10} = {B_o}/{H_1}$ $\pi_{11} = {L}/{H_1}$ $\pi_{12} = S_i$

$\pi_{13} = S_o$ $\pi_{14} = {Q}/{VH_1^2}$ $\pi_{15} = {H_1 g}/{V^2}$ $\pi_{16} = {\Phi}/{H_1}$

$\pi_{17} = {A_s}/{H_1}$ $\pi_{18} = {A_p}/{H_1}$

By substituting the values of (π) in to Equation (3.21)3.21) which can be formulated with the Equation (3.22)3.22):

$$f\left(\boldsymbol{\Delta E/H_1},\ \boldsymbol{E_1/H_1},\ \boldsymbol{E_2/H_1},\ \boldsymbol{P/H_1},\ \boldsymbol{W/H_1},\ \boldsymbol{W_i/H_1},\ \boldsymbol{W_o/H_1},\ \boldsymbol{B/H_1},\ \boldsymbol{B_i/H_1},\ \boldsymbol{B_o/H_1},\ \boldsymbol{L/H_1},\ \boldsymbol{S_i},\ \boldsymbol{S_o},\ \boldsymbol{Q/VH_1^2},\ \boldsymbol{H_1 g/V^2},\ \boldsymbol{\Phi/H_1},\ \boldsymbol{A_s/H_1^2},\ \boldsymbol{A_p/H_1^2}\right) = \mathbf{0} \quad \textbf{.....(3.22)}$$

by using division ${\pi_1}/{\pi_2} = {\Delta E}/{E_1}$.

by using division ${\pi_3}/{\pi_2} = {E_2}/{E_1}$.

by using inverse $\pi_4 = {H_1}/{P}$.

by using division ${\pi_5}/{\pi_4} = {W}/{P}$.

by using division $\pi_6/\pi_7 = W_i/W_o$.

by using division $\pi_9/\pi_8 = B_i/B$.

by using division $\pi_{10}/\pi_8 = B_o/B$.

by using division $\pi_8/\pi_4 = \mathrm{B}/P$.

by using division $\pi_{11}/\pi_5 = L/W$.

by using division $\pi_{11}/\pi_4 = L/P$.

by using division $\pi_{14}/\pi_{16}{}^{0.5} = \mathrm{Q}/\mathrm{V}H_1{}^2 \Big/ \left(H_1 g/V^2\right)^{0.5} = Q/H_1{}^{2.5} g^{0.5} = Fr$

The final form of the dimensional analysis equations can be obtained which can be formulated with the Equation (3.23)3.23):

$$\Delta E/E_1 = f\left(E_2/E_1,\ H_1/P,\ W/P,\ W_i/W_o,\ B_i/B,\ B_o/B,\ B/P,\ L/W,\ L/P,\ S_i,\ S_o,\ Fr,\ \Phi/H_1,\ A_s/H_1{}^2,\ A_p/H_1{}^2\right) \quad \textbf{(3.23)}$$

Since the slope of the inlet and outlet key were taken as constant and also the length of the overhang upstream was equal to the length of the overhang downstream so, (B_i/B_o) and (S_i), can be neglected, and because the flow regime upstream of weirs built perpendicular to the river channel is usually subcritical, the Froude number is not taken when assessing the hydraulic features of these structures (Haghiabi et al., 2022).

Therefore, the Equation (3.23) becomes:

$$\Delta E/E_1 = f\left(E_2/E_1,\ H_1/P,\ W/P,\ W_i/W_o,\ B/P,\ L/W,\ L/P,\ \Phi/H_1,\ A_s/H_1{}^2,\ A_p/H_1{}^2\right) \quad \textbf{(3.24)}$$

The values of the non-dimensional variables were obtained for all models of the piano key type-A with the different screen walls and for all experiments, the number of which was 400 experiments, as shown in Table A.3.

4. RESULTS ANALYSIS

This chapter included the study and analysis of the results obtained from conducting laboratory experiments on piano key weir type-A.

The hydraulic behaviour of the flow passing through the piano key weir was studied when adding screen walls with and without holes, and the hydraulic behaviour was evaluated and described using these results.

The effect of changing the geometric parameters of the piano key weir on the hydraulic performance of the flow and its effect on the discharge coefficient and energy dissipation were also studied and analyzed.

The effect of changing the holes of the screen walls was also studied and analyzed in terms of the diameter of the holes, their shapes, and their porosity and their effect on hydraulic performance, discharge coefficient, and dissipated energy.

4.1 Description of the Hydraulic Behavior of the Flow Crossing the Piano Key Weir:

This research studies the analysis of two cases of the hydraulic behavior of the flow across PKW:

4.1.1 Case one: The hydraulic behaviour of the flow across PKW by adding a screen wall without holes to it.

This case represents the standard case. In the surrounding region of the Piano Key Weir where the piano key weir creates distinguish, complicated, and three-dimensional flow fields, these are the flow over the back crest of the inlet key, the front crest of the outlet key, and the flow over the lateral wall, The three separate types of flow combine to form the flow over a PKW.

The piano key weir functions similarly to a conventional linear weir with a very long crest length at low relative water level heads. where the flow through the three crests of the piano key, the side crest, the downstream crest, and the upstream crest are all directly perpendicular to one another, as shown in Figure 4.1.

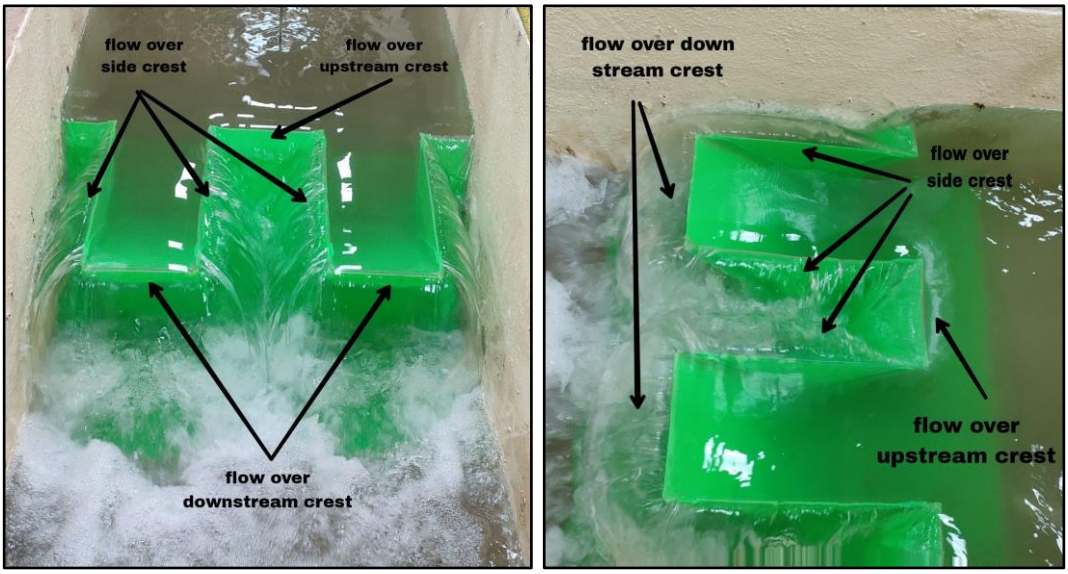

Figure 4.1: The flow across inlet and outlet key of PKW by adding screen wall type-X at the low head of flow $(H_1/P < 0.2)$.

The streamlines of the three-dimensional flow field of a PKW demonstrate that for low heads $(H_1/P < 0.2)$, the flow is approaching the upstream of the inlet key, the streamlines of the flow remain straight as it enters the inlet key, and the floor's slope propels the flow upward as shown in Figure 4.2.

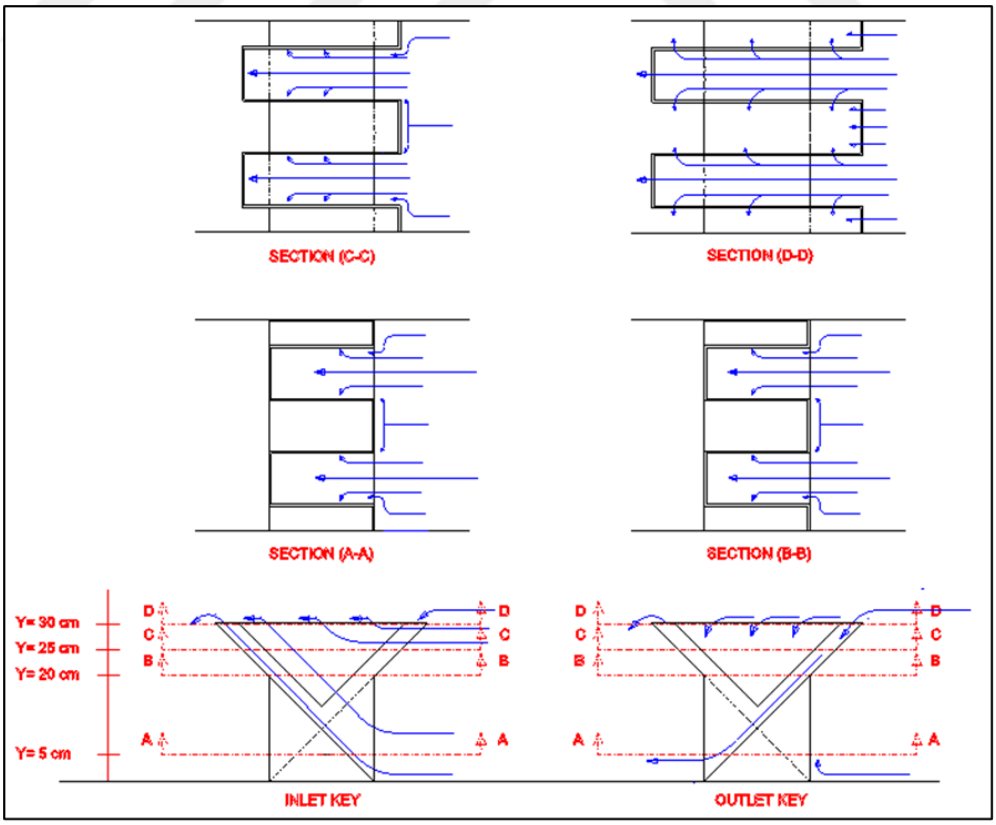

Figure 4.2: The streamlines flow across inlet and outlet key of PKW by adding screen wall type-X at the low head of flow $(H_1/P < 0.2)$.

The flow approaching the outlet key divides to both sides at the midline of the outlet key toward the inlet keys. As a result, the current running along the slopes always feeds the inlet's downstream key crest in meanwhile, only surface current enters the outlet key, and because of the flow inertia downstream, the partial flow from the front of the inlet key contributes to the discharge in its lateral portion in outlet key from over the lateral crest, and the current from the front of the outlet key contributes to the discharge in its upstream portion in outlet key.

For low heads, the whole weir crest flow is free outflow, and the nappe of water crossing over the near lateral crests enters the outlet key, In the outlet key, which leads to a collision of nappes coming from above the side wall and from both sides with the diaper coming from the upstream side of the outlet key, this collision occurs on the inclined surface of the outlet key which shows jet expansion and streams interaction in this key and leads the flow energy is dissipated through the interactions and collisions that occur in the outlet keys and the collision of flows and streams at the bottom of the PKW's base on the downstream side where the outflow from the outlet key and the toe of the weir base is highly aerated and three-dimensional with splash and spray regions within the outlet keys and at the base of the structure impact point as shown in Figure 4.3.

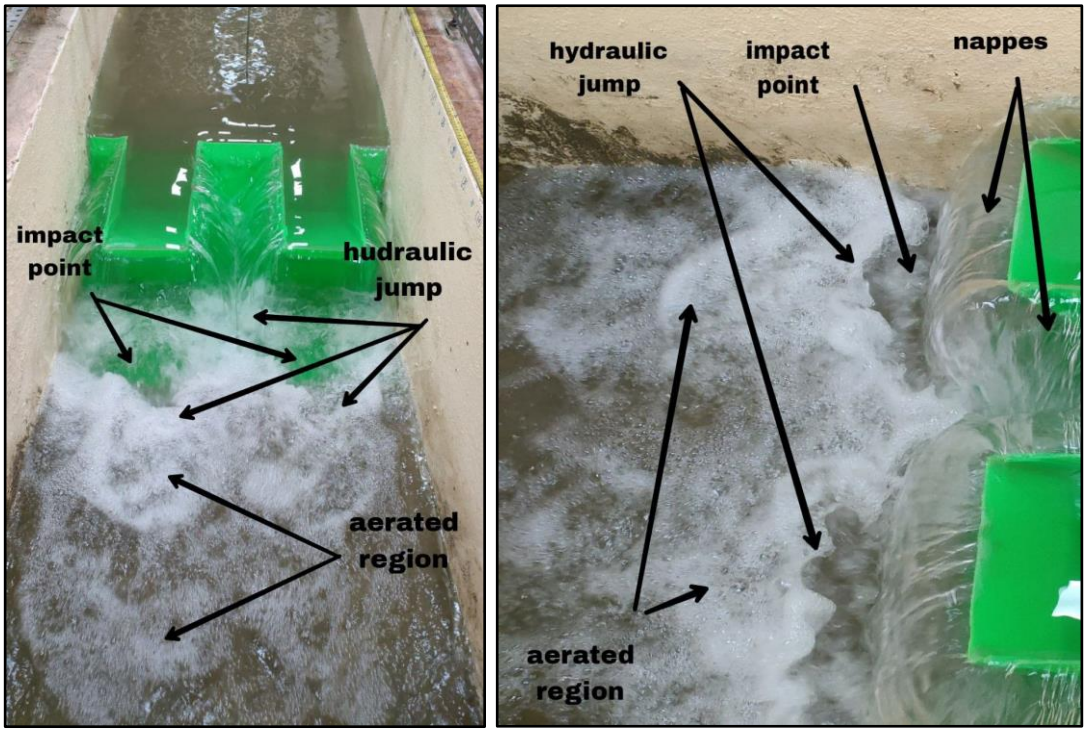

Figure 4.3: The location of the hydraulic jump and the impact point in addition to the aerated region

The hydraulic jump is then formed, the hydraulic jump is a phenomenon observed in fluid dynamics where there is an abrupt change in the depth and velocity of a flowing liquid. This occurs when a high velocity supercritical flow meets with a slower subcritical flow, and when these two types of flows interact then the energy in the flow is converted and causing a sudden increase in the water's depth and a decrease in its velocity.

The length and height of the hydraulic jump depend on the amount of flow and the amount of energy dissipated. As the amount of flow increases, the rotational jets generated from the outlet key increase, and this in turn increases the turbulence of the flow at the mouth of the weir as in the 4.3.

When the supercritical flow encounters a subcritical flow, energy dissipation happens, leading to turbulence, a rise in water level, and a decrease in flow velocity, this abrupt change can be observed as a distinct boundary between the rapid flow and the more tranquil deeper flow at downstream.

For high heads $(\mathrm{H}_1/\mathrm{P} > 0.2)$ the streamlines over the PKW are less uniformly, and for the outlet key of PKW which is similar in structure to a sharp-crested inclined weir it is supplied with flows coming from the upstream side and from the side flows that are coming nappes from the overflow of the inlet key as shown in Figure 4.4.

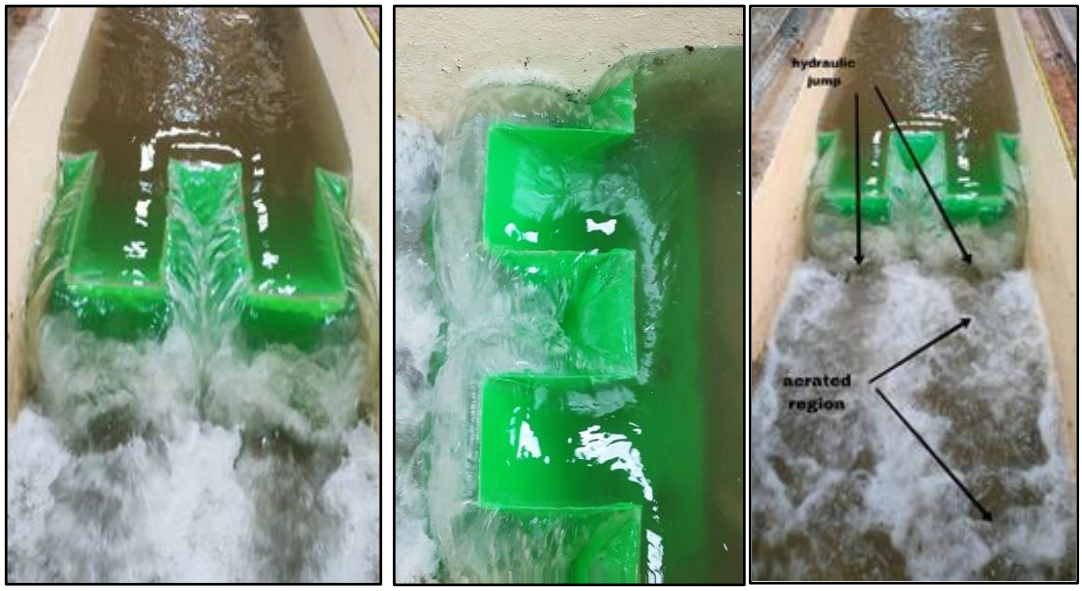

Figure 4.4: The flow across inlet and outlet key of PKW by adding screen wall type-X at the flow head much higher than $(H_1/P > 0.2)$

The increased velocity and longitudinal momentum of the flow in the input key lead the flow over the side crest to deviate from the normal direction with somewhat greater overflow heads. As a result, there is a minor reduction in the flow efficiency over the side crest, and the dimensions of the inlet and outlet keys become important with increasingly higher heads, as shown in Figure 4.5.

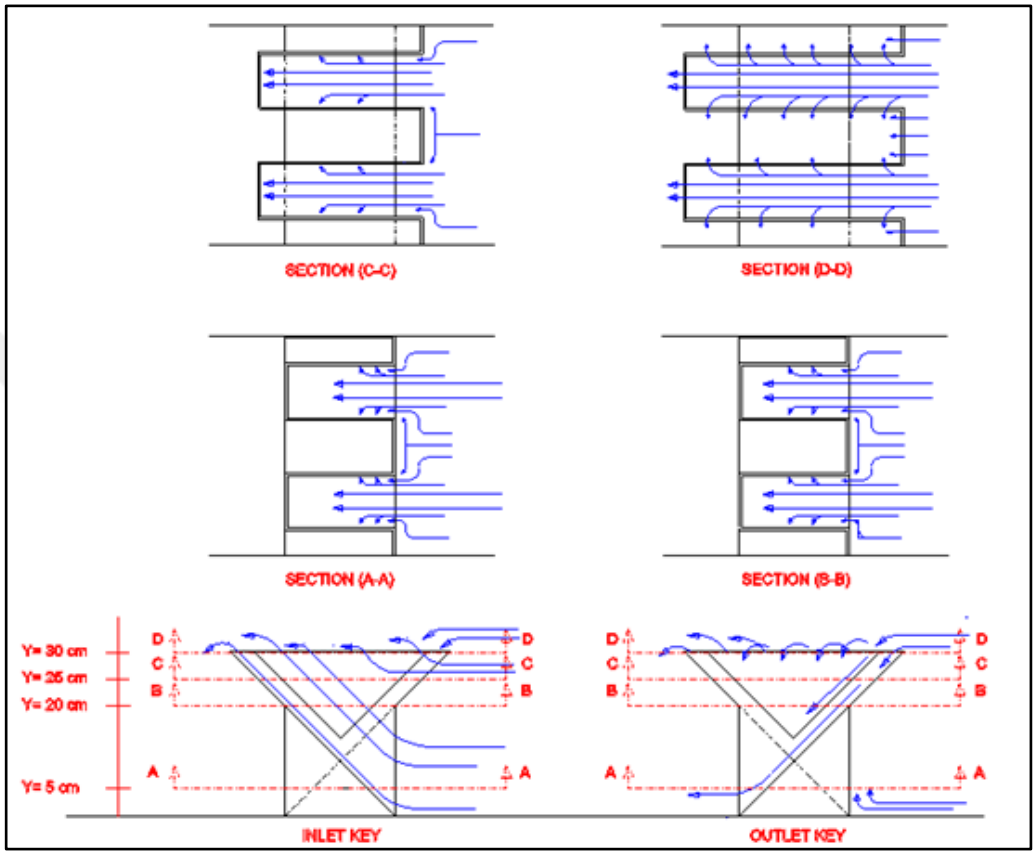

Figure 4.5: The streamlines flow across inlet and outlet key of PKW by adding screen wall type-X at the flow head is high than $(H_1/P > 0.2)$.

The nappe breaks free at 3/4 of the lateral crest length, and the opposing actions of the free nappe on the lateral crest cause the discharge coefficient (C_d) to decrease as H rises. The discharge coefficient rises when there is a hanging nappe on the upstream crest and a depressed nappe on the downstream crest.

Where the initial results show that as the approach flow head increases, The discharge coefficient (C_d) decreases. Furthermore, for constant (H), the discharge coefficient (C_d) increases with weir height; nevertheless, (H_1/P) has a major impact on the discharge coefficient (C_d).

In addition, the nappes that overflow from the nearby lateral crests to the outlet key clash, intensifying the local submergence effects; The resulting

interactions result in significant mixing and turbulence with a highly aerated rotating stream exiting from the outlet key that is directed downstream and immediately expands. Where that nappe acting in opposite directions contributes to energy dissipation.

One of its phenomena is the occurrence of a hydraulic jump, as well as the disturbance of the flow of the tailwater for a distance that depends on the amount of discharge and the strength of the hydraulic jump.

4.1.2 Case two: The hydraulic behavior of the flow across PKW by adding screen wall with holes to it

In the surrounding region of the Piano Key Weir where the piano key weir creates a distinguish, complicated, and four-dimensional flow field, these are the flow over the back crest of the inlet key, the front crest of the outlet key, and the flow over the lateral wall, and flow through holes in the lateral wall, the four separate types of flow combine to form the flow across the PKW as shown in Figure4.6.

Figure 4.6: The flow across inlet and outlet key of PKW by adding screen wall with holes to it at low head of flow $(H_1/P < 0.2)$.

We note in this case that the flow surface has become smoother and more flowing than the case in which screen walls were used type-X.

When the flow head is low $(\mathrm{H_1/P} < 0.2)$ the flow approaches the source of the inlet key, and the streamlines of flow remain straight when entering the inlet key, and the slope of the floor pushes the flow upward as shown in Figure 4.7. section A-A.

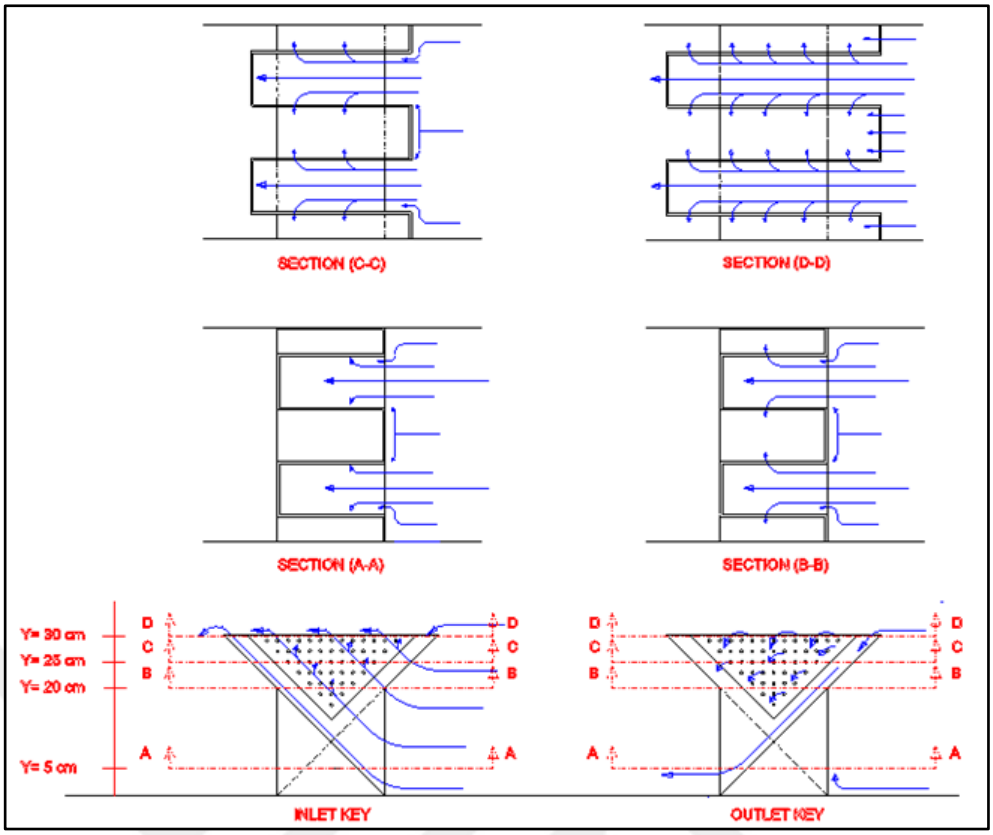

Figure 4.7: The streamlines flow across inlet and outlet key of PKW by adding screen wall with holes to it at low head of flow $(H_1/P < 0.2)$.

As the flow approaches the output key, it splits to both sides at the center line of the outlet key towards the inlet key.

When the flow reaches the level of the screen walls that contain the holes, the partial flow from the front of the inlet key will contribute to the discharge in the side part of it into the outlet key by flowing through the holes of the screen walls, with the form of jets that depends on the diameter and shape of the holes and on the amount of porosity of the screen walls, in addition to the amount of flow entering to the outlet key.

That jet increases as the height of the flow inside the inlet key increases and as the number of holes through it increases. The flow jets from it to the outlet key as in Figure 4.7 section, B-B and section C-C and Figure 4.7.

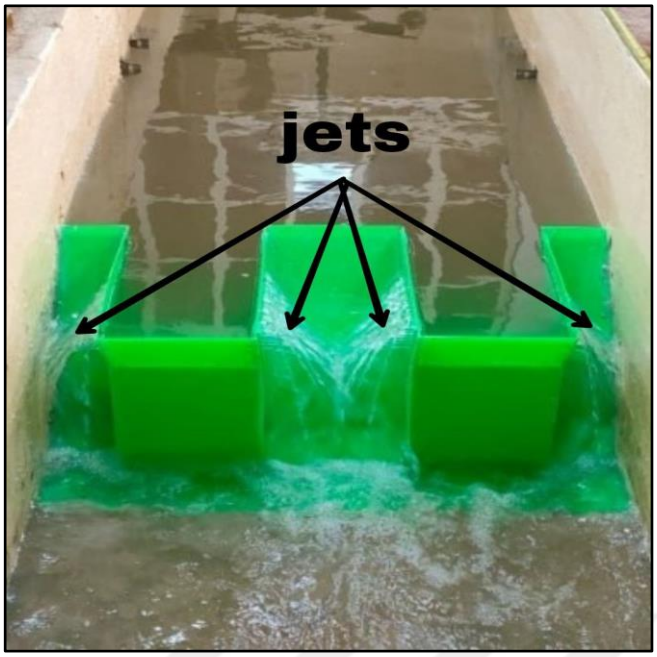

Figure 4.8: The flow jets through the holes in the screen walls when the flow rises to the level of the screen walls and below the level of the crest of PKW.

The flow jets emerging from the holes of the lateral screen walls reduce the hydraulic pressure generated inside the inlet key due to the flow coming to them from the upstream, which helps increase the carrying capacity of the inlet key to receive the flows coming to it from the upstream and thus increase the amount of discharge.

When the flow height reaches the crest level of the inlet key, the surplus part of the flow in the inlet key contributes to the discharge in the lateral part of it in the outlet key from above the crest of the lateral wall, as well as the discharge in the part downstream from the inlet key in the form of a nappe as shown in Figure 4.9.

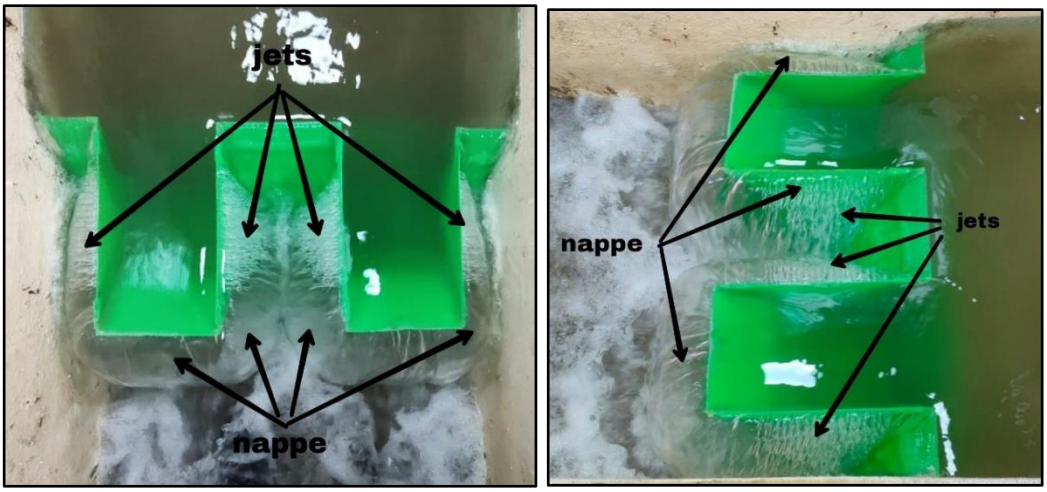

Figure 4.9: The nappes and jets that cross the crest and screen walls of the PKW.

The jets also work to reduce the intensity of the nappes flowing from the outlet Keys, and work to increase the dissipation of energy downstream of inlet key. These holes also increase the amount of water entering the outlet keys of the weir.

The side discharge over the lateral crest, which is in the form of a nappe, combines with the jets emerging from the holes of the screen walls to form a flow that flows into the outlet key, which is also supplied by the flow coming from the surface runoff on the upstream side of the outlet key. Together, they form a turbulent flow system emerging from the outlet key, as shown in Figure 4.9.

When increasing the head of the flow $(H_1/P > 0.2)$ at upstream and increasing the flow velocity, it works to enter the flow rapidly into the inlet key which causes pressure on the inlet key, then increases the lateral flow pressure on the lateral walls of the inlet key and on the added screen walls which containing holes which works to increase the discharge of flow through it, Which makes the flow jetting from it longer and stronger and in a greater amount than it were at normal speed and low running heads case, addition to the nappes that flows from above the downstream of the inlet key as well as from the over the lateral wall that will more and longer and stronger than its were at normal speed and low running heads case as shown in Figure 4.10 & Figure 4.11.

Figure 4.10: The flow across inlet and outlet key of PKW by adding screen wall with holes to it at high head of flow $(H_1/P > 0.2)$.

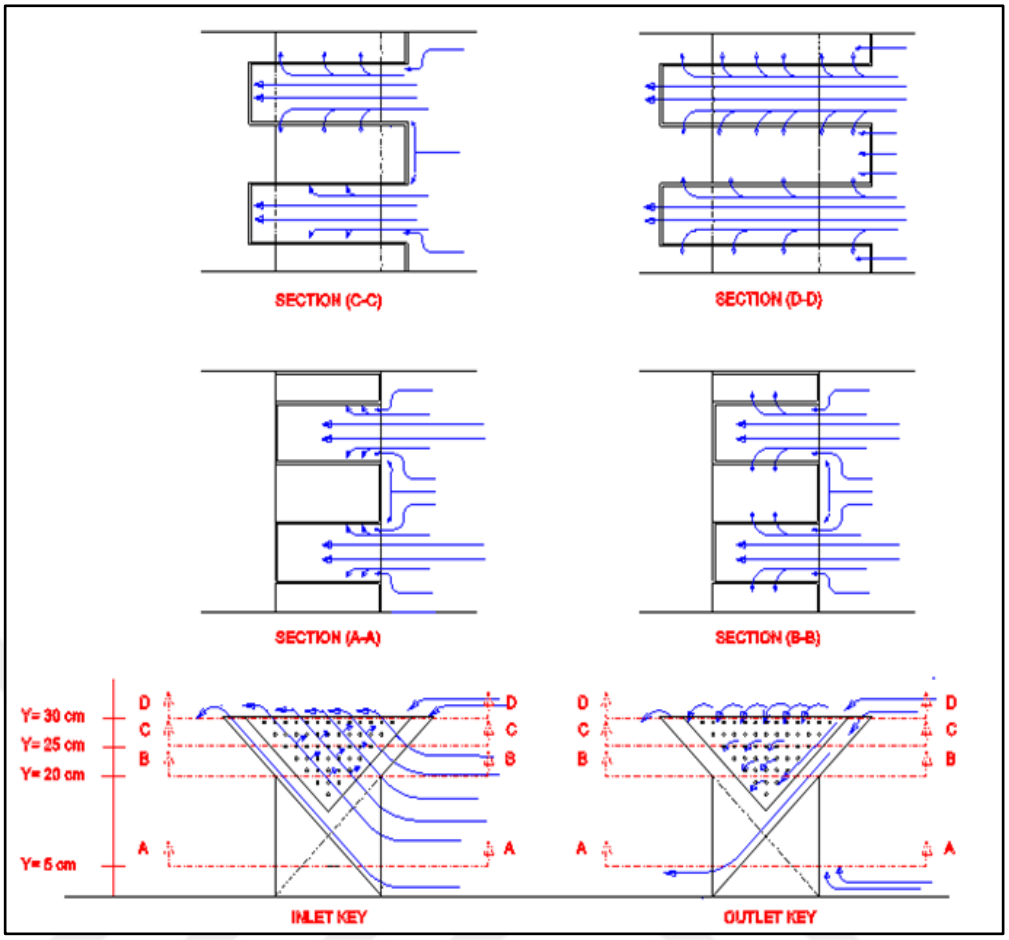

Figure 4.11: The streamlines flow across inlet and outlet key of PKW by adding screen wall with holes to it at high head of flow $(H_1/P > 0.2)$.

The continued increase in the heads of flow and the increase in the velocity of the flow will lead to an increase in the turbulence of the water currents inside the inlet key, which is more pressure on the circumference of the screen wall's holes for the side wall of the inlet key, and this increases the amount of water flowing from the holes to the outlet keys which makes it collide with the corresponding flows of it, in addition to increasing the pressure on the inlet key will increase the amount of nappes flowing over the crest of the lateral walls which increases the amount of water entering the outlet key and makes it in a local flooding.

This works to increase submerge the outlet key and thus leads to a decrease in energy dissipation the downstream of the outlet key. This can be seen by the weakening of the strength and length of the hydraulic jump. The flow disturbance decreases with the increase in the size and number of openings Figure 4.12.

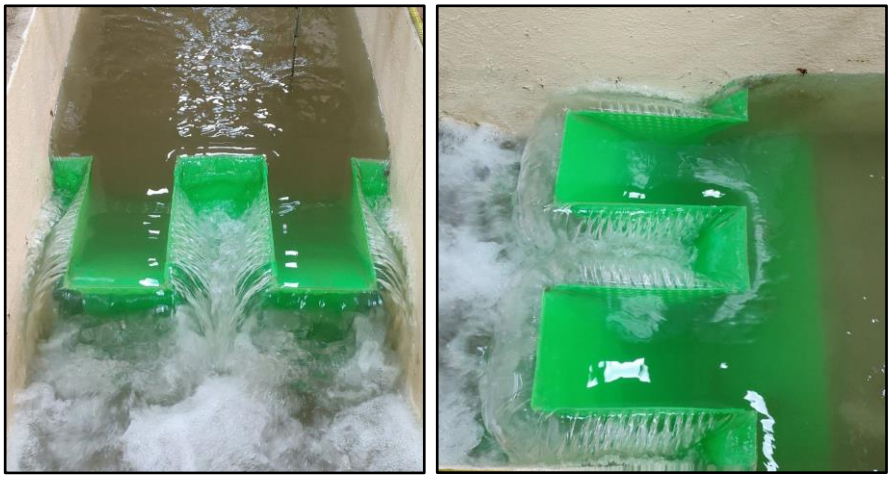

Figure 4.12: The flow across inlet and outlet key of PKW by adding screen wall with holes to it at head of flow much higher than $(H_1/P > 0.2)$.

The initial results showed that with the increasing head of the flowing flow, the discharge coefficient (C_d) decreases. Moreover, for the $(\mathrm{H_1/P} < 0.2)$ the discharge coefficient (C_d) increases with the height of PKW; However, (H_1/P) has a major impact on the coefficient of discharge (C_d).

4.2 Study the Effect of the Geometric Parameters of the Piano Key Weir by Adding Different Screen Walls on the Discharge Coefficient(C_d)

4.2.1 The effect of the ratio of the length of the crest edge of PKW to the width of the weir (L/W) by adding different screen walls on the discharge coefficient (C_d)

In light of the fact that PKW is an unstructured spillway that has been folded into a nonlinear shape, the goal of utilizing a PKW is to extend the total crest length developed for a specific spillway width. The fundamental factor determining the flow rate of PKW is, hence, the (L/W) magnification ratio. This ratio shows that it is possible to optimize the entire length of the crest edge (L) by employing the available width W in the design. The discharge coefficient (C_d) and (L/W) have a direct proportional connection.

The relationship between the discharge coefficient (C_d) and the ratio of the depth of water above the edge of the weir to height of weir (H_1/P) was drawn for different values (L/W) for all research experiments and when the screen walls were type-X without any holes at the same ratio (W_i/W_o) and model heights 30, 28, 26, and 24 cm. The (c) for *(P= 26 cm*), (d*) (P=24 cm*) shows a model of this relationship.

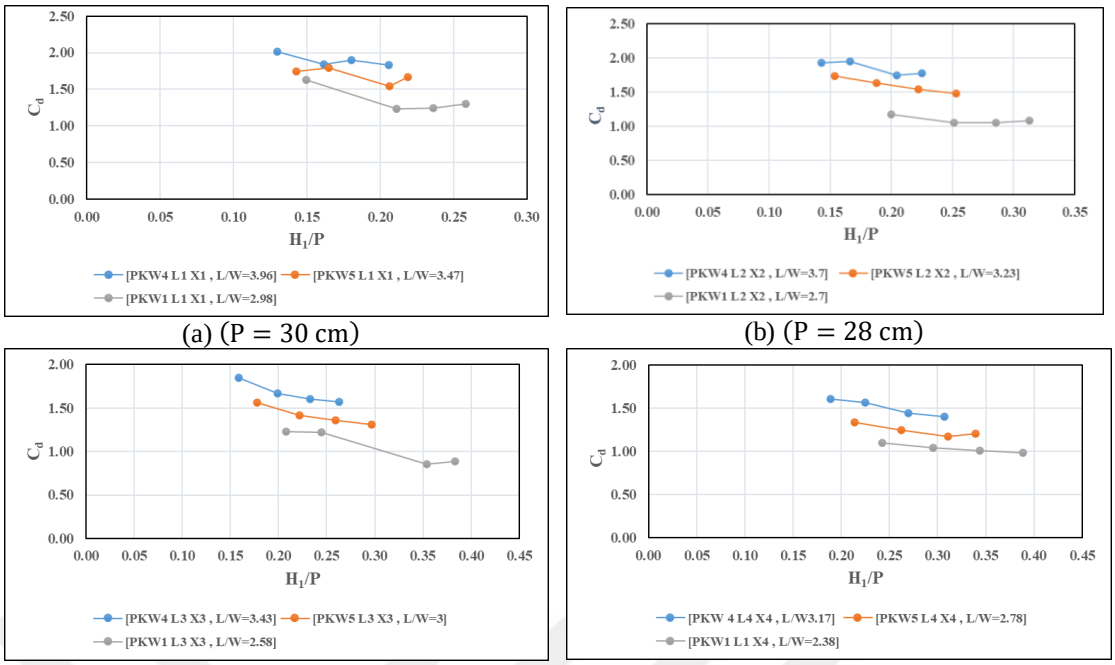

(a) (P = 30 cm) (b) (P = 28 cm)

(c) for (P = 26 cm) (d) (P = 24 cm)

Figure 4.13: The effect of the ratio of the length of crest edge of PKW to the width of the weir (L/W) on the discharge coefficient (C_d) by adding screen walls type-X.

It is clear from the Figure 4.13 that as (L/W) increases, the discharge coefficient increases. This is because of this (L/P) and to increase in the size of the inlet key and also increase in the length of the wet edge of the crest which increases the flow area to the downstream of PKW through the nappes emerging from above the back edges and side edges of the inlet key. This leads to the discharge of larger amounts of flow from the upstream of the weir towards the downstream, and this increase (C_d).

It is also noted that the greater the ratio (H_1/P). This increase leads to a decrease in the discharge coefficient in order to increase the amount of water entering the inlet key, where the inlet key accommodates the flow coming from the upstream as well as the side flow that wraps around the output key. This leads to an increase in pressure in the weir entry key which leads to an increase in the longitudinal velocity, making the flow more turbulent and less smooth and this is consistent with what was proposed by Ouamane & Lempérière, (2006).

The efficiency of the downstream hydro structure is decreased due to energy loss caused by convergent flow at the inlet key. Because of this, the side crest experiences flooding impacts at larger discharges, which decreases the weir's overall discharge efficiency.

It is observed in Figure 4.13 (a) the appearance of a variation of (C_d) with (L/W) which indicates that an increase in (L/W) leads to a significant increase in (C_d). As the increase in (W/L) from 2.98-3.96 at (H_1/P) approaching 1.5, the discharge coefficient increased by 18%. While the increase in the (W/L)ratio from 2.98-3.47 and when (P/H) approaches 1.5 led to an increase in (C_d) by 8%.

Also observed that as the flow height at the source increases while the weir height remains constant, we find that the discharge coefficient decreases, which gives an indication of a decrease in the weir efficiency.

It is noted that the different heights of the weirs gave different values for the (L/W) ratio, but they gave close values for the discharge coefficient within the close (H_1/P) limits.

Then, replacing type-X screen walls by type-B screen walls, which have circular holes with a diameter of $(\Phi = 0.5\ cm)$ and add them to PKW models for the same geometric parameters conducting experiments on them and obtaining results, then drawing the relationship between (C_d) and (H_1/P) for the same previous values of (L/W) ratios, as shown in the Figure 4.14.

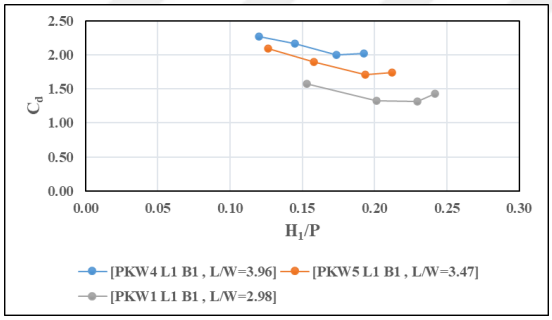

(a) (P = 30 cm)

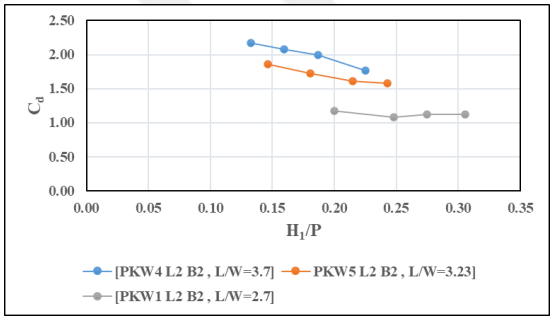

(b) (P = 28 cm)

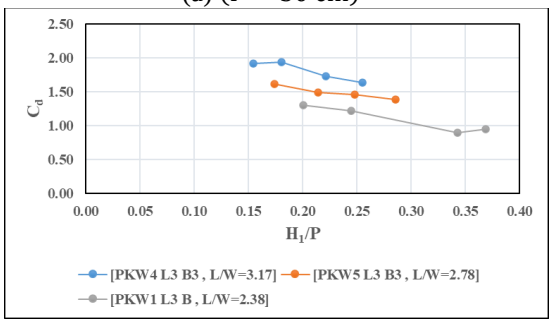

(c) (P = 26 cm)

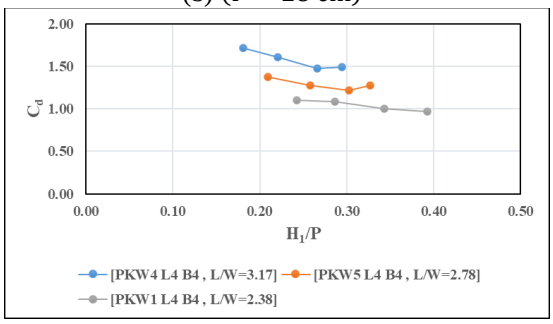

(d) (P = 24 cm)

Figure 4.14: The effect of the ratio of the length of crest edge of PKW to the width of the weir (L/W) on the discharge coefficient (C_d) by adding screen walls type-B

Observed from Figure 4.14 that adding screen walls type-B to the weir models led to an increase in the discharge coefficient over the weir models that do

not have holes in the screen walls and for the same ratio values (L/W) which means the holes in the screen walls were the reason of increasing the discharge coefficient, as the holes worked to reduce the head height at the front of the weir because these holes facilitated the flow through them from the entry key to the outlet key.

However, this increase in the discharge coefficient appears to be relatively small due to the small diameters of the holes. Also, larger ratios (L/W) still achieve a higher discharge coefficient. We also note that by increasing the (H_1/P) ratio for the same W/L ratio, the discharge coefficient decreases due to the increase in the head at the upstream relative to the weir height, which reduces the efficiency of the weir.

Also noted from Figure 4.14 (a) the increasing (L/W) ratio from 2.98 - 3.96 when (P/H) approaches 0.15 and the discharge coefficient increases by 37%, while the increase in the ratio $(W/L)$from 2.98 - 3.47 and when (P/H) approaches 0.15 it leads to an increase in (C_d) by 23%.

Then replacing type-B screen walls with type-D screen walls which have circular holes with a diameter of $(\Phi = 1.0\ cm)$, adding them to PKW models for the same geometric parameters and conducting experiments on them and obtaining results, then drawing the relationship between(C_d) and (H_1/P) for the same previous values of (W/L) ratios, as shown in the (c) *(P=26 cm)*, (d) *(P=24 cm)*.

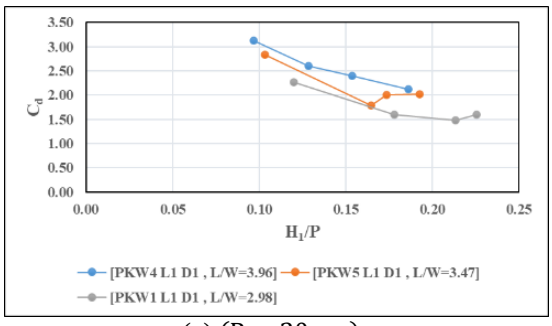

(a) (P = 30 cm)

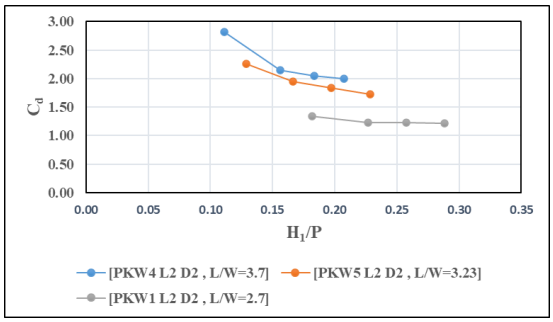

(b) (P = 28 cm)

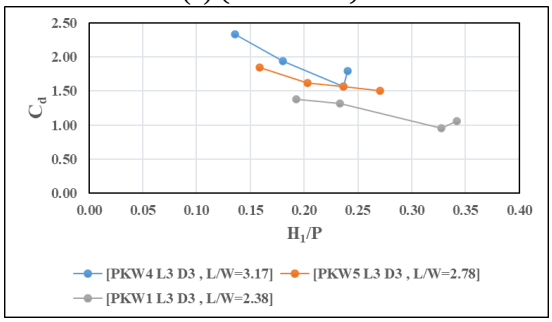

(c) (P = 26 cm)

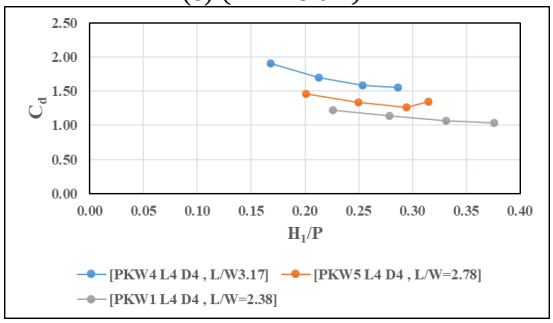

(d) (P = 24 cm)

Figure 4.15: The effect of the ratio of the length of crest edge of PKW to the width of the weir (L/W) on the discharge coefficient (C_d) by adding screen walls type-D.

It is noted that increasing the diameter of the screen wall holes to ($\Phi = 1.0\ cm$), gave a greater increase in the discharge coefficient than the screen walls have holes with diameter ($\Phi = 0.5\ cm$) which led to a higher discharge coefficient (C_d) and the value (H_1/P) is less. The reason is that the screen walls of the type-D that have hole diameter ($\Phi = 1.0\ cm$), allowed a larger amount of water entering the inlet keys to pass through it to the outlet keys in a smoother manner, which reduced the pressure on the inlet keys in receiving the flow coming to them from the upstream, and helped them Also, a large part of it drains through the walls of the screen and is not limited to just passing it over the edge of the weir only. We also note that the outlet key was supplied with larger quantities of water coming to it than the entry key through these holes, and it drained it to the estuary without any submergence occurring.

Noted from Figure 4.15 (a) that increasing the ratio W/L from 2.98 - 3.96 when P/H approaches 1.5 caused the discharge coefficient to increase by 48%, while the increase in the ratio (W/L) from 2.98 - 3.47 and when P/H approaches 1.5 it leads to an increase in (C_d) by 21%.

When drawing a relationship that combines the discharge coefficient (C_d) and the ratio (H_1/P) for the same weir height ($P = 30$) cm, the same ratio (L/W) and using the screen walls type-X, type-B, and type-D as shown in Figure 4.16.

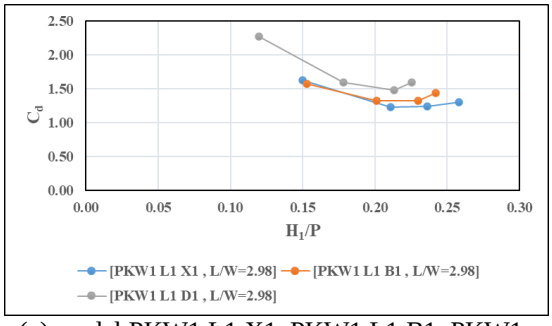

(a) model PKW1 L1 X1, PKW1 L1 B1, PKW1 L1 D1

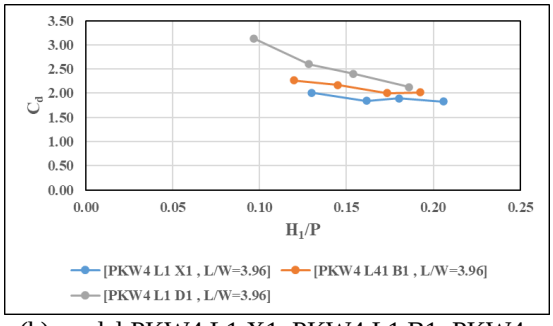

(b) model PKW4 L1 X1, PKW4 L1 B1, PKW4 L1 D1

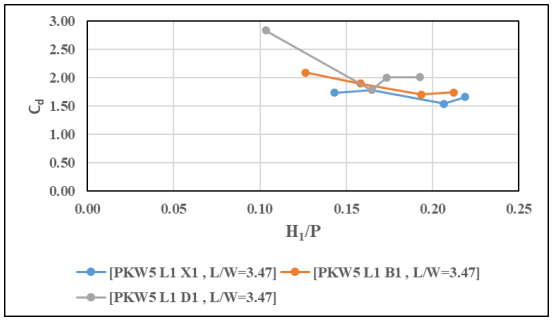

(c) model PKW5 L1 X1, PKW5 L1 B5, PKW5 L1 D1

Figure 4.16: The effect of adding screen walls type X, B and D to the models of PKW that have the same (L/W) and $P = 30\ cm$ on the discharge coefficient (C_d).

TheFigure 4.16 noted that screen walls type-D achieve the largest discharge coefficient for PKW models, followed by screen walls type-B and then type-X, respectively, for all PKW models used. This indicates that as the diameter of the screen wall holes increases, the discharge coefficient (C_d) increases, for an example, when the models PKW4 L1 X1, PKW4 L1 B1, PKW4 L1 D1 and at the ratio $(L/W = 3.96)$ for the same $(H_1/P = 1.5)$ the discharge coefficient increases by increases the diameter of the holes, where the $(C_d = 1.9, 2.2, \text{and } 2.4)$ for screen wall type-X, type-B, and type-D respectively. That is an increase of 15.7% for type-B and 26.3% for type-D.

It was also noted from all the figures linking the relationship between the discharge coefficient and the ratios (L/W) noted that low discharges give the highest values for the discharge coefficient, and high discharges give the lowest values for the discharge coefficient.

It is noted from Figure 4.17 that the effect of increasing the hole diameter of the screen wall on increasing the discharge coefficient is greater than the effect of increasing the geometric parameters (L/W) on it, and this effect increases with the increased diameter hole of the screen walls.

When adding the screen wall type-D to the model PKW1 L1 X1, the discharge coefficient increases from 1.5 - 2.0 by 33.3% at $H_1/P=1.5$, and when comparing model PKW1 L1 X1 with model PKW2 L1 X1 by $(C_d = 1.5, 1.8)$ respectively, at $(H_1/P = 0.15)$ where the resulting increase in the discharge coefficient 20% and this is less from 33.3%.

When (H_1/P) is low, the effect of the screen walls is more prominent than the effect of the geometric parameter (L/W), and as (H_1/P) increases, the effect of the screen walls decreases.

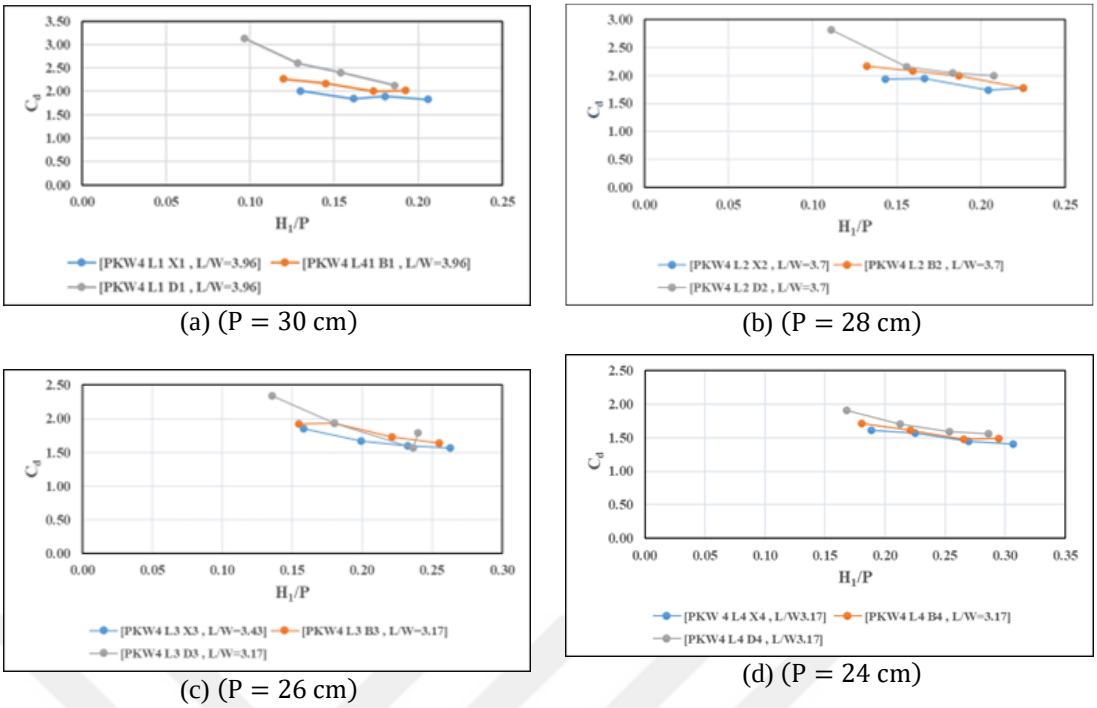

(a) (P = 30 cm) (b) (P = 28 cm)

(c) (P = 26 cm) (d) (P = 24 cm)

Figure 4.17: The effect of addition different screen walls to difference heights of PKW4 model on the discharge coefficient (C_d).

It is noted from Figure 4.17 that models with higher heights give a higher discharge coefficient, and the shorter the model, the lower the discharge coefficient. The reason is that as the height of the model increases, the height of the head upstream of the weir increases, which increases the immersion of the inlet and outlet keys, which reduces the discharge coefficient.

It was also noted that as the heights of the model decreased, the screen walls still gave the higher value of discharge coefficient, with type-D screen walls giving the best discharge, then type-B, then type-X, but this difference decreases with the shortness of the model.

4.2.2 The effect of the ratio of the width of the inlet key to the width of the outlet key of the piano key weir (Wi/Wo) by adding different screen walls on the discharge coefficient (C_d)

When using type X screen walls that do not contain any opening on different piano key weir models, and showing their effect with the ratio of the width of the entry key to the width of the exit key (Wi/Wo) and comparing it with the ratio of the height of the head at the source to the height of the weir for several discharges and for a different number of the heights weir as shown in Figure 4.18.

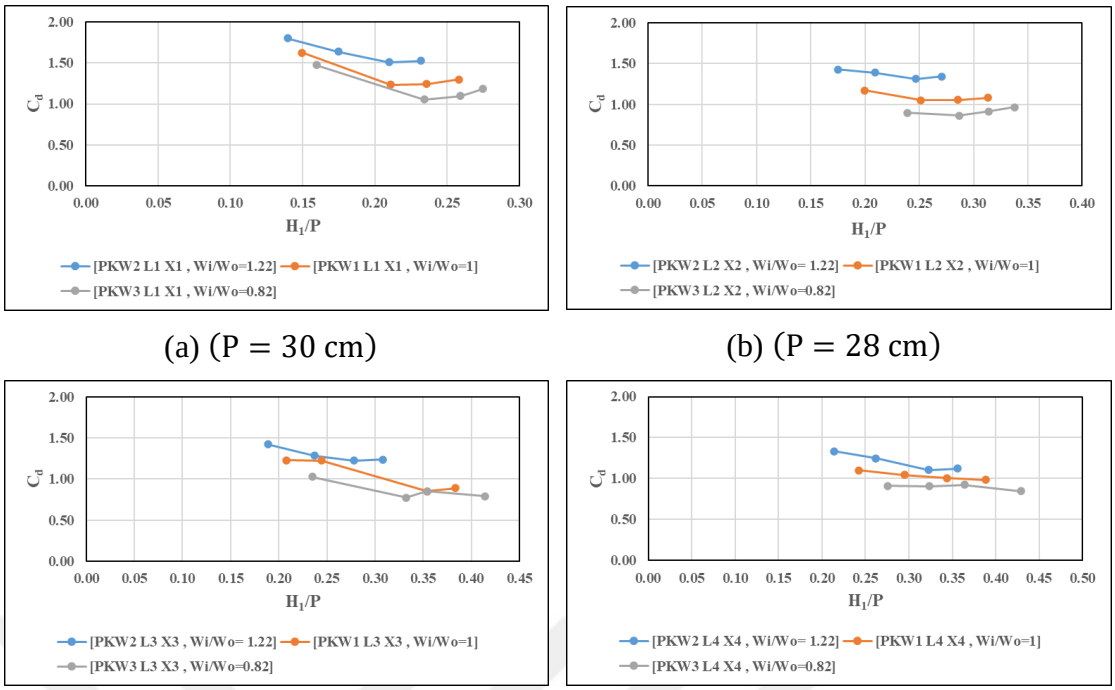

(a) (P = 30 cm) (b) (P = 28 cm)

(c) (P = 26 cm) (d) (P = 24 cm)

Figure 4.18: The effect of the ratio of the width of the inlet key to the width of the outlet key of the piano key weir (W_i/W_o) on the discharge coefficient (C_d) by adding screen walls type-X.

It is noted from the Figure 4.18 that the flow discharge coefficient (C_d) increases with the increase in the width of the inlet key to the width of the outlet key, as the flow discharge coefficient increases with the increase in the ratio (Wi/Wo). An increase in the ratio $(Wi/Wo > 1)$ means that the width of the inlet key is greater than the width of the outlet key of the weir, and this in turn leads to an increase in the carrying capacity of the flow coming from the upstream towards the inlet key, in addition to the flow wrapping around the front of the outlet key and coming to the inlet key, resulting in a decrease in the height of the head for the flow over the weir from the upstream side. The ratio $(Wi/Wo < 1)$ gives a lower discharge coefficient for the flow. The reason is due to the narrowness of the inlet key, which in turn causes a reduction in the carrying area for the flow coming from the upstream side, as the flow faces difficulty in entering the inlet key and notices a rise in the head of flow over the weir from the upstream side.

Also noted that as the height of the piano key weir models decreases and for approximately the same ratios $(H1/P)$, they give a lower discharge coefficient, and this is consistent with what was proposed by Anderson (2011) and Kabiri-Samani and Javaheri (2012), Lempérière and Jun (2005) and Hien et al. (2006).

Then replace type-X screen walls with type-B screen walls, which have circular holes with a diameter of $(\Phi = 0.5)$ cm adding them to PKW models for the same geometric parameters, conducting experiments on them and obtaining results, then drawing the relationship between (C_d) and (H_1/P) for the same previous values of (W_i/W_o) ratios as shown in Figure 4.19.

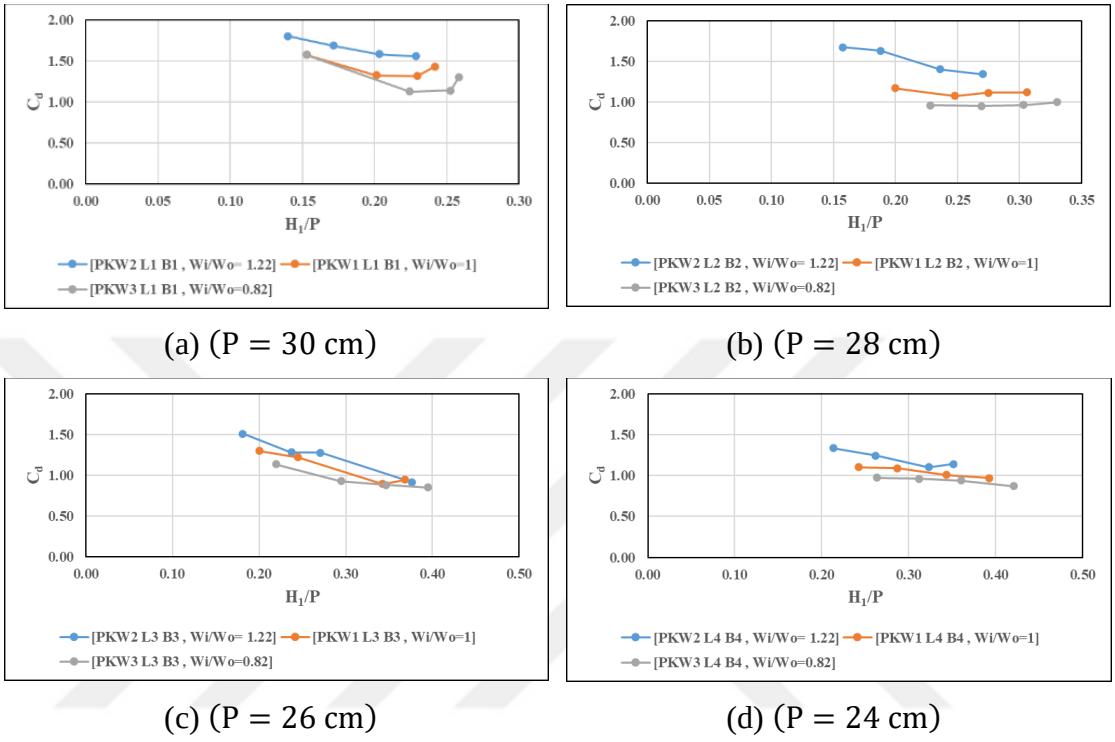

(a) (P = 30 cm) (b) (P = 28 cm)

(c) (P = 26 cm) (d) (P = 24 cm)

Figure 4.19: The effect of the ratio of the width of the inlet key to the width of the outlet key of the piano key weir (W_i/W_o) on the discharge coefficient (C_d) by adding screen walls type-B.

Figure 4.19 show a continued increase in the discharge coefficient for the ratios $(W_i/W_o = 1.22)$ higher than the ratios 1 and 0.82, respectively. Also noted that this increase is slight compared to the previous values of the discharge coefficient values when the screen walls were type-X not equipped with holes, for example in Figure 4.17 (a) and Figure 4.18 (a) notice a very slight increase in the discharge coefficient for the models equipped with type-B screen walls.

The reason is that when the ratio $(W_i/W_o > 1)$ was increased, it led to an increase in the flow coming from the front of the inlet key and into it. It also led to a reduction in the side flow wrapped around the front of the outlet key, which allowed water to flow through the holes in the screen walls, thus making room for an amount of water to enter greater than the water inside the inlet key and thus reduces the head at the upstream of the weir, but by reducing the ratio $(W_i/W_o < 1)$ lead to an

increase in the speed of the side flow which wraps around the outlet key and then enters the inlet key which will impede the flow of water from Through the screen holes, this is what noted in Figure 4.18 for the values of $(W_i/W_o = 1 \text{ and } 0.82)$in which the discharge coefficient increases slightly.

When replacing type-B screen walls with type-D screen walls that have openings with circular diameter $(\Phi = 1.0\ cm)$, and adding them to piano key weir models within the same geometric parameters, conducting experiments on them and drawing the relationship between (C_d) and (H_1/P) for the same Previous values of (W_i/W_o) as shown in Figure 4.20.

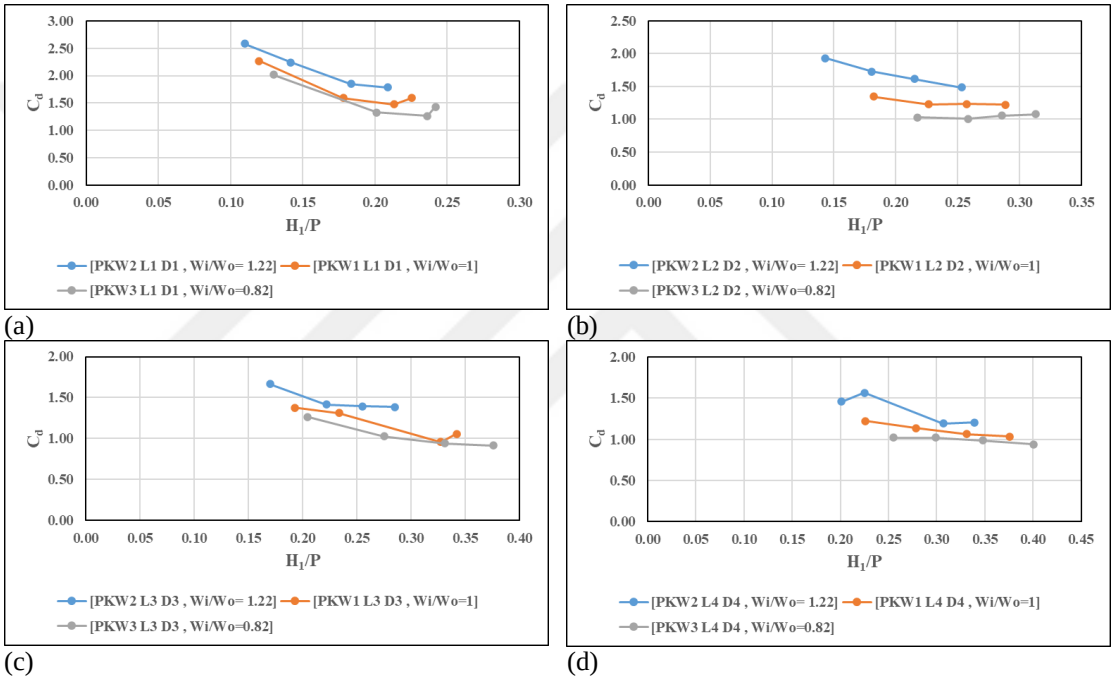

Figure 4.20: The effect of the ratio of the width of the inlet key to the width of the outlet key of the piano key weir (W_i/W_o) on the discharge coefficient (C_d) by adding screen walls type-D.

When observing Figure 4.20 (a), notice that the discharge coefficient for the different ratios (W_i/W_o) has increased noticeably, as the flow discharge coefficient at the $(P = 28\ cm)$ and the $(H_1/P = 1.5)$ for ratio $(W_i/W_o = 1, \text{and } 1.22)$ has increased by 25%, and 50%, respectively, compared to what was in the case of type-X screen walls. Also noted a decrease in the height of the head (H) of the flow at the upstream when using larger opening diameters. The reason is the increase in the amount of water that the holes allow to pass through the screen walls are type-D from the inlet key to the outlet keys, which thus works to reduce the pressure on the inlet keys as a result of the quantities of water coming into it from the upstream.

It is also noted that as the height of the water upstream of the weir increases in relation to the height of the weir, this will adversely affect the values of the discharge coefficient.

When drawing a relationship that combines the discharge coefficient (C_d) and the ratio (H_1/P) for the same weir height $(P = 30)$, the same ratio (W_i/W_o) and using the screen walls X, B, and D as shown in Figure 4.21.

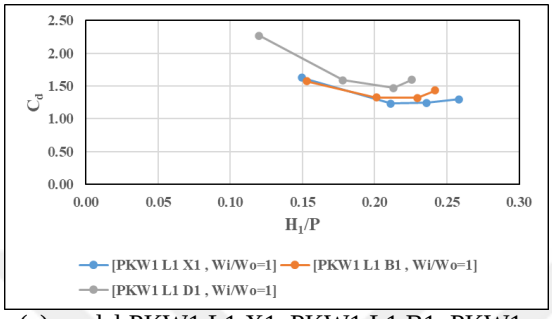

(a) model PKW1 L1 X1, PKW1 L1 B1, PKW1 L1 D1

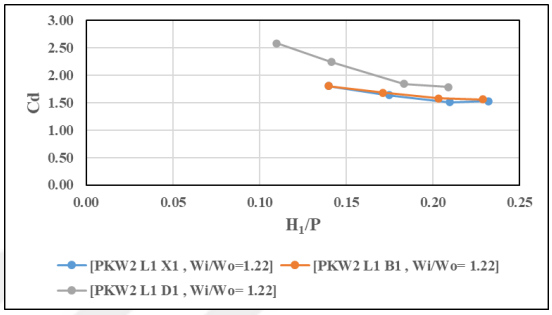

(b) model PKW2 L1 X1, PKW2 L1 B1, PKW2 L1 D1

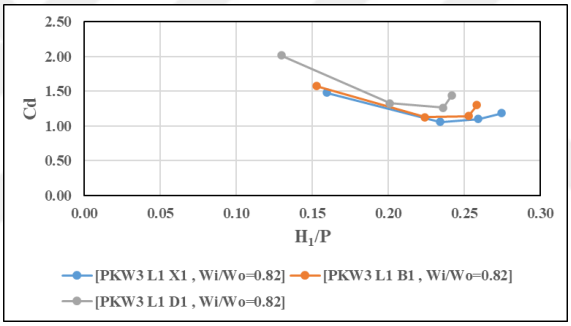

(c) model PKW3 L1 X1, PKW3 L1 B1, PKW3 L1 D1

Figure 4.21: The effect of adding screen walls type-X, type-B, and type-D to the models of PKW that have the same (W_i/W_o), and $P = 30\ cm$ on the discharge coefficient (C_d).

The Figure 4.21 noted that screen walls type-D achieve the largest discharge coefficient for PKW models, followed by screen walls type-B and then type-X, respectively, for all PKW models used. That indicates to the hole diameter of the screen wall increases with the discharge coefficient (C_d) increasing at the value of (W_i/W_o) a constant.

As an example, when used the models PKW3 L1 X1, PKW3 L1 B1, PKW3 L1 D1 and at the ratio $(W_i/W_o = 0.82)$, PKW2 L1 X1, PKW2 L1 B1, PKW2 L1 D1 and at the ratio $(W_i/W_o = 0.82)$ for the same $(H_1/P = 0.2)$, the discharge coefficient increases by increases the diameter of the holes, where the $(C_d = 1.55, 1.6 \text{ and } 1.9)$ for screen wall type-X, type-B, and type-D respectively. That is an increase of 3.2% for type-B, and 16% for type-D.

It was also noted from all the figures linking the relationship between the discharge coefficient, and the ratios $(W_i/W_o = 1.22, 1.0, \text{and } 0.82)$ noted that low discharges give the highest values for the discharge coefficient, and high discharges give the lowest values for the discharge coefficient.

It is noted from Figure 4.22 that the effect of increasing the hole diameter of the screen wall on increasing the discharge coefficient is greater than the effect of increasing the geometric parameters (W_i/W_o) on it, and this effect increases with the increased diameter holes of the screen walls.

When adding the screen wall type-D to the model PKW1 L1 X1, the discharge coefficient increases from 1.5 - 2.0 by 33.3% at $(H_1/P = 1.5)$, and when comparing model PKW1L1X1 with model PKW2 L1 X1 by $(C_d = 1.5, 1.7)$ respectively, at $(H_1/P = 0.15)$ where the resulting increase in the discharge coefficient 13.3% and this is less from 33.3%.

When (H_1/P) is low, the effect of the screen walls is more prominent than the effect of the geometric parameter (W_i/W_o), and as (H_1/P) increases, the effect of the screen walls decreases.

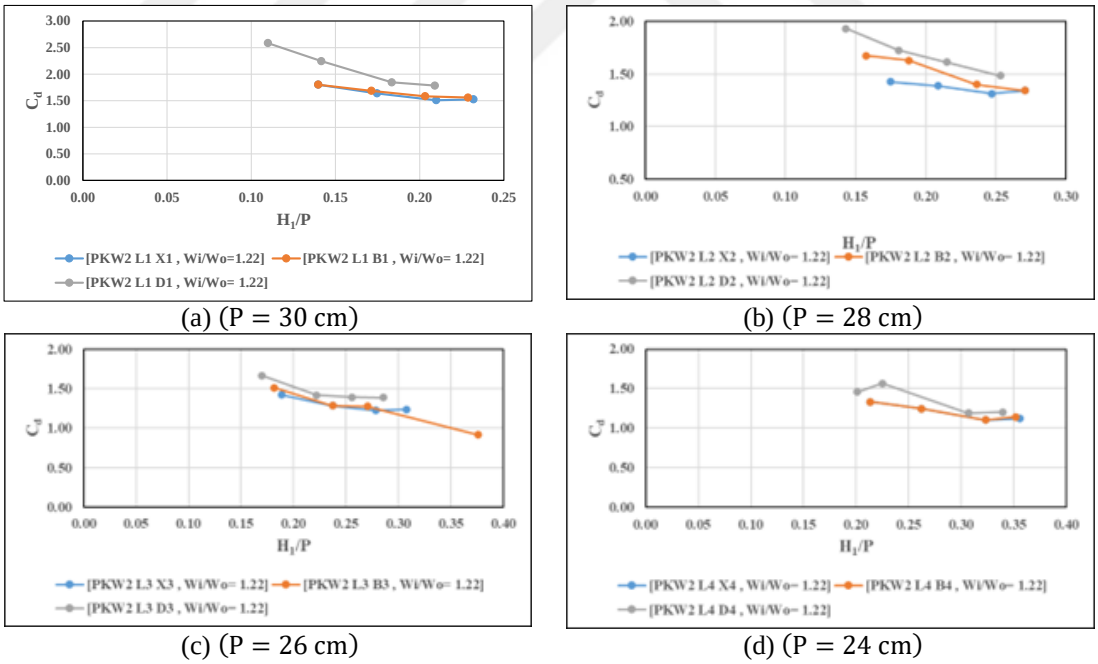

(a) (P = 30 cm) (b) (P = 28 cm)

(c) (P = 26 cm) (d) (P = 24 cm)

Figure 4.22: The effect of addition different screen walls to difference heights of PKW2 model on the discharge coefficient (C_d).

It is noted from Figure 4.22 that models with higher heights give a higher discharge coefficient, and the shorter the model, the lower the discharge coefficient. The reason is that as the height of the model increases, the size of the inlet key

decreases, and this works to raise the water above the weir. This leads to an increase in pressure in the weir entry key, which leads to an increase in the longitudinal velocity, making the flow more turbulent and less smooth, the efficiency of the downstream hydro structure is decreased due to energy loss caused by convergent flow at the inlet key. Because of this, the side crest experiences flooding impacts at larger discharges which decreases the weir's overall discharge coefficient.

It was also noted that as the heights of the model decreased, the screen walls still gave a higher value of discharge coefficient, with type-D screen walls giving the best discharge, then type-B, then type-X, but this difference decreased with the shortness of the model.

4.2.3 The effect of the ratio of the upstream-downstream length of the top of PKW to the height of the weir (B/P), by adding different screen walls on the discharge coefficient C_d

When using type-X screen walls that do not contain any opening on different PKW models, and showing their effect with the ratio of the length of the lateral length of the top of the weir to the height of the weir on the discharge coefficient and comparing it with the ratio of the head height to the weir height for several discharges and for a different number of weir heights as shown in Figure 4.23.

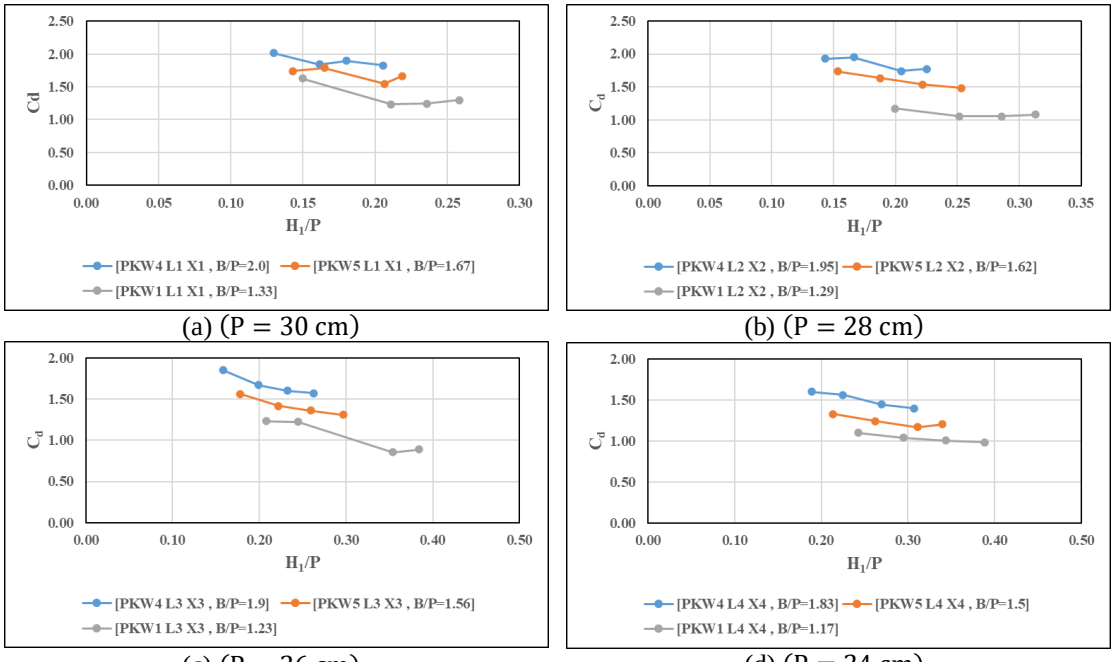

(a) (P = 30 cm) (b) (P = 28 cm)

(c) (P = 26 cm) (d) (P = 24 cm)

Figure 4.23: The effect of the ratio of the upstream-downstream length of the top of PKW to the height of the weir (B/P), on the discharge coefficient (C_d) by adding screen walls type-X.

Noted from the Figure 4.23 that the flow discharge coefficient (C_d) of the piano key weir increases with an increase in the ratio (B/P), where the length of the side edge of the weir top and its height affect the increase and decrease of the discharge coefficient, because increasing the length of the side edge of the weir works to enlarge the inlet flow area to the inlet key and also increases the length of the edge over which the flow flows to cross to the outlet key and downstream, and this in turn reduces the height of the heads in the upstream area.

It is noted that increasing the length of the top edge of the weir increases the discharge coefficient for the same weir heights. Also, increasing the height of the weir reduces the ratio (H_1/P), and this, in turn, increases the discharge coefficient of the weir, and this is consistent with what was proposed by (Machiels et al., 2014).

Also noted in Figure 4.24, when comparing the ratios (B/P) by other ratios of other PKW models that have the same geometric characteristics but at lower heights, noted that the higher heights of the weir models give the highest flow discharge coefficient, and this shows that the discharge coefficient increases by Increasing the height of the weir.

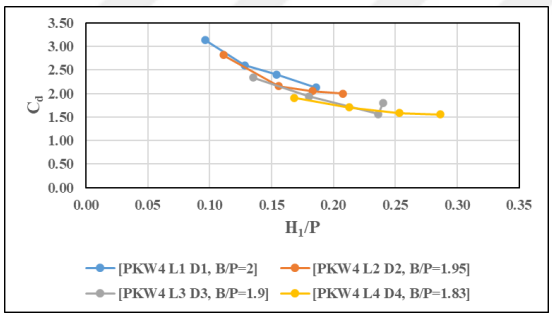

(a) Model PKW4 L1 B1 for $P = 30\ cm$, Model PKW4 L2 B2 for $(P = 28\ cm)$, Model PKW4 L3 B3 for $(P = 26\ cm)$, Model PKW4 L4 B4 for $(P = 24\ cm)$.

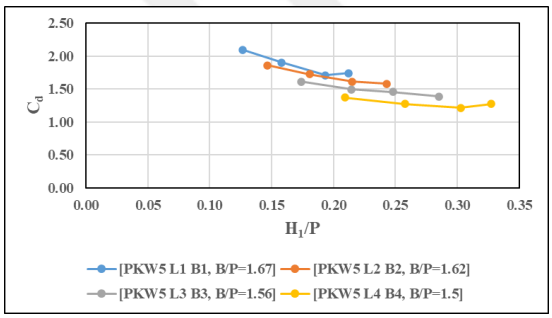

(b) Model PKW5 L1 B1 for $P = 30\ cm$, Model PKW5 L2 B2 for $(P = 28\ cm)$, Model PKW5 L3 B3 for $(P = 26\ cm)$, Model PKW5 L4 B4 for $(P = 24\ cm)$.

Figure 4.24: The effect of the different height of PKW on the discharge coefficient at the same (W_i/W_o), (S_i) and (S_o) on the discharge coefficient (C_d), as an example.

When replacing type-X screen walls with type-B screen walls, which have circular holes with diameter of$(\Phi = 0.5\ cm)$ and adding them to PKW models for the same geometric parameters and conducting experiments on them and obtaining results, then drawing the relationship between (C_d) and (H_1/P) for the same previous values of (B/P) ratios as shown in Figure 4.25.

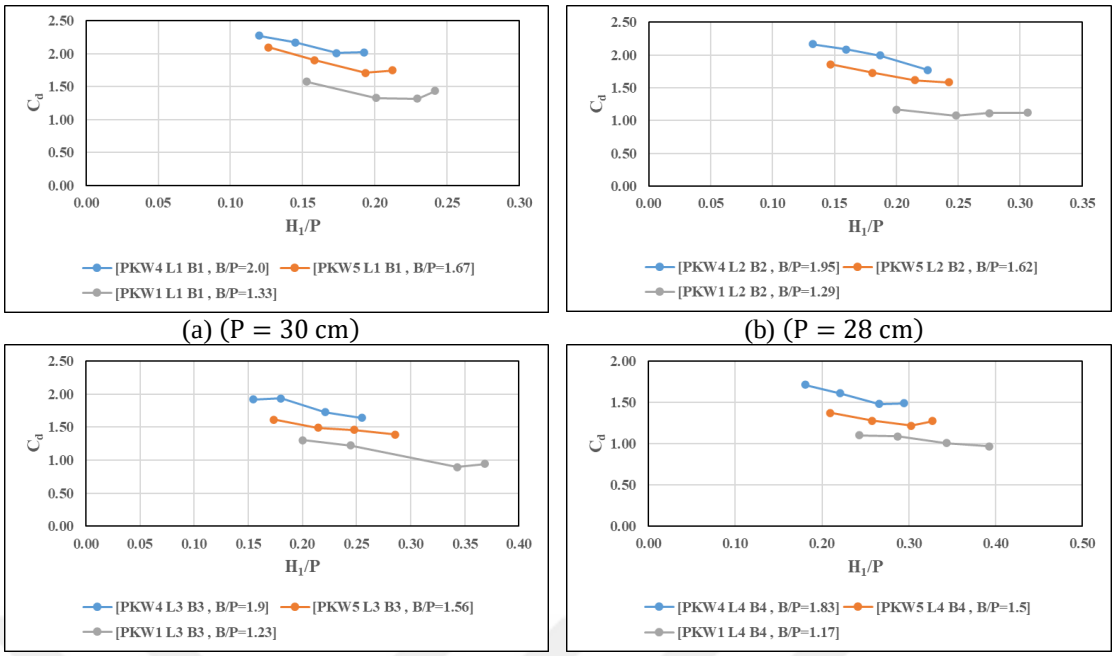

(a) (P = 30 cm) (b) (P = 28 cm)

(c) (P = 26 cm) (d) (P = 24 cm)

Figure 4.25: The effect of the ratio of the upstream-downstream length of the top of PKW to the height of the weir (B/P) on the discharge coefficient (C_d) by adding screen walls type-B.

Noted from Figure 4.25 that with adding type-B screen walls that have holes with diameter $(\Phi = 0.5\ cm)$ cm to the PKW models while keeping the same (B/P) ratios lead to a slight increase in the discharge coefficient at (H_1/P) is constant as noted from a comparison between Figure 4.24 (c) & Figure 4.25 (c) that the percentage of increasing for the discharge coefficient at $(H_1/P = 0.2)$ for the ratios $(B/P = 1.23, 1.56 \text{ and } 1.9)$ are 4%, 3.3% and 6% respectively.

When replacing type-B screen walls by type-D screen walls that have openings with circular diameter $(\Phi = 1.0\ cm)$, and adding them to piano key weir models within the same geometric parameters, conducting experiments on them and drawing the relationship between (C_d) and (H_1/P) for the same Previous values of (B/P) as shown in Figure 4.26.

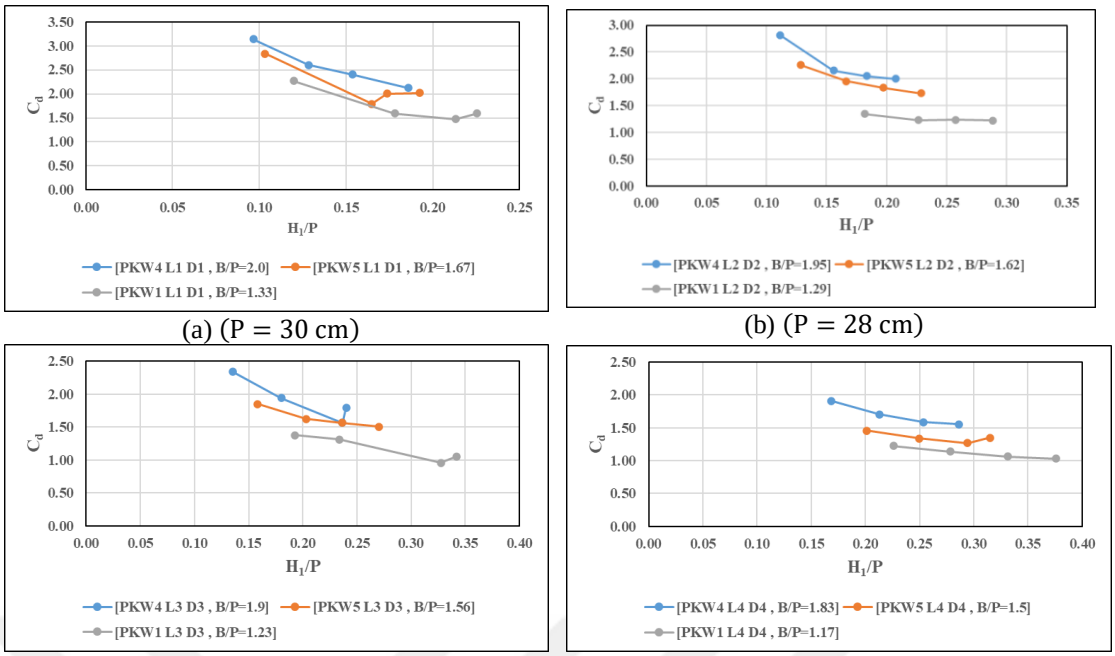

(a) (P = 30 cm) (b) (P = 28 cm)

(c) (P = 26 cm) (d) (P = 24 cm)

Figure 4.26: The effect of the ratio of the upstream-downstream length of the top of PKW to the height of the weir (B/P) on the discharge coefficient (C_d) by adding screen walls type-D.

The Figure 4.27 noted an increase in the coefficient of discharge for all ratios B/P, as well as a decrease in the values of the ratio (H_1/P).

A comparison between the walls of a screen type-D and type-X from the Figure 4.23& (c) Figure 4.26 noted at the value of $(H_1/P = 0.2)$ that the percentage increase in the discharge coefficient increases for the ratios $(B/P = 1.23, 1.56 \text{ and } 1.9)$ by 12%, 6.7%, and 6%, respectively. The reason for this is the flow occurring through the holes in the screen walls, which allows water to pass through them from the inlet key to the outlet key in the downstream direction. This works to reduce the pressure occurring in the inlet key as a result of the accumulation of additional water coming to it from the upstream side due to the increase in the length of the side edge inlet and outlet key.

When drawing a relationship that combines the discharge coefficient (C_d) and the ratio (H_1/P) for the same weir height $(P = 30\ cm)$, the same ratio (B/P) and using the screen walls type-X, type-B, and type-D, the following Figure 4.27 is obtained.

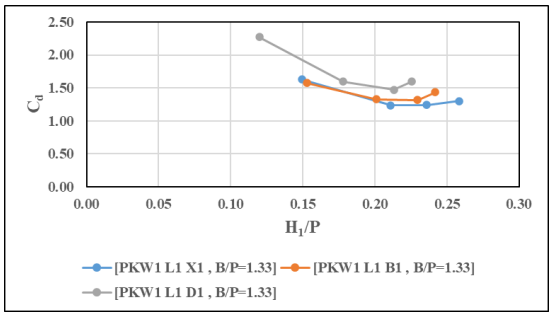

(a) model PKW1 L1 X1, PKW1 L1 B1, and PKW1 L1 D1

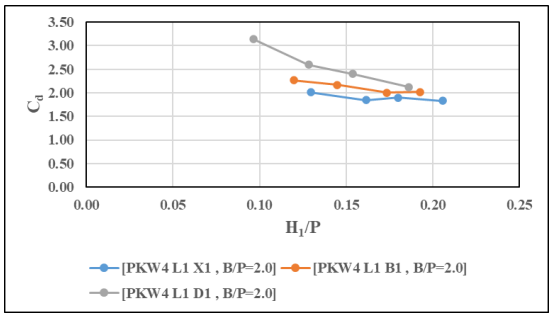

(b) model PKW4 L1 X1, PKW4 L1 B1, and PKW4 L1 D1

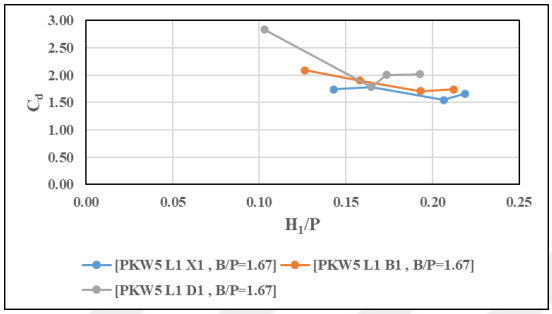

(c) model PKW5 L1 X1, PKW5 L1 B1, and PKW5 L1 D1

Figure 4.27: The effect of adding screen walls type-X, type-B and type-D to the models of PKW that have the same (B/P), (W_i/W_o), and $P = 30\ cm$ on the discharge coefficient (C_d).

The Figure 4.27 noted that screen walls type-D achieve the largest discharge coefficient for the piano key weir models, followed by screen walls type-B and type-X, respectively, for all PKW models used, this indicates that as the opening diameter of the screen wall increases, the discharge coefficient (C_d) increases. As an example, when used the models PKW5 L1 X1, PKW5 L1 B1, PKW5 L1 D1 and at the ratio $(B/P = 1.67)$, $(W_i/W_o = 1)$ and the ratio $(H_1/P = 0.15)$, the discharge coefficient increases by increasing the diameter of the holes, where the $(C_d = 1.6, 2.0, \text{and } 2.1)$ for screen wall type-X, type-B, and type-D respectively. That is an increase 25% for type-B, and 31% for type-D.

It was also noted from all the figures linking the relationship between the discharge coefficient and the ratios (B/P), noted that low discharges give the highest values for the discharge coefficient, and high discharges give the lowest values for the discharge coefficient.

It is noted from Figure 4.27 that the effect of increasing the hole diameter of the screen wall on increasing the discharge coefficient is greater than the effect of increasing the geometric parameters (B/P), on it, and this effect increases with the increased diameter holes of the screen walls.

When adding the screen wall type-D to the model PKW1 L1 X1, the discharge coefficient increases from 1.5 - 2.0 by 33.3% at $(H_1/P = 1.5)$, and when comparing model PKW1 L1 X1 with model PKW4 L1 X1 by $(C_d = 1.5, 1.8)$ respectively, at $(H_1/P = 0.15)$ where the resulting increase in the discharge coefficient 20% and this is less from 33.3%.

When (H_1/P) is low, the effect of the screen walls is more prominent than the effect of the geometric parameter (B/P), and as (H_1/P) increases, the effect of the screen walls decreases.

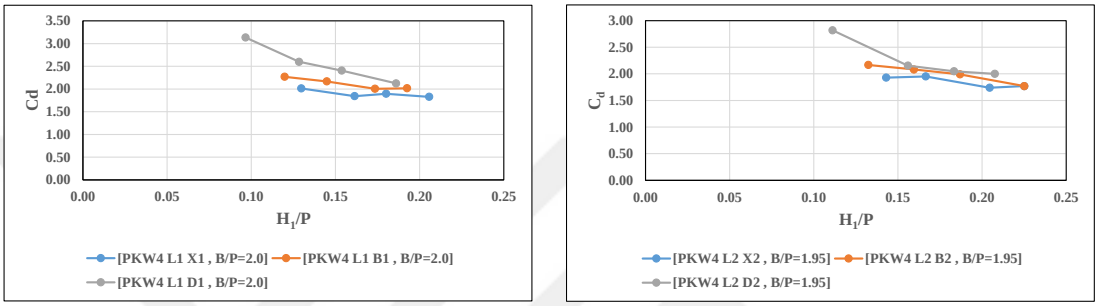

(a) (P = 30 cm)

(b) (P = 28 cm)

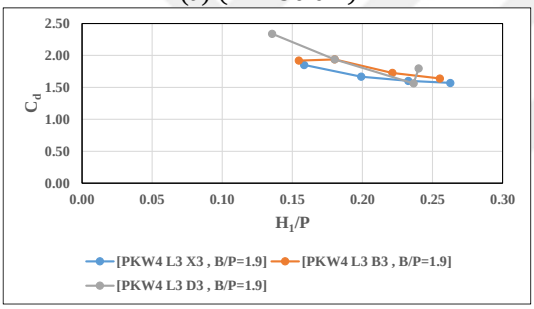

(c) (P = 26 cm)

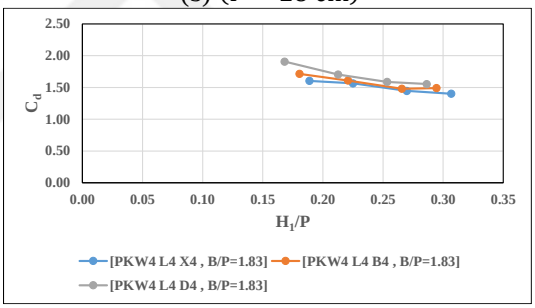

(d) (P = 24 cm)

Figure 4.28: The effect of addition different screen walls to difference heights of PKW4 model on the discharge coefficient (C_d).

It is noted from Figure 4.28 that models with higher heights give a higher discharge coefficient, and the shorter the model, the lower the discharge coefficient. The reason is that as the height of the model increases, the length of the overhang of PKW shortens, leading to shortness of the length of the edge of the weir, which reduces the discharge coefficient.

It was also noted that as the heights of the model decreased, the screen walls still gave the higher value of discharge coefficient, with type-D screen walls giving the best discharge, then type-B, then type-X, but this difference decreases with the shortness of the model.

4.2.4 The effect of adding screen walls that have holes with different diameters to PKW on the discharge coefficient (C_d)

The relationship between the flow discharge coefficient (C_d) and the ratio (H_1/P) was drawn by adding screen walls of type-X, type-A, type-B, type-C, type-D, and type-E have holes with different diameters to PKW models, which have the same geometric parameters but With different weir heights, Where the screen walls type-X no have holes, and the screen walls type-A have holes with diameter ($\Phi = 0.35\ cm$), type-B have holes with diameter ($\Phi = 0.5\ cm$), type-C have holes with diameter ($\Phi = 0.7\ cm$), type-D have holes with diameter ($\Phi = 1.0\ cm$), type-E have holes with diameter ($\Phi = 1.4\ cm$), as shown in Figure 4.29.

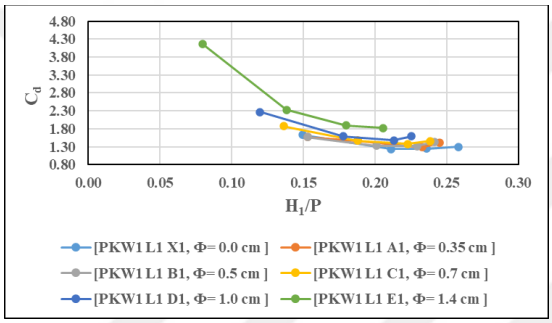

(a) model PKW1 L1 X1, PKW1 L1 A1, PKW1 L1 B1, PKW1 L1 C1, PKW1 L1 D1, PKW1 L1 E1

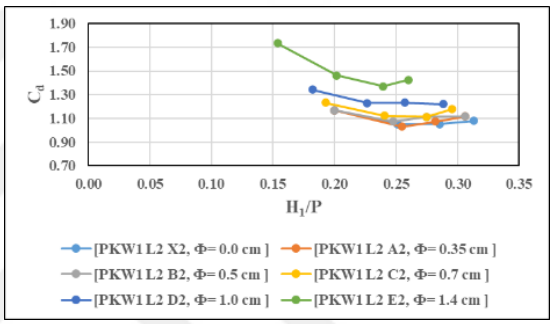

(b) model PKW1 L2 X2, PKW1 L2 A2, PKW1 L2 B2, PKW1 L2 C2, PKW1 L2 D2, PKW1 L2 E2

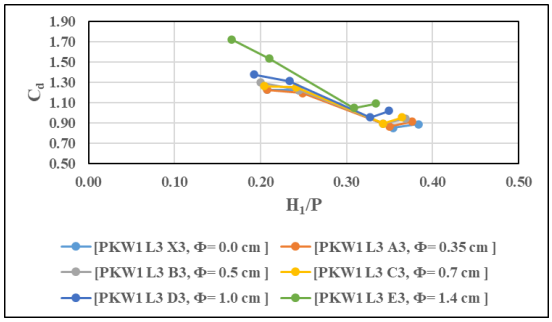

(c) model PKW1 L3 X3, PKW1 L3 A3, PKW1 L3 B3, PKW1 L3 C3, PKW1 L3 D3, PKW1 L3 E3

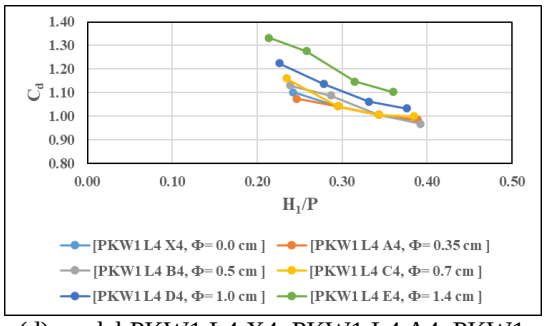

(d) model PKW1 L4 X4, PKW1 L4 A4, PKW1 L4 B4, PKW1 L4 C4, PKW1 L4 D4, PKW1 L4 E4

Figure 4.29: The effect of adding screen walls that have holes with different diameters to PKW on the discharge coefficient (C_d).

Noted from Figure 4.29 the screen walls type-E give the highest coefficient of discharge and the highest efficiency, followed by type-D, type-C, type-B, type-A, and type-X, respectively.

Also noted from the figure that the screen walls type-E have holes with diameter ($\Phi = 1.4\ cm$), giving the largest coefficient of discharge and the lowest

head height at the upstream. This causes the discharge coefficient increase by increasing the diameter of holes in the screen wall.

It is also noted that the diameter of holes in the screen wall achieves a greater discharge coefficient at a decrease (H_1/P).

Also noted that for screen walls of type-X, type-A, type-B, and type-C with holes diameters are less than diameters $(\Phi = 1.4\,cm)$, and $(\Phi = 1.0\,cm)$, the difference in the increase in the discharge coefficient between them is small, as an example, when used the models PKW1 L1 X1, PKW1 L1 A1, PKW1 L1 B1, PKW1 L1 C1, PKW1 L1 D1, PKW1 L1 E1 for the same geometric parameters and the same value of $(H_1/P = 1.5)$ the discharge coefficient increases by increases the diameter of the holes, where the $(C_d = 1.55, 1.6, 1.6, 1.75, 1.9, \text{and } 2.2)$ for screen wall type-X, type-A, type-B, type-C, type-D, and type-E respectively. That is, an increase 3.2% for type-A, and 3.2% for type-B, 12.9% for type-C, 22.6% for type-D, and 42% for type-E respectively.

It is noted that models with higher heights give a higher discharge coefficient, and the shorter the model, the lower the discharge coefficient.

It was also noted that as the heights of the model decreased, the higher diameter of the holes of screen walls still gave the higher value of discharge coefficient, with type-E screen walls giving the best discharge, then type-D, then type-C, type-B, type-A and type-X.

It was also noted from all the figures linking the relationship between the discharge coefficient and the different diameters of holes of screen walls noted that low discharges give the highest values for the discharge coefficient, and high discharges give the lowest values for the discharge coefficient.

4.2.5 The effect of adding screen walls that have holes with different porosity to PKW on the discharge coefficient (C_d)

The relationship between the flow discharge coefficient (C_d) and the ratio (H_1/P) was drawn by adding screen walls of type-X, type-B, type-F, type-G, and type-H, which have holes with different porosity to PKW models, which have the same geometric parameters but with different weir heights as shown in Figure 4.30.

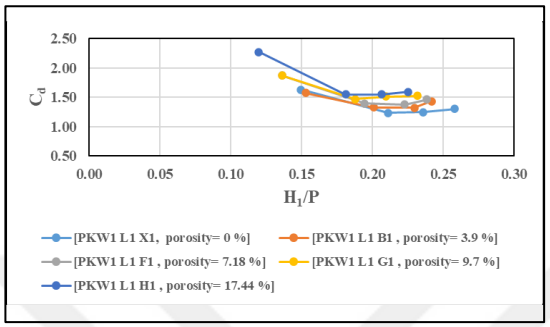

(a) model PKW1 L1 X1, PKW1 L1 B1, PKW1 L1 F1, PKW1 L1 G1, and PKW1 L1 H1

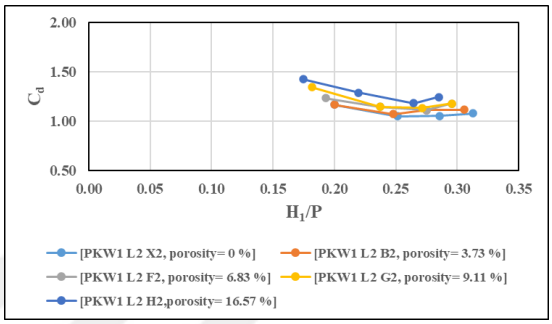

(b) model PKW1 L2 X2, PKW1 L2 B2, PKW1 L2 F2, PKW1 L2 G2, and PKW1 L2 H2

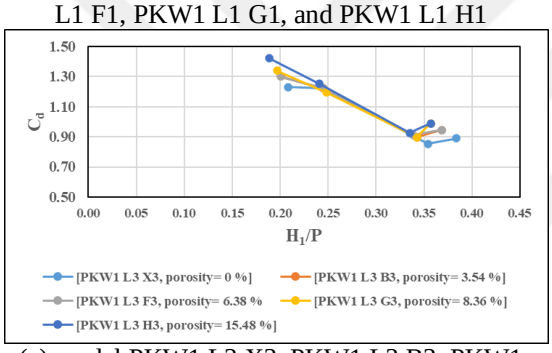

(c) model PKW1 L3 X3, PKW1 L3 B3, PKW1 L3 F3, PKW1 L3 G3, and PKW1 L3 H3

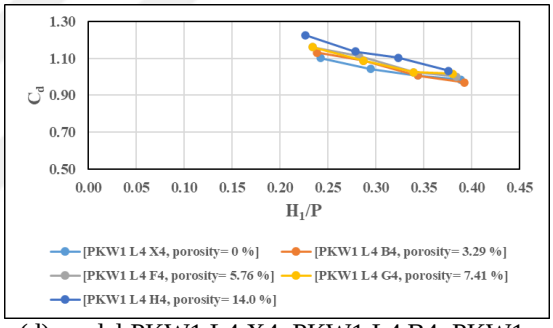

(d) model PKW1 L4 X4, PKW1 L4 B4, PKW1 L4 F4, PKW1 L4 G4, and PKW1 L4 H4

Figure 4.30: The effect of adding screen walls have holes with different porosity to PKW on the discharge coefficient (C_d).

Noted from Figure 4.30 that the discharge coefficient (C_d) increases as we use screen walls with greater porosity, and this increase in the discharge coefficient (C_d) is accompanied by a decrease in heads at the upstream of the weir, which explains this because screen walls with greater porosity allow flow to pass through them in a greater and smoother manner from the inlet key to the outlet key and then downstream which reduces the hydraulic pressure on the inlet key and thus reduces the flow out through the upper edges of the inlet key towards the outlet key and downstream.

Also noted from the figure is that the screen walls type-H gave the largest discharge coefficient and the lowest head height upstream of the weir.

The screen walls type-H gave the highest coefficient of discharge and the highest efficiency, followed by type-G, type-F, and type-B, respectively. Also note that for screen walls of type-G, type-F, and type-B lower porosity, the difference in the increase in the discharge coefficient between them is small, as an example, when used the models PKW1 L1 X1, PKW1 L1 B1, PKW1 L1 F1, PKW1 L1 G1, PKW1 L1 H_1 for the same geometric parameters and the same value of $(H_1/P = 2)$the discharge coefficient increases by increases the porosity of screen walls, where the $(C_d = 1.3, 1.35, 1.4, 1.5 \text{ and } 1.6)$ for screen wall type-X, type-B, type-F, type-G, and type-H respectively. That is, an increase of 3.8% for type-B, and 7.7% for type-F, 15.4% for type-G, and 23% for type-H, respectively.

It was also noted from all the figures linking the relationship between the discharge coefficient, and the different porosity of screen walls noted that low discharges give the highest values for the discharge coefficient, and high discharges give the lowest values for the discharge coefficient.

It is noted that models with higher heights give a higher discharge coefficient, and the shorter the model, the lower the discharge coefficient.

It was also noted that as the heights of the model decreased, that the higher porosity of screen walls still give higher value of discharge coefficient, with type-H screen walls giving the best discharge, then type-G, then type-F, type-B, and type-X.

4.2.6 The effect of adding screen walls that have holes with different shapes to PKW on the discharge coefficient (C_d)

The relationship between the flow discharge coefficient (C_d) and the ratio (H_1/P) was drawn by adding screen walls of type-X, type-D, type-I, type-J, type-K, and type-M that have holes with different shapes but with the same areas as PKW models, which have the same Geometric parameters, but at different weir heights as shown in Figure 4.31.

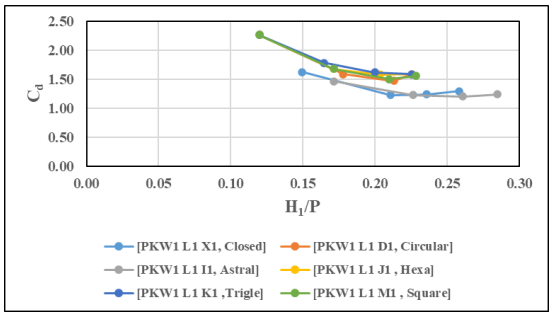

(a) model PKW1 L1 X1, PKW1 L1 D1, PKW1 L1 I1, PKW1 L1 J1, PKW1 L1 K1 and PKW1 L1 M1

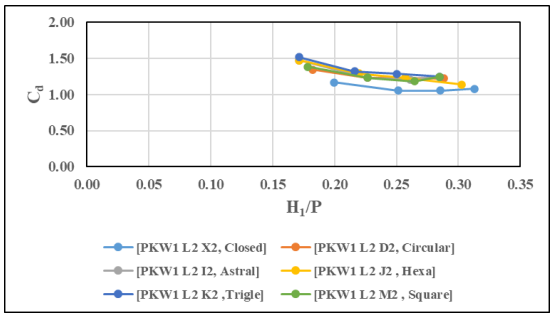

(b) model PKW1 L2 X2, PKW1 L2 D2, PKW1 L2 I2, PKW1 L2 J2, PKW1 L2 K2 and PKW1 L2 M2

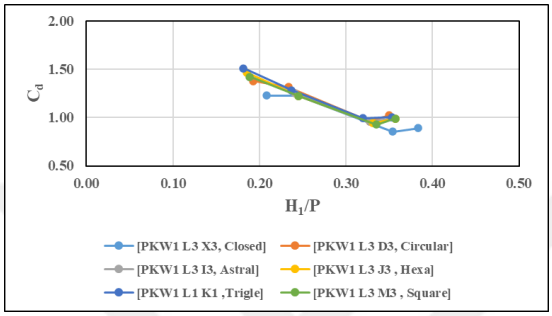

(c) model PKW1 L3 X3, PKW1 L3 D3, PKW1 L3 I3, PKW1 L3 J3, PKW1 L3 K3 and PKW1 L3 M3

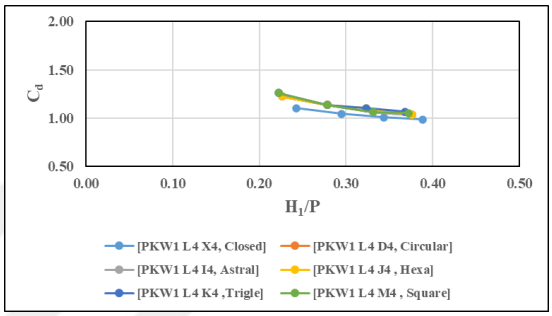

(d) model PKW1 L4 X4, PKW1 L4 D4, PKW1 L4 I4, PKW1 L4 J4, PKW1 L4 K4 and PKW1 L4 M4

Figure 4.31: The effect of adding screen walls have holes with different shapes to PKW on the discharge coefficient (C_d)

Noted from Figure 4.31 that the discharge coefficient (C_d) increases by using screen walls that have holes with different shapes type-D, type-I, type-J, type-K, and type-M than the discharge coefficient if using a screen wall type-X.

It is also noted that the diameter of holes in the screen wall achieves a greater discharge coefficient at a decrease (H_1/P).

But it always remains clear that screen walls type-K with tringle holes give the highest discharge coefficient at all weir heights, followed by screen walls type-J with hexagonal holes, then screen walls type-M with square holes, type-D circular holes, and type-I with astral holes, respectively, as an example, when used the models PKW1 L1 X1, PKW1 L1 D1, PKW1 L1 I1, PKW1 L1 J1, PKW1 L1 K1, PKW1 L1 M1 for the same geometric parameters for the same geometric parameters and the same value of $(H_1/P = 0.2)$ the discharge coefficient increase, Where $(C_d = 1.25, 1.3, 1.5, 1.52, 1.55 \text{ and } 1.6)$ for screen wall type-X, type-I, type-D, type-M, type-J, and type-K respectively. That is, an increase 4% for type-I, 20% for type-D, 21% for type-M, 23% for type-J, and 28% for type-K, respectively.

Noted the Convergence between values of (C_d) for type-K, type-M, type-J, and type-K.

It is noted that models with higher heights give a higher discharge coefficient, and the shorter the model, the lower the discharge coefficient.

It was also noted that as the heights of the model decreased, the screen walls that achieved a higher (C_d) still gave the higher value of discharge coefficient, with type-K screen walls giving the best discharge, then type-J, then type-M, type-D, type-I, and type-X.

It was also noted from all the figures linking the relationship between the discharge coefficient, and the different shapes of the holes of screen walls noted that low discharges give the highest values for the discharge coefficient, and high discharges give the lowest values for the discharge coefficient.

4.3 Studying the effect of the geometric parameters of the piano key weir by adding different screen walls on the Energy Dissipation $((\boldsymbol{E_1 - E_2})/\boldsymbol{E_1})$ and the Residual Energy $(\boldsymbol{E_2/E_1})$

4.3.1 The effect of the ratio of the length of crest edge of PKW to the width of the weir $(\boldsymbol{L/W})$ by adding different screen walls on the energy dissipation $((\boldsymbol{E_1 - E_2})/\boldsymbol{E_1})$ and the residual energy $(\boldsymbol{E_2/E_1})$

The relationship between the Relative Energy Dissipation $((E_1 - E_2)/E_1)$ and the ratio of the depth of water above the edge of the weir to its height (H_1/P) was drawn for different values of the ratio of the length of the edge of the weir to its width (L/W) for all research experiments and when the screen walls were type-X without any holes when the same ratio (W_i/W_o) and model heights 30 cm, 28 cm, 26 cm, and 24 cm. Figure 4.32 shows a model of this relationship.

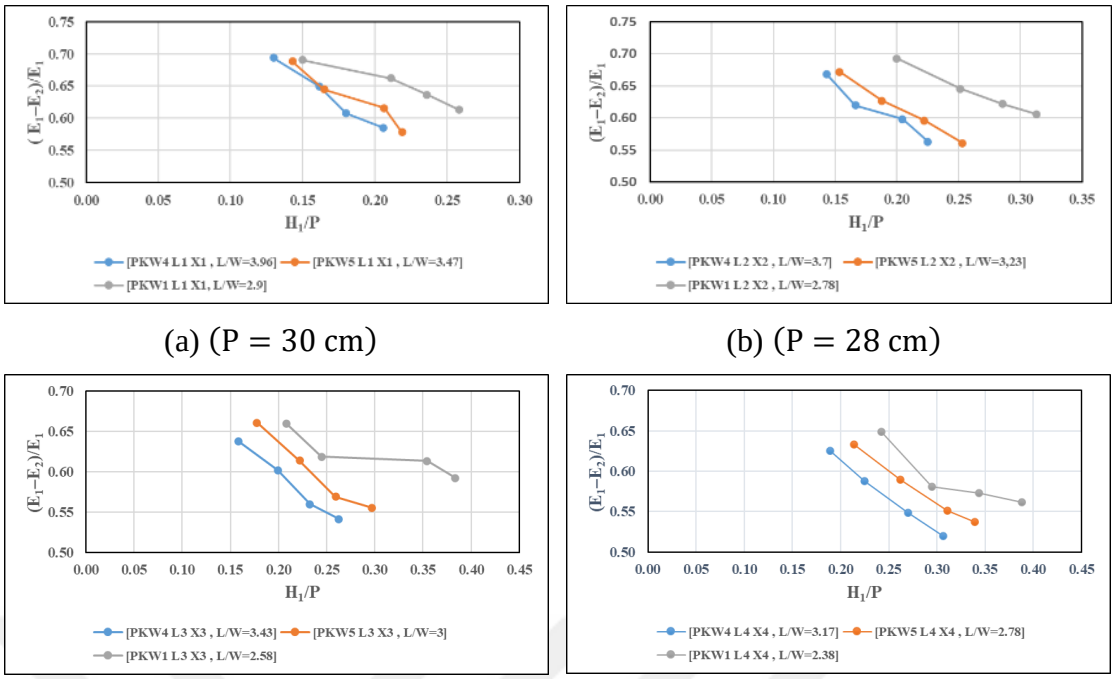

(a) (P = 30 cm) (b) (P = 28 cm)

(c) (P = 26 cm) (d) (P = 24 cm)

Figure 4.32: The effect of the ratio of the length of crest edge of PKW to the width of the weir (L/W) on the relative Energy Dissipation $((E_1 - E_2)/E_1)$ by adding screen wall type-X.

It is clear from the Figure 4.32 that as the ratio of the length of the weir edge to its width (L/W) increases, the Relative Energy Dissipation $((E_1 - E_2)/E_1)$ decreases, as Increasing this ratio leads to an increase in the amount of flow leaving PKW. This is because increasing this ratio leads to an increase in the size of the inlet key, and also increase in the length of the wet edge of the crest which increases the flow area to the downstream of PKW through the nappes emerging from above the back edges and side edges of the inlet key to outlet key. This leads to the discharge of larger amounts of flow from the upstream of the weir towards the downstream and then increases the depth of tailwater, which causes increased force of flow downstream and decreases Energy Dissipation $((E_1 - E_2)/E_1)$; this is consistent with (Eslinger & Crookston, 2020).

It is also noted from Figure 4.32 that the greater the height of the head of flow to the height of the weir, that is, the greater the ratio (H_1/P) this increase leads to a decrease in the Relative Energy Dissipation $((E_1 - E_2)/E_1)$.

Notice from Figure 4.32 (a) that by increasing the (L/W) ratio from 2.9–3.96 when (H_1/P) approaches 0.2 and the Relative Energy Dissipation $((E_1 - E_2)/E_1)$ decreases by 12%, Because increasing the ratio (L/W) means increasing the length

of the wet edge of the weir top, which allows larger amounts of flow to pass by the nappes especially the lateral nappes, which flows above long lateral crest to the outlet key. These nappes collide with the nappes opposite them, and in addition to the flow Coming from the front of the outlet key, all of this will increase the local immersion of the outlet key, which will increase the amount of flow at the downstream of PKW and increase the depth of the tailwater which reduces energy dissipation. This is consistent with(Eslinger & Crookston, 2020).

Type-A of PKW dissipate energy very effectively at low H_1/P, A crucial hydraulic parameter is the PKW's (L/W) ratio. In fact, this ratio demonstrates how successfully a design maximizes the crest length (L) by optimizing the available width W. The flow control section must be situated along the evolved crest length (L) in order to maximize discharge.

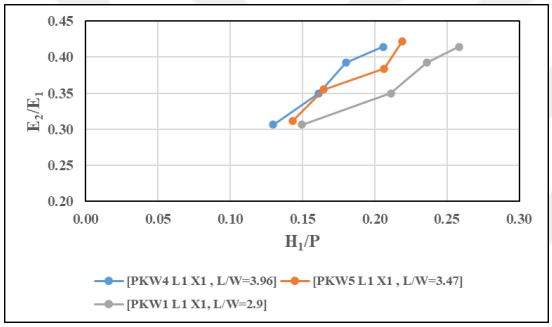

(a) (P = 30 cm)

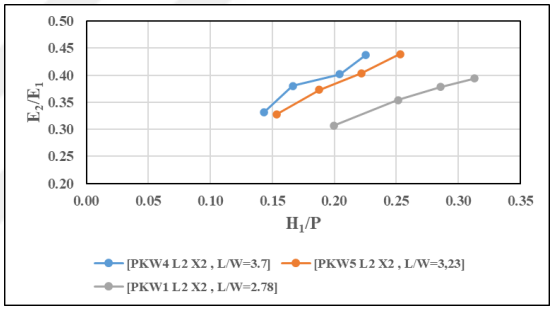

(b) (P = 28 cm)

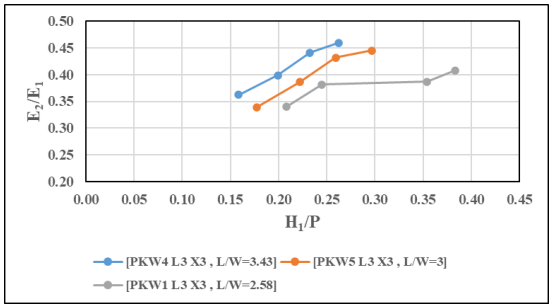

(c) (P = 26 cm)

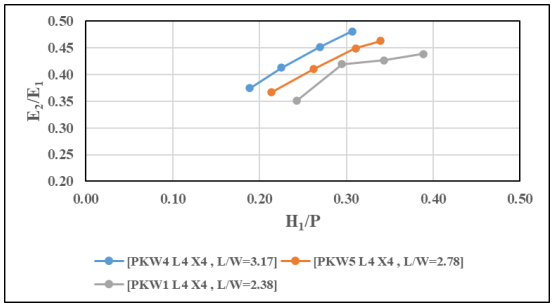

(d) (P = 24 cm)

Figure 4.33: The effect of the ratio of the length of crest edge of PKW to the width of the weir (L/W) on the Residual Energy (E_2/E_1) by adding screen wall type-X.

The Figure 4.33 shows that the greater value of (L/W) leads to an increase in the Residual Energy (E_2/E_1) as the relative energy dissipation in this case is rather lower, which leads to retaining of more energy of the flow in the waterway.

It is also noted in Figure 4.33 that the increase ratio (H_1/P) leads to increase in the Residual Energy (E_2/E_1), in order to increase the amount of water entering the

inlet key, where the inlet key accommodates the flow coming from the upstream as well as the side flow that it wraps around the output key at upstream, This leads to increase in pressure in the weir inlet key which leads to an increase in the longitudinal velocity, and increase the amount of flow from the keys of PKW toward the downstream which cause increase the tail depth and then increase the Residual Energy.

The screen walls type-X that do not contain holes were replaced by the screen walls type-B that contain holes with diameter of ($\Phi = 0.5\ cm$), and installed it on the same models of PKW within the same geometric parameters. Laboratory results were obtained, and by plotting these laboratory results by a relationship between (H_1/P) and energy dissipation ($(E_1 - E_2)/E_1$), the Figure 4.34 was obtained.

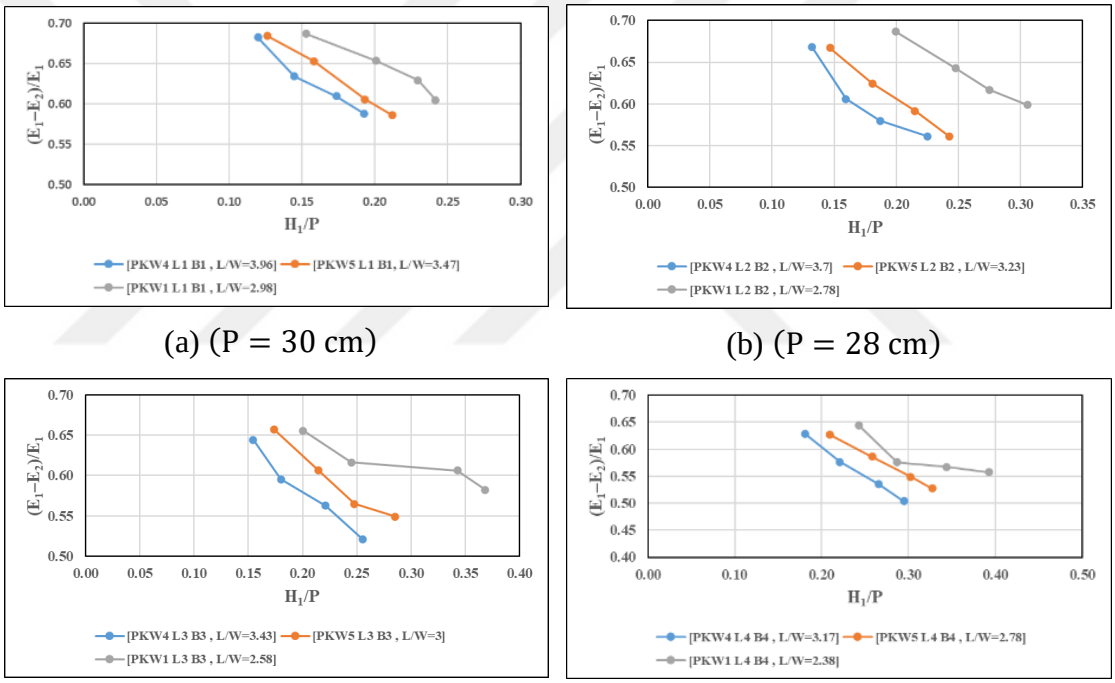

(a) (P = 30 cm) (b) (P = 28 cm)

(c) (P = 26 cm) (d) (P = 24 cm)

Figure 4.34: The effect of the ratio of the length of crest edge of PKW to the width of the weir (L/W) on the relative Energy Dissipation ($(E_1 - E_2)/E_1$) by adding screen wall type-B.

Note that when the screen wall was replaced with type-B, the ratio ($L/W = 2.98$) still gave a higher energy dissipation than the other ratios ($L/W = 3.47, 3.96$).

Also note that by using screen walls of type-B, instead of screen walls of type-X the energy dissipation decreased slightly, in the Figure 4.32 (a) when using screen walls of type-X and when H_1/P=0.2noted that the ratio ($L/W = 2.98$) had the

energy dissipation $((E_1 - E_2)/E_1 = 0.67)$, while in the Figure 4.34 (a) when using a screen wall type-B and at the same discharge, the energy dissipation $((E_1 - E_2)/E_1 = 0.65)$.

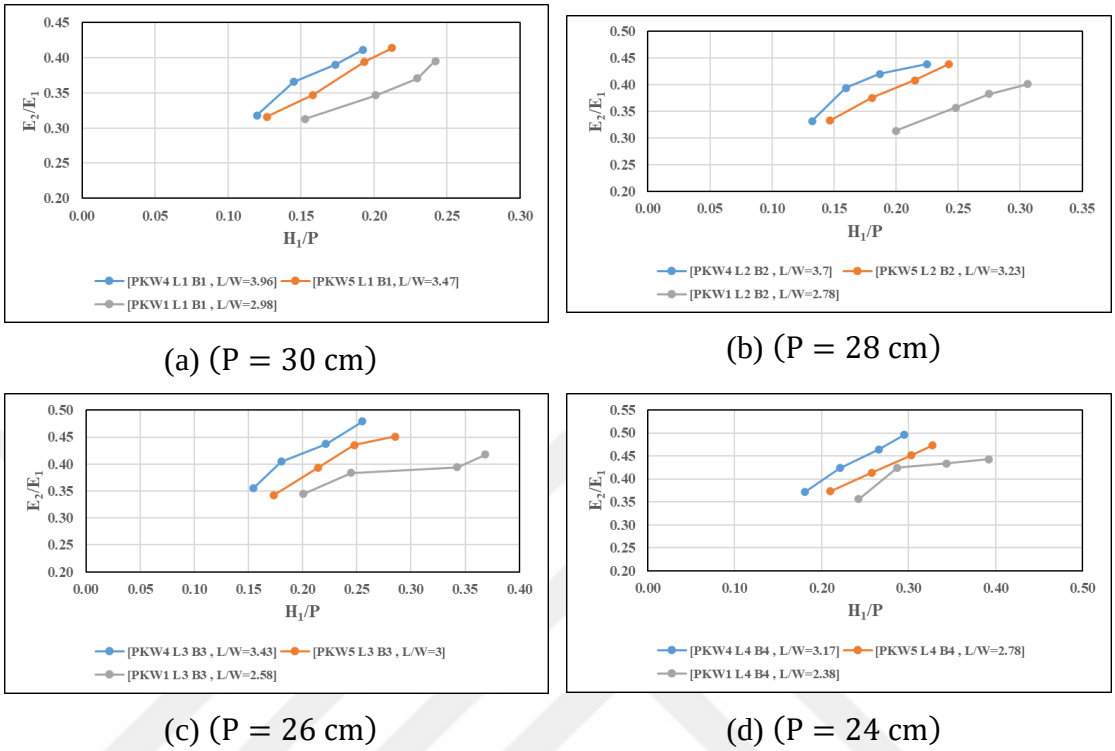

(a) (P = 30 cm) (b) (P = 28 cm)

(c) (P = 26 cm) (d) (P = 24 cm)

Figure 4.35: The effect of the ratio of the length of crest edge of PKW to the width of the weir (L/W) on the Residual Energy (E_2/E_1) by adding screen wall type-B.

The Figure 4.35 shows that the greater the ratio of (L/W) leads to an increase in the Residual Energy (E_2/E_1), where the relative energy dissipation in this case is small, which leads to the flow in the waterway retaining more energy than if the ratio of (L/W) was lower, which causes an increase in energy dissipation, Therefore, the Residual Energy is less.

Noted from Figure 4.35 (a) that when replacing the screen wall with type-B, the ratio $(L/W = 3.97)$ still gives a higher residual energy than the other ratios $(L/W = 3.47 \; and \; 2.98)$ respectively.

Also note that by using type-B screen walls instead of type-X screen walls, the residual energy increased slightly in Figure 4.30 when using type-X screen walls and when $(H_1/P = 0.2)$ noted that the ratio $(L/W = 2.9)$ had the Residual Energy $(E_2/E_1 = 0.34)$ in Figure 4.32 when using a screen wall of type-B and at the same time discharging, and the Residual Energy is 0.35.

When replacing type-B screen walls with type-D screen walls that have an opening circular diameter Φ=1.0 cm and adding them to piano key weir models within the same geometric parameters, conducting experiments on them and drawing the relationship between $((E_1 - E_2)/E_1)$ and (H_1/P) for the same Previous values of (L/W) ratios, the results are obtained as in the Figure 4.36.

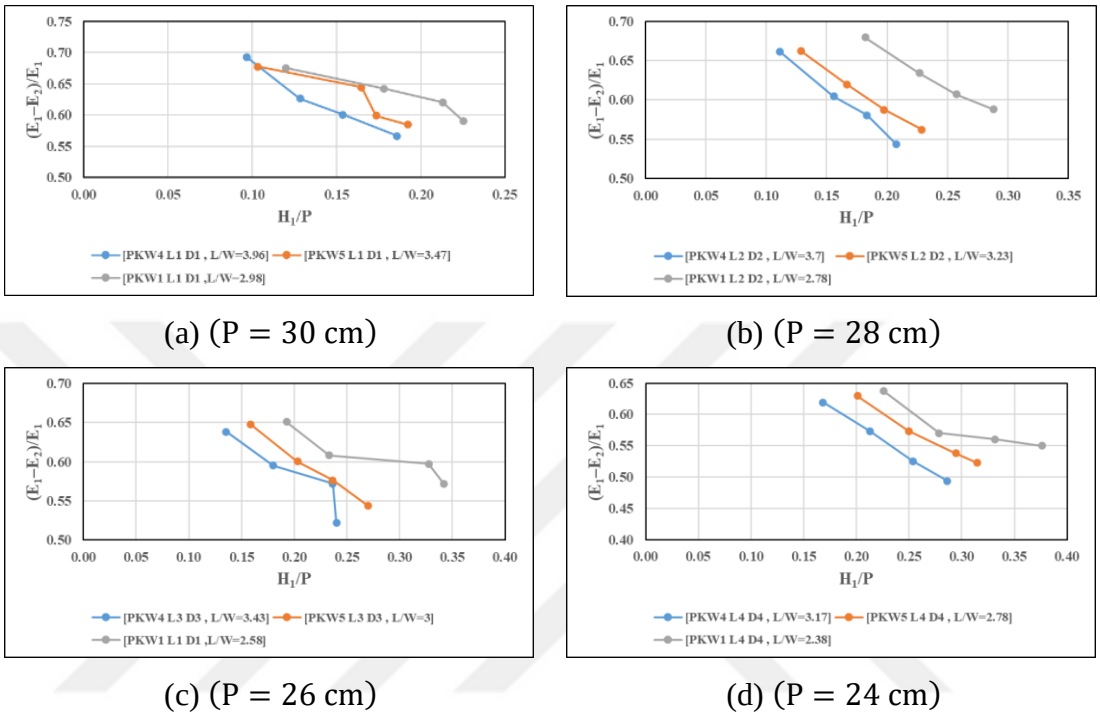

(a) (P = 30 cm) (b) (P = 28 cm)

(c) (P = 26 cm) (d) (P = 24 cm)

Figure 4.36: The effect of the ratio of the length of crest edge of PKW to the width of the weir (L/W) on the relative Energy Dissipation $((E_1 - E_2)/E_1)$ by adding screen wall type-D.

Noted from Figure 4.36 (a), the energy dissipation decreased when using screen wall type-D more than type-B and type-X, respectively.

Which causes an increase in the number of jets inside it, depending on the diameter of the hole in the screen wall. These jets mix and interfere with the nappes jumping over the edge of the side wall, as well as with the flow coming down from the front of the outlet key. This, in turn, causes a relative increase in local immersion of the outlet key. Increasing the local immersion of the outlet key causes a greater amount of flow to be pushed out with light velocity to the toe of PKW, where the flow coming out of the outlet key collides with the tailwater upstream in a somewhat less forceful way than the case of using screen walls without holes, and the collision distance is closer to the toe of the PKW, and this makes the length of the hydraulic jump shorter. In addition, the nappes that jump from the back of the inlet key are

shorter due to the reduction of hydraulic pressure in the inlet key due to the holes of the screen walls and their ability to pass flow through it smoothly. The increase in flow coming from the weir will cause an increase in the depth of the tail water, and this explains the reduction in energy dissipation, as the increase in energy dissipation is related to the decrease in the depth of the tail water.as shown in Figure 4.37.

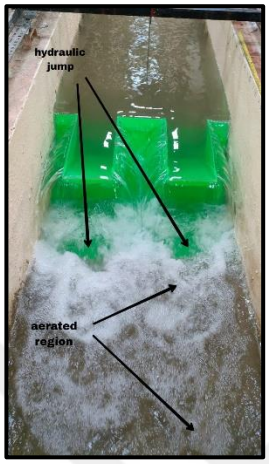

(a) when use Screen walls type-X as $(Q = 37\ lt/s)$

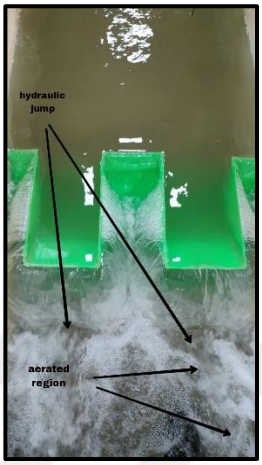

(b) when use Screen walls type-B as $(Q = 37\ lt/s)$

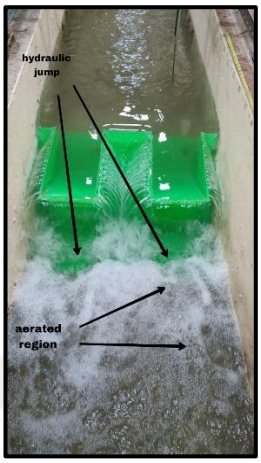

(c) when use screen walls type-D as $(Q = 37\ lt/s)$

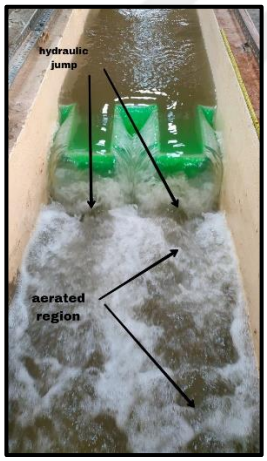

(d) when use Screen walls type-X as $(Q = 57\ lt/s)$

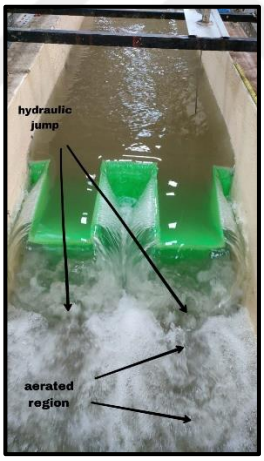

(e) when use Screen walls type-B as $(Q = 57\ lt/s)$

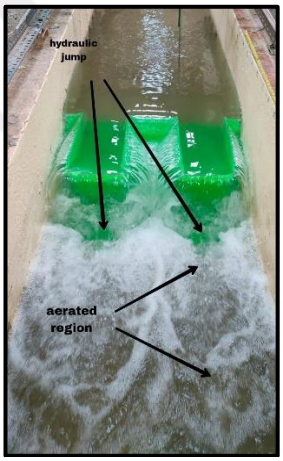

(f) when use screen walls type-D as $(Q = 57\ lt/s)$

Figure 4.37: The hydraulic jump, the nappes, and aerated Region for the flow at downstream as adding different screen walls.

Using screen walls type-D, the ratio $(L/W = 0.98)$ still gives the largest value of energy dissipation than the other ratios $(L/W = 3.47)$ and $(L/W = 3.96)$, but this value is low compared to using screen walls type-X and B.

From the Figure 4.32 (b), Figure 4.34 (b) and Figure 4.36 (b) noted that the ratio $(L/W = 2.78)$ at the $(H_1/P = 0.25)$ when using screen walls type-D is the

amount of energy dissipation $((E_1 - E_2)/E_1 = 0.61)$ while when using screen walls type-B and type-X the amount of energy dissipation is 0.64 and 0.65 respectively.

The effect of energy dissipation also continues to be affected by the ratio H_1/P, as the energy dissipation decreases as the ratio (H_1/P) increases.

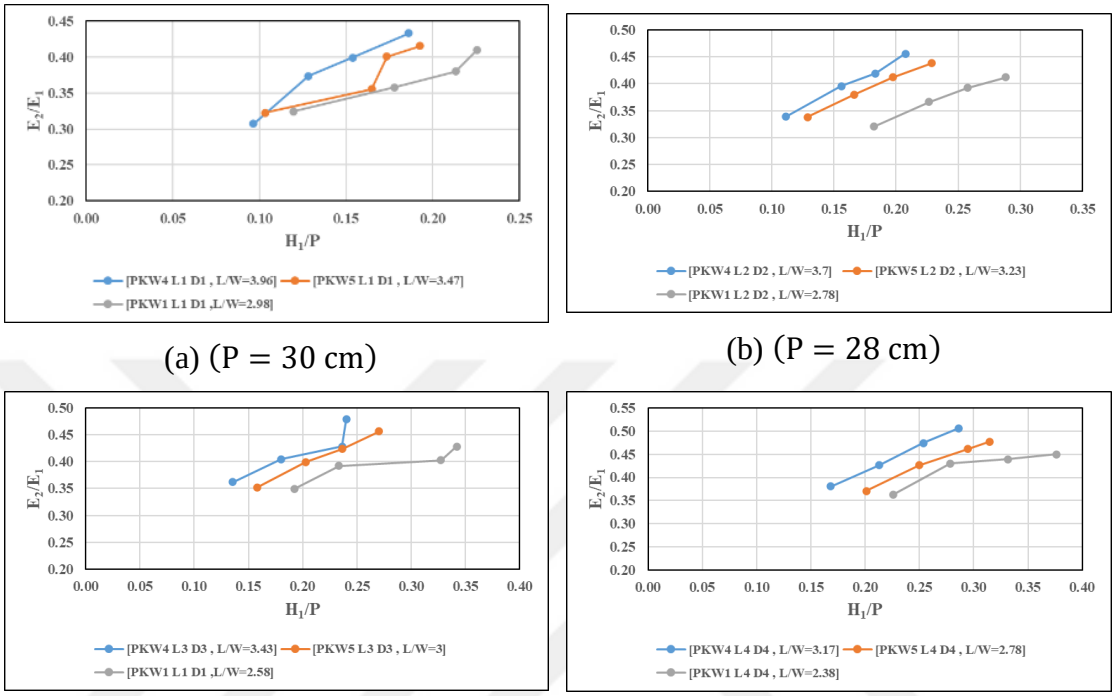

(a) (P = 30 cm) (b) (P = 28 cm)

(c) (P = 26 cm) (d) (P = 24 cm)

Figure 4.38: The effect of the ratio of the length of crest edge of PKW to the width of the weir (L/W) on the Residual Energy (E_2/E_1) by adding screen wall type-D.

Figure 4.38 shows that the greater value of (L/W) leads to an increase in the Residual Energy (E_2/E_1) as the relative energy dissipation, in this case, is rather lower, which leads to retaining of more energy of the flow in the waterway.

Note Figure 4.38 that when replacing the screen wall with type-D, the ratio L/W=3.97 still gives a higher residual energy than the other ratios $(L/W =$ 3.47 and 2.98) respectively.

Also noted that by using type-D screen walls instead of type-X screen walls, the residual energy increased slightly, in Figure 4.33 (a) when using type-X screen walls and when $(H_1/P = 0.2)$ noted that the ratio $(L/W = 2.9)$ had the Residual Energy $((E_2/E_1)$=0.34), but in Figure 4.38 (a) when using a screen wall of type-D and at the same time discharging, and the Residual Energy $((E_2/E_1)$=0.37).

When drawing a relationship that combines the Energy Dissipation $((E_1 - E_2)/E_1)$ and the ratio (H/P) for the same weir height P=30cm, the same ratio (L/W) and using the screen walls type-X, type-B, and type-D as shown in Figure 4.39.

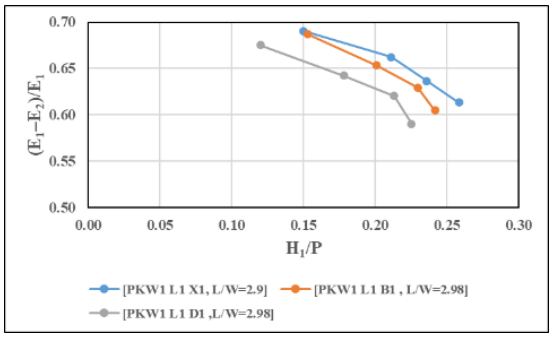

(a) model PKW1 L1 X1, PKW1 L1 B1, PKW1 L1 D1

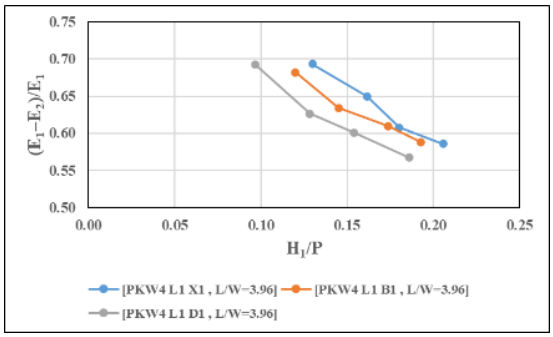

(b) model PKW4 L1 X1, PKW4 L1 B1, PKW4 L1 D1

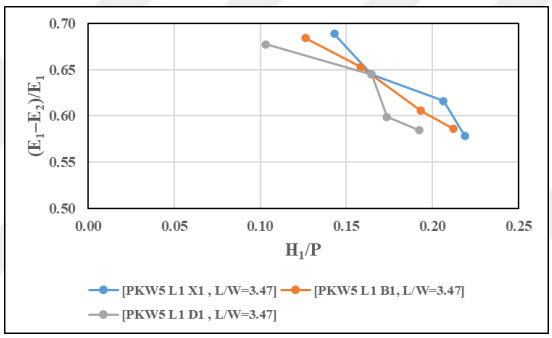

(c) model PKW5 L1 X1, PKW5 L1 B5, PKW5 L1 D1

Figure 4.39: The effect of adding screen walls type X, B and D to the models of PKW that have the same (L/W) and P=30cm on the Energy Dissipation $((E_1 - E_2)/E_1)$.

From the Figure 4.39 noted that screen walls type-X achieve the largest Energy Dissipation $((E_1 - E_2)/E_1)$ for PKW models, followed by screen walls type-B and then type-D respectively, for all PKW models used which indicates that as the diameter of the screen wall holes increases, the Energy Dissipation $((E_1 - E_2)/E_1)$ decreases.

As an example, when used the models PKW4 L1 X1, PKW4 L1 B1, PKW4 L1 D1 and at the ratio $(L/W = 3.96)$ for the same $(H_1/P = 0.15)$, the Energy Dissipation decreases by increases the diameter of the holes, where $((E_1 - E_2)/E_1 = 0.67, 0.63, \text{and } 0.61)$ for screen wall type-X, type-B, and type-D respectively. That is, a decrease 59% for type-B, and 61% for type-D.

Noted from the Figure 4.39 the effect of increasing the holes diameter of screen wall on decrease of the Energy Dissipation is smaller than the effect of increasing the geometric parameters (L/W) on it, and this effect increases with the increase diameter holes of the screen walls.

When adding the screen wall type-D to the model PKW1 L1 X1, the Energy Dissipation decreases from 0.67 - 0.63 by 6% at $(H_1/P = 0.2)$, and when comparing model PKW1 L1 X1 with model PKW4 L1 X1 by $((E_1 - E_2)/E_1 = 0.67, 0.59)$ respectively, at $(H_1/P = 0.2)$ where the resulting decrease in the Energy Dissipation 8% and this is greater from 6%.

When (H_1/P) is low, the effect of the screen walls is more prominent on decrease of the Energy Dissipation than the effect of the geometric parameter (L/W), and as (H_1/P) increases, the effect of the screen walls decreases.

It was also noted from all the figures linking the relationship between the Relative Energy Dissipation $((E_1 - E_2)/E_1)$ and the ratios (L/W) noted that low discharges give the highest values for the Relative Energy Dissipation, and high discharges give the lowest values for the Relative Energy Dissipation.

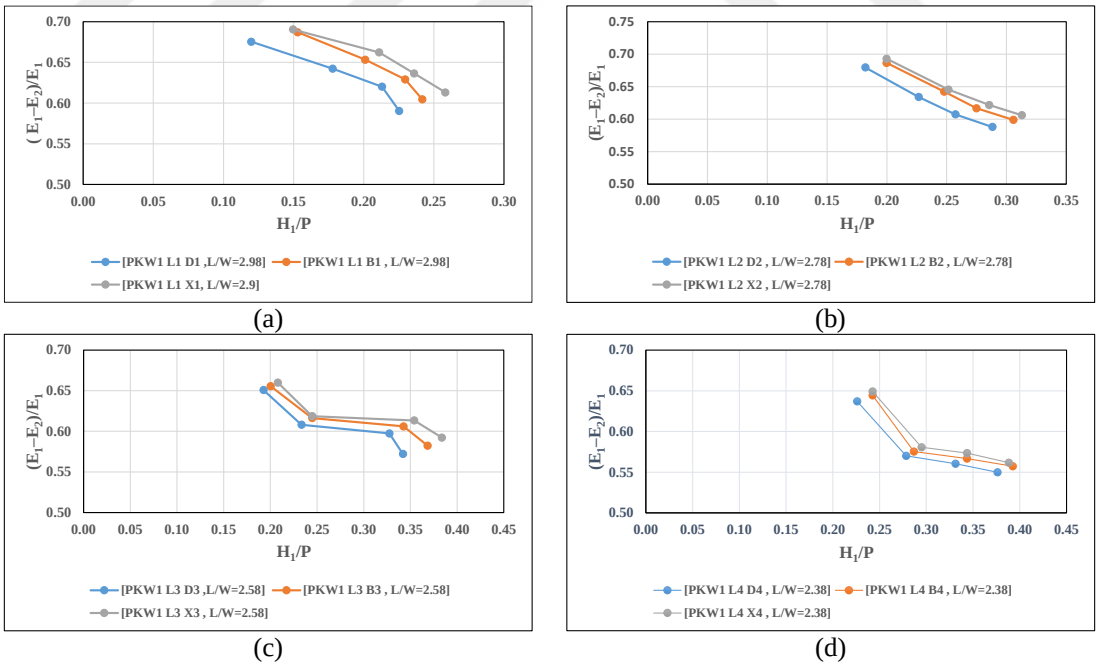

Figure 4.40: The effect of addition different screen walls to difference heights of PKW4 model on the Energy Dissipation $((E_1 - E_2)/E_1)$.

Noted from the Figure 4.41 Type X screen walls still give the highest energy dissipation with a decrease in the height of the weir, followed by Type B and Type D.

Energy dissipation decreases as the height of model PKW decreases due to the increased head height upstream which causes more immersion of the weir keys. This leads to a decrease in energy dissipation and an increase the Residual Energy in downstream.

Also, when drawing a relationship that combines the Residual Energy (E_2/E_1) and the ratio (H_1/P) for the same weir height $(P = 30)$, the same ratio (L/W) and using the screen walls type-X, type-B, and type-D as shown in Figure 4.41.

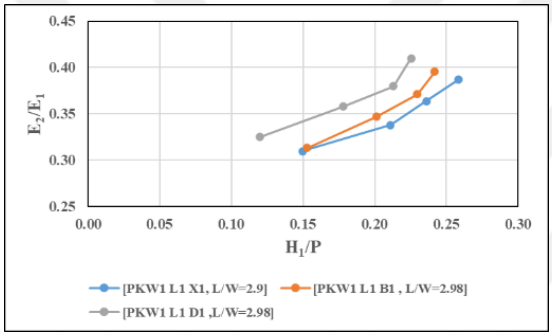

(a) model PKW1 L1 X1, PKW1 L1 B1, PKW1 L1 D1

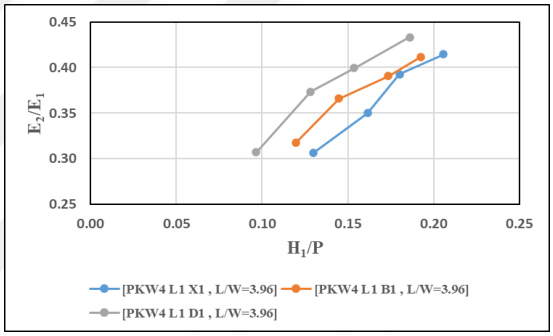

(b) model PKW4 L1 X1, PKW4 L1 B1, PKW4 L1 D1

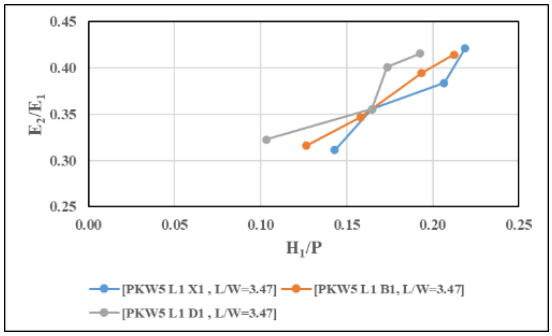

(c) model PKW5 L1 X1, PKW5 L1 B5, PKW5 L1 D1

Figure 4.41: The effect of adding screen walls type X, B and D to the models of PKW that have the same (L/W) and P=30cm on the Residual Energy (E_2/E_1).

From the Figure 4.41 noted that screen walls type-D achieve the Largest Residual Energy (E_2/E_1) for PKW models, followed by screen walls type-B and then type-X respectively, for all PKW models used which indicates that as the diameter of the screen wall holes increases, the Residual Energy (E_2/E_1) increases.

As an example, when used the models PKW1 L1 X1, PKW1 L1 B1, PKW1 L1 D1 and at the ratio $(L/W = 3.96)$ for the same $(H_1/P = 0.15)$, the Residual

Energy (E_2/E_1) increase by increases the diameter of the holes, where $((E_2/E_1)$=0.33, 0.37 and 0.4) for screen wall type-X, type-B, and type-D respectively. That is, an increase 12% for type-B, and 18.1% for type-D.

It was also noted from all the figures linking the relationship between the Residual Energy (E_2/E_1) and the ratios (L/W) noted that high discharges give the highest values for the Residual Energy, and low discharges give the lowest values for the Residual Energy.

4.3.2 The effect of the ratio of the width of the inlet key to the width of the outlet key of the piano key weir (W_i/W_o) by adding different screen walls on the energy dissipation $((E_1 - E_2)/E_1)$ and the residual energy(E_2/E_1)

The relationship between the Relative Energy Dissipation $((E_1 - E_2)/E_1)$ and the ratio of the depth of water above the edge of the weir to its height (H_1/P) was drawn for different values of the ratio of the width of the inlet key to the width of the outlet key of the piano key weir (W_i/W_o) for all research experiments and when the screen walls were type-X without any holes when the same ratio (L/W), (B/P), and model heights 30 cm, 28 cm, 26 cm, and 24 cm. Figure 4.42 shows a model of this relationship.

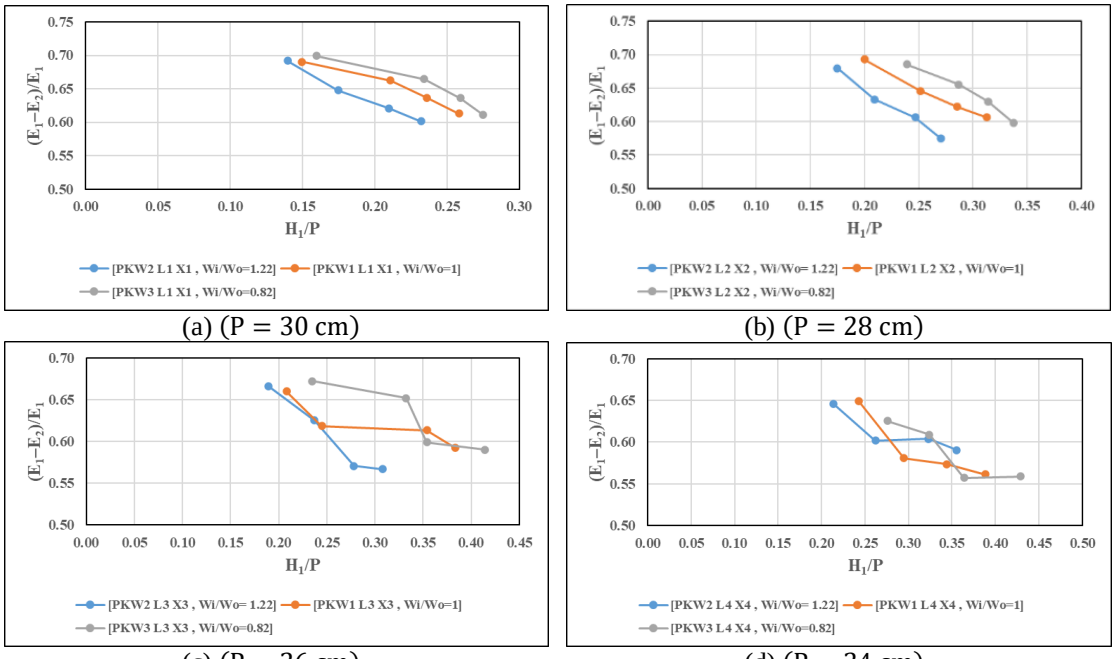

(a) (P = 30 cm) (b) (P = 28 cm)

(c) (P = 26 cm) (d) (P = 24 cm)

Figure 4.42: The effect of the ratio of the width of the inlet key to the width of the outlet key of the piano key weir (W_i/W_o) on the Relative Energy Dissipation $((E_1 - E_2)/E_1)$ by adding screen walls type-X.

From the Figure 4.42 it is clear that the energy dissipation is higher at the ratio $(W_i/W_o = 0.82)$ than $(W_i/W_o = 1)$, $(W_i/W_o = 1.22)$.

Whereas the highest value of the ratio of the width of the inlet key to the width of the outlet key (W_i/W_o) gives the least energy dissipation, while the low ratio (W_i/W_o) gives a higher energy dissipation. In the case of a high (W_i/W_o) this means that the width of the inlet key is wide which allows easier entry flow to it. It reduces losses in the flow head at the upstream, and this increases the amount of flow and distribution through it, and this, in turn, increases the effects of immersion in the outlet key. Due to the effects of immersion in the outlet key, the energy dissipation decreases, where Less energy is dissipated across the weir's toe as a result of jet clash and downstream impact changes in energy loss.

Observed that as the ratio of (H_1/P) increases, the percentage of energy dissipation decreases. This is consistent with what he mentioned (Eslinger and Crookston, 2020).

In the Figure 4.39 (a) the ratio $(W_i/W_o = 0.82)$ when (H_1/P) increases from 0.16 to 0.27, and percentage of energy dissipation decreases from 0.70 to 0.61.

In Figure 4.42 (c), and (d), notice that the total energy dissipation values vary in proportions (W_i/W_o) and are sometimes overlapping, especially at low weir heights and the flow discharge is high and the flow head is not low, as the secretions or heads increase and the nappes flow changes from aerate to partially aerate, and this in turn will increase turbulence at the bottom of the weir, reducing energy dissipation.

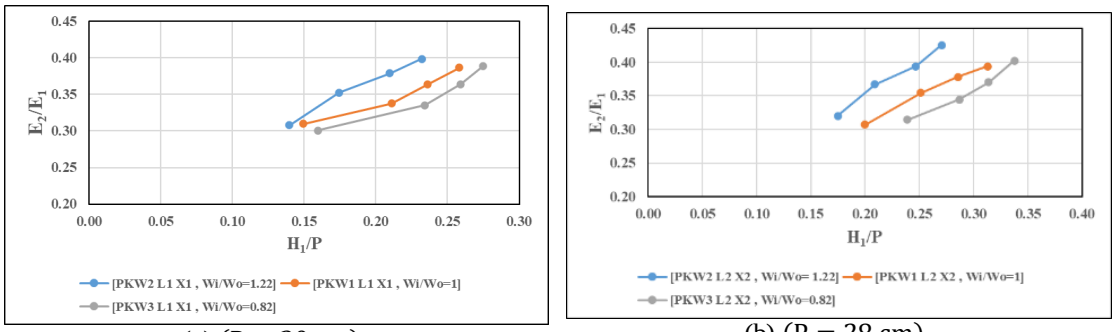

(a) (P = 30 cm)

(b) (P = 28 cm)

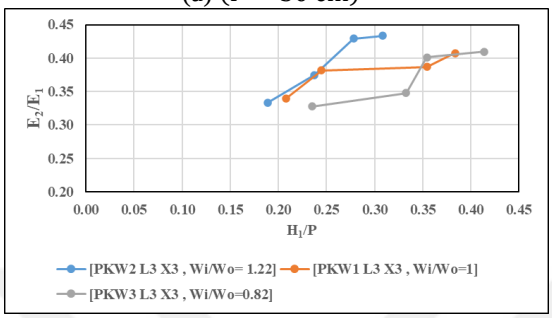

(c) (P = 26 cm)

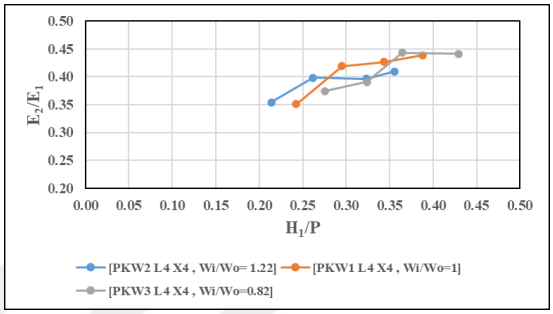

(d) (P = 24 cm)

Figure 4.43: The effect of the ratio of the width of the inlet key to the width of the outlet key of the piano key weir (W_i/W_o) on the Residual Energy (E_2/E_1) by adding screen wall type-X.

Noted from Figure 4.43 that the amount of the Residual energy increases with the increase in the ratio (W_i/W_o), meaning that the Residual energy increases as the width of the inlet key increases and the width of the outlet key decreases, as this leads to a greater amount of flow entering the inlet key in a smoother manner and flowing from it through the nappes, this increases the amount of flow at the downstream of PKW, thus increasing the depth of the tailwater and thus increasing the Residual energy at the downstream.

It also noted is that as the head-to-weir height ratio increases (H_1/P), the Residual energy downstream increases.

The screen walls type-X that do not contain holes were replaced by the screen walls type-B that contain holes with a diameter of $(\Phi = 0.5\ cm)$, and installed on the same models of PKW within the same geometric parameters and for the same values of (W_i/W_o). Laboratory results were obtained, and by plotting these laboratory results by a relationship between (H_1/P) and energy dissipation $((E_1 - E_2)/E_1)$, Figure 4.44 was obtained.

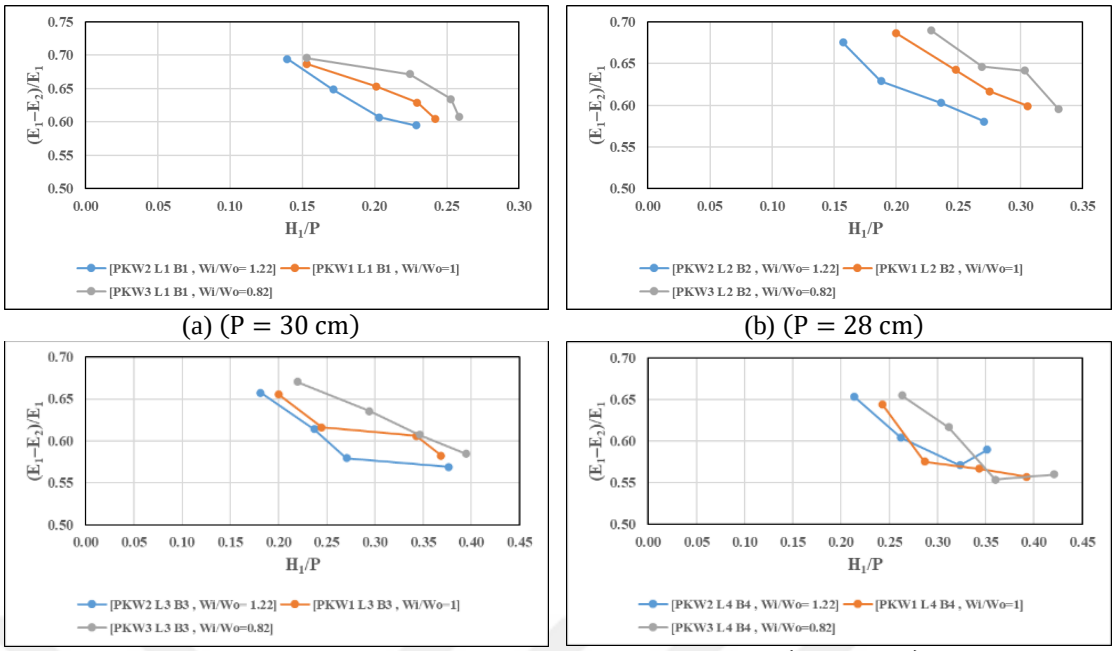

(a) (P = 30 cm) (b) (P = 28 cm)

(c) (P = 26 cm) (d) (P = 24 cm)

Figure 4.44: The effect of the ratio of the width of the inlet key to the width of the outlet key of the piano key weir (W_i/W_o) on the Relative Energy Dissipation $((E_1 - E_2)/E_1)$ by adding screen walls type-B.

Also noted that by using screen walls of type-B, instead of screen walls of type-X the energy dissipation decreased slightly, in Figure 4.42 (a) when using screen walls of type-X and when H_1/P=0.2 noted that the ratio $(W_i/W_o = 1.22)$ had the energy dissipation $((E_1 - E_2)/E_1 = 0.63)$, while in Figure 4.44 (a) when using a screen wall type-B and at the same discharge, the energy dissipation $((E_1 - E_2)/E_1 = 0.60)$.

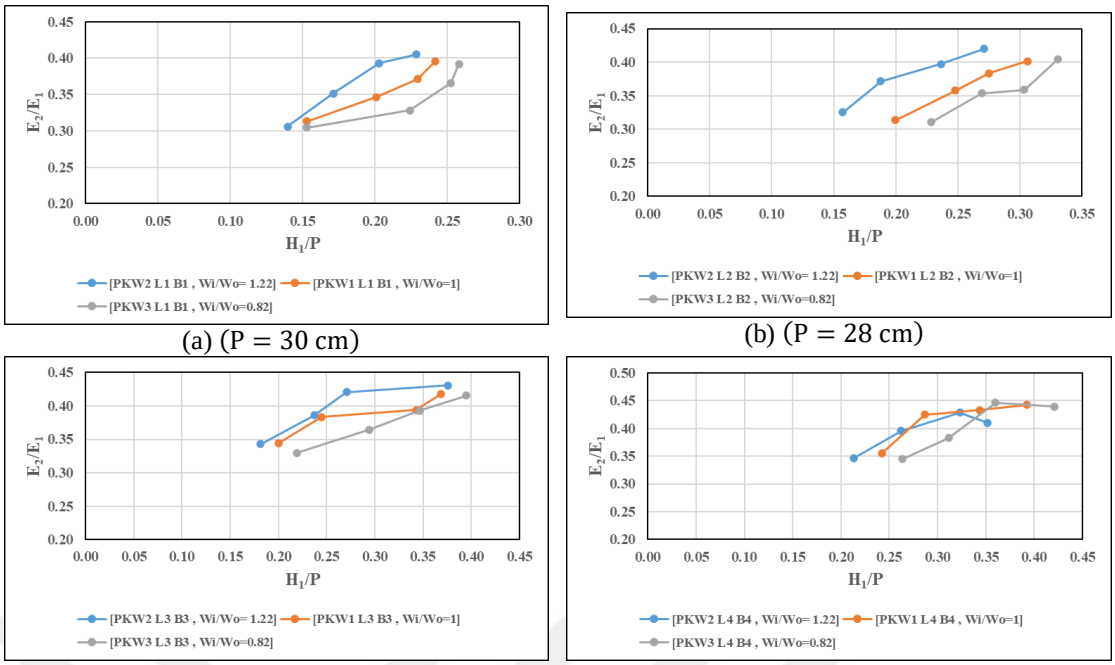

(a) (P = 30 cm) (b) (P = 28 cm)

(c) (P = 26 cm) (d) (P = 24 cm)

Figure 4.45: The effect of the ratio of the width of the inlet key to the width of the outlet key of the piano key weir (W_i/W_o) on the Residual Energy (E_2/E_1) by adding screen wall type-B.

The Figure 4.45 shows that the greater value of (W_i/W_o) leads to an increase in the Residual Energy (E_2/E_1) as the relative energy dissipation in this case is rather lower which leads to retaining of more energy of the flow in the waterway.

Noted from Figure 4.45 (a) that when replacing the screen wall by type-B, the ratio $(W_i/W_o = 1.22)$ still gives a higher residual energy than the other ratios $(W_i/W_o = 1.0 \text{ and } 0.82)$ respectively.

Also, it is clear that increasing the ratio of head to weir height (H_1/P) led to an increase in the down stream's Residual energy.

Note from Figure 4.45 & Figure 4.43 that the Residual Energy (E_2/E_1) was not greatly affected with replacing the screen walls type-B instead of type-X due to the large amount of nappe that flows over the edge walls of the inlet key, which is a large amount compared to the amount of water that flows through the holes with diameter $(\Phi = 0.5\ cm)$.

When replacing type-B screen walls by type-D screen walls that have holes with circular diameter $(\Phi = 1.0\ cm)$, and adding them to piano key weir models within the same geometric parameters, conducting experiments on them and drawing

the relationship between $((E_1 - E_2)/E_1)$ and (H_1/P) for the same Previous values of (W_i/W_o) ratios, the results are obtained as in the Figure 4.46.

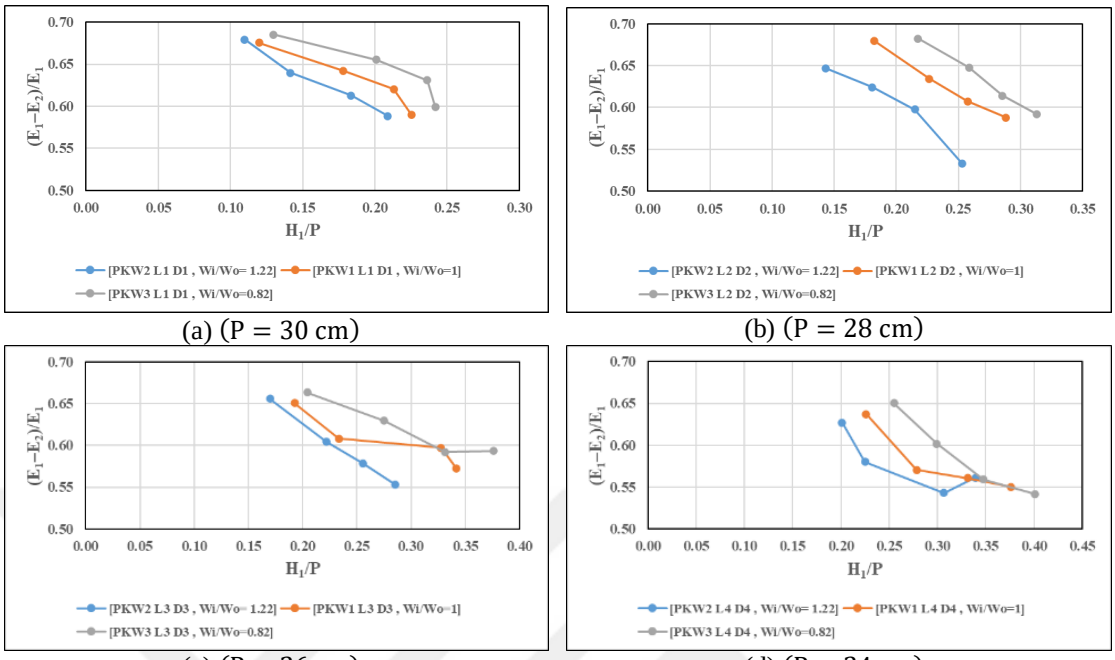

(a) (P = 30 cm) (b) (P = 28 cm)

(c) (P = 26 cm) (d) (P = 24 cm)

Figure 4.46: The effect of the ratio of the width of the inlet key to the width of the outlet key of the piano key weir (W_i/W_o) on the Relative Energy Dissipation $((E_1 - E_2)/E_1)$ by adding screen walls type-D.

Noted from Figure 4.46 the energy dissipation decreased when screen wall type-D was used more than type-B and type-X, respectively. The reason for this is that by using screen walls that contain openings will cause water to pass in the form of jets from the inlet key to the outlet key and mix with the water coming from the upstream of the outlet key, which leads to local flooding inside the outlet key which reduces energy dissipation.

Also noted that by using screen walls of type-D instead of screen walls of type-X the energy dissipation decreased, in Figure 4.42 (a) when using screen walls of type-X, and when H_1/P=0.2 noted that the ratio $(W_i/W_o = 1.0)$ had the energy dissipation $((E_1 - E_2)/E_1 = 0.68)$, while in Figure 4.46 (a) when using a screen wall type-D and at the same discharge, the energy dissipation $((E_1 - E_2)/E_1 = 0.65)$.

It also noted that the energy dissipation decreases by (H_1/P) increases.

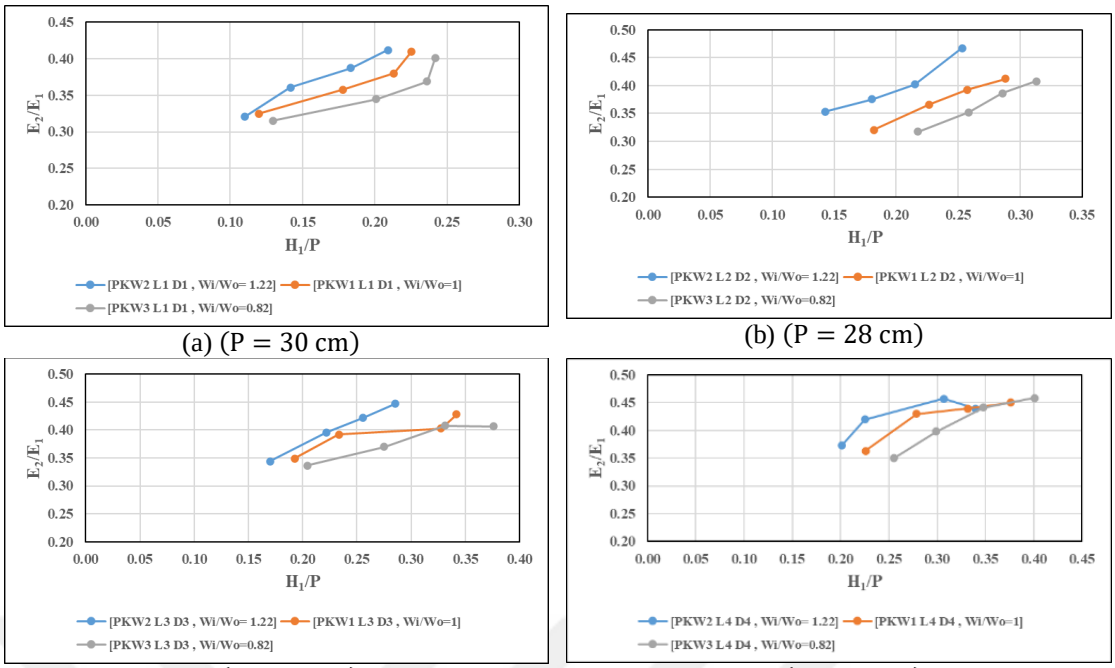

(a) (P = 30 cm) (b) (P = 28 cm)

(c) (P = 26 cm) (d) (P = 24 cm)

Figure 4.47: The effect of the ratio of the width of the inlet key to the width of the outlet key of the piano key weir (W_i/W_o) on the Residual Energy (E_2/E_1) by adding screen wall type-D.

The 4.47 shows that the greater value of (W_i/W_o) leads to an increase in the Residual Energy (E_2/E_1) as the relative energy dissipation in this case is rather lower which leads to retaining of more energy of the flow in the waterway.

Noted from Figure 4.47 (a) that when replacing the screen wall by type-D, the ratio $(W_i/W_o = 1.22)$ still gives a higher residual energy than the other ratios $(W_i/W_o = 1.0, \text{and } 0.82)$ respectively.

Also noted that as the head to weir height ratio increases (H_1/P), the Residual energy downstream increases.

Noted from Figure 4.47 and Figure 4.43 that the Residual Energy (E_2/E_1) was not greatly affected by replacing the screen walls with type-D instead of type-X due to the large amount of nappe that flow over the edge walls of the inlet key which is a large amount compared to the amount of water that flows through the holes with diameter $(\Phi = 1.0\ cm)$.

When drawing a relationship that combines the Energy Dissipation $((E_1 - E_2)/E_1)$ and the ratio (H/P) for the same weir height $(P = 30\ cm)$, the same ratio (W_i/W_o) and using the screen walls X, B, and D as shown in Figure 4.43.

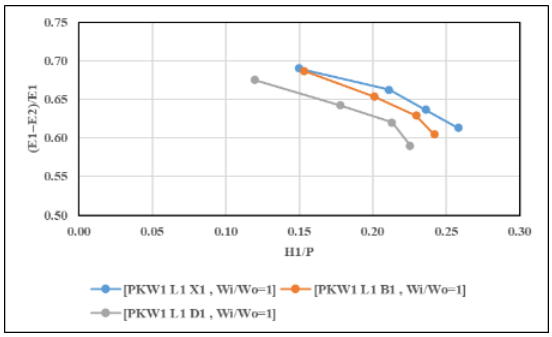

(a) model PKW1 L1 X1, PKW1 L1 B1, PKW1 L1 D1

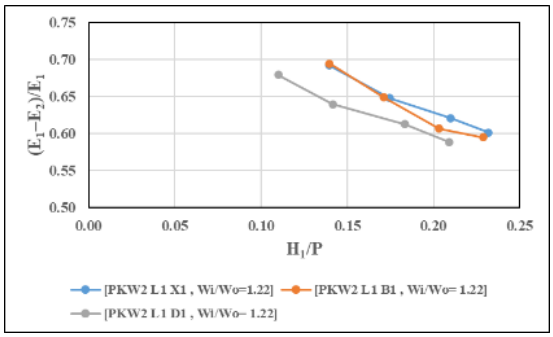

(b) model PKW2 L1 X1, PKW2 L1 B1, PKW2 L1 D1

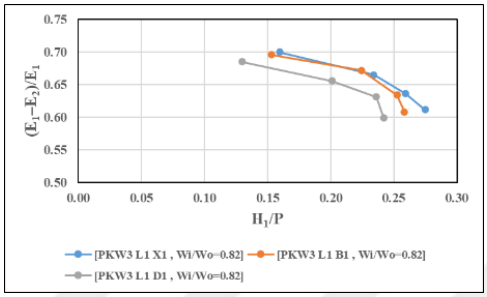

(c) model PKW3 L1 X1, PKW3 L1 B1, PKW3 L1 D1

Figure 4.48: The effect of adding screen walls type X, B and D to the models of PKW that have the same (W_i/W_o) and P=30cm on the Energy Dissipation $((E_1 - E_2)/E_1)$.

The Figure 4.48 noted that screen walls type-X achieve the largest Energy Dissipation $((E_1 - E_2)/E_1)$ for PKW models, followed by screen walls type-B and then type-D, respectively, for all PKW models used, which indicates that as the diameter of the screen wall holes increases, the Energy Dissipation $((E_1 - E_2)/E_1)$ decreases.

As an example, when using the models PKW1 L1 X1, PKW1 L1 B1, PKW1 L1 D1 and at the ratio $(W_i/W_o = 1.0)$ for the same $(H_1/P = 0.2)$, the Energy Dissipation decreases by increasing the diameter of the holes, where $((E_1 - E_2)/E_1 = 0.67, 0.65, \text{and } 0.67)$ for screen wall type-X, type-B, and type-D respectively. That is, a decrease of 3% for type-B, and 6% for type-D.

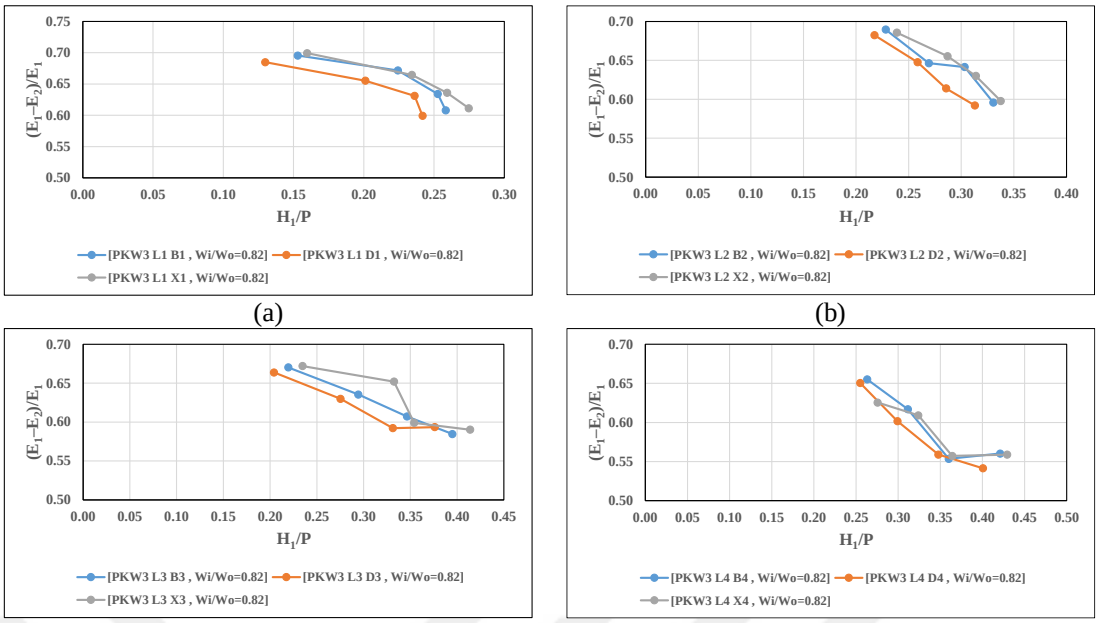

Figure 4.49: The effect of addition different screen walls to difference heights of PKW3 model on the Energy Dissipation $((E_1 - E_2)/E_1)$.

Noted from Figure 4.49 Type X screen walls still give the highest energy dissipation with a decrease in the height of the weir, followed by Type B and Type D.

Energy dissipation decreases as the height of model PKW decreases due to the increased head height upstream which causes more immersion of the weir keys. This leads to a decrease in energy dissipation and an increase in residual Energy downstream.

Also, when drawing a relationship that combines the Residual Energy (E_2/E_1) and the ratio (H/P) for the same weir height $P = 30\ cm$, the same ratio (W_i/W_o) and using the screen walls X, B, and D as shown in Figure 4.50.

It was also noted from all the figures linking the relationship between the Relative Energy Dissipation $((E_1 - E_2)/E_1)$ and the ratios $(W_i/W_o = 1.22, 1.0, \text{and } 0.82)$ noted that low discharges give the highest values for the Relative Energy Dissipation, and high discharges give the lowest values for the Relative Energy Dissipation.

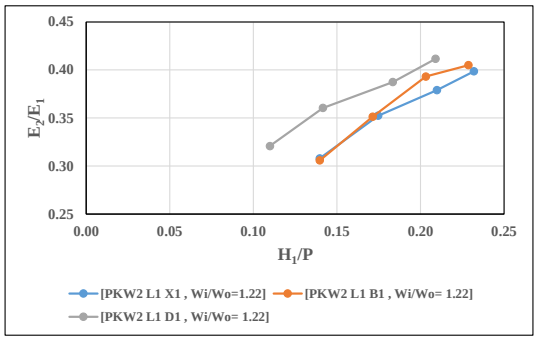

(a) model PKW1 L1 X1, PKW1 L1 B1, PKW1 L1 D1

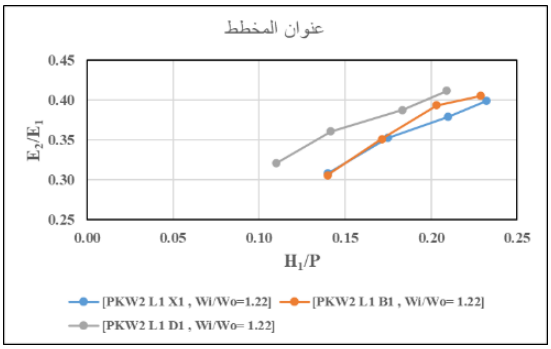

(b) model PKW2 L1 X1, PKW2 L1 B1, PKW2 L1 D1

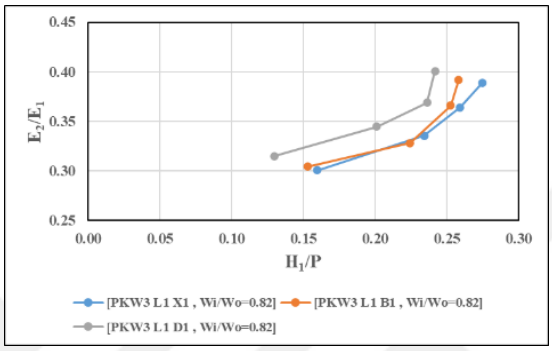

(c) model PKW3 L1 X1, PKW3 L1 B1, PKW3 L1 D1

Figure 4.50: The effect of adding screen walls type X, B and D to the models of PKW that have the same (W_i/W_o) and P=30cm on the Residual Energy (E_2/E_1).

The Figure 4.50 noted that screen walls type-D achieve the Residual Energy (E_2/E_1) for PKW models, followed by screen walls type-B and then type-X, respectively, for all PKW models used, which indicates that as the diameter of the screen wall holes increases, the Residual Energy (E_2/E_1) increases.

As an example, when using the models PKW1 L1 X1, PKW1 L1 B1, PKW1 L1 D1 and at the ratio $(W_i/W_o = 1.0)$for the same $(H_1/P = 0.22)$, the Residual Energy (E_2/E_1) increases by increasing the diameter of the holes, where $(E_2/E_1 = 0.35, 0.36, \text{and } 0.38)$ for screen wall type-X, type-B, and type-D respectively. That is an increase of 2.8% for type-B, and 8.5% for type-D.

It was also noted from all the figures linking the relationship between the Residual Energy (E_2/E_1) and the ratios $(W_i/W_o = 1.22, 1.0, \text{and } 0.82)$ noted that high discharges give the highest values for the Residual Energy, and low discharges give the lowest values for the Residual Energy.

4.3.3 The effect of the ratio of the upstream-downstream length of the top of PKW to the height of the weir (B/P), by adding different screen walls on the energy dissipation $((E_1 - E_2)/E_1)$ and the residual energy (E_2/E_1)

When using type-X screen walls that do not contain any opening on different piano key weir models, and showing their effect with the ratio of the length of the side crest of the weir to the height of the weir on the Energy Dissipation and comparing it with the ratio of the head height to the weir height for several discharges and for a different number of weir heights, getting the Figure 4.51.

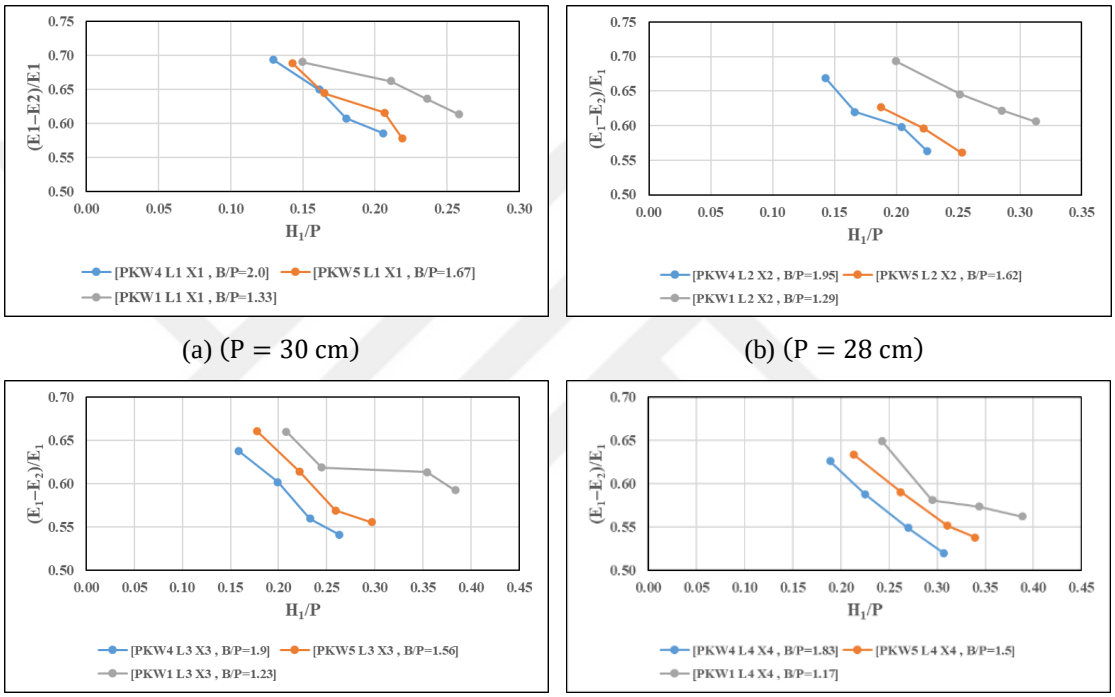

(a) (P = 30 cm) (b) (P = 28 cm)

(c) (P = 26 cm) (d) (P = 24 cm)

Figure 4.51: The effect of the ratio of the upstream-downstream length of the top of PKW to the height of the weir (B/P), on the Relative Energy Dissipation $((E_1 - E_2)/E_1)$ by adding screen walls type-X.

It is also clear from Figure 4.51 that the Relative Energy Dissipation $((E_1 - E_2)/E_1)$ of the piano key weir decreases with an increase in the ratio (B/P), where the length of the side edge of the weir top and its height affect the increase and decrease of the Relative Energy Dissipation Because increasing the ratio (B/P) means increasing the length of the wet edge of the weir top which allows larger amounts of flow to pass by the nappes especially the lateral nappes which flows above long lateral crest to the outlet key. These nappes collide with the nappes opposite them, and in addition to the flow Coming from the front of the outlet key,

all of this will increase the local immersion of the outlet key, which will increase the amount of flow at the downstream of PKW and increase the depth of the tailwater which reduces energy dissipation. This is consistent with (Eslinger & Crookston, 2020).

Note that increasing the length of the top edge of the weir decreases the Relative Energy Dissipation $((E_1 - E_2)/E_1)$ for the same weir heights.

Also, decreasing the value of (H_1/P) leads to reducing the value of energy dissipation for the same weir height.

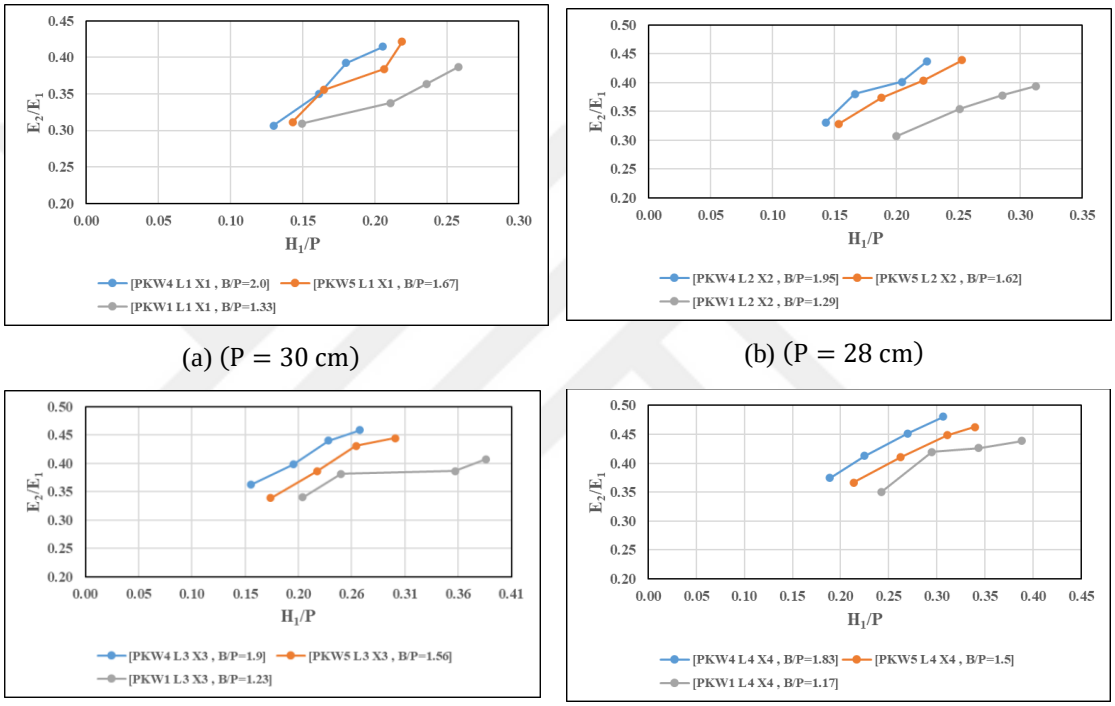

(a) (P = 30 cm) (b) (P = 28 cm)

(c) (P = 26 cm) (d) (P = 24 cm)

Figure 4.52: The effect of the ratio of the upstream-downstream length of the top of PKW to the height of the weir (B/P), on Residual Energy (E_2/E_1) by adding screen walls type-X.

Figure 4.52 shows that the greater value of (B/P) leads to an increase in the Residual Energy (E_2/E_1) as the relative energy dissipation, in this case, is rather lower, which leads to retaining of more energy of the flow in the waterway.

It is also noted in Figure 4.52 that the increased ratio(H_1/P) leads to an increase in the Residual Energy (E_2/E_1), in order to increase the amount of water entering the inlet key, where the inlet key accommodates the flow coming from the upstream as well as the side flow that it wraps around the output key at upstream, This leads to increase in pressure in the weir inlet key which leads to an increase in

the longitudinal velocity, and increase the amount of flow from the keys of PKW toward the downstream which cause increase the tail depth and then increase the Residual Energy.

The screen walls type-X that do not contain holes were replaced by the screen walls type-B that contain holes with diameter Φ=0.5 cm and installed on the same models of PKW within the same geometric parameters and for the same values of (B/P). Laboratory results were obtained, and by plotting these laboratory results by a relationship between (H_1/P) and energy dissipation $((E_1 - E_2)/E_1)$, Figure 4.53 was obtained.

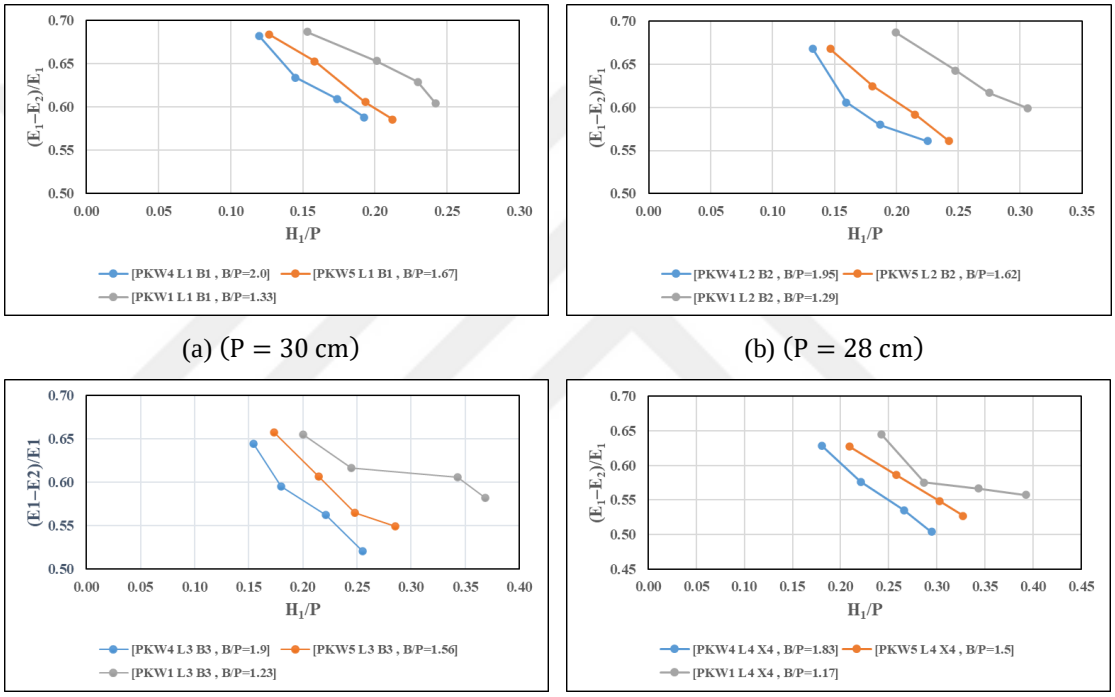

(a) (P = 30 cm) (b) (P = 28 cm)

(c) (P = 26 cm) (d) (P = 24 cm)

Figure 4.53: The effect of the ratio of the upstream-downstream length of the top of PKW to the height of the weir (B/P), on the Relative Energy Dissipation $((E_1 - E_2)/E_1)$ by adding screen walls type-B.

Note that when the screen wall was replaced with type-B, that the ratio $(B/P = 1.33)$ still gives a higher energy dissipation than the other ratios $(B/P = 1.67$ and $2.0)$ respectively.

Also noted that by using screen walls of type-B, instead of screen walls of type-X, the energy dissipation decreased slightly, in Figure 4.51 (a) when using screen walls of type-X and when $(H_1/P = 0.2)$ noted that the ratio $(B/P = 1.33)$ had the energy dissipation $((E_1 - E_2)/E_1 = 0.67)$, while in Figure 4.53 (a) when

using a screen wall type-B and at the same discharge, the energy dissipation ($(E_1 - E_2)/E_1 = 0.65$).

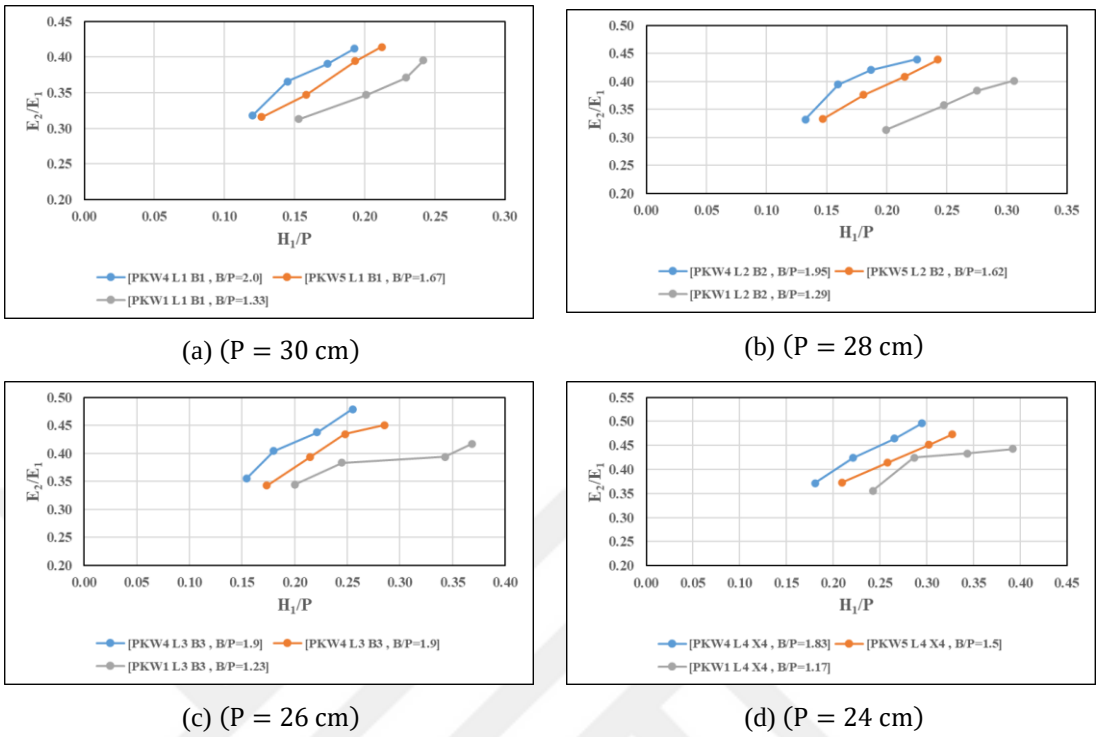

Figure 4.54: The effect of the ratio of the upstream-downstream length of the top of PKW to the height of the weir (B/P), on Residual Energy (E_2/E_1) by adding screen walls type-B.

Figure 4.54 shows that the greater value of (B/P) leads to an increase in the Residual Energy (E_2/E_1) as the relative energy dissipation, in this case, is rather lower which leads to retaining of more energy of the flow in the waterway.

Noted from Figure 4.54 (a) that when replacing the screen wall by type-B, the ratio $(B/P = 2.0)$ still gives a higher residual energy than the other ratios $(B/P = 1.67)$, and 1.33, respectively.

Also noted that by using type-B screen walls instead of type-X screen walls, the residual energy increased slightly, in Figure 4.52 (a) when using type-X screen walls and when $(H_1/P = 0.2)$ noted that the ratio $(B/P = 1.33)$ had the Residual Energy $(E_2/E_1 = 0.37)$ in Figure 4.54 (a) when using a screen wall of type-B and at the same time discharging, and the Residual Energy $(E_2/E_1 = 0.4)$.

When replacing type-B screen walls with type-D screen walls having opening circular diameter $(\Phi = 1.0\ cm)$, and adding them to PKW models within the same geometric parameters, conducting experiments on them and drawing the relationship

between $((E_1 - E_2)/E_1)$ and (H_1/P) for the same Previous values of (B/P) ,ratios, the results are obtained as in the Figure 4.55.

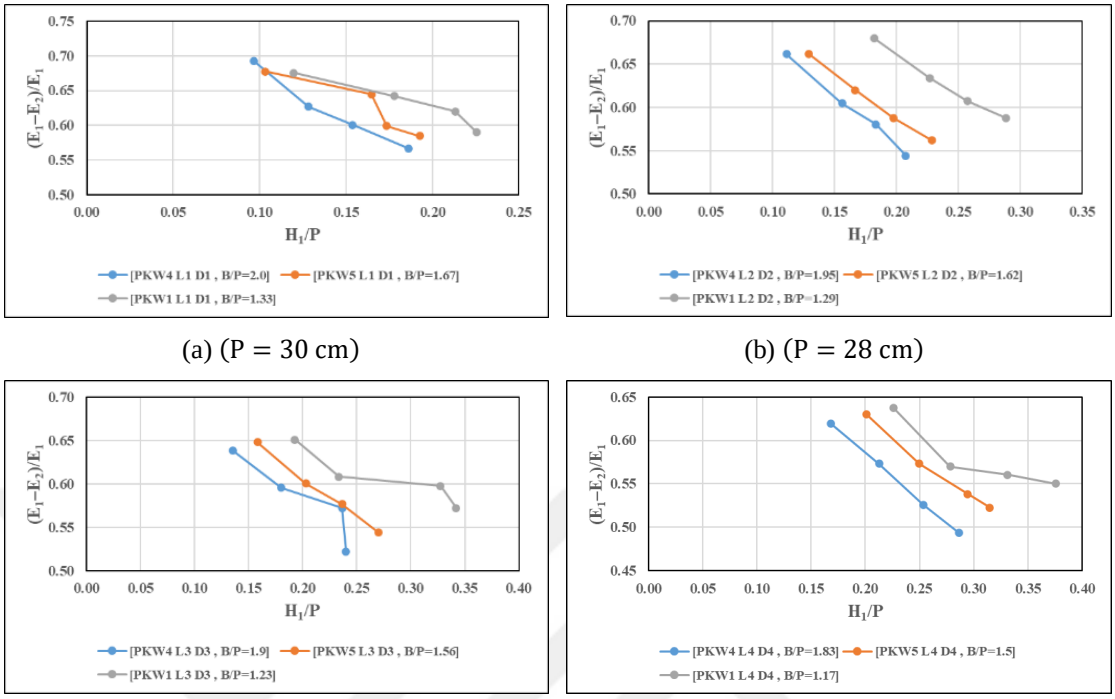

(a) (P = 30 cm) (b) (P = 28 cm)

(c) (P = 26 cm) (d) (P = 24 cm)

Figure 4.55: The effect of the ratio of the upstream-downstream length of the top of PKW to the height of the weir (B/P), on the Relative Energy Dissipation $((E_1 - E_2)/E_1)$ by adding screen walls type-D.

Noted from Figure 4.50 the energy dissipation decreased when screen wall type-D was used more than type-B and type-X, respectively. The reason for this is that by using screen walls that contain openings will cause water to pass in the form of jets from the inlet key to the outlet key and mix with the water coming from the upstream of the outlet key, which leads to local flooding inside the outlet key which reduces energy dissipation.

Noted that when the screen wall was replaced by the type-D, that the ratio $(B/P = 1.33)$ still gives a higher energy dissipation than the other ratios $(B/P = 1.67\ and\ 2.0)$ respectively.

Also noted that by using screen walls of type-D instead of screen walls of type-X, the energy dissipation decreased slightly, in Figure 4.51 (b) when using screen walls of type-X and when $(H_1/P = 0.2)$ noted that the ratio $(B/P = 1.29)$ had the energy dissipation $((E_1 - E_2)/E_1 = 0.65)$, while in the Figure 4.55 (b) when using a screen wall type-D, the energy dissipation $((E_1 - E_2)/E_1 = 0.62)$.

It was also noted from all the figures linking the relationship between the Relative Energy Dissipation $((E_1 - E_2)/E_1)$ and the ratios (B/P), noted that low discharges give the highest values for the Relative Energy Dissipation, and high discharges give the lowest values for the Relative Energy Dissipation.

When drawing a relationship that combines the energy dissipation $((E_1 - E_2)/E_1)$ and the ratio (H_1/P) for the same weir height $(P = 30\ cm)$, the same ratio (B/P), and using the screen walls type-X, type-B, and type-D following Figure 4.56 is obtained.

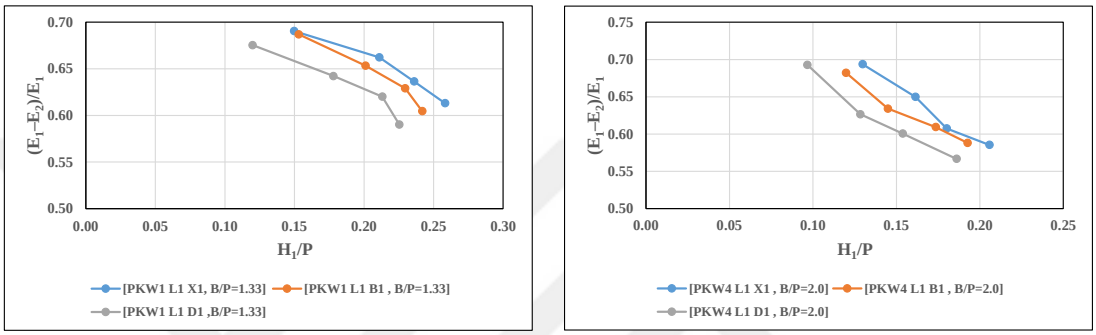

(a) model PKW1 L1 X1, PKW1 L1 B1, and PKW1 L1 D1

(b) model PKW4 L1 X1, PKW4 L1 B1, and PKW4 L1 D1

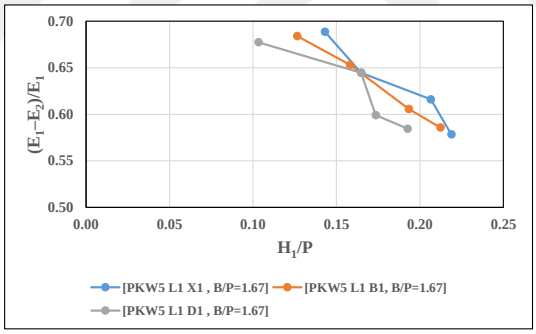

(c) model PKW5 L1 X1, PKW5 L1 B1, and PKW5 L1 D1

Figure 4.56: The effect of adding screen walls type-X, type-B and type-D to the models of PKW that have the same B/P, (W_i/W_o), and $(P = 30\ cm)$ on the energy dissipation $((E_1 - E_2)/E_1)$.

The Figure 4.56 noted that screen walls type-X achieve the largest Energy Dissipation $((E_1 - E_2)/E_1)$ for PKW models, followed by screen walls type-B and then type-D, respectively, for all PKW models used, which indicates that as the diameter of the screen wall holes increases, the Energy Dissipation $((E_1 - E_2)/E_1)$ decreases.

As an example, when used the models PKW1 L1 X1, PKW1 L1 B1, PKW1 L1 D1 and at the ratio $(L/W = 3.96)$ for the same $(H_1/P = 0.2)$ the Energy

Dissipation decreases by increasing the diameter of the holes, where $((E_1 - E_2)/E_1 = 0.67, 0.65$ and $0.63)$ for screen wall type-X type-B, and type-D respectively. That is, a decrease of 16.6% for type-B and 3.1% for type-D.

Noted from Figure 4.56 that the effect of increasing the hole diameter of the screen wall on decrease of the Energy Dissipation is smaller than the effect of increasing the geometric parameters (B/P), on it, and this effect increases with the increase diameter holes of the screen walls.

When adding the screen wall type-D to the model PKW1 L1 X1, the Energy Dissipation decreases from 0.67 - 0.63 by 6% at $(H_1/P = 0.2)$, and when comparing model PKW1 L1 X1 with model PKW4 L1 X1 by $((E_1 - E_2)/E_1 = 0.67, 0.59)$ respectively, at $(H_1/P = 0.2)$ where the resulting decrease in the Energy Dissipation 8% and this is greater from 6%.

When (H_1/P) is low, the effect of the screen walls is more prominent on decrease of the Energy Dissipation than the effect of the geometric parameters (B/P), and as (H_1/P) increases, the effect of the screen walls decreases.

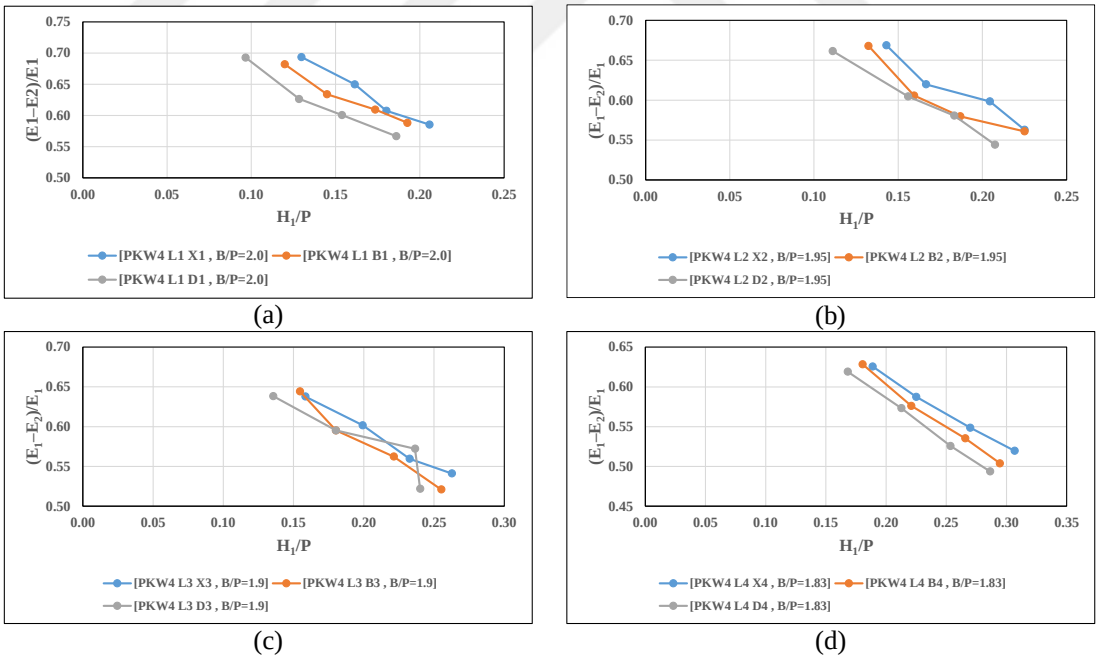

Figure 4.57: The effect of addition different screen walls to difference heights of PKW4 model on the Energy Dissipation $(E_1 - E_2)/E_1)$.

Noted from, Figure 4.57 Type X screen walls still give the highest energy dissipation with a decrease in the height of the weir, followed by Type B and Type D.

Energy dissipation decreases as the height of model PKW decreases due to the increased head height upstream, which causes more immersion of the weir keys. This leads to a decrease in energy dissipation and an increase the Residual Energy in downstream.

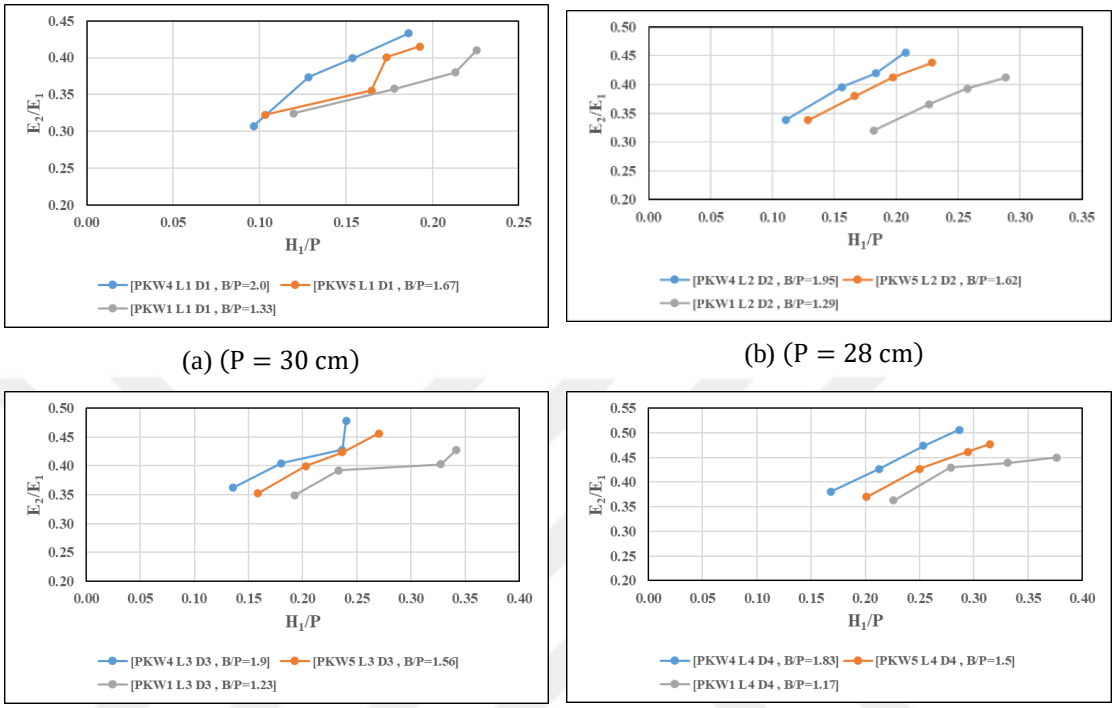

(a) (P = 30 cm)

(b) (P = 28 cm)

(c) (P = 26 cm)

(d) (P = 24 cm)

Figure 4.58: The effect of the ratio of the upstream-downstream length of the top of PKW to the height of the weir (B/P), on Residual Energy (E_2/E_1) by adding screen walls type-D.

Figure 4.58 shows that the greater the ratio of (B/P) ,leads to an increase in the Residual Energy (E_2/E_1), as the relative energy dissipation in this case is small, which leads to the flow in the waterway retaining more energy than if the ratio of (B/P) ,was lower which causes an increase in energy dissipation, Therefore, the Residual Energy is less.

Noted from Figure 4.58 (a) that when replacing the screen wall by type-D, the ratio $(B/P = 2.0)$ still gives a higher residual energy than the other ratios $(B/P = 1.67)$, and 1.33, respectively.

Also noted that by using type-D screen walls instead of type-X screen walls, the residual energy increased slightly, in Figure 4.58 (a) when using type-X screen walls and when $(H_1/P = 0.15)$ noted that the ratio $(B/P = 2.0)$ had the Residual

Energy ($E_2/E_1 = 0.32$) in Figure 4.58 (a) when using a screen wall of type-D and at the same time discharging, and the Residual Energy ($E_2/E_1 = 0.41$).

It was also noted from all the figures linking the relationship between the Residual Energy (E_2/E_1) and the ratios (B/P), noted that high discharges give the highest values for the Residual Energy, and low discharges give the lowest values for the Residual Energy.

When drawing a relationship that combines the Residual Energy (E_2/E_1) and the ratio (H_1/P) for the same weir height ($P = 30\ cm$), the same ratio (B/P), and using the screen walls type-X, type-B, and type-D following Figure 4.59 s obtained.

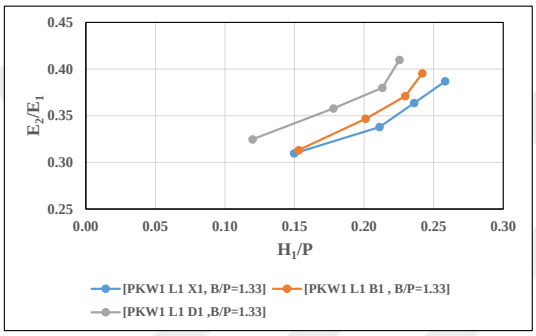

(a) model PKW1 L1 X1, PKW1 L1 B1, and PKW1 L1 D1

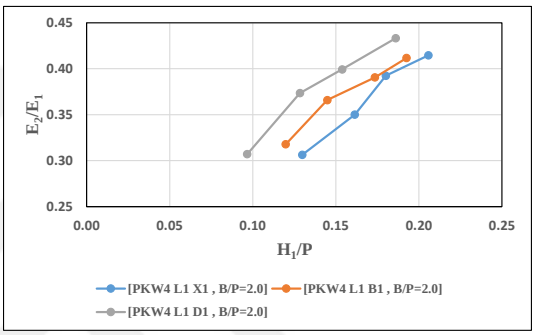

(b) model PKW4 L1 X1, PKW4 L1 B1, and PKW4 L1 D1

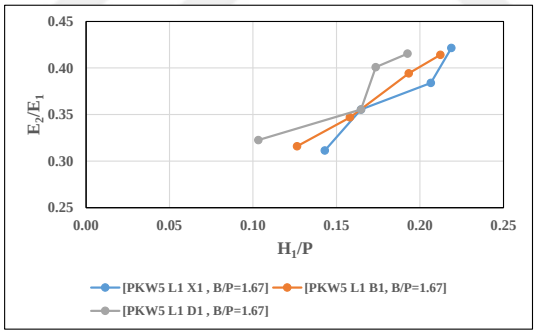

(c) model PKW5 L1 X1, PKW5 L1 B1, and PKW5 L1 D1

Figure 4.59: The effect of adding screen walls type-X, type-B and type-D to the models of PKW that have the same B/P, (W_i/W_o), and $P = 30\ cm$ on the Residual Energy (E_2/E_1).

Figure 4.59 noted that screen walls type-D achieve the largest the Residual Energy (E_2/E_1) for the piano key weir models, followed by screen walls type-B and type-X, respectively for all PKW models used which indicates that as the opening diameter of the screen wall increases, the Residual Energy (E_2/E_1) increases, as an example, when used the models PKW1 L1 X1, PKW1 L1 B1, PKW1 L1 D1 and the ratio H_1/P=0.2, the discharge coefficient increases by increasing the diameter of the

holes, where the $(E_2/E_1 = 0.33, 0.35 \text{ and } 0.37)$ for screen wall type-X, type-B, and type-D respectively. That is, an increase of 6% for type-B and 15% for type-D.

4.3.4 The effect of adding screen walls that have holes with different diameters to PKW on the energy dissipation $((E_1 - E_2)/E_1)$ and the residual energy (E_2/E_1)

The relationship between the flow of the Relative Energy Dissipation $((E_1 - E_2)/E_1)$ and the ratio (H_1/P) was drawn by adding screen walls of type-X, type-A, type-B, type-C, type-D, and type-E have holes with different holes diameters to PKW models, which have the same geometric parameters, but With a different weir heights, Where the screen walls type-X no have holes, and the screen walls type-A have holes with diameter $(\Phi = 0.35\ cm)$, type-B have holes with diameter $(\Phi = 0.5\ cm)$, type-C have holes with diameter $(\Phi = 0.7\ cm)$, type-D have holes with diameter $(\Phi = 1.0\ cm)$, type-E have holes with diameter $(\Phi = 1.4\ cm)$, as shown in Figure 4.60.

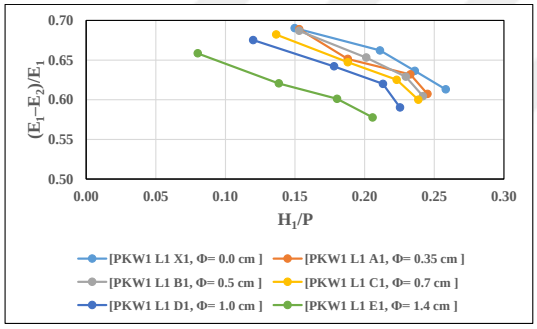

(a) model PKW1 L1 X1, PKW1 L1 A1, PKW1 L1 B1, PKW1 L1 C1, PKW1 L1 D1, PKW1 L1 E1

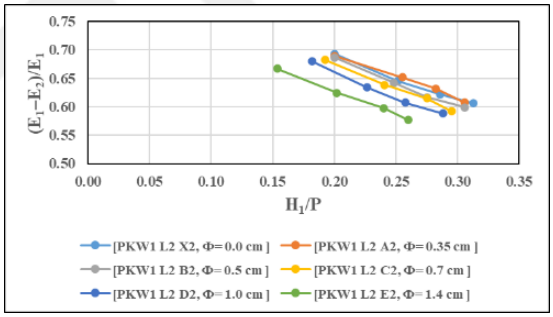

(b) model PKW1 L2 X2, PKW1 L2 A2, PKW1 L2 B2, PKW1 L2 C2, PKW1 L2 D2, PKW1 L2 E2

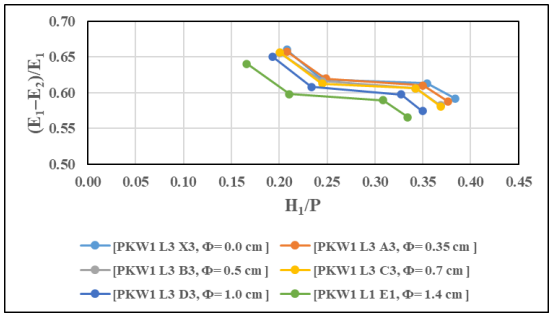

(c) model PKW1 L3 X3, PKW1 L3 A3, PKW1 L3 B3, PKW1 L3 C3, PKW1 L3 D3, PKW1 L3 E3

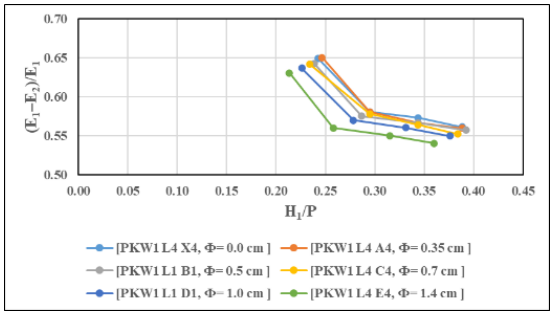

(d) model PKW1 L4 X4, PKW1 L4 A4, PKW1 L4 B4, PKW1 L4 C4, PKW1 L4 D4, PKW1 L4 E4

Figure 4.60: The effect of adding screen walls have holes with different diameters to PKW on the Energy Dissipation $((E_1 - E_2)/E_1)$.

Noted from Figure 4.60 The screen walls type-X give the highest Relative Energy Dissipation $((E_1 - E_2)/E_1)$ followed by screen walls type-A, type-B, type-C, type-D, and type-E, respectively. The reason for this is that using screen walls that contain holes will cause water to pass in the form of jets from the inlet key to the outlet key in addition to the lateral nappes and mix with the water coming from the upstream the outlet key which leads to local flooding inside the outlet key, which reduces energy dissipation.

Also noted from Figure 4.60 that the screen walls type-E have holes with diameter $(\Phi = 1.4\, cm)$, giving the lowest Relative Energy Dissipation $((E_1 - E_2)/E_1)$.

The screen walls type-E give the lowest Relative Energy Dissipation $((E_1 - E_2)/E_1)$ followed by screen walls type-D, type-C, type-B, and type-A, respectively.

Also noted that for screen walls of screen type-A, type-B, type-C and type-D with holes with diameters $(\Phi \geq 0.35\, cm)$, the difference in the Relative Energy Dissipation $((E_1 - E_2)/E_1)$ between them is small, as an example, when used the models PKW1 L1 X1, PKW1 L1 A1, PKW1 L1 B1, PKW1 L1 C1, PKW1 L1 D1, PKW1 L1 E1 for the same geometric parameters and the same $(H_1/P = 0.2)$, the Relative Energy Dissipation decrease by increases the diameter of the holes, where $((E_1 - E_2)/E_1 = 0.67, 0.66, 0.65, 0.64, 0.63, 0.58 \text{ and } 0.6)$ for screen wall type-X, type-A, type-B, type-C, type-D, and type-E respectively. That is, a decrease of 1.5% for type-A, and 3% for type-B, 4.5% for type-C, 6% for type-D, and 13% for type-E, respectively.

It was also noted from all the figures linking the relationship between the Relative Energy Dissipation $((E_1 - E_2)/E_1)$ and the different diameters of the holes of screen walls noted low discharges give the highest values for Relative Energy Dissipation and high discharges give the lowest values for the Relative Energy Dissipation for the same screen wall.

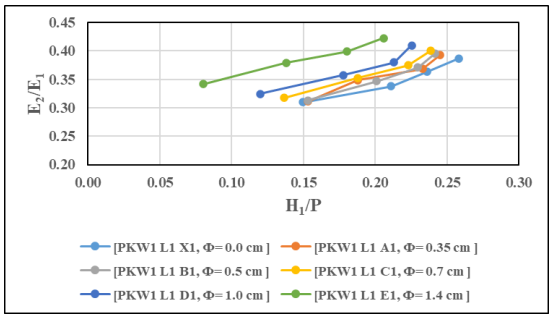

(a) model PKW1 L1 X1, PKW1 L1 A1, PKW1 L1 B1, PKW1 L1 C1, PKW1 L1 D1, PKW1 L1 E1

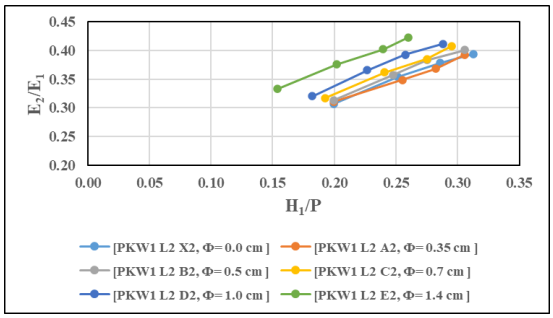

(b) model PKW1 L2 X2, PKW1 L2 A2, PKW1 L2 B2, PKW1 L2 C2, PKW1 L2 D2, PKW1 L2 E2

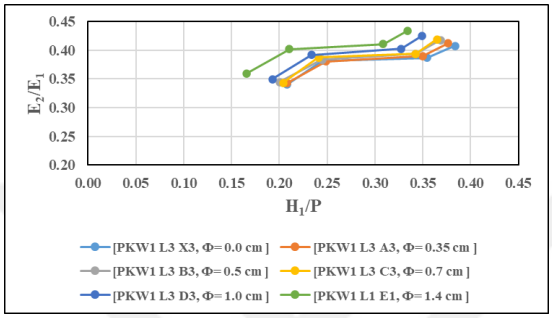

(c) model PKW1 L3 X3, PKW1 L3 A3, PKW1 L3 B3, PKW1 L3 C3, PKW1 L3 D3, PKW1 L3 E3

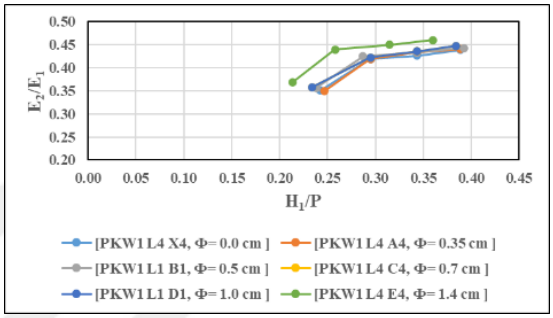

(d) model PKW1 L4 X4, PKW1 L4 A4, PKW1 L4 B4, PKW1 L4 C4, PKW1 L4 D4, PKW1 L4 E4

Figure 4. 61: The effect of adding screen walls have holes with different diameters to PKW on the Residual Energy (E_2/E_1).

Noted from the Figure 4.61 The screen walls type-X give the lowest the Residual Energy (E_2/E_1) followed by type-A, type-B, type-C, type-D and type-E, respectively.

Also noted from the Figure 4.61 that the screen walls type-E with a diameter $(\Phi = 1.4\ cm)$ which gave the largest of the Residual Energy (E_2/E_1) at the same value of H1/P , explains this because screen walls with big diameter holes allow flow to pass through them in a greater and smoother manner from The inlet key to the outlet key and then to the downstream which decrease the hydraulic pressure on the inlet key and thus decrease the hydraulic flow out through the upper edges of the inlet key, and increase the hydraulic flow from the outlet key towards downstream, this causes a decrease in Energy dissipation, and thus the Residual Energy (E_2/E_1) will increase.

The screen walls type-E gave the largest Residual Energy (E_2/E_1) followed by type-D, type-C, type-B, type-A and type-X, respectively.

Also noted that for screen walls of type-A, type-B, type-C and type-D have holes with diameters are lowest than $(\Phi = 1.4\ cm)$, the difference in the Residual Energy (E_2/E_1) between them is small, as an example, when used the models PKW1 L1 X1, PKW1 L1 A1, PKW1 L1 B1, PKW1 L1 C1, PKW1 L1 D1, PKW1 L1 E1 for the same geometric parameters and the same $(H_1/P = 0.2)$, the Relative Energy Dissipation increase by increases the diameter of the holes, where $(E_2/E_1 = 0.33, 0.35, 0.35, 0.36, 0.37 \text{ and } 0.42)$ for screen wall type-X, type-A, type-B, type-C, type-D, and type-E respectively. That is, an increase of 6% for type-A and 6% for type-B, 9% for type-C, 12% for type-D, and 27% for type-E respectively.

It was also noted from all the figures linking the relationship between the relative Energy Dissipation $((E_1 - E_2)/E_1)$ and the different shapes of the holes of screen walls noted that high discharges give the highest values for Residual Energy and low discharges give the lowest values for Residual Energy for the same screen wall.

4.3.5 The effect of adding screen walls that have holes with different porosity to PKW on the energy dissipation $((\boldsymbol{E_1 - E_2})/\boldsymbol{E_1})$ and the residual energy $(\boldsymbol{E_2/E_1})$

The relationship between the Relative Energy Dissipation $((E_1 - E_2)/E_1)$ and the ratio (H_1/P) was drawn by adding screen walls of type-X, type-B, type-F, type-G, and type-H of different porosity to the piano key weir models which have the same geometric parameters but with different weir heights.

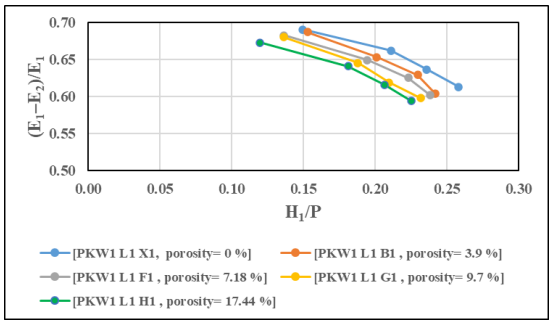

(a) model PKW1 L1 X1, PKW1 L1 B1, PKW1 L1 F1, PKW1 L1 G1, PKW1 L1 H1

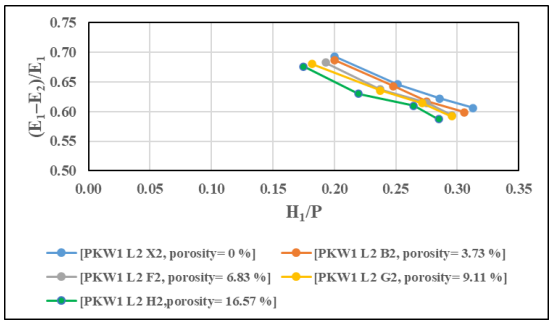

(b) model PKW1 L2 X2, PKW1 L2 B2, PKW1 L2 F2, PKW1 L2 G2, PKW1 L2 H2

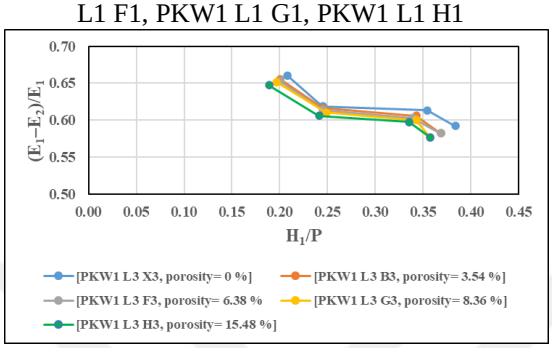

(c) model PKW1 L3 X3, PKW1 L3 B3, PKW1 L3 F3, PKW1 L3 G3, PKW1 L3 H3

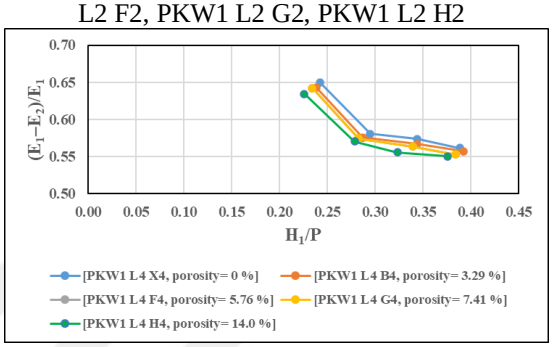

(d) model PKW1 L4 X4, PKW1 L4 B4, PKW1 L4 F4, PKW1 L4 G4, PKW1 L4 H4

Figure 4.62: The effect of adding screen walls have holes with different porosity to PKW on the Energy Dissipation $((E_1 - E_2)/E_1)$

Noted from Figure 4.62 that the Relative Energy Dissipation $((E_1 - E_2)/E_1)$ decreases as used screen walls with greater porosity and is accompanied by a decrease in heads at the upstream of the weir, The reason for this is that by using screen walls with greater porosity, this will cause water to pass in the form of jets from the inlet key to the outlet key in addition to the lateral nappes and mix with the water coming from the upstream of the outlet key which leads to local immersion inside the outlet key which reduces energy dissipation.

Noted from Figure 4.62 that the screen walls type-H gave the lowest of the Relative Energy Dissipation $((E_1 - E_2)/E_1)$ for the same value of (H_1/P), also noted from Figure 4.62 that the highest of the height of PKW models give the highest value of the Relative Energy Dissipation $((E_1 - E_2)/E_1)$ comparing with the lowest of the height of PKW models.

The screen walls type-X gave the largest of Relative Energy Dissipation $((E_1 - E_2)/E_1)$ followed by screen walls type-B, type-F, type-G, and type-H, respectively, also noted that for screen walls of type-X, type-B, type-F, type-G, there are no big different in the Relative Energy Dissipation between them, as an example, when used the models PKW1 L1 X1, PKW1 L1 B1, PKW1 L1 F1, PKW1 L1 G1,

PKW1 L1 H_1, for the same geometric parameters and the same $(H_1/P = 0.2)$, the Relative Energy Dissipation by increases the porosity of the screen wall, where the $((E_1 - E_2)/E_1 = 0.67, 0.65, 0.64, 0.63 \text{ and } 0.62)$ for screen wall type-X, type-B, type-F, type-G, and type-H, respectively. That is a decrease of 3% for type-B, 4.4% for type-F, 6% for type-G, and 7.4% for type-H respectively.

It was also noted from all the figures linking the relationship between the Relative Energy Dissipation $((E_1 - E_2)/E_1)$ and the different shapes of the holes of screen walls that low discharges give the highest values for Relative Energy Dissipation and high discharges give the lowest values for Relative Energy Dissipation for the same screen wall.

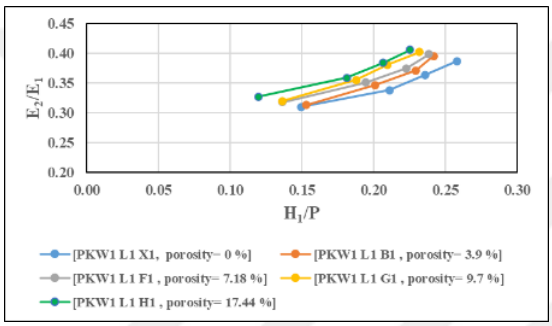

(a) model PKW1 L1 X1, PKW1 L1 B1, PKW1 L1 F1, PKW1 L1 G1, PKW1 L1 H1

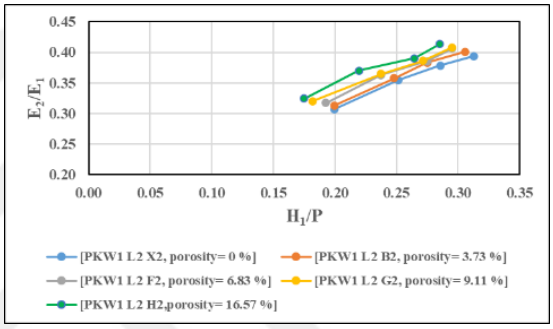

(b) model PKW1 L2 X2, PKW1 L2 B2, PKW1 L2 F2, PKW1 L2 G2, PKW1 L2 H2

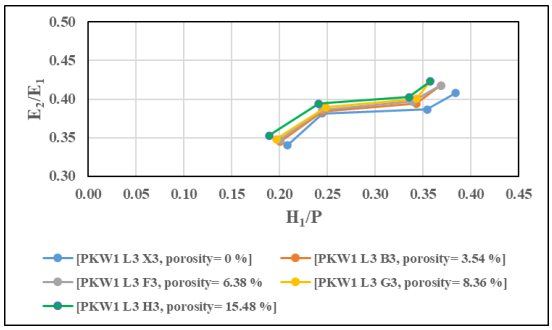

(c) model PKW1 L3 X3, PKW1 L3 B3, PKW1 L3 F3, PKW1 L3 G3, PKW1 L3 H3

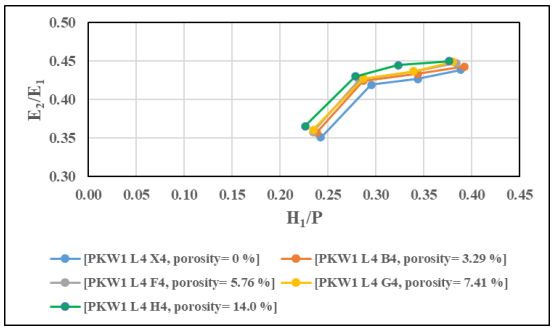

(d) model PKW1 L4 X4, PKW1 L4 B4, PKW1 L4 F4, PKW1 L4 G4, PKW1 L4 H4

Figure 4.63: The effect of adding screen walls have holes with different porosity to PKW on the Residual Energy (E_2/E_1).

Noted from Figure 4.63 that the Residual Energy (E_2/E_1) increases as used screen walls with greater porosity and is accompanied by a decrease in heads at the upstream of the weir. The reason for this is that using screen walls with greater porosity this will cause water to pass in the form of jets from the inlet key to the outlet key in addition to the lateral nappes and mix with the water coming from the front of the outlet key which leads to local immersion inside the outlet key which

increase amount of the flow at the downstream with increase the depth of the tailwater and decrease the Residual Energy.

Noted from Figure 4.63 that the screen walls type-H gave the largest of the Residual Energy (E_2/E_1) at the same (H_1/P) the lowest head height upstream of weir at the same discharges.

The screen walls type-X gave the lowest Residual Energy (E_2/E_1) followed by screen walls type-B, type-F, type-G and type-H, respectively, also noted that for screen walls of type-X, type-B, type-F, and type-G there are no big different in the Residual Energy (E_2/E_1) between them, as an example, when used the models PKW1 L1 X1, PKW1 L1 B1, PKW1 L1 F1, PKW1 L1 G1, PKW1 L1 H_1, for the same geometric parameters and the same $(H_1/P = 0.15)$, the Residual Energy by increases the porosity of the screen wall, where the $(E_2/E_1 = 0.31, 0.32, 0.33, 0.33 \text{ and } 0.34)$ for screen wall type-X, type-B, type-F, type-G, and type-H, respectively. That is an increase of 3.2% for type-B, 6.4% for type-F, 6.4% for type-G, and 9.6% for type-H, respectively.

It was also noted from all the figures linking the relationship between the Residual Energy (E_2/E_1) and the different shapes of the holes of screen walls that high discharges give the highest values for the Residual Energy and low discharges give the lowest values for the Residual Energy for the same screen wall.

4.3.6 The effect of adding screen walls that have holes with different shapes to PKW on the energy dissipation $((\boldsymbol{E_1 - E_2})/\boldsymbol{E_1})$ and the residual energy $(\boldsymbol{E_2/E_1})$

The relationship between the Relative Energy Dissipation $((E_1 - E_2)/E_1)$ and the ratio (H_1/P) was drawn by adding screen walls of type-X, type-D, type-I, type-J, type-K, and type-M with different shapes of holes but with the same areas to PKW models, which have the same Geometric parameters, but at different weir heights.

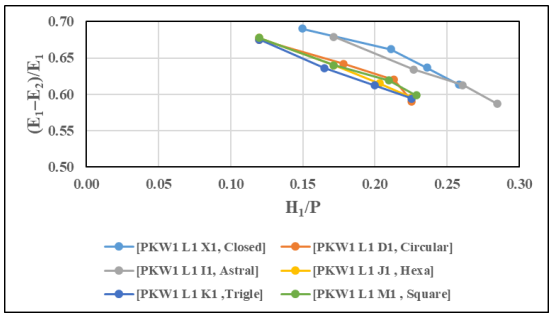

(a) model PKW1 L1 X1, PKW1 L1 D1, PKW1 L1 I1, PKW1 L1 J1, PKW1 L1 K1, PKW1 L1 M1

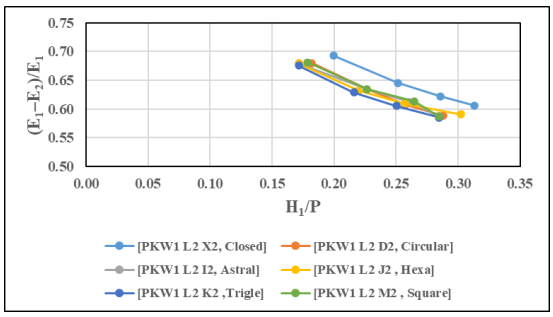

(b) model PKW1 L2 X2, PKW1 L2 D2, PKW1 L2 I2, PKW1 L2 J2, PKW1 L2 K2, PKW1 L2 M2

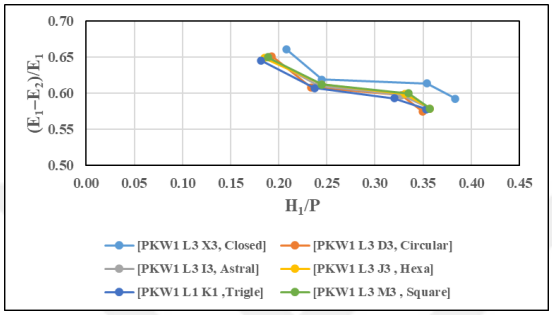

(c) model PKW1 L3 X3, PKW1 L3 D3, PKW1 L3 I3, PKW1 L3 J3, PKW1 L3 K3, PKW1 L3 M3

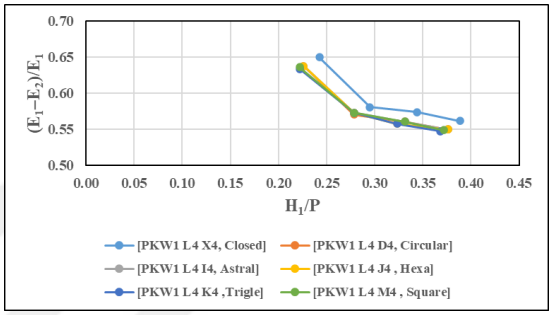

(d) model PKW1 L4 X4, PKW1 L4 D4, PKW1 L4 I4, PKW1 L4 J4, PKW1 L4 K4, PKW1 L4 M4

Figure 4.64: The effect of adding screen walls have holes with different shapes to PKW on the Energy Dissipation $((E_1 - E_2)/E_1)$.

Noted from Figure 4.64 that the Relative Energy Dissipation $((E_1 - E_2)/E_1)$ decreases by using screen walls with holes of different shapes type-D, type-I, type-J, type-K, and type-M than screen wall type-X.

Noted from Figure 4.64 that the screen walls all give very similar results by decreasing Relative Energy Dissipation $((E_1 - E_2)/E_1)$, but they sometimes differ in their sequences by giving a higher the Relative Energy Dissipation $((E_1 - E_2)/E_1)$. This slight difference appears when changing the heights of the weir and at high discharges.

But it always remains clear that screen walls type-K with tringle holes gave the lowest Relative Energy Dissipation for all weir heights, followed by screen walls type-J with hexagonal holes, then screen walls type-M with square holes, type-D with circular holes, and type-I with astral holes, respectively, as an example, when used the models PKW1 L1 X1, PKW1 L1 D1, PKW1 L1 I1, PKW1 L1 J1, PKW1 L1 K1, PKW1 L1 M1 for the same geometric parameters and the same $(H_1/P = 0.2)$, the Relative Energy Dissipation

$((E_1 - E_2)/E_1 = 0.67, 0.66, 0.63, 0.63, 0.62$ and $0.61)$ for screen wall type-X, type-I, type-D, type-M, type-J, and type-K respectively. That is, a decrease 1.5% for type-I, 6% for type-D, 6% for type-M, 4% for type-J, and 9% for type-K respectively.

It was also noted from all the figures linking the relationship between the Relative Energy Dissipation $((E_1 - E_2)/E_1)$ and the different shapes of the holes of screen walls that low discharges give the highest values for Relative Energy Dissipation and high discharges give the lowest values for Relative Energy Dissipation for the same screen wall.

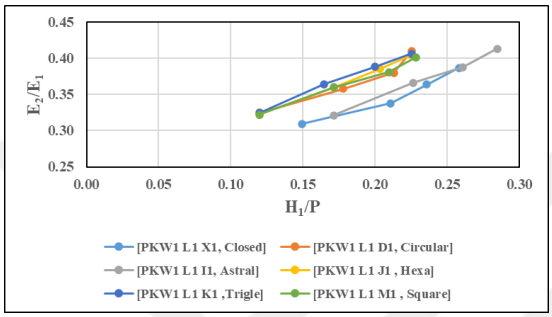

(a) model PKW1 L1 X1, PKW1 L1 D1, PKW1 L1 I1, PKW1 L1 J1, PKW1 L1 K1, PKW1 L1 M1

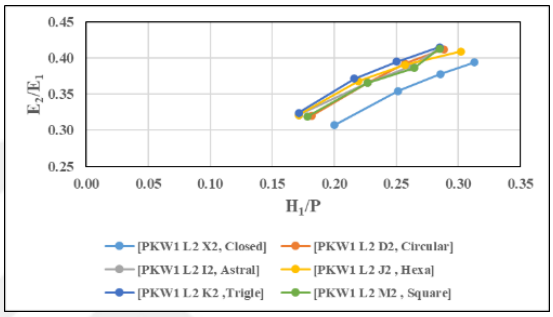

(b) model PKW1 L2 X2, PKW1 L2 D2, PKW1 L2 I2, PKW1 L2 J2, PKW1 L2 K2, PKW1 L2 M2

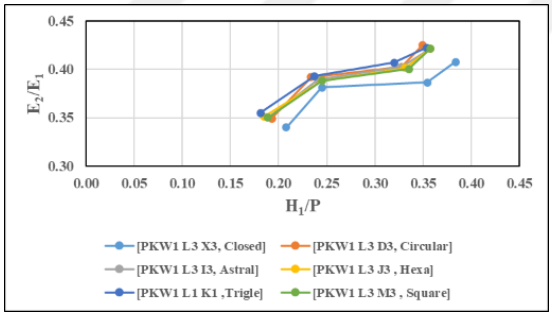

(c) model PKW1 L3 X3, PKW1 L3 D3, PKW1 L3 I3, PKW1 L3 J3, PKW1 L3 K3, PKW1 L3 M3

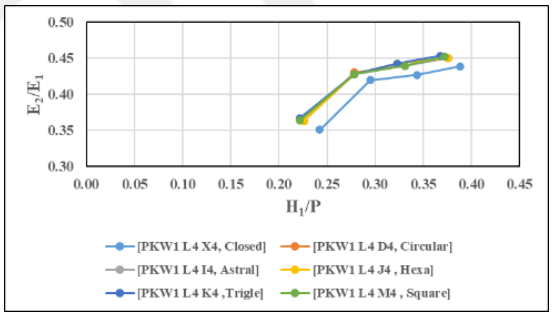

(d) model PKW1 L4 X4, PKW1 L4 D4, PKW1 L4 I4, PKW1 L4 J4, PKW1 L4 K4, PKW1 L4 M4

Figure 4.65: The effect of adding screen walls have holes with different shapes to PKW on the Residual Energy (E_2/E_1).

Noted from Figure 4.65 that the Residual Energy (E_2/E_1) increases by using screen walls with holes of different shapes type-D, type-I, type-J, type-K, and type-M than the Residual Energy (E_2/E_1) if we use a screen wall type-X.

Noted from Figure 4.65 that the screen walls all give very similar results in increasing Residual Energy (E_2/E_1), but they sometimes differ in their sequences by giving a higher the Residual Energy (E_2/E_1). This slight difference appears when changing the heights of the weir and at high discharge.

But it always remains clear that screen walls type-K with tringle holes gave the largest Residual Energy (E_2/E_1) at all weir heights, followed by screen walls type-J with hexagonal holes, then screen walls type-M with square holes, type-D with circular holes, and type-I with astral holes, respectively, as an example, when used the models PKW1 L1 X1, PKW1 L1 D1, PKW1 L1 I1, PKW1 L1 J1, PKW1 L1 K1, PKW1 L1 M1 for the same geometric parameters and the same $(H_1/P = 0.2)$, the Residual Energy $(E_2/E_1 = 0.33, 0.34, 0.37, 0.37, 0.38 \text{ and } 0.39)$ for screen wall type-X, type-I, type-D, type-M, type-J, and type-K respectively. That is, an increase 3% for type-I, and 9% for type-D, 5% for type-M, 12% for type-J, and 18% for type-K respectively.

It was also noted from all the figures linking the relationship between the Residual Energy (E_2/E_1) and the different shapes of the holes of screen wall that high discharges give the highest values for the Residual Energy and low discharges give the lowest values for the Residual Energy for the same screen wall.

4.4 Study of Choosing the Optimal Case for Adding A Screen Wall to PKW Type-A

Based on the previous results obtained in the laboratory for the values of the flow discharge coefficients and the flow energy dissipation rates for the laboratory models, and by conducting a comparison for the discharge coefficients of the screen walls in terms of the diameters of the holes, it was found that the screen wall type-E achieve the highest flow discharge coefficient, followed by the screen walls type-D, and it is In terms of the porosity of the screen walls, it was found that type-H screen wall give the highest discharge coefficient within their group, and in terms of the shape of the screen wall holes, it was shown that type-K achieves almost higher results than type-J, type-M, type-D and type-I, respectively, with a very slight difference.

A comparison is made between all of these walls to determine the best discharge coefficient through the following Figure 4.66.

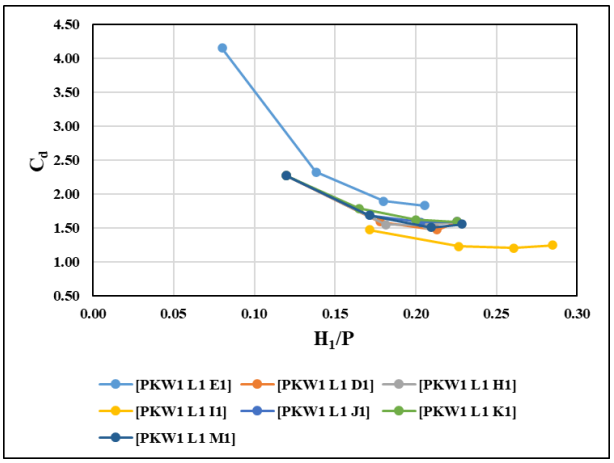

Figure 4.66: Comparing of the discharge coefficient for model PKW1 L1 E1, PKW1 L1 D1, PKW1 L1 H1, PKW1 L1 K1, PKW1 L1 J1, PKW1 L1 M1, PKW1 L1 I1.

It is noted from Figure 4.66 that the highest discharge coefficient is achieved by the screen wall type-E, and the lowest value of discharge coefficient is for the screen wall type-I. As for the rest of the screen walls, type-K, type-J, type-M, type-D, and type-H, they are very close in the coefficient of discharge, especially when (H_1/P) is low, and a slight discrepancy is observed when the head of flow is high, that is, at $(H_1/P = 0.2)$.

In order to compare screen walls that give the highest discharge coefficient with the highest possible amount of energy dissipation, a comparison is made to screen walls type-E, type-K, type-J, type-M, type-D, and type-H in terms of flow energy dissipation with the screen wall type-I excluded from the comparison because it gives a lower coefficient of discharge than the rest of the screen walls that compared. As shown in Figure 4.67.

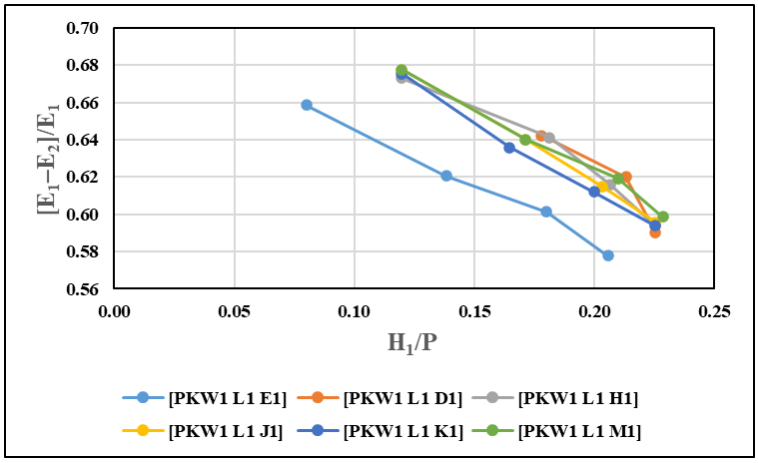

Figure 4.67: Comparing of the energy dissipation for model PKW1 L1 E1, PKW1 L1 D1, PKW1 L1 H_1, PKW1 L1 K1, PKW1 L1 J1, PKW1 L1 M1.

It is noted from Figure 4.67 that the lowest energy dissipation is achieved by screen wall type-E, as the difference is very clear between it and the rest of the screen walls that were compared.

It is also noted that the screen wall type-K gives a lower dissipation than the rest of the screen walls, as the energy dissipation of the screen walls at $(H_1/P = 0.2)$ as follows: $(type - D = 0.63, type - H = 0.62, type - M = 0.62, type - J = 0.62, type - K = 0.61, and\ type - E = 0.58)$.

These ratios are somewhat close to each other, noting that the type-D screen wall gives the highest rates of energy dissipation, albeit with a slight difference, and this makes determining the superiority of the performance of one of them over the performance of the rest of the screen walls a relative issue. It is preferable to use screen walls with large openings over screen walls with smaller openings because they are less affected by blockages resulting from the accumulation of sediment, debris, and small driftwood coming from the source of the waste.

In addition, it is preferable to use screen walls with smooth, circular edges free of corners and protrusions to facilitate the passage of water algae, fish, etc., without causing blockage.

For this reason, it will be preferable to use type D screen walls, as well as type E, despite the fact that it dissipates less energy than the rest of the walls, but it has other priorities which were mentioned earlier.

To know the extent of the benefit of adding a screen wall to the piano key weir in developing the hydraulic performance of this dam, a comparison was made between the five PKW models that were studied in the case of adding a screen wall type-X to them (PKW1 L1 X1, PKW2 L1 X1, PKW3 L1 X1, PKW4 L1 X1, PKW5 L1 X1) to represent the absence of any holes in the lateral walls of the weir, against the model PKW1 L1 to represent the traditional case for the PKW type-A with add to it the screen walls type-E and type-D that it has been previously identified.

PKW1 L1 model was chosen from among the five models for reasons including it represents the most structurally balanced state for this type of weirs, in addition to its optimal resistance to push flow due to its small cross-section and small size of its overhangs compared to the rest of the other models which face difficulty in resisting the forces of push flow that Coming to it from the upstream.

A comparison was made between the two models (PKW1 L1 E1, PKW1 L1 D1) and the five models (PKW1 L1 X1, PKW2 L1 X1, PKW3 L1 X1, PKW4 L1 X1, PKW5 L1 X1) In terms of the coefficient of discharge and the dissipated energy, as shown in Figure 4.68 & Figure 4.69.

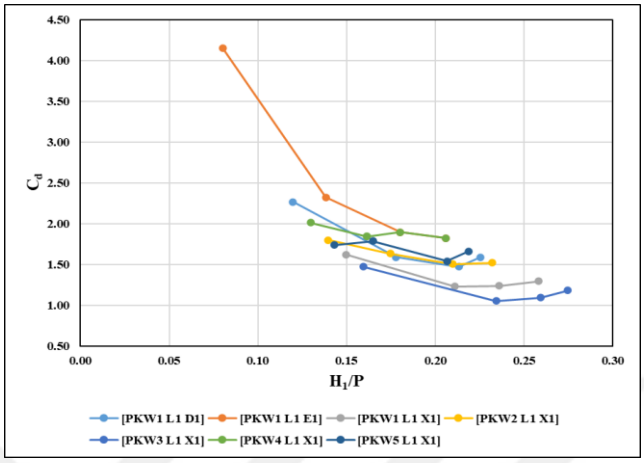

Figure 4.68: Comparing of the discharge coefficient for model PKW1 L1 E1, PKW1 L1 D1 with the five models PKW1 L1 X1, PKW2 L1 X1, PKW3 L1X1, PKW4 L1 X1, PKW5 L1 X1.

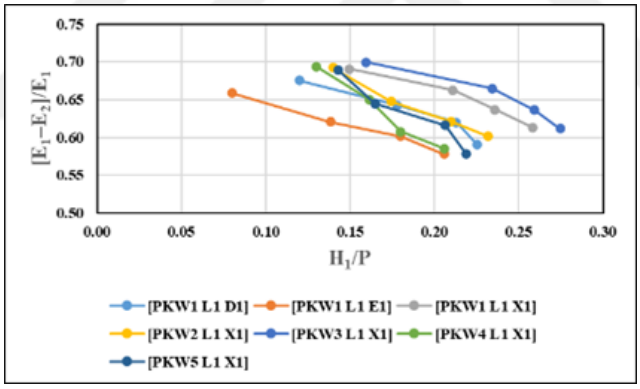

Figure 4.69: Comparing of the dissipated energy for model PKW1 L1 E1, PKW1 L1 D1 with the five models PKW1 L1 X1, PKW2 L1 X1, PKW3 L1X1, PKW4 L1 X1, PKW5 L1 X1.

From Figure4.69, it was noted that the model PKW1 L1 E1 gave a clearly higher coefficient of discharge than the rest of the other models, but it gave a lower value of energy dissipation than the rest of the models. This gives an indication of the possibility of using this model in cases where there is a need to pass large amounts of discharge at times of peak floods, with the possibility of energy dissipation being slightly lower than other models. It is also characterized by its ability to clean deposits well due to the size of the holes in the screen walls.

It was also noted that the model PKW1 L1 D1 gives a good value of the coefficient of discharge that can compete with models with longer top edges such as the model PKW4 L1 X1, PKW5 L1 X1 and models with large inlet keys such as the model PKW2 L1 X1. It was also distinguished by the fact that its energy dissipation rate was good, which means that adding screen walls to it greatly increases its performance, so it is possible to dispense with models with longer edges or large inlet keys and just develop the model PKW1 by adding a screen wall to it.

A comparison was also made to the model PKW3 L1 by adding a screen wall of type-D with the seven models ago PKW1 L1 E1, PKW1 L1 D1, PKW1 L1 X1, PKW2 L1 X1, PKW3 L1 X1, PKW4 L1 X1, PKW5 L1 X1, to determine the extent of its performance in increasing discharge coefficient and energy dissipation, as it always gives the highest of energy dissipation, and comparing it with all seven models that were compared. As shown in Figure 4.70 & Figure 4.71.

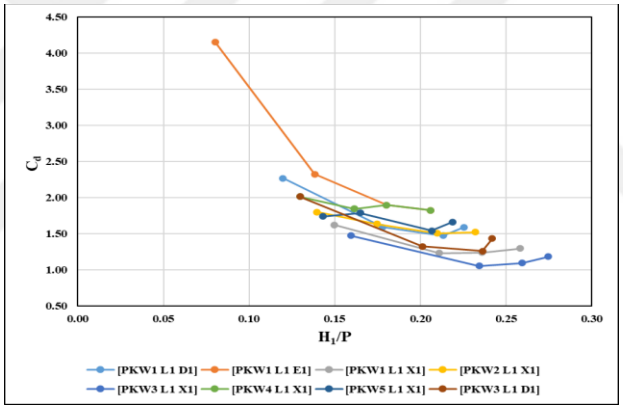

Figure 4.70: Comparing of the discharge coefficient for model PKW3 L1 D1 with the five models PKW1 L1 E1, PKW1, PKW1 L1 X1, PKW2 L1 X1, PKW3 L1X1, PKW4 L1 X1, PKW5 L1 X1.

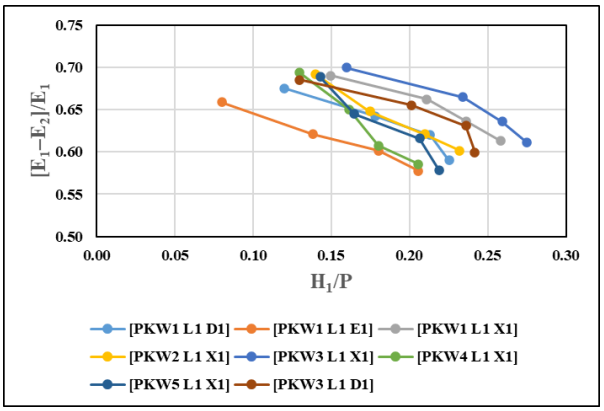

Figure 4.71: Comparing of the dissipated energy for model PKW3 L1 D1 with the five models PKW1 L1 E1, PKW1 L1 D1, PKW1 L1 X1, PKW2 L1 X1, PKW3 L1X1, PKW4 L1 X1, PKW5 L1 X1.

Noted from the Figure 4.71 that the model PKW3 L1 D1 gave a fairly good discharge coefficient due to reducing the hydraulic pressure on the input key after adding screen walls with openings, and its performance is still good in dissipating energy.

When comparing the discharge coefficient between the five main PKW models for the same type of screen walls PKW1 L1 D1, PKW2 L1 D1, PKW3 L1 D1, PKW4 L1 D1, PKW5 L1 D1 as in the Figure 4.72.

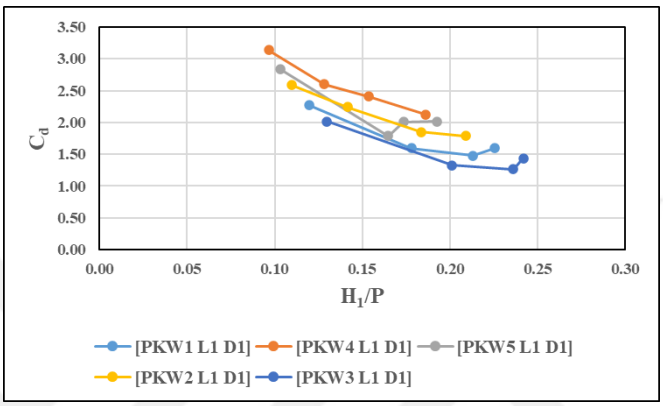

Figure 4.72: Comparing of the discharge coefficient for model PKW3 L1 D1 with the five models PKW1 L1 D1, PKW1, PKW2 L1 D1, PKW3 L1 D1, PKW4 L1 D1, and PKW5 L1 D1.

Noted that model PKW4 L1 D1 achieves a greater discharge coefficient than the rest of the other models, followed by the models PKW5 L1 D1, PKW2 L1 D1, PKW1 L1 D1, and PKW3 L1 D1, respectively.

When comparing the energy dissipation of these five main PKW models for the same type of screen walls as in Figure 4.73.

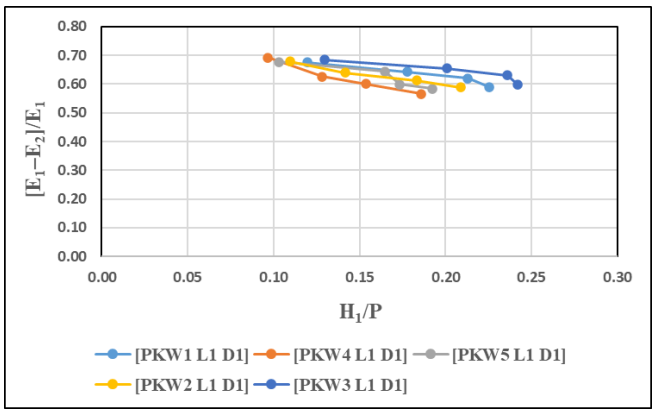

Figure 4.73: Comparing of the energy dissipation for model PKW3 L1 D1 with the five models PKW1 L1 D1, PKW1, PKW2 L1 D1, PKW3 L1 D1, PKW4 L1 D1, and PKW5 L1 D1.

Noted that the model PKW4 L1 D1 gave a good rate of energy dissipation, relatively close to other models, and this makes it the optimal model that can be chosen for discharging large amounts of runoff during times of river floods and heavy rains. Next comes PKW5 L1 D1 model.

5. CONCLUSIONS

5.1 Conclusions of the Experimental Study

In this research, the addition of different screen walls in terms of diameters of holes, porosity of screen wall, and shapes of holes to the side walls of the piano key weir was studied to determine the extent of their effect on the discharge coefficient, energy dissipation, and residual energy.

The different screen walls are applied to five main models of the piano key weir type-A, with a rectangular shape (PKW1, PKW2, PKW3, PKW4, and PKW5) which Different geometric parameters and each model have four heights ($P = 30, 28, 26, 24\ cm$) and additional 13 models of screen walls with different holes and divided into three groups; the group of diameters it includes type-A ($\Phi = 0.35cm$), type-B ($\Phi = 0.5cm$), type-c ($\Phi = 0.7cm$), type-D ($\Phi = 1.0cm$), type-E ($\Phi = 1.4cm$), and the group of porosity it includes type-B ($porosity = 3.9\%$), type-F ($porosity = 7.18$), type-G ($porosity = 9.7\%$), type-H ($porosity = 17.44\%$) and the group of shapes it includes type-D (circular), type-I (astral), type-J (hexagonal), type-K(triangular), type-M (square).

The experiments laboratory was conducted in the hydraulics laboratory of the College of Engineering, University of Mosul, where 400 Experiment conducted by passing 4 flow discharges 37,47,57 and 67 lt/s through a horizontal concrete channel with a length of 24.64 m, width of 0.81 m and depth of 0.6 m, with concrete walls 0.2 m thick. The case of flow was free flow and clear water, and the model of PKW was not immersed.

5.2 Conclusions about Adding Different Screen Walls to PKW TYPE-A Models Based on the Discharge Coefficient C_d

1. The discharge coefficient of PKW models increases by increasing the values of (L/W), (W_i/W_o), and (B/P), when the value of (H_1/P) is constant, for all cases of study. as Increasing this value leads to an increase in the amount of flow

leaving PKW. This is because by increasing this ratio leads to an increase in the size of the inlet key, and also increase in the length of the wet edge of the crest which increases the flow area to the downstream of PKW through the nappes emerging from above the back edges and side edges of the inlet key. This leads to the discharge of larger amounts of flow from the upstream of the weir towards the downstream.

2. The discharge coefficient of PKW models decreases by increasing the value of H_1/P, when the value of (L/W), (W_i/W_o), and (B/P) ,is constant, for all cases of study Because increasing this value means an increase in the head of flow at the upstream of PKW and above the inlet key, and this increases the hydraulic pressure in the inlet key which leads to an increase the flow speed in it, and which causes an increase in the size and length of the lateral nappes emerging from it which leads to an increase in the collision of these nappes with the corresponding nappes inside the outlet key, in addition to the flow descending from the upstream side of the outlet key which causes local immersion of the outlet key which causes obstruction of the flow at the toe of. These factors lead to a decrease in the actual discharge passing through the model dam and, thus, a decrease in the discharge coefficient.

3. By adding screen walls containing holes to PKW models, the discharge coefficient increases when the value of (H_1/P) is constant for all cases of study, as the holes in the screen walls allow the flow to pass through them to the outlet key in jets form, which reduces the hydraulic pressure generated inside the inlet key and thus reduces speed disturbance, and this allows the flow to pass more smoothly. It also keeps the head height upstream at low levels, thus increasing the discharge coefficient.

4. The discharge coefficient of PKW models increases by addition of the screen walls to them and with increasing values of (L/W), (W_i/W_o), (B/P), at constant value H_1/P, for all cases of study, more than it increases with increasing values (L/W), (W_i/W_o), (B/P), only.

5. The effect of increasing the holes diameter of the screen wall on increasing the discharge coefficient of the PKW models is greater than the effect of increasing

the geometric parameters (L/W), (W_i/W_o), (B/P), on it, and this effect increases with the increased diameter of holes of the screen walls.

6. The discharge coefficient of PKW models increases by decreasing the value of (H_1/P) when adding screen walls, for all cases of study and the rate of increase of the discharge coefficient decreases with increasing high discharges.
7. The discharge coefficient of PKW models increases by increasing the diameters of the holes in the screen walls, with a constant (H_1/P) for all cases of study. The type-E screen walls achieved the highest discharge coefficient, followed by type D, type C, type B, and type A, respectively. The increase in the discharge coefficient is caused by the greater the diameter of the holes, the greater amounts of flow are allowed to drain through them to the outlet key, which leads to a decrease in the head at the upstream of the weir and the discharge coefficient increases.
8. The discharge coefficient of PKW models increases by increasing the porosity of the screen walls, with a constant (H_1/P) for all cases of study. The type-H screen walls achieved the highest discharge coefficient, followed by type G, type F, and type B, respectively. The increase in the discharge coefficient is caused by the greater the number of holes, the greater amounts of flow are allowed to drain through them to the outlet key, which leads to a decrease in the head upstream of the weir and the discharge coefficient increases.
9. The screen walls, which have different shapes holes and equal area holes which are added to PKW models, gave close values for the discharge coefficients when (H_1/P) constant, where type-K screen wall achieved the highest discharge coefficient, then type-J, type-M, type-D, and type-I, respectively.
10. PKW models with higher the heights give a higher discharge coefficient value, and the shorter the heights of the models, the lower the discharge coefficient value for all cases, The reason is because as decrease the height of the model, the head at the upstream which increases the immersion of the inlet and outlet keys which reduces the discharge coefficient.
11. As the heights of PKW models decreased, the screen walls still gave the higher value of discharge coefficient for all cases, with type-D screen walls giving the

best discharge, then type-B, then type-X, but this difference decreases with a decrease in the height of the model.

12. Screen walls type-E gave the highest value for the discharge coefficient, with a very large difference from the rest of the screen walls at low discharges, and this difference decreases with increasing discharges.
13. The model PKW4 gives the highest discharge coefficient, and then PKW5, PKW2, PKW1 and PKW3, respectively, use the same screen walls.

5.3 Conclusions about adding different screen walls to the PKW TYPE-A models based on the energy dissipation $((\boldsymbol{E_1 - E_2})/\boldsymbol{E_1})$ and the Residual Energy $(\boldsymbol{E_2/E_1})$

1. The energy dissipation of PKW models decreases by increasing the values of L/W, (W_i/W_o), and (B/P), when the value of (H_1/P) is constant, for all cases of study. As increasing this value leads to an increase in the amount of flow leaving PKW, this is because by increasing this ratio leads to an increase in the size of the inlet key, and also increase in the length of the wet edge of the crest which increases the flow area to the downstream of PKW through the nappes emerging from above the back edges and side edges of the inlet key to outlet key. This leads to the discharge of larger amounts of flow from the upstream of the weir towards the downstream and then increases the depth of tailwater, which causes an increase in the force of flow and the Residual Energy (E_2/E_1) downstream and decreases Energy Dissipation $((E_1 - E_2)/E_1)$.
2. The Energy Dissipation of PKW models decreases by increasing the value of H_1/P when the values of (L/W), (W_i/W_o), and (B/P) ,is constant, for all cases of study Because increasing this value means an increase in the head of flow at the upstream of PKW and above the inlet key, and this increases the hydraulic pressure in the inlet key which leads to an increase the flow speed in it, and which causes an increase in the size and length of the lateral nappes emerging from it which leads to an increase in the collision of these nappes With the corresponding nappes inside the outlet key, in addition to the flow descending from the upstream side of the outlet key which causes local immersion of the

outlet key, and this will increase the turbulence inside it, and will increase the energy that exits out it which reduces energy dissipation.

3. By adding screen walls containing holes to PKW models, the energy dissipation decreases when the value of (H_1/P) is constant for all cases of study, as the holes in the screen walls allow the flow to pass through them to the outlet key in jets form. These jets mix and interfere with the nappes jumping over the edge the side wall, as well as with the flow coming down from the front of the outlet key. This causes a relative increase in local immersion of the outlet key, which means it increases the flow coming from the weir and, therefore, increases the depth of the tail water, increases the Residual Energy and decreases the energy dissipation.
4. The energy dissipation of the PKW models decreases by the addition of the screen walls to them and with increasing values of (L/W), (W_i/W_o), (B/P), at constant value H_1/P, for all cases of study, less than it decreases with increasing values (L/W), (W_i/W_o), (B/P), only.
5. The effect of increasing the holes diameter of the screen wall on the decrease of the Energy Dissipation of PKW models is smaller than the effect of increasing the geometric parameters (L/W), (W_i/W_o), (B/P), on it, and this effect increases with the increase in diameter of holes of the screen walls.
6. The energy dissipation of PKW models increases by decreasing the value of (H_1/P) when adding screen walls for all cases of study.
7. The energy dissipation of PKW models decreases by increasing the diameters of the holes in the screen walls, with a constant (H_1/P) for all cases of study. The type-A screen walls achieved the highest energy dissipation, followed by type B, type C, type D, and type E, respectively. The decrease in the energy dissipation is caused by the greater the diameter of the holes, the greater amounts of flow are allowed to drain through them to the outlet key, which causes a local immersion of the outlet key.
8. The energy dissipation of PKW models decreases by increasing the porosity of the screen walls, with a constant (H_1/P) for all cases of study. The type-B screen walls achieved the highest energy dissipation, followed by type F, type G, and type H, respectively. The decrease in the energy dissipation is caused by the

greater the number of holes, the greater amounts of flow are allowed to drain through them to the outlet key, which causes a local immersion of the outlet key.

9. The screen walls, which have different shapes holes and equal area holes which are added to PKW models, gave close values for the energy dissipation when (H_1/P) is constant, where type-I screen wall achieved the highest energy dissipation, then type-D, type-M, type-J, and type-K, respectively.
10. PKW models with higher heights give a higher Energy dissipation value, and the shorter the heights of the models. The lower the Energy dissipation value for all cases, the reason is because as decrease the height of the model, the head at the upstream increases which increases the immersion of the inlet and outlet keys, this leads to a decrease in energy dissipation and an increase the Residual Energy in downstream.
11. The model PKW3 gives the highest energy dissipation, and then PKW1, PKW2, PKW5 and PKW4, respectively, at use same the screen wall.
12. The hydraulic jump approaches the bottom of the dam as the diameter of the screen wall holes increases. It also shortens the length of the ventilation area which is good for reducing the area of the corrosion area below the dam.

5.4 Conclusion of the Optimal Model for This Study

1. PKW1 model represents the most structurally balanced state among the five models and its optimal resistance to push flow due to the short length of its overhangs, small inlet keys, and small cross-section.
2. Models PKW4 L1 D1 and PKW5 L1 D1 give the best performance in terms of balance between increasing the discharge coefficient with good energy dissipation.

5.5 Advantages of Adding Screen Walls to Piano Key Weir

1. It increases the discharge coefficient, which increases the amount of safe discharge of flow through it, thus reducing the risk of flooding.

2. It reduces the flow head upstream, especially at peak times of floods and large rain waves, thus preserving neighboring lands from the danger of flow lagging on them.
3. It is structurally easy to manufacture, and its manufacture or construction does not require effort or increased economic costs. It can be implemented during the construction of the dam.
4. It can be made in several geometric shapes or measurements according to what the situation needs or the surrounding conditions require. It can also be made liftable and replaceable as needed.
5. It is easy to maintain and does not cause mechanical or electrical malfunctions. It is not like hydromechanical gates or electric gates are expensive.
6. It reduces the hydraulic pressure on the dam and on the inlet keys by draining the flow through their holes. This is what makes the dam structurally safe.
7. Using screen walls reduces the need to increase the geometric parameters, increase the sizes of the inlet and outlet keys of PKW, increase the length of the overhangs, or increase the edge length of the crest, as it gives high drainage coefficients, a smaller size of the weir, and greater energy dissipation than increasing the size of the geometric parameters.
8. The hydraulic jump approaches the bottom of the dam as the diameter of the screen wall holes increases. It also shortens the length of the ventilation area which is good for reducing the area of the corrosion area below the dam.
9. It allows sediment and silt to pass through it, especially if the screen wall holes are large, which reduces the accumulation of sediment upstream of the dam.
10. It allows aquatic plants, fish, and other aquatic animals to pass through it, especially if the diameters of the holes in the screen walls are large, which gives more balance to nature on both sides of the dam.

5.6 Disadvantage of Adding Screen Walls to Piano Key Weir

1. It reduces energy dissipation slightly due to the amount of water that passes through it to the downstream of the PKW and increases the amount of remaining energy.

2. There is a constant need to clean the holes of the screen walls from blockages that occur due to silt, debris, and driftwood.
3. Difficulty controlling the amount of storage volume of the dam at the upstream due to the presence of holes that continue to drain water through them.
4. The role of the screen wall holes decreases at high discharges due to the increased flow velocity of the flow, as well as due to the high head upstream, which makes the flow jump over the edge of the crest to the outlet keys; it causes it to be submerged.

5.7 Recommendations

1. Study the effect of adding screen walls to other types of piano key weirs, type-B, type-C, and type-D.
2. Study the effect of adding screen walls to the piano key weir on the scouring downstream of PKW.
3. Study the effect of adding screen walls to the labyrinth weir.
4. Study the effect of adding screen walls on other shapes of piano key weirs, such as triangle, trapezoid, and circular.
5. Study the effect of adding screen walls to piano key weir on the transfer of sediments from the upstream to downstream of PKW.
6. Study the effect of adding screen walls to piano key weir at the end of the outlet key and also on the back slope floor of the inlet key.
7. Numerical study of the effect of adding screen walls to the piano key weir.

REFERENCES

Abhash, A., & Pandey, K. K. (2022). A review of Piano Key Weir as a superior alternative for dam rehabilitation. *ISH Journal of Hydraulic Engineering*, *28*(sup1), 541–551. https://doi.org/10.1080/09715010.2020.1767516.

Ackers, J. C., Bennett, F. C. J., Scott, T. A., & Karunaratne, G. (2014). Raising the bellmouth spillway at Black Esk reservoir using Piano Key weirs. *Labyrinth Piano Key Weirs II-PKW 2013*, 235–242. https://doi.org/10.1201/b15985-32.

Al-Baghdadi, M. B. N., & Khassaf, S. I. (2018). Evaluation of crest length effect on piano key weir discharge coefficient. *International Journal of Energy and Environment*, *9*(5). http://ijee.ieefoundation.org/vol2/public_html/ijeeindex/-vol2/issue4/IJEE_03_v2n4.pdf.

Al-Hafith, A. I. M., & Noori, B. M. A. (2007). Laboratory Study Of Scour In Stone Beds Downstream Triangular Plan Form Weirs. *Al-Rafidain Engineering Journal (AREJ)*, *15*(2), 47–62. https://doi.org/10.33899/rengj.2007.44966.

Al-Shukur, A.-H. K., & Al-Khafaji, G. H. (2018). Experimental study of the hydraulic performance of piano key weir. *International Journal of Energy and Environment*, *9*(1), 63–70.

Alrahhawi, G., & Hayawi, G. (2011, November). *Laboratory Study Of Scour Downstream Screen Walls Used As Energy Dissipaters*. ResearchGate Logo. https://www.researchgate.net/publication/350327745%0ALABORATORY.

Anderson, R. M. (2011). *Piano Key Weir Head Discharge Relationships* [All Graduate Theses and Dissertations]. https://digitalcommons.usu.edu/etd/880.

Anderson, R. M., & Tullis, B. P. (2013). Piano Key Weir Hydraulics and Labyrinth Weir Comparison. *Journal of Irrigation and Drainage Engineering*, *139*(3), 246–253. https://doi.org/doi:10.1061/(ASCE)IR.1943-4774.0000530.

Anderson, R. M., Tullis, B. P., & Asce, M. (2012a). Comparison of Piano Key and Rectangular Labyrinth Weir Hydraulics. *Journal of Hydraulic Engineering*, *139*, 246–253. https://doi.org/10.1061/(ASCE)IR.

Anderson, R. M., Tullis, B. P., & Asce, M. (2012b). Piano Key Weir : Reservoir versus Channel Application Piano Key Weir : Reservoir versus Channel Application. *Journal of Irrigation and Drainage Engineering*, *138*(8), 1–5. https://doi.org/10.1061/(ASCE)IR.1943-4774.0000464.

Aslankara, V. (2007). *Experimental Investigation of Tailwater Effect on The Energy Dissipation Through Screens, [M.S. - Master of Science]*. Middle East Technical University.

Association of State Dam Safety Officials. (2020). *Spencer Dam Failure Investigation Report*. https://damsafety.org/SpencerDamReport

Balkiş, G. (2004). *Experimental Investigation of Energy Dissipation Through Inclined Screens, [M.S. - Master of Science]*. Middle East Technical University.

Barcouda, M., Cazaillet, O., Cochet, P., Jones, B. A., Lacroix, S., Laugier, F., Odeyer, C., & Vingny, J. P. (2006). Cost effective increase in storage and safety of most dams using fusing or P.K. Weirs. *22nd Congress of ICOLD Q86, R3*.

Bekheet, A. A., Aboulatta, N. M., Saad, N. Y., & El-molla, D. A. (2022). Effect of the shape and type of piano key weirs on the flow efficiency. *Ain Shams Engineering Journal*, *13*. https://doi.org/10.1016/j.asej.2021.10.015.

Belaabed, F., Goudjil, K., Leila, A., & Ouamane, A. (2021). Utilization of computational intelligence approaches to estimate the relative head of PK-Weir for submerged flow. *Neural Computing and Applications*, *33*, 1–13. https://doi.org/10.1007/s00521-021-05996-7.

Belaabed, F., & Ouamane, A. (2013). Submerged Flow Regimes of Piano Key Weir. In S. ERPICUM & et al. (Eds.), *Labyrinth and Piano KeyWeirs II*. Taylor & Francis.

Bhukya, R. K., Pandey, M., Valyrakis, M., & Michalis, P. (2022). Discharge Estimation over Piano Key Weirs: A Review of. *Water 2022*, *14*(3029), 1–17. Panagiotis Michalis

Bieri, M., Federspiel, M., Boillat, J., Houdant, B., Faramond, L., & Delorme, F. (2011). Energy dissipation downstream of Piano Key Weirs – Case study of Gloriettes Dam (France). In S. Erpicum, F. Laugier, J. L. Boillat, M. Pirotton, B. Reverchon, & A. Schleiss (Eds.), *Labyrinth and Piano Key Weirs-PKW 2011*. CRC Press.

Blancher, B., Montarros, F., & Laugier, F. (2011). Hydraulic Comparison between Piano Key Weirs and Labyrinth Spillways. *Proceedings of the International Conference on Labyrinth and Piano Key Weirs (PKW 2011)*, 141–150.

Bozkus, Z., Çakir, P., & Ger, A. M. (2007). Energy dissipation by vertically placed screens. *Canadian Journal of Civil Engineering*, *34*, 557–564. https://doi.org/10.1139/L06-158.

Bozkuş, Z., Güngör, E., & Ger, M. (2006, November). Energy Dissipation by Triangular Screens. *Seventh International Congress on Advances in Civil Engineering*. https://www.researchgate.net/publication/303738740.

Chow, V. . (1959). *Open-channel hydraulics*. McGraw-Hill Book Company.

Cicero, G.-M., Carol, G., Marilyne, L., Thomas, P., Alexandre, L., & Pierre-, B. (2010, May). Experimental Optimization of A Piano Key Weir to Increase The Spillway Capacity of The Malarce Dam. *1st IAHR European Congress*.

Cicero, G.-M., & Delisle, J. R. (2013). Discharge characteristics of Piano Key weirs under submerged flow. In S. Erpicum, F. Laugier, M. Pfister, M. Pirotton, G.-M. Cicero, & A. J. Schleiss (Eds.), *Labyrinth Piano Key Weirs II-PKW 2013* (pp. 101–109). Taylor & Francis.

Cicero, G.-M., Vermeulen, J., & Laugier, F. (2016). Influence of Some Geometrical Parameters on Piano Key Weir Discharge Efficiency. In B. Crookston & B. Tullis (Eds.), *Hydraulic Structures and Water System Management*. https://doi.org/10.15142/T3320628160853.

Climate-ADAPT. (2019, February 6). *Flood risk management for hydropower plants in France*. https://climate-adapt.eea.europa.eu/en/metadata/case-studies/fd/-energy-cs1_hydropower-france_figure-2.jpg/image_view_fullscreen.

Crookston, B. M., Crowley, L., & Pfister, M. (2016). Piano Key Weir for Enlargement of the West Fork of Eno River Reservoir. In B. Crookston & B. Tullis (Eds.), *Hydraulic Structures and Water System Management*. 6th IAHR International Symposium on Hydraulic Structures. https://doi.org/10.15142/T3300628160853

Crookston, B. M., & Tullis, B. P. (2012). Labyrinth weirs: Nappe interference and local submergence. *Journal of Irrigation and Drainage Engineering*, *138*(8), 757–767.

Denys, F. (2017, May). *Piano Key Weir spillway standard design principles and flow induced vibrations*. ResearchGate. https://www.researchgate.net/publication-/316889515.

Eichenberger, P. (2013). The first commercial piano keyweir in Switzerland. In S. Erpicum, F. Laugier, M. Pfister, M. Pirotton, G.-M. Cicero, & A. J. Schleiss (Eds.), *Labyrinth Piano Key Weirs II-PKW 2013*. Taylor & Francis. https://doi.org/10.1201/b15985.

Elaswad, S., Elnikhili, E., & Saleh, O. (2021). Effect of different screen widths on the submerged hydraulic jump characteristics. *The Egyptian International Journal of Engineering Sciences and Technology*, *34*, 1–10. https://eijest.journals.ekb.eg/.

Erpicum, S., Archambeau, P., Pirotton, M., & Dewals, B. J. (2014). Geometric parameters influence on Piano Key Weir hydraulic performances. *5th International Symposium on Hydraulic Structures*, 25–27. https://doi.org/10.14264/uql.2014.31.

Erpicum, S., Laugier, F., Pfister, M., Pirotton, M., Cicero, G.-M., & Schleiss, A. J. (2013). *Labyrinth Piano Key Weirs II-PKW 2013*. Taylor & Francis.

Erpicum, S., Lempérière, F., Ouamane, A., Khanh, M. H. T., Laugier, F., Tullis, B., & Crookston, B. (Eds.). (2013). Piano Key Weirs Spillways. In *Labyrinth and Piano Key Weirs II-PKW 2013*. CRC Press.

Erpicum, S., Machiels, O., Archambeau, P., Dewals, B., & Pirotton, M. (2010, June). 1d Numerical Approach to Model The Flow Over A Piano déversoir en touches de piano (PKW). *Hydraulic Modeling and Uncertainty*.

Erpicum, S., Machiels, O., Archambeau, P., Dewals, B., Pirotton, M., & Daux, C. (2011). Energy dissipation on a stepped spillway downstream of a Piano Key Weir—Experimental study. In S. Erpicum, F. Laugier, M. Pfister, M. Pirotton, G.-M. Cicero, & A. J. Schleiss (Eds.), *Labyrinth and Piano Key Weirs-PKW 2011* (pp. 105–112). CRC Press.

Eslinger, K. R., & Crookston, B. M. (2020). Energy Dissipation of Type a Piano Key Weirs. *Water*, *12*(1253). http://creativecommons.org/licenses/by/4.0/.

Farhadi, H., Moghadam, M. K., Sabzevari, T., & Noroozpour, S. (2023). Study of relative energy dissipation of trapezoidal and arced piano key weirs equipped with baffles. *Water Supply*, *23*(1), 80–93. https://doi.org/10.2166/ws.2022.427.

Guo, X., Wang, T., Fu, H., & Li, J. (2018). Discharge capacity evaluation and hydraulic design of a piano key weir. *Water Science & Technology: Water Supply*. https://doi.org/10.2166/ws.2018.134.

Haghiabi, A. H., Ghaleh Nou, M. R., & Parsaie, A. (2022). The energy dissipation of flow over the labyrinth weirs. *Alexandria Engineering Journal*, *61*(5), 3729–3733. https://doi.org/10.1016/j.aej.2021.08.075.

Hammel, P. (2023, April 15). *Family of man who was washed away in collapse of Spencer Dam loses court appeal*. 10 11 Now Koln Kgin. https://www.1011now.com/.

Hammer, J. (2020, October 9). *City Asks You To Imagine A Day Without Water*. Rihno Times. https://www.rhinotimes.com/news/city-asks-you-to-imagine-a-day-without-water/.

Hayawi, G. A. A.-M. (2006). *Labratory Study of Protected Downstream Slope of Rockfill Weirs Using Gabions, Doctor Thesis*. University of Mosul.

Hien, T. C., Son, H. T., & Khanh, M. H. T. (2006). Results of some Piano Keys weir hydraulic model tests in Vietnam. Proc. *22nd Congress of Large Dams, Question 87, Response 39, International Commission on Large Dams (ICOLD)*.

Jalil, S. A., Yaseen, M. S., & Mahmoud, H. A. (2013). Performance of Screen Wall Openings Shape on Energy Dissipation. *International Journal of Scientific & Engineering Research*, *4*(11). https://www.researchgate.net/publication/3155-22805%0APerformance.

Jayatillake, H. M., & Perera, K. T. N. (2013). Design of a Piano-Key Weir for Giritale Dam spillway in Sri Lanka. *Jaya Tillake 2013 Design OA*. https://api.semanticscholar.org/CorpusID:114056219.

Jüstrich, S., Pfister, M., & Schleiss, A. (2016). Mobile Riverbed Scour Downstream of a Piano Key Weir. *Journal of Hydraulic Engineering*, *142*(11), 1–2. https://doi.org/p.04016043.

Kabiri-samani, A., & Javaheri, A**. (2012). Discharge coefficients for free and** submerged flow over Piano Key weirs. *Journal of Hydraulic Research*, *50*(1). https://doi.org/10.1080/00221686.2011.647888.

Karimi, C. M., Nazari, S., & Mahmoodian, S. M. (2019). Experimental and numerical simulation of arced trapezoidal piano key weirs. In *Flow Measurement and Instrumentation 68*. https://doi.org/10.1016/j.flowmeasinst.2019.10157.

Khanh, M. H. T. (2017). History and development of Piano Key Weirs in Vietnam from 2004 to 2016. In S. Erpicum, F. Laugier, M. Pfister, M. Pirotton, G.-M. Cicero, & A. J. Schleiss (Eds.), *Labyrinth and Piano Key Weirs II-PKW 2013* (3rd ed., pp. 3–16). https://www.taylorfrancis.com/chapters/edit/10.1201/-9781315169064-38/study-design-construction-van-phong-piano-key-weirs-quat-dinh-sy-nguyen-luong-hung-nguyen-manh.

Khanh, M. H. T., Hein, T. C., & Hai, N. T. (2011). Main Results of the PK Weir Model Tests in Vietnam (2004–2010). In *Labyrinth and Piano Key Weirs-PKW 2011* (pp. 191–198). CRC Press.

Khanh, M. H. T., Hien, T. C., & Quat, D. S. (2012). Study and construction of PK Weirs in Vietnam (2004 to 2011). *Fourth International Conference on Water Resources and Renewable Energy Development in Asia*.

Khassaf, S. I., & Al-Baghdadi, M. B. (2015). Experimental study of non-rectangular piano key weir discharge coefficien. *International Journal of Energy and Environment (IJEE)*, *6*(5). https://www.researchgate.net/publication/281643667-%0AExperimental.

Khassaf, S. I., Aziz, L. J., & Elkatib, Z. A. (2016). Hydraulic Behavior of Piano Key Weir Type B Under Free Flow Conditions. *IInternational Journal Of Scientific & Technology Research*, *5*(03), 2–7.

Kumar, M., Sihag, P., & Subodh, N. K. T. (2020). Experimental study and modelling discharge coefficient of trapezoidal and rectangular piano key weirs. *Applied Water Science*, *10*(43), 1–9. https://doi.org/10.1007/s13201-019-1104-8.

Landers, J. (2021, September 15). *Static liquefaction likely caused Edenville Dam failure, report says*. The American Society of Civil Engineers (ASCE). https://www.asce.org/publications-and-news/civil-engineering-source/civil-engineering-magazine/article/2021/09/static-liquefaction-likely-caused-edenville-dam-failure-report-says.

Laugier, F. (2007). Design and construction of the first Piano Key Weirs spillway at the Goulours dam. *Hypdopower and Dams*, *14*(5), 94–101.

Laugier, F., Lochu, A., Gille, C., Ribeiro, M. L., & Boillat, J.-L. (2009). Design and Construction of a Labyrinth PKW Spillway at Saint-Marc Dam, France. *Hydropower & Dams*, *5*.

Laugier, F., Vermeulen, J., & Blancher, B. (2017). Overview of design and construction of 11 piano key weirs spillways developed in France by EDF from 2003 to 2016. In S. Erpicum, F. Lempérière, A. Ouamane, M. H. T. Khanh, F. Laugier, B. Tullis, & B. Crookston (Eds.), *Labyrinth and Piano Key Weirs II-PKW 2013*. CRC Press.

Laugier, F., Vermeulen, J., & Lefebvre, V. (2013). Overview of Piano Key Weirs experience developed at EDF during the past few years. In S. Erpicum, F. Laugier, M. Pfister, M. Pirotton, G.-M. Cicero, & A. J. Schleiss (Eds.), *Labyrinth Piano Key Weirs II-PKW 2013*. Taylor & Francis.

Lempérière, F., & Jun, G. (2005). Low Cost Increase of Dams Storage and Flood Mitigation: The Piano Keys weir. *19th Congress International Commission on Irrigation and Drainage (ICID)*.

Lempérière, F., & Ouamane, A. (2003). The Piano Keys Weir: a new cost-effective solution for spillways. *International Journal on Hydropower and Dams*, *5*.

Lempérière, F., Ouamane, A., & Vigny, J.-P. (2013). *Piano Keys Weirs (PK weirs) could be used for most African spillways*. HydroCoop. http://www.hydrocoop.org/piano-keys-weirs-could-be-used-for-most-african-spillways/:

Lemperiere, F., Yigny, J.-P., & Ouamane, A. (2011). General comments on Labyrinths and Piano Key Weirs: The past and present. In S. Erpicum, F. Lempérière, A. Ouamane, M. H. T. Khanh, F. Laugier, B. Tullis, & B. Crookston (Eds.), *Labyrinth and Piano Key Weirs-PKW 2011*. Taylor & Francis.

Li, S., Li, G., Jiang, D., & Ning, J. (2020). Influence of auxiliary geometric parameters on discharge capacity of piano key weirs. *Flow Measurement and Instrumentation*, *72*(101719). https://doi.org/10.1016/j.flowmeasinst.2020.-101719.

Lopes, R., Matos, J., & Melo, J. F. de. (2006). Discharge Capacity and Residual Energy of Labyrinth Weirs. In J. Matos & H. Chanson (Eds.), *Hydraulic Structures: A Challenge to Engineers and Researchers* (CH61/06). Division of Civil Engineering at the University of Queensland. http://www.eng.uq.edu.au/civil/%0AFirst.

Lopes, R., Matos, J., & Melo, J. F. de. (2011). Flow properties and residual energy downstream of labyrinth weirs. In S. Erpicum, F. Laugier, J. L. Boillat, M. Pirotton, B. Reverchon, & A. Schleiss (Eds.), *Labyrinth and Piano Key Weirs-PKW 2011*. CRC Press/Balkema.

Machiels, O., Erpicum, S., Archambeau, P., Dewals, B. J., & Pirotton, M. (2009). Large scale experimental study of piano key weirs. *33rd IAHR Congress*, 1030–1037.

Machiels, O., Erpicum, S., Archambeau, P., Dewals, B. J., & Pirotton, M. (2010). Experimental study of the hydraulic behavior of Piano Key Weirs. *Proceedings of IAHR-APD*, 2–11.

Machiels, O., Erpicum, S., Archambeau, P., Dewals, B., & Pirotton, M. (2013). Parapet Wall Effect on Piano Key Weir Efficiency. *Journal of Irrigation and Drainage Engineering*, *139*(6), 506–511. https://doi.org/10.1061/(ASCE)IR.-1943-4774.0000566.

Machiels, O., Pirotton, M., Pierre, A., Dewals, B., & Erpicum, S. (2014). Experimental parametric study and design of Piano Key Weirs. *Journal of Hydraulic Research*, *53*(3), 543–545.

https://doi.org/10.1080/00221686.2015.1054323.

Magalhaes, A. P., & Lorena, M. (1994). Perdas de energiado do escoamento sobre soleiras em labirinto. *Proc. 68 SILUSB/18 SILUSBA*, 203–211.

Mehboudi, A., Attari, J., & Hosseini, S. (2016). Experimental study of discharge coefficient for trapezoidal piano key weirs. In *Flow Measurement and Instrumentation 50* (pp. 65–72). https://doi.org/10.1016/j.flowmeasinst.-2016.06.00.

Merkel, J., Belzner, F., Gebhardt, M., & Thorenz, C. (2018). Energy Dissipation Downstream of Labyrinth Weirs. In D. Bung & B. Tullis (Eds.), *7th IAHR International Symposium on Hydraulic Structures*. https://doi.org/10.15142/T32D2V.

News Detail En. (2017, March 28). *Ground Anchors at Hazelmere Dam Raising*. Paul. https://prestressed-concrete.paul.eu/en/news/news-detail-en?tx_news_pi1%5Baction%5D=detail&tx_news_pi1%5Bcontroller%5D=News&tx_news_pi1%5Bnews%5D=28&cHash=b68397d1c3db9540a597ca525c008235:

Noui, A., & Ouamane, A. (2011). Study of optimization of the Piano Key Weir. In Epicum & E. Al. (Eds.), *Labyrinth and Piano Key Weirs-PKW 2011*. https://www.researchgate.net/publication/274640702%0ATurbulence.

Ouamane, A. (2011). Nine years of study of the Piano Key Weir in the university laboratory of Biskra (lessons and reflections). *Proceedings of the International Conference on Labyrinth Piano Key Weirs-PKW 2011*, 51–58. https://doi.org/10.1201/b12349-9.

Ouamane, A., & Lempérière, F. (2006). Design of a new economic shape of weir. In Berga & E. Al (Eds.), *Dams and Reservoirs, Societies and Environment in the 21st Century*. Taylor& Francis.

Paxson, G., Tullis, B. P., & Hertel, D. J. (2014). Comparison of piano keyweirs with labyrinth and gated spillways: Hydraulics, cost, constructability and operations. In *ResearchGate*. https://www.researchgate.net/publication/290525667%0-AComparison.

Pfister, M., Boillat, J.-L., Schleiss, A. J., Laugier, F., & Ribeiro, M. L. (2012, June). Piano Key Weirs as Efficient Spillway Structure. *Vingt Quatrième Congrès Des Grands Barrages Kyoto*.

Pfister, M., Schleiss, A. J., & Tullis, B. P. (2013). *Effect of driftwood on hydraulic head of Piano Key weirs*. 255–265.

Philips, M., & Lesleighter, E. (2013). Piano Key Weir spillway: Upgrade option for a major dam. *2nd International Workshop on Labyrinth and Piano Key Weirs III-PKW 2013*, 159–168.

Phillips, D. S. (2023). *Sona 2023 Implications for The Department of Water And Sanitation*. artment of Water And Sanitation/ Republic of South Africa.

Pralong, J., Vermeulen, J., Blancher, B., Laugier, F., Erpicum, S., Machiels, O., Pirotton, M., Boillat, J.-L., Leite Ribeiro, M., & Schleiss, A. (2011). A naming convention for the Piano Key Weirs geometrical parameters. In S. Erpicum, F. Laugier, J.-L. Boillat, M. Pirotton, B. Reverchon, & A. Schleiss (Eds.), *Labyrinth and Piano Key Weirs-PKW 2011* (pp. 271–

278). Taylor & Francis. https://doi.org/10.1201/b12349-40.

Reporter, W. (2022, May 22). *release water from Hazelmere Dam, in KZN*. The Witness. https://www.citizen.co.za/witness/news/kzn/kzn-floods-umgeni-water-to-release-water-from-hazelmere-dam-in-kzn-20220522/.

Ribeiro, M. L., Bieri, M., Boillat, J.-L., Schleiss, A. J., Delorme, F., & Laugier, F. (2009, May). Hydraulic Capacity Improvement of Existing Spillways – Design of Piano Key Weirs. *Vingt Troisième Congrès Des Grands Barrages Brasilia*.

Ribeiro, M. L., Bieri, M., Boillat, J.-L., Schleiss, A. J., Singhal, G., & Sharma, N. (2012). Discharge Capacity of Piano Key Weirs. *Journal of Hydraulic Engineering*, *138*(2), 199–203. https://doi.org/10.1061/(asce)hy.1943-7900.0000490.

Ribeiro, M. L., Boillat, J., Schleiss, A. J., & Doucen, O. Le. (2011). Experimental parametric study for hydraulic design of PKWs. *Proceedings of the International Conference Labyrinth and Piano Key Weirs-PKW 2011*, 183–190.

Ribeiro, M. L., Boillat, J., Schleiss, A. J., & Laugier, F. (2007). *Rehabilitation of St-Marc Dam Experimental Optimization of a Piano Key Weir*. ResearchGate.

Ribeiro, M. L., Pfister, M., Schleiss, A. J., & Boillat, J. (2012). Hydraulic design of A-type Piano Key Weirs. *Journal of Hydraulic Research*. https://doi.org/10.1080/00221686.2012.695041.

SA News. (2022, March 18). *Raising of Hazelmere Dam wall on track*. South African Goverment News Agency. https://www.sanews.gov.za/south-africa/raising-hazelmere-dam-wall-track

Salmasi, F., & Abraham, J. P. (2020). Discharge coefficients for ogeeweirs including the effects of a sloping upstream face. *Water Supply*, *22*(5), 5376–5392. https://doi.org/10.2166/ws.2022.129.

Sangsefidi, Y., Tavakol-davani, H., Ghodsian, M., Mehraein, M., & Zarei, R. (2021). Hydrodynamics and Free-Flow Characteristics of Piano Key Weirs with Different Plan Shapes. *Water*, *13*(2108). https://doi.org/10.3390/w13152108.

Schleiss, A. J. (2011). From Labyrinth to Piano Key Weirs-A historical review. *International Conference on Labyrinth and Piano Key Weirs-PKW 2011*, *5*, 581–595. https://www.researchgate.net/publication/265905378_From_Labyrinth_to-Piano_Key_Weirs_-_A_historical_review.

Silvestri, A., Archambeau, P., Pirotton, M., Dewals, B. J., & Erpicum, S. (2013). Comparative analysis of the energy dissipation on a stepped spillway downstream of a Piano Key Weir. *2nd International Workshop on Labyrinth and Piano Key Weirs Paris - Chatou, France 20-22 November 2013*.

Singh, D., & Kumar, M. (2023). Study of the Energy Dissipation over the Type-A Piano Key Weir. *KSCE Journal of Civil Engineering*, *27*(4), 1568–1584.

Sjösten, W., & Vadling, V. (2020). *CFD Simulations of Flow Characteristics of a Piano Key Weir Spillway*. Uppsala University.

Suprapto, M. (2013). Increase Spillway Capacity using Labyrinth Weir. *Procedia Engineering*, *54*, 440–446. https://doi.org/10.1016/j.proeng.2013.03.039

The Associated Press. (2022, May 6). *Report says Michigan 2020 dam failures were preventable*. Michigan Radio. https://www.michiganradio.org/transportation-infrastructure/2022-05-06/report-says-michigan-2020-dam-failures-were-preventable:

Tiwari, H., & Sharma, N. (2015). Turbulence study in the vicinity of piano key weir: relevance, instrumentation, parameters and methods. *Applied Water Science*, *7*. https://doi.org/10.1007/s13201-015-0275-1.

Tuan, L. A., & Hiramatsu, K. (2020). Hydraulic Investigation of Piano Key Weir. *Reviews in Agricultural Science*, *8*, 310–322. https://dx.doi.org/10.7831/ras.8.0_310.

Tullis, B., Crookston, B., & Young, N. (2020). Scale effects in free-flow nonlinear weir head-discharge relationships. *Journal of Hydraulic Engineering*, *146*(2).

Waymark. (2013, September 6). *Lake Brazos Labyrinth Weir - Waco, Texas*. United States of Texas. https://www.waymarking.com/waymarks/WMJ0TT_Lake-Brazos_Labyrinth_Weir_Waco_Texas.

Yazdi, A. M., Hoseini, S., Nazari, S., & Fazeli, M. (2022). Numerical and experimental analysis of scour downstream of piano key weirs. *Sadhana - Academy Proceedings in Engineering Sciences*, *4*(47). https://doi.org/10.1007/s12046-022-01960-w.

Yousif, A. A. (2020). Experimental Investigation On Hydraulic Performance Of Non-Rectangular Piano Key Weir (PKW). *International Journal of Advanced Science and Technology*, *29*(8), 4467–4480.

Zayed, M., El, A., & Sallah, M. (2018). An experimental investigation of head loss through a triangular (V- shaped) screen. *Journal of Advanced Research*, *10*, 69–76. https://doi.org/10.1016/j.jare.2017.12.005.

APPENDICES

Table A.1: The Description of the Different Screen Wall Models that were used in the Experimental Work

No of (Screen Wall) Model	Code of (Screen Wall) Model	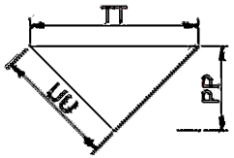			Area of the Screen Wall (cm^2)	Number of holes of screen wall	Shapes of opening of screen wall	Diameters of holes of screen wall Φ (cm)	Area of opening of screen wall ($cm^{\wedge 2}$)	Total area of holes of the screen wall (cm^2)	% Porosity of screen walls with diameter (0.5 cm)
		TT (cm)	UU (cm)	PP (cm)							
1	X1	31.51	22.28	15.76	248.3	0	-	0	0	0	0
2	X2	27.51	19.46	13.76	189.2	0	-	0	0	0	0
3	X3	23.51	16.63	11.76	138.2	0	-	0	0	0	0
4	X4	19.51	13.8	9.76	95.2	0	-	0	0	0	0
5	A1	31.51	22.28	15.76	248.3	49	Circular	0.35	0.0962	4.71	-
6	A2	27.51	19.46	13.76	189.2	36	Circular	0.35	0.0962	3.36	-
7	A3	23.51	16.63	11.76	138.2	25	Circular	0.35	0.0962	2.4	-
8	A4	19.51	13.8	9.76	95.2	16	Circular	0.35	0.0962	1.54	-
9	B1	31.51	22.28	15.76	248.3	49	Circular	0.5	0.196	9.6	3.9 %
10	B2	27.51	19.46	13.76	189.2	36	Circular	0.5	0.196	7.0	3.73 %
11	B3	23.51	16.63	11.76	138.2	25	Circular	0.5	0.196	4.9	3.54 %
12	B4	19.51	13.8	9.76	95.2	16	Circular	0.5	0.196	3.13	3.3 %
13	C1	31.51	22.28	15.76	248.3	49	Circular	0.7	0.384	18.81	-

No of (Screen Wall) Model	Code of (Screen Wall) Model	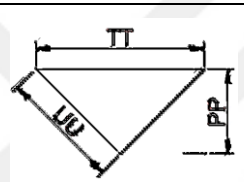			Area of the Screen Wall (cm^2)	Number of holes of screen wall	Shapes of opening of screen wall	Diameters of holes of screen wall Φ (cm)	Area of opening of screen wall ($cm^{\wedge 2}$)	Total area of holes of the screen wall (cm^2)	% Porosity of screen walls with diameter (0.5 cm)
		TT (cm)	UU (cm)	PP (cm)							
14	C2	27.51	19.46	13.76	189.2	36	Circular	0.7	0.384	13.82	-
15	C3	23.51	16.63	11.76	138.2	25	Circular	0.7	0.384	9.6	-
16	C4	19.51	13.8	9.76	95.2	16	Circular	0.7	0.384	6.14	-
17	D1	31.51	22.28	15.76	248.3	49	Circular	1.0	0.785	38.46	-
18	D2	27.51	19.46	13.76	189.2	36	Circular	1.0	0.785	28.26	-
19	D3	23.51	16.63	11.76	138.2	25	Circular	1.0	0.785	19.62	-
20	D4	19.51	13.8	9.76	95.2	16	Circular	1.0	0.785	12.56	-
21	E1	31.51	22.28	15.76	248.3	49	Circular	1.4	1.54	75.45	-
22	E2	27.51	19.46	13.76	189.2	36	Circular	1.4	1.54	55.44	-
23	E3	23.51	16.63	11.76	138.2	25	Circular	1.4	1.54	38.5	-
24	E4	19.51	13.8	9.76	95.2	16	Circular	1.4	1.54	24.64	-
25	F1	31.51	22.28	15.76	248.3	91	Circular	0.5	0.196	17.83	7.18 %
26	F2	27.51	19.46	13.76	189.2	66	Circular	0.5	0.196	12.93	6.84 %
27	F3	23.51	16.63	11.76	138.2	45	Circular	0.5	0.196	10.58	6.38 %
28	F4	19.51	13.8	9.76	95.2	28	Circular	0.5	0.196	5.48	5.76 %
29	G1	31.51	22.28	15.76	248.3	123	Circular	0.5	0.196	24.1	9.7 %
30	G2	27.51	19.46	13.76	189.2	88	Circular	0.5	0.196	17.24	9.11 %
31	G3	23.51	16.63	11.76	138.2	59	Circular	0.5	0.196	11.56	8.36 %
32	G4	19.51	13.8	9.76	95.2	36	Circular	0.5	0.196	7.05	7.41 %
33	H_1	31.51	22.28	15.76	248.3	221	Circular	0.5	0.196	43.31	17.44 %

No of (Screen Wall) Model	Code of (Screen Wall) Model	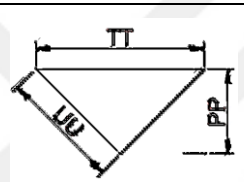			Area of the Screen Wall (cm^2)	Number of holes of screen wall	Shapes of opening of screen wall	Diameters of holes of screen wall Φ (cm)	Area of opening of screen wall ($cm^{\wedge 2}$)	Total area of holes of the screen wall (cm^2)	% Porosity of screen walls with diameter (0.5 cm)
		TT (cm)	UU (cm)	PP (cm)							
34	H2	27.51	19.46	13.76	189.2	160	Circular	0.5	0.196	31.36	16.57 %
35	H3	23.51	16.63	11.76	138.2	109	Circular	0.5	0.196	21.36	15.46 %
36	H4	19.51	13.8	9.76	95.2	68	Circular	0.5	0.196	13.32	14.0 %
37	I1	31.51	22.28	15.76	248.3	49	astral	-	0.785	38.46	-
38	I2	27.51	19.46	13.76	189.2	36	astral	-	0.785	28.26	-
39	I3	23.51	16.63	11.76	138.2	25	astral	-	0.785	19.62	-
40	I4	19.51	13.8	9.76	95.2	16	astral	-	0.785	12.56	-
41	J1	31.51	22.28	15.76	248.3	49	Hexagonal	-	0.785	38.46	-
42	J2	27.51	19.46	13.76	189.2	36	Hexagonal	-	0.785	28.26	-
43	J3	23.51	16.63	11.76	138.2	25	Hexagonal	-	0.785	19.62	-
44	J4	19.51	13.8	9.76	95.2	16	Hexagonal	-	0.785	12.56	-
45	K1	31.51	22.28	15.76	248.3	49	triangle	-	0.785	38.46	-
46	K2	27.51	19.46	13.76	189.2	36	triangle	-	0.785	28.26	-
47	K3	23.51	16.63	11.76	138.2	25	triangle	-	0.785	19.62	-
48	K4	19.51	13.8	9.76	95.2	16	triangle	-	0.785	12.56	-
49	M1	31.51	22.28	15.76	248.3	49	Square	-	0.785	38.46	-
50	M2	27.51	19.46	13.76	189.2	36	Square	-	0.785	28.26	-
51	M3	23.51	16.63	11.76	138.2	25	Square	-	0.785	19.62	-
52	M4	19.51	13.8	9.76	95.2	16	Square	-	0.785	12.56	-

Table A.2: THE laboratory results for upstream and downstream flow heights of PKW

No. of model	Name of Model	Q (lt/s)	P (cm)	Depth of water in Upstream flow Y_1 (cm)	Height of Water over PKW Model in Upstream Flow H_1 (cm)	Height of Tail Water in Downstream Flow h_2 (cm)
1	PKW1 L1 X1	67	30	37.5	7.5	12.3
		57		36.9	6.9	11.7
		47		36.2	6.2	10.8
		37		34.4	4.4	9.5
1	PKW1 L1 A1	67	30	37.1	7.1	12.4
		57		36.8	6.8	11.8
		47		35.5	5.5	11
		37		34.5	4.5	9.6
1	PKW1 L1 B1	67	30	37	7	12.5
		57		36.7	6.7	11.9
		47		35.9	5.9	11.1
		37		34.5	4.5	9.7
1	PKW1 L1 C1	67	30	36.9	6.9	12.7
		57		36.5	6.5	12
		47		35.5	5.5	11.2
		37		34	4	9.7
1	PKW1 L1 D1	67	30	36.5	6.5	13
		57		36.2	6.2	12.1
		47		35.2	5.2	11.3
		37		33.5	3.5	9.8
1	PKW1 L1 E1	67	30	35.9	5.9	13.3
		57		35.2	5.2	12.5
		47		34	4	11.7
		37		32.3	2.3	10
1	PKW1 L1 F1	67	30	36.9	6.9	12.6
		57		36.5	6.5	12

No. of model	Name of Model	Q (lt/s)	P (cm)	Depth of water in Upstream flow Y_1 (cm)	Height of Water over PKW Model in Upstream Flow H_1 (cm)	Height of Tail Water in Downstream Flow h_2 (cm)
		47		35.7	5.7	11.2
		37		34	4	9.7
1	PKW1 L1 G1	67	30	36.7	6.7	12.7
		57		36.1	6.1	12.1
		47		35.5	5.5	11.3
		37		34	4	9.8
1	PKW1 L1 H_1	67	30	36.5	6.5	12.8
		57		36	6	12.2
		47		35.3	5.3	11.4
		37		33.5	3.5	9.9
1	PKW1 L1 I1	67	30	36.5	6.5	12.5
		57		36	6	12.1
		47		35	5	11.3
		37		33.5	3.5	9.7
1	PKW1 L1 J1	67	30	36.5	6.5	12.7
		57		35.9	5.9	12.2
		47		35	5	11.3
		37		33.5	3.5	9.7
1	PKW1 L1 K1	67	30	36.5	6.5	12.8
		57		35.8	5.8	12.3
		47		34.8	4.8	11.4
		37		33.5	3.5	9.8
1	PKW1 L1 M1	67	30	36.6	6.6	12.6
		57		36.1	6.1	12.1
		47		35	5	11.3
		37		33.5	3.5	9.7
2	PKW1 L2 X2	67	28	36.5	8.5	12.1

No. of model	Name of Model	Q (lt/s)	P (cm)	Depth of water in Upstream flow Y_1 (cm)	Height of Water over PKW Model in Upstream Flow H_1 (cm)	Height of Tail Water in Downstream Flow h_2 (cm)
		57		35.8	7.8	11.8
		47		34.9	6.9	11
		37		33.5	5.5	9
2	PKW1 L2 A2	67	28	36.3	8.3	12.3
		57		35.7	7.7	11.9
		47		35	7	11.1
		37		33.5	5.5	9.2
2	PKW1 L2 B2	67	28	36.3	8.3	12.4
		57		35.5	7.5	11.9
		47		34.8	6.8	11.1
		37		33.5	5.5	9.3
2	PKW1 L2 C2	67	28	36	8	12.6
		57		35.5	7.5	12
		47		34.6	6.6	11.2
		37		33.3	5.3	9.4
2	PKW1 L2 D2	67	28	35.8	7.8	12.7
		57		35	7	12.1
		47		34.2	6.2	11.2
		37		33	5	9.4
2	PKW1 L2 E2	67	28	34	7	12.8
		57		34.5	6.5	12.3
		47		33.5	5.5	11.3
		37		32.2	4.2	9.6
2	PKW1 L2 F2	67	28	36	8	12.5
		57		35.5	7.5	12
		47		34.5	6.5	11.2
		37		33.3	5.3	9.4

No. of model	Name of Model	Q (lt/s)	P (cm)	Depth of water in Upstream flow Y_1 (cm)	Height of Water over PKW Model in Upstream Flow H_1 (cm)	Height of Tail Water in Downstream Flow h_2 (cm)
2	PKW1 L2 G2	67	28	36	8	12.6
		57		35.4	7.4	12
		47		34.5	6.5	11.3
		37		33	5	9.4
2	PKW1 L2 H2	67	28	35.7	7.7	12.7
		57		35.2	7.2	12.1
		47		34	6	11.3
		37		32.8	4.8	9.5
2	PKW1 L2 I2	67	28	35.7	7.7	12.7
		57		35.1	7.1	11.9
		47		34.2	6.2	11.2
		37		32.7	4.7	9.3
2	PKW1 L2 J2	67	28	36.2	8.2	12.8
		57		35	7	12
		47		34	6	11.2
		37		32.7	4.7	9.3
2	PKW1 L2 K2	67	28	35.7	7.7	12.8
		57		34.8	6.8	12.1
		47		33.9	5.9	11.3
		37		32.6	4.6	9.4
2	PKW1 L2 M2	67	28	35.7	7.7	12.7
		57		35.2	7.2	11.9
		47		34.2	6.2	11.2
		37		32.9	4.9	9.3
3	PKW1 L3 X3	67	26	35.7	9.7	12.4
		57		35	9	11.9
		47		32.2	6.2	10.9

No. of model	Name of Model	Q (lt/s)	P (cm)	Depth of water in Upstream flow Y_1 (cm)	Height of Water over PKW Model in Upstream Flow H_1 (cm)	Height of Tail Water in Downstream Flow h_2 (cm)
		37		31	5.3	9.5
3	PKW1 L3 A3	67	26	35.5	9.5	12.5
		57		34.9	8.9	11.9
		47		32.3	6.3	10.9
		37		31.3	5.3	9.6
3	PKW1 L3 B3	67	26	35.3	9.3	12.7
		57		34.7	8.7	12
		47		32.2	6.2	11
		37		32.1	5.1	9.6
3	PKW1 L3 C3	67	26	35.2	9.2	12.7
		57		34.7	8.7	12
		47		32.1	6.1	11.1
		37		31.2	5.2	9.6
3	PKW1 L3 D3	67	26	34.8	8.8	12.8
		57		34.3	8.3	12.2
		47		31.9	5.9	11.2
		37		30.9	4.9	9.7
3	PKW1 L3 E3	67	26	34.4	8.4	13
		57		33.8	7.8	12.3
		47		31.3	5.3	11.3
		37		30.2	4.2	9.8
3	PKW1 L3 F3	67	26	35.3	9.3	12.7
		57		34.6	8.6	12.1
		47		32.2	6.2	11.1
		37		31.1	5.1	9.7
3	PKW1 L3 G3	67	26	35	9	12.8
		57		34.7	8.7	12.3

No. of model	Name of Model	Q (lt/s)	P (cm)	Depth of water in Upstream flow Y_1 (cm)	Height of Water over PKW Model in Upstream Flow H_1 (cm)	Height of Tail Water in Downstream Flow h_2 (cm)
		47		32.3	6.3	11.3
		37		31	5	9.7
3	PKW1 L3 H3	67	26	35	9	12.8
		57		34.5	8.5	12.3
		47		32.1	6.1	11.4
		37		30.8	4.8	9.8
3	PKW1 L3 I3	67	26	35	9	12.7
		57		34.3	8.3	12.2
		47		32.1	6.1	11.2
		37		30.8	4.8	9.7
3	PKW1 L3 J3	67	26	35	9	12.7
		57		34.4	8.4	12.2
		47		32.2	6.2	11.2
		37		30.7	4.7	9.7
3	PKW1 L3 K3	67	26	34.9	8.9	12.7
		57		34.1	8.1	12.3
		47		32	6	11.3
		37		30.6	4.6	9.8
3	PKW1 L3 M3	67	26	35	9	12.7
		57		34.5	8.5	12.2
		47		32.2	6.2	11.2
		37		30.8	4.8	9.7
4	PKW1 L4 X4	67	24	33	9	12.3
		57		32	8	12
		47		30.9	6.9	11.8
		37		29.7	5.7	9.2
4	PKW1 L4 A4	67	24	33	9	12.4

No. of model	Name of Model	Q (lt/s)	P (cm)	Depth of water in Upstream flow Y_1 (cm)	Height of Water over PKW Model in Upstream Flow H_1 (cm)	Height of Tail Water in Downstream Flow h_2 (cm)
		57		32	8	12.3
		47		30.9	6.9	11.8
		37		29.8	5.8	9.2
4	PKW1 L4 B4	67	24	33.1	9.1	12.6
		57		32	8	12.3
		47		30.7	6.7	11.9
		37		29.6	5.6	9.4
4	PKW1 L4 C4	67	24	32.9	8.9	12.7
		57		32	8	12.4
		47		30.9	6.9	11.9
		37		29.5	5.5	9.4
4	PKW1 L4 D4	67	24	32.7	8.7	12.7
		57		31.7	7.7	12.4
		47		30.5	6.5	12
		37		29.3	5.3	9.5
4	PKW1 L4 E4	67	24	32.3	8.3	12.9
		57		31.3	7.3	12.6
		47		30	6	12.1
		37		29	5	9.6
4	PKW1 L4 F4	67	24	32.9	8.9	12.7
		57		31.9	7.9	12.4
		47		30.6	6.6	11.9
		37		29.5	5.5	9.4
4	PKW1 L4 G4	67	24	32.8	8.8	12.7
		57		31.9	7.9	12.4
		47		30.7	6.7	12
		37		29.5	5.5	9.5

No. of model	Name of Model	Q (lt/s)	P (cm)	Depth of water in Upstream flow Y_1 (cm)	Height of Water over PKW Model in Upstream Flow H_1 (cm)	Height of Tail Water in Downstream Flow h_2 (cm)
4	PKW1 L4 H4	67	24	32.7	8.7	12.7
		57		31.5	7.5	12.5
		47		30.5	6.5	12
		37		29.3	5.3	9.6
4	PKW1 L4 I4	67	24	32.7	8.7	12.7
		57		31.7	7.7	12.4
		47		30.5	6.5	11.9
		37		29.3	5.3	9.5
4	PKW1 L4 J4	67	24	32.7	8.7	12.7
		57		31.5	7.5	12.4
		47		30.5	6.5	11.9
		37		29.3	5.3	9.5
4	PKW1 L4 K4	67	24	32.5	8.5	12.7
		57		31.5	7.5	12.4
		47		30.5	6.5	11.9
		37		29.2	5.2	9.6
4	PKW1 L4 M4	67	24	32.6	8.6	12.7
		57		31.7	7.7	12.4
		47		30.5	6.5	11.9
		37		29.2	5.2	9.5
5	PKW2 L1 X1	67	30	36.7	6.7	12.5
		57		36.1	6.1	12
		47		35.1	5.1	11
		37		34.1	4.1	9.3
5	PKW2 L1 B1	67	30	36.6	6.6	12.8
		57		35.9	5.9	12.6
		47		35	5	10.9

No. of model	Name of Model	Q (lt/s)	P (cm)	Depth of water in Upstream flow Y_1 (cm)	Height of Water over PKW Model in Upstream Flow H_1 (cm)	Height of Tail Water in Downstream Flow h_2 (cm)
		37		34.1	4.1	9.2
5	PKW2 L1 D1	67	30	36	6	12.8
		57		35.3	5.3	12
		47		34.1	4.1	10.9
		37		33.2	3.2	9.5
6	PKW2 L2 X2	67	28	35.3	7.3	12.1
		57		34.7	6.7	12
		47		33.7	5.7	11
		37		32.8	4.8	9.3
6	PKW2 L2 B2	67	28	35.3	7.3	12.8
		57		34.4	6.4	12
		47		33.1	5.1	10.9
		37		32.3	4.3	9.3
6	PKW2 L2 D2	67	28	34.8	6.8	14.8
		57		33.8	5.8	11.9
		47		32.9	4.9	11
		37		31.9	3.9	10.3
7	PKW2 L3 X3	67	26	33.7	7.7	12.5
		57		33	7	12.7
		47		32	6	10.5
		37		30.8	4.8	9
7	PKW2 L3 B3	67	26	35.5	9.5	13.5
		57		32.8	6.8	12.2
		47		32	6	11
		37		30.6	4.6	9.3
7	PKW2 L3 D3	67	26	33.1	7.1	12.8
		57		32.4	6.4	12

No. of model	Name of Model	Q (lt/s)	P (cm)	Depth of water in Upstream flow Y_1 (cm)	Height of Water over PKW Model in Upstream Flow H_1 (cm)	Height of Tail Water in Downstream Flow h_2 (cm)
		47		31.6	5.6	11.2
		37		30.3	4.3	9.2
8	PKW2 L4 X4	67	24	32.2	8.2	8.5
		57		31.5	7.5	10.1
		47		30.1	6.1	10.5
		37		29	5	9
8	PKW2 L4 B4	67	24	32.1	8.1	9
		57		31.5	7.5	11.8
		47		30.1	6.1	10.4
		37		29	5	8.7
8	PKW2 L4 D4	67	24	31.8	7.8	7
		57		31.1	7.1	12.8
		47		29.2	5.2	10.9
		37		28.7	4.7	9.6
9	PKW3 L1 X1	67	30	38	8	12.7
		57		37.6	7.6	12
		47		36.9	6.9	11
		37		34.7	4.7	9.2
9	PKW3 L1 B1	67	30	37.5	7.5	12.6
		57		37.4	7.4	12
		47		36.6	6.6	10.5
		37		34.5	4.5	9.3
9	PKW3 L1 D1	67	30	37	7	12.8
		57		36.9	6.9	11.9
		47		35.9	5.9	11
		37		33.8	3.8	9.5
10	PKW3 L2 X2	67	28	37.2	9.2	13

No. of model	Name of Model	Q (lt/s)	P (cm)	Depth of water in Upstream flow Y_1 (cm)	Height of Water over PKW Model in Upstream Flow H_1 (cm)	Height of Tail Water in Downstream Flow h_2 (cm)
		57		36.6	8.6	11.8
		47		35.9	7.9	11
		37		34.6	6.6	9.8
10	PKW3 L2 B2	67	28	37	9	13
		57		36.3	8.3	11
		47		35.4	7.4	11.2
		37		34.3	6.3	9.5
10	PKW3 L2 D2	67	28	36.5	8.5	12.9
		57		35.8	7.8	12.2
		47		35.1	7.1	11
		37		34	6	9.7
11	PKW3 L3 X3	67	26	36.5	10.5	13
		57		35	9	12.5
		47		34.5	8.5	10.5
		37		32	6	9.3
11	PKW3 L3 B3	67	26	36	10	13
		57		34.8	8.8	12
		47		33.5	7.5	10.8
		37		31.6	5.6	9.2
11	PKW3 L3 D3	67	26	35.5	9.5	12.2
		57		34.4	8.4	12.5
		47		33	7	10.8
		37		31.2	5.2	9.3
12	PKW3 L4 X4	67	24	34	10	13.1
		57		32.5	8.5	13
		47		31.6	7.6	11
		37		30.5	6.5	10.5

No. of model	Name of Model	Q (lt/s)	P (cm)	Depth of water in Upstream flow Y_1 (cm)	Height of Water over PKW Model in Upstream Flow H_1 (cm)	Height of Tail Water in Downstream Flow h_2 (cm)
12	PKW3 L4 B4	67	24	33.8	9.8	12.9
		57		32.4	8.4	13.1
		47		31.3	7.3	10.5
		37		30.2	6.2	9.2
12	PKW3 L4 D4	67	24	33.3	9.3	13.5
		57		32.1	8.1	12.7
		47		31	7	11
		37		30	6	9.3
13	PKW4 L1 X1	67	30	35.9	5.9	12.9
		57		35.2	5.2	12.2
		47		34.7	4.7	10.7
		37		33.8	3.8	9.1
13	PKW4 L1 B1	67	30	35.5	5.5	12.5
		57		35	5	12
		47		34.2	4.2	11.2
		37		33.5	3.5	9.5
13	PKW4 L1 D1	67	30	35.3	5.3	13.5
		57		34.4	4.4	12.1
		47		33.7	3.7	11.3
		37		32.8	2.8	8.7
14	PKW4 L2 X2	67	28	34	6	12.9
		57		33.5	5.5	11.7
		47		32.5	4.5	11
		37		31.9	3.9	9.4
14	PKW4 L2 B2	67	28	34	6	13
		57		33	5	12.3
		47		32.3	4.3	11.5

No. of model	Name of Model	Q (lt/s)	P (cm)	Depth of water in Upstream flow Y_1 (cm)	Height of Water over PKW Model in Upstream Flow H_1 (cm)	Height of Tail Water in Downstream Flow h_2 (cm)
		37		31.6	3.6	9.3
14	PKW4 L2 D2	67	28	33.5	5.5	13.5
		57		32.9	4.9	12.2
		47		32.2	4.2	11.5
		37		31	3	9.3
15	PKW4 L3 X3	67	26	32.5	6.5	13
		57		31.8	5.8	12.5
		47		31	5	11
		37		30	4	9.8
15	PKW4 L3 B3	67	26	32.3	6.3	13.8
		57		31.5	5.5	12.2
		47		30.5	4.5	11
		37		29.9	3.9	9.5
15	PKW4 L3 D3	67	26	31.9	5.9	13.5
		57		31.9	5.9	12
		47		30.5	4.5	11
		37		29.4	3.4	9.5
16	PKW4 L4 X4	67	24	31	7	13
		57		30.2	6.2	12
		47		29.2	5.2	10.6
		37		28.4	4.4	9.5
16	PKW4 L4 B4	67	24	30.7	6.7	13.5
		57		30.1	6.1	12.5
		47		29.1	5.1	11
		37		28.2	4.2	9.3
16	PKW4 L4 D4	67	24	30.5	6.5	13.8
		57		29.8	5.8	12.7

No. of model	Name of Model	Q (lt/s)	P (cm)	Depth of water in Upstream flow Y_1 (cm)	Height of Water over PKW Model in Upstream Flow H_1 (cm)	Height of Tail Water in Downstream Flow h_2 (cm)
		47		28.9	4.9	11
		37		27.9	3.9	9.5
17	PKW5 L1 X1	67	30	36.3	6.3	13.5
		57		36	6	12.2
		47		34.8	4.8	11
		37		34.2	4.2	9.5
17	PKW5 L1 B1	67	30	36.1	6.1	13
		57		35.6	5.6	12.5
		47		34.6	4.6	10.5
		37		33.7	3.7	9.5
17	PKW5 L1 D1	67	30	35.5	5.5	12.7
		57		35	5	12.5
		47		34.8	4.8	11
		37		33	3	9.5
18	PKW5 L2 X2	67	28	34.8	6.8	13.5
		57		34	6	12.1
		47		33.1	5.1	11
		37		32.2	4.2	9.4
18	PKW5 L2 B2	67	28	34.5	6.5	13.3
		57		33.8	5.8	12.2
		47		32.9	4.9	11
		37		32	4	9.5
18	PKW5 L2 D2	67	28	34.1	6.1	13
		57		33.3	5.3	12.1
		47		32.5	4.5	11
		37		31.5	3.5	9.5
19	PKW5 L3 X3	67	26	33.4	7.4	12.9

No. of model	Name of Model	Q (lt/s)	P (cm)	Depth of water in Upstream flow Y_1 (cm)	Height of Water over PKW Model in Upstream Flow H_1 (cm)	Height of Tail Water in Downstream Flow h_2 (cm)
		57		32.5	6.5	12.5
		47		31.6	5.6	10.8
		37		30.5	4.5	9.1
19	PKW5 L3 B3	67	26	33.1	7.1	13
		57		32.2	6.2	12.5
		47		31.4	5.4	11
		37		30.4	4.4	9.2
19	PKW5 L3 D3	67	26	32.7	6.7	13
		57		31.9	5.9	11.8
		47		31.1	5.1	11.1
		37		30	4	9.4
20	PKW5 L4 X4	67	24	31.8	7.8	12.7
		57		31.2	7.2	12.5
		47		30.1	6.1	11
		37		29	5	9.5
20	PKW5 L4 B4	67	24	31.5	7.5	13
		57		31	7	12.5
		47		30	6	11.1
		37		28.9	4.9	9.7
20	PKW5 L4 D4	67	24	31.2	7.2	13
		57		30.8	6.8	12.8
		47		29.8	5.8	11.5
		37		28.7	4.7	9.5

Table A.3: The values of the non-dimensional variables were obtained for all models of the piano key (type-A) with the different screen wall and for all experiments.

Name of Model	Qa (lt/s)	P (cm)	h_1 (cm)	V_1 (m/s)	H_1 (cm)	H_1/P	Qt (lt/s)	C_d	E_1 (m)	h_2 (cm)	V_2 (m/s)	E_2 (m)	L/W	W_i/W_o	B/P	$\frac{(E_1-E_2)}{E_1}$	E_2/E_1	Fr
PKW1 L1 X1	67	30	7.5	0.221	7.7	0.26	51.6	1.30	0.377	12.3	0.672	0.146	2.98	1.00	1.33	0.61	0.39	0.11
	57		6.9	0.187	7.1	0.24	45.0	1.24	0.371	11.7	0.591	0.135				0.64	0.36	0.10
	47		6.2	0.160	6.3	0.21	38.1	1.23	0.363	10.8	0.537	0.123				0.66	0.34	0.08
	37		4.4	0.133	4.5	0.15	22.8	1.63	0.345	9.5	0.481	0.107				0.69	0.31	0.07
PKW1 L1 A1	67	30	7.1	0.223	7.4	0.25	47.7	1.40	0.374	12.4	0.667	0.147	2.98	1.00	1.33	0.61	0.39	0.12
	57		6.8	0.191	7.0	0.23	44.2	1.29	0.370	11.8	0.596	0.136				0.63	0.37	0.10
	47		5.5	0.163	5.6	0.19	32.0	1.47	0.356	11.0	0.527	0.124				0.65	0.35	0.09
	37		4.5	0.132	4.6	0.15	23.5	1.57	0.346	9.6	0.476	0.108				0.69	0.31	0.07
PKW1 L1 B1	67	30	7	0.224	7.3	0.24	46.7	1.43	0.373	12.5	0.662	0.147	2.98	1.00	1.33	0.60	0.40	0.12
	57		6.7	0.192	6.9	0.23	43.2	1.32	0.369	11.9	0.591	0.137				0.63	0.37	0.10
	47		5.9	0.162	6.0	0.20	35.4	1.33	0.360	11.1	0.523	0.125				0.65	0.35	0.09
	37		4.5	0.132	4.6	0.15	23.5	1.57	0.346	9.7	0.471	0.108				0.69	0.31	0.07
PKW1 L1 C1	67	30	6.9	0.224	7.2	0.24	45.8	1.46	0.372	12.7	0.651	0.149	2.98	1.00	1.33	0.60	0.40	0.12
	57		6.5	0.193	6.7	0.22	41.4	1.38	0.367	12.0	0.586	0.138				0.63	0.37	0.10
	47		5.5	0.163	5.6	0.19	32.0	1.47	0.356	11.2	0.518	0.126				0.65	0.35	0.09
	37		4	0.134	4.1	0.14	19.8	1.87	0.341	9.7	0.471	0.108				0.68	0.32	0.07
PKW1 L1 D1	67	30	6.5	0.227	6.8	0.23	42.1	1.59	0.368	13.0	0.636	0.151	2.98	1.00	1.33	0.59	0.41	0.12
	57		6.2	0.194	6.4	0.21	38.7	1.47	0.364	12.1	0.582	0.138				0.62	0.38	0.10
	47		5.2	0.165	5.3	0.18	29.5	1.59	0.353	11.3	0.513	0.126				0.64	0.36	0.09
	37		3.5	0.136	3.6	0.12	16.3	2.27	0.336	9.8	0.466	0.109				0.68	0.32	0.08
PKW1 L1 E1	67	30	5.9	0.230	6.2	0.21	36.7	1.83	0.362	13.3	0.622	0.153	2.98	1.00	1.33	0.58	0.42	0.12

Name of Model	Qa (lt/s)	P (cm)	h_1 (cm)	V_1 (m/s)	H_1 (cm)	H_1/P	Qt (lt/s)	C_d	E_1 (m)	h_2 (cm)	V_2 (m/s)	E_2 (m)	L/W	W_i/W_o	B/P	$\frac{(E_1-E_2)}{E_1}$	E_2/E_1	Fr
	57		5.2	0.200	5.4	0.18	30.0	1.90	0.354	12.5	0.563	0.141				0.60	0.40	0.11
	47		4	0.171	4.1	0.14	20.2	2.33	0.341	11.7	0.496	0.130				0.62	0.38	0.09
	37		2.3	0.141	2.4	0.08	8.9	4.16	0.324	10.0	0.457	0.111				0.66	0.34	0.08
PKW1 L1 F1	67	30	6.9	0.224	7.2	0.24	45.8	1.46	0.372	12.6	0.656	0.148	2.98	1.00	1.33	0.60	0.40	0.12
	57		6.5	0.193	6.7	0.22	41.4	1.38	0.367	12.0	0.586	0.138				0.63	0.37	0.10
	47		5.7	0.163	5.8	0.19	33.7	1.39	0.358	11.2	0.518	0.126				0.65	0.35	0.09
	37		4	0.134	4.1	0.14	19.8	1.87	0.341	9.7	0.471	0.108				0.68	0.32	0.07
PKW1 L1 G1	67	30	6.7	0.225	7.0	0.23	43.9	1.53	0.370	12.7	0.651	0.149	2.98	1.00	1.33	0.60	0.40	0.12
	57		6.1	0.195	6.3	0.21	37.8	1.51	0.363	12.1	0.582	0.138				0.62	0.38	0.10
	47		5.5	0.163	5.6	0.19	32.0	1.47	0.356	11.3	0.513	0.126				0.65	0.35	0.09
	37		4	0.134	4.1	0.14	19.8	1.87	0.341	9.8	0.466	0.109				0.68	0.32	0.07
PKW1 L1 H_1	67	30	6.5	0.227	6.8	0.23	42.1	1.59	0.368	12.8	0.646	0.149	2.98	1.00	1.33	0.59	0.41	0.12
	57		6	0.195	6.2	0.21	36.9	1.55	0.362	12.2	0.577	0.139				0.62	0.38	0.10
	47		5.3	0.164	5.4	0.18	30.3	1.55	0.354	11.4	0.509	0.127				0.64	0.36	0.09
	37		3.5	0.136	3.6	0.12	16.3	2.27	0.336	9.9	0.461	0.110				0.67	0.33	0.08
PKW1 L1 I1	67	30	6.5	0.227	6.8	0.23	42.1	1.59	0.368	12.5	0.662	0.147	2.98	1.00	1.33	0.60	0.40	0.12
	57		6	0.195	6.2	0.21	36.9	1.55	0.362	12.1	0.582	0.138				0.62	0.38	0.10
	47		5	0.166	5.1	0.17	27.9	1.69	0.351	11.3	0.513	0.126				0.64	0.36	0.09
	37		3.5	0.136	3.6	0.12	16.3	2.27	0.336	9.7	0.471	0.108				0.68	0.32	0.08
PKW1 L1 J1	67	30	6.5	0.227	6.8	0.23	42.1	1.59	0.368	12.7	0.651	0.149	2.98	1.00	1.33	0.60	0.40	0.12
	57		5.9	0.196	6.1	0.20	36.0	1.58	0.361	12.2	0.577	0.139				0.62	0.38	0.10
	47		5	0.166	5.1	0.17	27.9	1.69	0.351	11.3	0.513	0.126				0.64	0.36	0.09
	37		3.5	0.136	3.6	0.12	16.3	2.27	0.336	9.7	0.471	0.108				0.68	0.32	0.08

Name of Model	Qa (lt/s)	P (cm)	h_1 (cm)	V_1 (m/s)	H_1 (cm)	H_1/P	Qt (lt/s)	C_d	E_1 (m)	h_2 (cm)	V_2 (m/s)	E_2 (m)	L/W	W_i/W_o	B/P	$\frac{(E_1-E_2)}{E_1}$	E_2/E_1	Fr
PKW1 L1 K1	67	30	6.5	0.227	6.8	0.23	42.1	1.59	0.368	12.8	0.646	0.149	2.98	1.00	1.33	0.59	0.41	0.12
	57		5.8	0.197	6.0	0.20	35.1	1.62	0.360	12.3	0.572	0.140				0.61	0.39	0.10
	47		4.8	0.167	4.9	0.16	26.3	1.79	0.349	11.4	0.509	0.127				0.64	0.36	0.09
	37		3.5	0.136	3.6	0.12	16.3	2.27	0.336	9.8	0.466	0.109				0.68	0.32	0.08
PKW1 L1 M1	67	30	6.6	0.226	6.9	0.23	43.0	1.56	0.369	12.6	0.656	0.148	2.98	1.00	1.33	0.60	0.40	0.12
	57		6.1	0.195	6.3	0.21	37.8	1.51	0.363	12.1	0.582	0.138				0.62	0.38	0.10
	47		5	0.166	5.1	0.17	27.9	1.69	0.351	11.3	0.513	0.126				0.64	0.36	0.09
	37		3.5	0.136	3.6	0.12	16.3	2.27	0.336	9.7	0.471	0.108				0.68	0.32	0.08
PKW1 L2 X2	67	28	8.5	0.227	8.8	0.31	62.0	1.08	0.368	12.1	0.684	0.145	2.78	1.00	1.29	0.61	0.39	0.12
	57		7.8	0.197	8.0	0.29	54.1	1.05	0.360	11.8	0.596	0.136				0.62	0.38	0.10
	47		6.9	0.166	7.0	0.25	44.7	1.05	0.350	11.0	0.527	0.124				0.65	0.35	0.09
	37		5.5	0.136	5.6	0.20	31.7	1.17	0.336	9.0	0.508	0.103				0.69	0.31	0.08
PKW1 L2 A2	67	28	8.3	0.228	8.6	0.31	60.0	1.12	0.366	12.3	0.672	0.146	2.78	1.00	1.29	0.60	0.40	0.12
	57		7.7	0.197	7.9	0.28	53.1	1.07	0.359	11.9	0.591	0.137				0.62	0.38	0.11
	47		7	0.166	7.1	0.26	45.6	1.03	0.351	11.1	0.523	0.125				0.64	0.36	0.09
	37		5.5	0.136	5.6	0.20	31.7	1.17	0.336	9.2	0.497	0.105				0.69	0.31	0.08
PKW1 L2 B2	67	28	8.3	0.228	8.6	0.31	60.0	1.12	0.366	12.4	0.667	0.147	2.78	1.00	1.29	0.60	0.40	0.12
	57		7.5	0.198	7.7	0.28	51.1	1.12	0.357	11.9	0.591	0.137				0.62	0.38	0.11
	47		6.8	0.167	6.9	0.25	43.7	1.07	0.349	11.1	0.523	0.125				0.64	0.36	0.09
	37		5.5	0.136	5.6	0.20	31.7	1.17	0.336	9.3	0.491	0.105				0.69	0.31	0.08
PKW1 L2 C2	67	28	8	0.230	8.3	0.30	56.9	1.18	0.363	12.6	0.656	0.148	2.78	1.00	1.29	0.59	0.41	0.12
	57		7.5	0.198	7.7	0.28	51.1	1.12	0.357	12.0	0.586	0.138				0.61	0.39	0.11
	47		6.6	0.168	6.7	0.24	41.9	1.12	0.347	11.2	0.518	0.126				0.64	0.36	0.09

Name of Model	Qa (lt/s)	P (cm)	h_1 (cm)	V_1 (m/s)	H_1 (cm)	H_1/P	Qt (lt/s)	C_d	E_1 (m)	h_2 (cm)	V_2 (m/s)	E_2 (m)	L/W	W_i/W_o	B/P	$\frac{(E_1-E_2)}{E_1}$	E_2/E_1	Fr
	37		5.3	0.137	5.4	0.19	30.0	1.23	0.334	9.4	0.486	0.106				0.68	0.32	0.08
PKW1 L2 D2	67	28	7.8	0.231	8.1	0.29	54.9	1.22	0.361	12.7	0.651	0.149	2.78	1.00	1.29	0.59	0.41	0.12
	57		7	0.201	7.2	0.26	46.3	1.23	0.352	12.1	0.582	0.138				0.61	0.39	0.11
	47		6.2	0.170	6.3	0.23	38.2	1.23	0.343	11.2	0.518	0.126				0.63	0.37	0.09
	37		5	0.138	5.1	0.18	27.5	1.34	0.331	9.4	0.486	0.106				0.68	0.32	0.08
PKW1 L2 E2	67	28	7	0.236	7.3	0.26	47.0	1.42	0.353	12.8	0.646	0.149	2.78	1.00	1.29	0.58	0.42	0.13
	57		6.5	0.204	6.7	0.24	41.6	1.37	0.347	12.3	0.572	0.140				0.60	0.40	0.11
	47		5.5	0.173	5.7	0.20	32.1	1.46	0.337	11.3	0.513	0.126				0.62	0.38	0.10
	37		4.2	0.142	4.3	0.15	21.3	1.73	0.323	9.6	0.476	0.108				0.67	0.33	0.08
PKW1 L2 F2	67	28	8	0.230	8.3	0.30	56.9	1.18	0.363	12.5	0.662	0.147	2.78	1.00	1.29	0.59	0.41	0.12
	57		7.5	0.198	7.7	0.28	51.1	1.12	0.357	12.0	0.586	0.138				0.61	0.39	0.11
	47		6.5	0.168	6.6	0.24	41.0	1.15	0.346	11.2	0.518	0.126				0.64	0.36	0.09
	37		5.3	0.137	5.4	0.19	30.0	1.23	0.334	9.4	0.486	0.106				0.68	0.32	0.08
PKW1 L2 G2	67	28	8	0.230	8.3	0.30	56.9	1.18	0.363	12.6	0.656	0.148	2.78	1.00	1.29	0.59	0.41	0.12
	57		7.4	0.199	7.6	0.27	50.1	1.14	0.356	12.0	0.586	0.138				0.61	0.39	0.11
	47		6.5	0.168	6.6	0.24	41.0	1.15	0.346	11.3	0.513	0.126				0.64	0.36	0.09
	37		5	0.138	5.1	0.18	27.5	1.34	0.331	9.4	0.486	0.106				0.68	0.32	0.08
PKW1 L2 H2	67	28	7.7	0.232	8.0	0.28	53.9	1.24	0.360	12.7	0.651	0.149	2.78	1.00	1.29	0.59	0.41	0.12
	57		7.2	0.200	7.4	0.26	48.2	1.18	0.354	12.1	0.582	0.138				0.61	0.39	0.11
	47		6	0.171	6.1	0.22	36.5	1.29	0.341	11.3	0.513	0.126				0.63	0.37	0.09
	37		4.8	0.139	4.9	0.17	25.9	1.43	0.329	9.5	0.481	0.107				0.68	0.32	0.08
PKW1 L2 I2	67	28	6.5	0.227	6.8	0.23	42.1	1.59	0.368	12.5	0.662	0.147	2.98	1.00	1.33	0.60	0.40	0.12
	57		6	0.195	6.2	0.21	36.9	1.55	0.362	12.1	0.582	0.138				0.62	0.38	0.10

Name of Model	Qa (lt/s)	P (cm)	h_1 (cm)	V_1 (m/s)	H_1 (cm)	H_1/P	Qt (lt/s)	C_d	E_1 (m)	h_2 (cm)	V_2 (m/s)	E_2 (m)	L/W	W_i/W_o	B/P	$\frac{(E_1-E_2)}{E_1}$	E_2/E_1	Fr
	47		5	0.166	5.1	0.17	27.9	1.69	0.351	11.3	0.513	0.126				0.64	0.36	0.09
	37		3.5	0.136	3.6	0.12	16.3	2.27	0.336	9.7	0.471	0.108				0.68	0.32	0.08
PKW1 L2 J2	67	28	8.2	0.228	8.5	0.30	58.9	1.14	0.365	12.8	0.646	0.149	2.78	1.00	1.29	0.59	0.41	0.12
	57		7	0.201	7.2	0.26	46.3	1.23	0.352	12.0	0.586	0.138				0.61	0.39	0.11
	47		6	0.171	6.1	0.22	36.5	1.29	0.341	11.2	0.518	0.126				0.63	0.37	0.09
	37		4.7	0.140	4.8	0.17	25.1	1.47	0.328	9.3	0.491	0.105				0.68	0.32	0.08
PKW1 L2 K2	67	28	7.7	0.232	8.0	0.28	53.9	1.24	0.360	12.8	0.646	0.149	2.78	1.00	1.29	0.59	0.41	0.12
	57		6.8	0.202	7.0	0.25	44.4	1.28	0.350	12.1	0.582	0.138				0.61	0.39	0.11
	47		5.9	0.171	6.0	0.22	35.6	1.32	0.340	11.3	0.513	0.126				0.63	0.37	0.09
	37		4.6	0.140	4.7	0.17	25.1	1.52	0.327	9.4	0.486	0.106				0.68	0.32	0.08
PKW1 L2 M2	67	28	7.7	0.232	8.0	0.28	53.9	1.24	0.360	12.7	0.651	0.149	2.78	1.00	1.29	0.59	0.41	0.12
	57		7.2	0.200	7.4	0.26	48.2	1.18	0.354	11.9	0.591	0.137				0.61	0.39	0.11
	47		6.2	0.170	6.3	0.23	38.2	1.23	0.343	11.2	0.518	0.126				0.63	0.37	0.09
	37		4.9	0.139	5.0	0.18	26.7	1.38	0.330	9.3	0.491	0.105				0.68	0.32	0.08
PKW1 L3 X3	67	26	9.7	0.232	10.0	0.38	75.3	0.89	0.360	12.4	0.667	0.147	2.58	1.00	1.23	0.59	0.41	0.12
	57		9	0.201	9.2	0.35	66.8	0.85	0.352	11.9	0.591	0.137				0.61	0.39	0.11
	47		6.2	0.180	6.4	0.24	38.4	1.22	0.324	10.9	0.532	0.123				0.62	0.38	0.10
	37		5.3	0.146	5.4	0.21	30.1	1.23	0.314	9.5	0.481	0.107				0.66	0.34	0.08
PKW1 L3 A3	67	26	9.5	0.233	9.8	0.38	73.1	0.92	0.358	12.5	0.662	0.147	2.58	1.00	1.23	0.59	0.41	0.12
	57		8.9	0.202	9.1	0.35	65.7	0.87	0.351	11.9	0.591	0.137				0.61	0.39	0.11
	47		6.3	0.180	6.5	0.25	39.3	1.20	0.325	10.9	0.532	0.123				0.62	0.38	0.10
	37		5.3	0.146	5.4	0.21	30.1	1.23	0.314	9.6	0.476	0.108				0.66	0.34	0.08
PKW1 L3 B3	67	26	9.3	0.234	9.6	0.37	70.9	0.94	0.356	12.7	0.651	0.149	2.58	1.00	1.23	0.58	0.42	0.13

Name of Model	Qa (lt/s)	P (cm)	h_1 (cm)	V_1 (m/s)	H_1 (cm)	H_1/P	Qt (lt/s)	C_d	E_1 (m)	h_2 (cm)	V_2 (m/s)	E_2 (m)	L/W	W_i/W_o	B/P	$\frac{(E_1-E_2)}{E_1}$	E_2/E_1	Fr
	57		8.7	0.203	8.9	0.34	63.6	0.90	0.349	12.0	0.586	0.138				0.61	0.39	0.11
	47		6.2	0.180	6.4	0.24	38.4	1.22	0.324	11.0	0.527	0.124				0.62	0.38	0.10
	37		5.1	0.147	5.2	0.20	28.4	1.30	0.312	9.6	0.476	0.108				0.66	0.34	0.08
PKW1 L3 C3	67	26	9.2	0.235	9.5	0.36	69.8	0.96	0.355	12.7	0.651	0.149	2.58	1.00	1.23	0.58	0.42	0.13
	57		8.7	0.203	8.9	0.34	63.6	0.90	0.349	12.0	0.586	0.138				0.61	0.39	0.11
	47		6.1	0.181	6.3	0.24	37.5	1.25	0.323	11.1	0.523	0.125				0.61	0.39	0.10
	37		5.2	0.146	5.3	0.20	29.3	1.26	0.313	9.6	0.476	0.108				0.66	0.34	0.08
PKW1 L3 D3	67	26	8.8	0.238	9.1	0.35	65.5	1.02	0.351	12.8	0.646	0.149	2.58	1.00	1.23	0.57	0.43	0.13
	57		8.3	0.205	8.5	0.33	59.4	0.96	0.345	12.2	0.577	0.139				0.60	0.40	0.11
	47		5.9	0.182	6.1	0.23	35.8	1.31	0.321	11.2	0.518	0.126				0.61	0.39	0.10
	37		4.9	0.148	5.0	0.19	26.8	1.38	0.310	9.7	0.471	0.108				0.65	0.35	0.08
PKW1 L3 E3	67	26	8.4	0.240	8.7	0.33	61.3	1.09	0.347	13.0	0.636	0.151	2.58	1.00	1.23	0.57	0.43	0.13
	57		7.8	0.208	8.0	0.31	54.3	1.05	0.340	12.3	0.572	0.140				0.59	0.41	0.11
	47		5.3	0.185	5.5	0.21	30.6	1.53	0.315	11.3	0.513	0.126				0.60	0.40	0.11
	37		4.2	0.151	4.3	0.17	21.5	1.72	0.303	9.8	0.466	0.109				0.64	0.36	0.09
PKW1 L3 F3	67	26	9.3	0.234	9.6	0.37	70.9	0.94	0.356	12.7	0.651	0.149	2.58	1.00	1.23	0.58	0.42	0.13
	57		8.6	0.203	8.8	0.34	62.6	0.91	0.348	12.1	0.582	0.138				0.60	0.40	0.11
	47		6.2	0.180	6.4	0.24	38.4	1.22	0.324	11.1	0.523	0.125				0.61	0.39	0.10
	37		5.1	0.147	5.2	0.20	28.4	1.30	0.312	9.7	0.471	0.108				0.65	0.35	0.08
PKW1 L3 G3	67	26	9	0.236	9.3	0.36	67.7	0.99	0.353	12.8	0.646	0.149	2.58	1.00	1.23	0.58	0.42	0.13
	57		8.7	0.203	8.9	0.34	63.6	0.90	0.349	12.3	0.572	0.140				0.60	0.40	0.11
	47		6.3	0.180	6.5	0.25	39.3	1.20	0.325	11.3	0.513	0.126				0.61	0.39	0.10
	37		5	0.147	5.1	0.20	27.6	1.34	0.311	9.7	0.471	0.108				0.65	0.35	0.08

Name of Model	Qa (lt/s)	P (cm)	h_1 (cm)	V_1 (m/s)	H_1 (cm)	H_1/P	Qt (lt/s)	C_d	E_1 (m)	h_2 (cm)	V_2 (m/s)	E_2 (m)	L/W	W_i/W_o	B/P	$\frac{(E_1-E_2)}{E_1}$	E_2/E_1	Fr
PKW1 L3 H3	67	26	9	0.236	9.3	0.36	67.7	0.99	0.353	12.8	0.646	0.149	2.58	1.00	1.23	0.58	0.42	0.13
	57		8.5	0.204	8.7	0.34	61.5	0.93	0.347	12.3	0.572	0.140				0.60	0.40	0.11
	47		6.1	0.181	6.3	0.24	37.5	1.25	0.323	11.4	0.509	0.127				0.61	0.39	0.10
	37		4.8	0.148	4.9	0.19	26.0	1.42	0.309	9.8	0.466	0.109				0.65	0.35	0.09
PKW1 L3 I3	67	26	9	0.236	9.3	0.36	67.7	0.99	0.353	12.7	0.651	0.149	2.58	1.00	1.23	0.58	0.42	0.13
	57		8.3	0.205	8.5	0.33	59.4	0.96	0.345	12.2	0.577	0.139				0.60	0.40	0.11
	47		6.1	0.181	6.3	0.24	37.5	1.25	0.323	11.2	0.518	0.126				0.61	0.39	0.10
	37		4.8	0.148	4.9	0.19	26.0	1.42	0.309	9.7	0.471	0.108				0.65	0.35	0.09
PKW1 L3 J3	67	26	9	0.236	9.3	0.36	67.7	0.99	0.353	12.7	0.651	0.149	2.58	1.00	1.23	0.58	0.42	0.13
	57		8.4	0.205	8.6	0.33	60.5	0.94	0.346	12.2	0.577	0.139				0.60	0.40	0.11
	47		6.2	0.180	6.4	0.24	38.4	1.22	0.324	11.2	0.518	0.126				0.61	0.39	0.10
	37		4.7	0.149	4.8	0.19	25.3	1.47	0.308	9.7	0.471	0.108				0.65	0.35	0.09
PKW1 L3 K3	67	26	8.9	0.237	9.2	0.35	66.6	1.01	0.352	12.7	0.651	0.149	2.58	1.00	1.23	0.58	0.42	0.13
	57		8.1	0.206	8.3	0.32	57.4	0.99	0.343	12.3	0.572	0.140				0.59	0.41	0.11
	47		6	0.181	6.2	0.24	36.6	1.28	0.322	11.3	0.513	0.126				0.61	0.39	0.10
	37		4.6	0.149	4.7	0.18	24.5	1.51	0.307	9.8	0.466	0.109				0.64	0.36	0.09
PKW1 L3 M3	67	26	9	0.236	9.3	0.36	67.7	0.99	0.353	12.7	0.651	0.149	2.58	1.00	1.23	0.58	0.42	0.13
	57		8.5	0.204	8.7	0.34	61.5	0.93	0.347	12.2	0.577	0.139				0.60	0.40	0.11
	47		6.2	0.180	6.4	0.24	38.4	1.22	0.324	11.2	0.518	0.126				0.61	0.39	0.10
	37		4.8	0.148	4.9	0.19	26.0	1.42	0.309	9.7	0.471	0.108				0.65	0.35	0.09
PKW1 L4 X4	67	24	9	0.251	9.3	0.39	68.1	0.98	0.333	12.3	0.672	0.146	2.38	1.00	1.17	0.56	0.44	0.14
	57		8	0.220	8.2	0.34	56.6	1.01	0.322	12.0	0.586	0.138				0.57	0.43	0.12
	47		6.9	0.188	7.1	0.29	45.1	1.04	0.311	11.8	0.492	0.130				0.58	0.42	0.11

Name of Model	Qa (lt/s)	P (cm)	h_1 (cm)	V_1 (m/s)	H_1 (cm)	H_1/P	Qt (lt/s)	C_d	E_1 (m)	h_2 (cm)	V_2 (m/s)	E_2 (m)	L/W	W_i/W_o	B/P	$\frac{(E_1-E_2)}{E_1}$	E_2/E_1	Fr
	37		5.7	0.154	5.8	0.24	33.6	1.10	0.298	9.2	0.497	0.105				0.65	0.35	0.09
PKW1 L4 A4	67	24	9	0.251	9.3	0.39	68.1	0.98	0.333	12.4	0.667	0.147	2.38	1.00	1.17	0.56	0.44	0.14
	57		8	0.220	8.2	0.34	56.6	1.01	0.322	12.3	0.572	0.140				0.57	0.43	0.12
	47		6.9	0.188	7.1	0.29	45.1	1.04	0.311	11.8	0.492	0.130				0.58	0.42	0.11
	37		5.8	0.153	5.9	0.25	34.5	1.07	0.299	9.2	0.497	0.105				0.65	0.35	0.09
PKW1 L4 B4	67	24	9.1	0.250	9.4	0.39	69.1	0.97	0.334	12.6	0.656	0.148	2.38	1.00	1.17	0.56	0.44	0.14
	57		8	0.220	8.2	0.34	56.6	1.01	0.322	12.3	0.572	0.140				0.57	0.43	0.12
	47		6.7	0.189	6.9	0.29	43.2	1.09	0.309	11.9	0.488	0.131				0.58	0.42	0.11
	37		5.6	0.154	5.7	0.24	32.7	1.13	0.297	9.4	0.486	0.106				0.64	0.36	0.09
PKW1 L4 C4	67	24	8.9	0.251	9.2	0.38	67.0	1.00	0.332	12.7	0.651	0.149	2.38	1.00	1.17	0.55	0.45	0.14
	57		8	0.220	8.2	0.34	56.6	1.01	0.322	12.4	0.568	0.140				0.56	0.44	0.12
	47		6.9	0.188	7.1	0.29	45.1	1.04	0.311	11.9	0.488	0.131				0.58	0.42	0.11
	37		5.5	0.155	5.6	0.23	31.9	1.16	0.296	9.4	0.486	0.106				0.64	0.36	0.09
PKW1 L4 D4	67	24	8.7	0.253	9.0	0.38	64.9	1.03	0.330	12.7	0.651	0.149	2.38	1.00	1.17	0.55	0.45	0.14
	57		7.7	0.222	8.0	0.33	53.6	1.06	0.320	12.4	0.568	0.140				0.56	0.44	0.13
	47		6.5	0.190	6.7	0.28	41.3	1.14	0.307	12.0	0.484	0.132				0.57	0.43	0.11
	37		5.3	0.156	5.4	0.23	30.2	1.22	0.294	9.5	0.481	0.107				0.64	0.36	0.09
PKW1 L4 E4	67	24	8.3	0.256	8.6	0.36	60.7	1.10	0.326	12.9	0.641	0.150	2.38	1.00	1.17	0.54	0.46	0.14
	57		7.3	0.225	7.6	0.31	49.7	1.15	0.316	12.6	0.558	0.142				0.55	0.45	0.13
	47		6	0.193	6.2	0.26	36.8	1.28	0.302	12.1	0.480	0.133				0.56	0.44	0.11
	37		5	0.158	5.1	0.21	27.8	1.33	0.291	9.6	0.476	0.108				0.63	0.37	0.09
PKW1 L4 F4	67	24	8.9	0.251	9.2	0.38	67.0	1.00	0.332	12.7	0.651	0.149	2.38	1.00	1.17	0.55	0.45	0.14
	57		7.9	0.221	8.1	0.34	55.6	1.02	0.321	12.4	0.568	0.140				0.56	0.44	0.12

Name of Model	Qa (lt/s)	P (cm)	h_1 (cm)	V_1 (m/s)	H_1 (cm)	H_1/P	Qt (lt/s)	C_d	E_1 (m)	h_2 (cm)	V_2 (m/s)	E_2 (m)	L/W	W_i/W_o	B/P	$\frac{(E_1-E_2)}{E_1}$	E_2/E_1	Fr
	47		6.6	0.190	6.8	0.28	42.3	1.11	0.308	11.9	0.488	0.131				0.57	0.43	0.11
	37		5.5	0.155	5.6	0.23	31.9	1.16	0.296	9.4	0.486	0.106				0.64	0.36	0.09
PKW1 L4 G4	67	24	8.8	0.252	9.1	0.38	65.9	1.02	0.331	12.7	0.651	0.149	2.38	1.00	1.17	0.55	0.45	0.14
	57		7.9	0.221	8.1	0.34	55.6	1.02	0.321	12.4	0.568	0.140				0.56	0.44	0.12
	47		6.7	0.189	6.9	0.29	43.2	1.09	0.309	12.0	0.484	0.132				0.57	0.43	0.11
	37		5.5	0.155	5.6	0.23	31.9	1.16	0.296	9.5	0.481	0.107				0.64	0.36	0.09
PKW1 L4 H4	67	24	8.7	0.253	9.0	0.38	64.9	1.03	0.330	12.7	0.651	0.149	2.38	1.00	1.17	0.55	0.45	0.14
	57		7.5	0.223	7.8	0.32	51.6	1.10	0.318	12.5	0.563	0.141				0.56	0.44	0.13
	47		6.5	0.190	6.7	0.28	41.3	1.14	0.307	12.0	0.484	0.132				0.57	0.43	0.11
	37		5.3	0.156	5.4	0.23	30.2	1.22	0.294	9.6	0.476	0.108				0.63	0.37	0.09
PKW1 L4 I4	67	24	8.7	0.253	9.0	0.38	64.9	1.03	0.330	12.7	0.651	0.149	2.38	1.00	1.17	0.55	0.45	0.14
	57		7.7	0.222	8.0	0.33	53.6	1.06	0.320	12.4	0.568	0.140				0.56	0.44	0.13
	47		6.5	0.190	6.7	0.28	41.3	1.14	0.307	11.9	0.488	0.131				0.57	0.43	0.11
	37		5.3	0.156	5.4	0.23	30.2	1.22	0.294	9.5	0.481	0.107				0.64	0.36	0.09
PKW1 L4 J4	67	24	8.7	0.253	9.0	0.38	64.9	1.03	0.330	12.7	0.651	0.149	2.38	1.00	1.17	0.55	0.45	0.14
	57		7.5	0.223	7.8	0.32	51.6	1.10	0.318	12.4	0.568	0.140				0.56	0.44	0.13
	47		6.5	0.190	6.7	0.28	41.3	1.14	0.307	11.9	0.488	0.131				0.57	0.43	0.11
	37		5.3	0.156	5.4	0.23	30.2	1.22	0.294	9.5	0.481	0.107				0.64	0.36	0.09
PKW1 L4 K4	67	24	8.5	0.255	8.8	0.37	62.8	1.07	0.328	12.7	0.651	0.149	2.38	1.00	1.17	0.55	0.45	0.14
	57		7.5	0.223	7.8	0.32	51.6	1.10	0.318	12.4	0.568	0.140				0.56	0.44	0.13
	47		6.5	0.190	6.7	0.28	41.3	1.14	0.307	11.9	0.488	0.131				0.57	0.43	0.11
	37		5.2	0.156	5.3	0.22	29.4	1.26	0.293	9.6	0.476	0.108				0.63	0.37	0.09
PKW1 L4 M4	67	24	8.6	0.254	8.9	0.37	63.8	1.05	0.329	12.7	0.651	0.149	2.38	1.00	1.17	0.55	0.45	0.14

Name of Model	Qa (lt/s)	P (cm)	h_1 (cm)	V_1 (m/s)	H_1 (cm)	H_1/P	Qt (lt/s)	C_d	E_1 (m)	h_2 (cm)	V_2 (m/s)	E_2 (m)	L/W	W_i/W_o	B/P	$\frac{(E_1-E_2)}{E_1}$	E_2/E_1	Fr
	57		7.7	0.222	8.0	0.33	53.6	1.06	0.320	12.4	0.568	0.140				0.56	0.44	0.13
	47		6.5	0.190	6.7	0.28	41.3	1.14	0.307	11.9	0.488	0.131				0.57	0.43	0.11
	37		5.2	0.156	5.3	0.22	29.4	1.26	0.293	9.5	0.481	0.107				0.64	0.36	0.09
PKW2 L1 X1	67	30	6.7	0.225	7.0	0.23	43.9	1.53	0.370	12.5	0.662	0.147	2.98	1.22	1.33	0.60	0.40	0.12
	57		6.1	0.195	6.3	0.21	37.8	1.51	0.363	12.0	0.586	0.138				0.62	0.38	0.10
	47		5.1	0.165	5.2	0.17	28.7	1.64	0.352	11.0	0.527	0.124				0.65	0.35	0.09
	37		4.1	0.134	4.2	0.14	20.5	1.80	0.342	9.3	0.491	0.105				0.69	0.31	0.07
PKW2 L1 B1	67	30	6.6	0.226	6.9	0.23	43.0	1.56	0.369	12.8	0.646	0.149	2.98	1.22	1.33	0.59	0.41	0.12
	57		5.9	0.196	6.1	0.20	36.0	1.58	0.361	12.6	0.558	0.142				0.61	0.39	0.10
	47		5	0.166	5.1	0.17	27.9	1.69	0.351	10.9	0.532	0.123				0.65	0.35	0.09
	37		4.1	0.134	4.2	0.14	20.5	1.80	0.342	9.2	0.497	0.105				0.69	0.31	0.07
PKW2 L1 D1	67	30	6	0.230	6.3	0.21	37.5	1.78	0.363	12.8	0.646	0.149	2.98	1.22	1.33	0.59	0.41	0.12
	57		5.3	0.199	5.5	0.18	30.9	1.85	0.355	12.0	0.586	0.138				0.61	0.39	0.11
	47		4.1	0.170	4.2	0.14	20.9	2.24	0.342	10.9	0.532	0.123				0.64	0.36	0.09
	37		3.2	0.138	3.3	0.11	14.3	2.58	0.333	9.5	0.481	0.107				0.68	0.32	0.08
PKW2 L2 X2	67	28	7.3	0.234	7.6	0.27	49.9	1.34	0.356	12.1	0.684	0.145	2.78	1.22	1.29	0.59	0.41	0.13
	57		6.7	0.203	6.9	0.25	43.4	1.31	0.349	12.0	0.586	0.138				0.61	0.39	0.11
	47		5.7	0.172	5.9	0.21	33.9	1.39	0.339	11.0	0.527	0.124				0.63	0.37	0.09
	37		4.8	0.139	4.9	0.17	25.9	1.43	0.329	9.3	0.491	0.105				0.68	0.32	0.08
PKW2 L2 B2	67	28	7.3	0.234	7.6	0.27	49.9	1.34	0.356	12.8	0.646	0.149	2.78	1.22	1.29	0.58	0.42	0.13
	57		6.4	0.205	6.6	0.24	40.7	1.40	0.346	12.0	0.586	0.138				0.60	0.40	0.11
	47		5.1	0.175	5.3	0.19	28.8	1.63	0.333	10.9	0.532	0.123				0.63	0.37	0.10
	37		4.3	0.141	4.4	0.16	22.1	1.67	0.324	9.3	0.491	0.105				0.68	0.32	0.08

Name of Model	Qa (lt/s)	P (cm)	h_1 (cm)	V_1 (m/s)	H_1 (cm)	H_1/P	Qt (lt/s)	C_d	E_1 (m)	h_2 (cm)	V_2 (m/s)	E_2 (m)	L/W	W_i/W_o	B/P	$\frac{(E_1-E_2)}{E_1}$	E_2/E_1	Fr
PKW2 L2 D2	67	28	6.8	0.238	7.1	0.25	45.1	1.48	0.351	14.8	0.559	0.164	2.78	1.22	1.29	0.53	0.47	0.13
	57		5.8	0.208	6.0	0.22	35.3	1.61	0.340	11.9	0.591	0.137				0.60	0.40	0.11
	47		4.9	0.176	5.1	0.18	27.2	1.73	0.331	11.0	0.527	0.124				0.62	0.38	0.10
	37		3.9	0.143	4.0	0.14	19.2	1.93	0.320	10.3	0.443	0.113				0.65	0.35	0.08
PKW2 L3 X3	67	26	7.7	0.245	8.0	0.31	54.2	1.24	0.340	12.5	0.662	0.147	2.58	1.22	1.23	0.57	0.43	0.13
	57		7	0.213	7.2	0.28	46.5	1.23	0.332	12.7	0.554	0.143				0.57	0.43	0.12
	47		6	0.181	6.2	0.24	36.6	1.28	0.322	10.5	0.553	0.121				0.63	0.37	0.10
	37		4.8	0.148	4.9	0.19	26.0	1.42	0.309	9.0	0.508	0.103				0.67	0.33	0.09
PKW2 L3 B3	67	26	9.5	0.233	9.8	0.38	73.1	0.92	0.358	13.5	0.613	0.154	2.58	1.22	1.23	0.57	0.43	0.12
	57		6.8	0.215	7.0	0.27	44.6	1.28	0.330	12.2	0.577	0.139				0.58	0.42	0.12
	47		6	0.181	6.2	0.24	36.6	1.28	0.322	11.0	0.527	0.124				0.61	0.39	0.10
	37		4.6	0.149	4.7	0.18	24.5	1.51	0.307	9.3	0.491	0.105				0.66	0.34	0.09
PKW2 L3 D3	67	26	7.1	0.250	7.4	0.29	48.3	1.39	0.334	12.8	0.646	0.149	2.58	1.22	1.23	0.55	0.45	0.14
	57		6.4	0.217	6.6	0.26	40.9	1.39	0.326	12.0	0.586	0.138				0.58	0.42	0.12
	47		5.6	0.184	5.8	0.22	33.2	1.42	0.318	11.2	0.518	0.126				0.60	0.40	0.10
	37		4.3	0.151	4.4	0.17	22.2	1.67	0.304	9.2	0.497	0.105				0.66	0.34	0.09
PKW2 L4 X4	67	26	8.2	0.257	8.5	0.36	59.7	1.12	0.325	8.5	0.973	0.133	2.38	1.22	1.17	0.59	0.41	0.14
	57		7.5	0.223	7.8	0.32	51.6	1.10	0.318	10.1	0.697	0.126				0.60	0.40	0.13
	47		6.1	0.193	6.3	0.26	37.7	1.25	0.303	10.5	0.553	0.121				0.60	0.40	0.11
	37		5	0.158	5.1	0.21	27.8	1.33	0.291	9.0	0.508	0.103				0.65	0.35	0.09
PKW2 L4 B4	67	26	8.1	0.258	8.4	0.35	58.6	1.14	0.324	9.0	0.919	0.133	2.38	1.22	1.17	0.59	0.41	0.14
	57		7.5	0.223	7.8	0.32	51.6	1.10	0.318	11.8	0.596	0.136				0.57	0.43	0.13
	47		6.1	0.193	6.3	0.26	37.7	1.25	0.303	10.4	0.558	0.120				0.60	0.40	0.11

Name of Model	Qa (lt/s)	P (cm)	h_1 (cm)	V_1 (m/s)	H_1 (cm)	H_1/P	Qt (lt/s)	C_d	E_1 (m)	h_2 (cm)	V_2 (m/s)	E_2 (m)	L/W	W_i/W_o	B/P	$\frac{(E_1-E_2)}{E_1}$	E_2/E_1	Fr
	37		5	0.158	5.1	0.21	27.8	1.33	0.291	8.7	0.525	0.101				0.65	0.35	0.09
PKW2 L4 D4	67	26	7.8	0.260	8.1	0.34	55.6	1.21	0.321	7.0	1.182	0.141	2.38	1.22	1.17	0.56	0.44	0.15
	57		7.1	0.226	7.4	0.31	47.8	1.19	0.314	12.8	0.550	0.143				0.54	0.46	0.13
	47		5.2	0.199	5.4	0.23	30.0	1.57	0.294	10.9	0.532	0.123				0.58	0.42	0.12
	37		4.7	0.159	4.8	0.20	25.4	1.46	0.288	9.6	0.476	0.108				0.63	0.37	0.09
PKW3 L1 X1	67	26	8	0.218	8.2	0.27	56.6	1.18	0.382	12.7	0.651	0.149	2.98	0.82	1.33	0.61	0.39	0.11
	57		7.6	0.187	7.8	0.26	51.9	1.10	0.378	12.0	0.586	0.138				0.64	0.36	0.10
	47		6.9	0.157	7.0	0.23	44.5	1.06	0.370	11.0	0.527	0.124				0.66	0.34	0.08
	37		4.7	0.132	4.8	0.16	25.1	1.48	0.348	9.2	0.497	0.105				0.70	0.30	0.07
PKW3 L1 B1	67	26	7.5	0.221	7.7	0.26	51.6	1.30	0.377	12.6	0.656	0.148	2.98	0.82	1.33	0.61	0.39	0.11
	57		7.4	0.188	7.6	0.25	49.9	1.14	0.376	12.0	0.586	0.138				0.63	0.37	0.10
	47		6.6	0.159	6.7	0.22	41.7	1.13	0.367	10.5	0.553	0.121				0.67	0.33	0.08
	37		4.5	0.132	4.6	0.15	23.5	1.57	0.346	9.3	0.491	0.105				0.70	0.30	0.07
PKW3 L1 D1	67	26	7	0.224	7.3	0.24	46.7	1.43	0.373	12.8	0.646	0.149	2.98	0.82	1.33	0.60	0.40	0.12
	57		6.9	0.191	7.1	0.24	45.1	1.26	0.371	11.9	0.591	0.137				0.63	0.37	0.10
	47		5.9	0.162	6.0	0.20	35.4	1.33	0.360	11.0	0.527	0.124				0.66	0.34	0.09
	37		3.8	0.135	3.9	0.13	18.4	2.01	0.339	9.5	0.481	0.107				0.68	0.32	0.07
PKW3 L2 X2	67	26	9.2	0.222	9.5	0.34	69.5	0.96	0.375	13.0	0.636	0.151	2.78	0.82	1.29	0.60	0.40	0.12
	57		8.6	0.192	8.8	0.31	62.3	0.91	0.368	11.8	0.596	0.136				0.63	0.37	0.10
	47		7.9	0.162	8.0	0.29	54.5	0.86	0.360	11.0	0.527	0.124				0.66	0.34	0.09
	37		6.6	0.132	6.7	0.24	41.4	0.89	0.347	9.8	0.466	0.109				0.69	0.31	0.07
PKW3 L2 B2	67	26	9	0.224	9.3	0.33	67.3	0.99	0.373	13.0	0.636	0.151	2.78	0.82	1.29	0.60	0.40	0.12
	57		8.3	0.194	8.5	0.30	59.2	0.96	0.365	11.0	0.640	0.131				0.64	0.36	0.10

Name of Model	Qa (lt/s)	P (cm)	h_1 (cm)	V_1 (m/s)	H_1 (cm)	H_1/P	Qt (lt/s)	C_d	E_1 (m)	h_2 (cm)	V_2 (m/s)	E_2 (m)	L/W	W_i/W_o	B/P	$\frac{(E_1-E_2)}{E_1}$	E_2/E_1	Fr
	47		7.4	0.164	7.5	0.27	49.5	0.95	0.355	11.2	0.518	0.126				0.65	0.35	0.09
	37		6.3	0.133	6.4	0.23	38.6	0.96	0.344	9.5	0.481	0.107				0.69	0.31	0.07
PKW3 L2 D2	67	24	8.5	0.227	8.8	0.31	62.0	1.08	0.368	12.9	0.641	0.150	2.78	0.82	1.29	0.59	0.41	0.12
	57		7.8	0.197	8.0	0.29	54.1	1.05	0.360	12.2	0.577	0.139				0.61	0.39	0.10
	47		7.1	0.165	7.2	0.26	46.6	1.01	0.352	11.0	0.527	0.124				0.65	0.35	0.09
	37		6	0.134	6.1	0.22	36.0	1.03	0.341	9.7	0.471	0.108				0.68	0.32	0.07
PKW3 L3 X3	67	26	10.5	0.227	10.8	0.41	84.4	0.79	0.368	13.0	0.636	0.151	2.58	0.82	1.23	0.59	0.41	0.12
	57		9	0.201	9.2	0.35	66.8	0.85	0.352	12.5	0.563	0.141				0.60	0.40	0.11
	47		8.5	0.168	8.6	0.33	60.8	0.77	0.346	10.5	0.553	0.121				0.65	0.35	0.09
	37		6	0.143	6.1	0.23	36.1	1.03	0.321	9.3	0.491	0.105				0.67	0.33	0.08
PKW3 L3 B3	67	26	10	0.230	10.3	0.39	78.7	0.85	0.363	13.0	0.636	0.151	2.58	0.82	1.23	0.58	0.42	0.12
	57		8.8	0.202	9.0	0.35	64.7	0.88	0.350	12.0	0.586	0.138				0.61	0.39	0.11
	47		7.5	0.173	7.7	0.29	50.6	0.93	0.337	10.8	0.537	0.123				0.64	0.36	0.10
	37		5.6	0.145	5.7	0.22	32.6	1.13	0.317	9.2	0.497	0.105				0.67	0.33	0.08
PKW3 L3 D3	67	26	9.5	0.233	9.8	0.38	73.1	0.92	0.358	12.2	0.678	0.145	2.58	0.82	1.23	0.59	0.41	0.12
	57		8.4	0.205	8.6	0.33	60.5	0.94	0.346	12.5	0.563	0.141				0.59	0.41	0.11
	47		7	0.176	7.2	0.28	45.8	1.03	0.332	10.8	0.537	0.123				0.63	0.37	0.10
	37		5.2	0.146	5.3	0.20	29.3	1.26	0.313	9.3	0.491	0.105				0.66	0.34	0.08
PKW3 L4 X4	67	24	10	0.243	10.3	0.43	79.1	0.85	0.343	13.1	0.631	0.151	2.38	0.82	1.17	0.56	0.44	0.13
	57		8.5	0.217	8.7	0.36	61.8	0.92	0.327	13.0	0.541	0.145				0.56	0.44	0.12
	47		7.6	0.184	7.8	0.32	51.8	0.91	0.318	11.0	0.527	0.124				0.61	0.39	0.10
	37		6.5	0.150	6.6	0.28	40.7	0.91	0.306	10.5	0.435	0.115				0.63	0.37	0.09
PKW3 L4 B4	67	24	9.8	0.245	10.1	0.42	76.8	0.87	0.341	12.9	0.641	0.150	2.38	0.82	1.17	0.56	0.44	0.13

Name of Model	Qa (lt/s)	P (cm)	h_1 (cm)	V_1 (m/s)	H_1 (cm)	H_1/P	Qt (lt/s)	C_d	E_1 (m)	h_2 (cm)	V_2 (m/s)	E_2 (m)	L/W	W_i/W_o	B/P	$\frac{(E_1-E_2)}{E_1}$	E_2/E_1	Fr
	57		8.4	0.217	8.6	0.36	60.8	0.94	0.326	13.1	0.537	0.146				0.55	0.45	0.12
	47		7.3	0.185	7.5	0.31	48.9	0.96	0.315	10.5	0.553	0.121				0.62	0.38	0.11
	37		6.2	0.151	6.3	0.26	38.0	0.97	0.303	9.2	0.497	0.105				0.66	0.34	0.09
PKW3 L4 D4	67	24	9.3	0.248	9.6	0.40	71.3	0.94	0.336	13.5	0.613	0.154	2.38	0.82	1.17	0.54	0.46	0.14
	57		8.1	0.219	8.3	0.35	57.7	0.99	0.323	12.7	0.554	0.143				0.56	0.44	0.12
	47		7	0.187	7.2	0.30	46.0	1.02	0.312	11.0	0.527	0.124				0.60	0.40	0.11
	37		6	0.152	6.1	0.25	36.2	1.02	0.301	9.3	0.491	0.105				0.65	0.35	0.09
PKW4 L1 X1	67	30	5.9	0.230	6.2	0.21	36.7	1.83	0.362	12.9	0.641	0.150	3.96	1.00	2.00	0.59	0.41	0.12
	57		5.2	0.200	5.4	0.18	30.0	1.90	0.354	12.2	0.577	0.139				0.61	0.39	0.11
	47		4.7	0.167	4.8	0.16	25.5	1.84	0.348	10.7	0.542	0.122				0.65	0.35	0.09
	37		3.8	0.135	3.9	0.13	18.4	2.01	0.339	9.1	0.502	0.104				0.69	0.31	0.07
PKW4 L1 B1	67	30	5.5	0.233	5.8	0.19	33.2	2.02	0.358	12.5	0.662	0.147	3.96	1.00	2.00	0.59	0.41	0.12
	57		5	0.201	5.2	0.17	28.4	2.01	0.352	12.0	0.586	0.138				0.61	0.39	0.11
	47		4.2	0.170	4.3	0.14	21.7	2.17	0.343	11.2	0.518	0.126				0.63	0.37	0.09
	37		3.5	0.136	3.6	0.12	16.3	2.27	0.336	9.5	0.481	0.107				0.68	0.32	0.08
PKW4 L1 D1	67	30	5.3	0.234	5.6	0.19	31.5	2.13	0.356	13.5	0.613	0.154	3.96	1.00	2.00	0.57	0.43	0.13
	57		4.4	0.205	4.6	0.15	23.7	2.41	0.346	12.1	0.582	0.138				0.60	0.40	0.11
	47		3.7	0.172	3.9	0.13	18.1	2.60	0.339	11.3	0.513	0.126				0.63	0.37	0.09
	37		2.8	0.139	2.9	0.10	11.8	3.13	0.329	8.7	0.525	0.101				0.69	0.31	0.08
PKW4 L2 X2	67	28	6	0.243	6.3	0.23	37.8	1.77	0.343	12.9	0.641	0.150	3.70	1.00	1.95	0.56	0.44	0.13
	57		5.5	0.210	5.7	0.20	32.8	1.74	0.337	11.7	0.601	0.135				0.60	0.40	0.12
	47		4.5	0.179	4.7	0.17	24.1	1.95	0.327	11.0	0.527	0.124				0.62	0.38	0.10
	37		3.9	0.143	4.0	0.14	19.2	1.93	0.320	9.4	0.486	0.106				0.67	0.33	0.08

Name of Model	Qa (lt/s)	P (cm)	h_1 (cm)	V_1 (m/s)	H_1 (cm)	H_1/P	Qt (lt/s)	C_d	E_1 (m)	h_2 (cm)	V_2 (m/s)	E_2 (m)	L/W	W_i/W_o	B/P	$\frac{(E_1-E_2)}{E_1}$	E_2/E_1	Fr
PKW4 L2 B2	67	28	6	0.243	6.3	0.23	37.8	1.77	0.343	13.0	0.636	0.151	3.70	1.00	1.95	0.56	0.44	0.13
	57		5	0.213	5.2	0.19	28.6	1.99	0.332	12.3	0.572	0.140				0.58	0.42	0.12
	47		4.3	0.180	4.5	0.16	22.6	2.08	0.325	11.5	0.505	0.128				0.61	0.39	0.10
	37		3.6	0.145	3.7	0.13	17.1	2.17	0.317	9.3	0.491	0.105				0.67	0.33	0.08
PKW4 L2 D2	67	28	5.5	0.247	5.8	0.21	33.5	2.00	0.338	13.5	0.613	0.154	3.70	1.00	1.95	0.54	0.46	0.14
	57		4.9	0.214	5.1	0.18	27.8	2.05	0.331	12.2	0.577	0.139				0.58	0.42	0.12
	47		4.2	0.180	4.4	0.16	21.8	2.15	0.324	11.5	0.505	0.128				0.60	0.40	0.10
	37		3	0.147	3.1	0.11	13.1	2.82	0.311	9.3	0.491	0.105				0.66	0.34	0.08
PKW4 L3 X3	67	26	6.5	0.255	6.8	0.26	42.7	1.57	0.328	13.0	0.636	0.151	3.43	1.00	1.90	0.54	0.46	0.14
	57		5.8	0.221	6.0	0.23	35.6	1.60	0.320	12.5	0.563	0.141				0.56	0.44	0.12
	47		5	0.187	5.2	0.20	28.2	1.67	0.312	11.0	0.527	0.124				0.60	0.40	0.11
	37		4	0.152	4.1	0.16	20.0	1.85	0.301	9.8	0.466	0.109				0.64	0.36	0.09
PKW4 L3 B3	67	26	6.3	0.256	6.6	0.26	40.9	1.64	0.326	13.8	0.599	0.156	3.43	1.00	1.90	0.52	0.48	0.14
	57		5.5	0.223	5.8	0.22	33.0	1.73	0.318	12.2	0.577	0.139				0.56	0.44	0.13
	47		4.5	0.190	4.7	0.18	24.3	1.94	0.307	11.0	0.527	0.124				0.60	0.40	0.11
	37		3.9	0.153	4.0	0.15	19.3	1.92	0.300	9.5	0.481	0.107				0.64	0.36	0.09
PKW4 L3 D3	67	26	5.9	0.259	6.2	0.24	37.3	1.80	0.322	13.5	0.613	0.154	3.43	1.00	1.90	0.52	0.48	0.15
	57		5.9	0.221	6.1	0.24	36.5	1.56	0.321	12.0	0.586	0.138				0.57	0.43	0.12
	47		4.5	0.190	4.7	0.18	24.3	1.94	0.307	11.0	0.527	0.124				0.60	0.40	0.11
	37		3.4	0.155	3.5	0.14	15.8	2.34	0.295	9.5	0.481	0.107				0.64	0.36	0.09
PKW4 L4 X4	67	24	7	0.267	7.4	0.31	47.8	1.40	0.314	13.0	0.636	0.151	3.17	1.00	1.83	0.52	0.48	0.15
	57		6.2	0.233	6.5	0.27	39.4	1.45	0.305	12.0	0.586	0.138				0.55	0.45	0.13
	47		5.2	0.199	5.4	0.23	30.0	1.57	0.294	10.6	0.547	0.121				0.59	0.41	0.12

Name of Model	Qa (lt/s)	P (cm)	h_1 (cm)	V_1 (m/s)	H_1 (cm)	H_1/P	Qt (lt/s)	C_d	E_1 (m)	h_2 (cm)	V_2 (m/s)	E_2 (m)	L/W	W_i/W_o	B/P	$\frac{(E_1-E_2)}{E_1}$	E_2/E_1	Fr
	37		4.4	0.161	4.5	0.19	23.1	1.60	0.285	9.5	0.481	0.107				0.63	0.37	0.10
PKW4 L4 B4	67	24	6.7	0.269	7.1	0.29	45.0	1.49	0.311	13.5	0.613	0.154	3.17	1.00	1.83	0.50	0.50	0.15
	57		6.1	0.234	6.4	0.27	38.5	1.48	0.304	12.5	0.563	0.141				0.54	0.46	0.14
	47		5.1	0.199	5.3	0.22	29.2	1.61	0.293	11.0	0.527	0.124				0.58	0.42	0.12
	37		4.2	0.162	4.3	0.18	21.6	1.71	0.283	9.3	0.491	0.105				0.63	0.37	0.10
PKW4 L4 D4	67	24	6.5	0.271	6.9	0.29	43.1	1.55	0.309	13.8	0.599	0.156	3.17	1.00	1.83	0.49	0.51	0.16
	57		5.8	0.236	6.1	0.25	35.9	1.59	0.301	12.7	0.554	0.143				0.53	0.47	0.14
	47		4.9	0.201	5.1	0.21	27.6	1.70	0.291	11.0	0.527	0.124				0.57	0.43	0.12
	37		3.9	0.164	4.0	0.17	19.4	1.91	0.280	9.5	0.481	0.107				0.62	0.38	0.10
PKW5 L1 X1	67	30	6.3	0.228	6.6	0.22	40.2	1.67	0.366	13.5	0.613	0.154	3.47	1.00	1.67	0.58	0.42	0.12
	57		6	0.195	6.2	0.21	36.9	1.55	0.362	12.2	0.577	0.139				0.62	0.38	0.10
	47		4.8	0.167	4.9	0.16	26.3	1.79	0.349	11.0	0.527	0.124				0.64	0.36	0.09
	37		4.2	0.134	4.3	0.14	21.3	1.74	0.343	9.5	0.481	0.107				0.69	0.31	0.07
PKW5 L1 B1	67	30	6.1	0.229	6.4	0.21	38.4	1.74	0.364	13.0	0.636	0.151	3.47	1.00	1.67	0.59	0.41	0.12
	57		5.6	0.198	5.8	0.19	33.4	1.71	0.358	12.5	0.563	0.141				0.61	0.39	0.11
	47		4.6	0.168	4.7	0.16	24.7	1.90	0.347	10.5	0.553	0.121				0.65	0.35	0.09
	37		3.7	0.136	3.8	0.13	17.7	2.09	0.338	9.5	0.481	0.107				0.68	0.32	0.07
PKW5 L1 D1	67	30	5.5	0.233	5.8	0.19	33.2	2.02	0.358	12.7	0.651	0.149	3.47	1.00	1.67	0.58	0.42	0.12
	57		5	0.201	5.2	0.17	28.4	2.01	0.352	12.5	0.563	0.141				0.60	0.40	0.11
	47		4.8	0.167	4.9	0.16	26.3	1.79	0.349	11.0	0.527	0.124				0.64	0.36	0.09
	37		3	0.138	3.1	0.10	13.0	2.84	0.331	9.5	0.481	0.107				0.68	0.32	0.08
PKW5 L2 X2	67	28	6.8	0.238	7.1	0.25	45.1	1.48	0.351	13.5	0.613	0.154	3.23	1.00	1.62	0.56	0.44	0.13
	57		6	0.207	6.2	0.22	37.1	1.54	0.342	12.1	0.582	0.138				0.60	0.40	0.11

Name of Model	Qa (lt/s)	P (cm)	h_1 (cm)	V_1 (m/s)	H_1 (cm)	H_1/P	Qt (lt/s)	C_d	E_1 (m)	h_2 (cm)	V_2 (m/s)	E_2 (m)	L/W	W_i/W_o	B/P	$\frac{(E_1-E_2)}{E_1}$	E_2/E_1	Fr
	47		5.1	0.175	5.3	0.19	28.8	1.63	0.333	11.0	0.527	0.124				0.63	0.37	0.10
	37		4.2	0.142	4.3	0.15	21.3	1.73	0.323	9.4	0.486	0.106				0.67	0.33	0.08
PKW5 L2 B2	67	28	6.5	0.240	6.8	0.24	42.3	1.58	0.348	13.3	0.622	0.153	3.23	1.00	1.62	0.56	0.44	0.13
	57		5.8	0.208	6.0	0.22	35.3	1.61	0.340	12.2	0.577	0.139				0.59	0.41	0.11
	47		4.9	0.176	5.1	0.18	27.2	1.73	0.331	11.0	0.527	0.124				0.62	0.38	0.10
	37		4	0.143	4.1	0.15	19.9	1.86	0.321	9.5	0.481	0.107				0.67	0.33	0.08
PKW5 L2 D2	67	28	6.1	0.243	6.4	0.23	38.7	1.73	0.344	13.0	0.636	0.151	3.23	1.00	1.62	0.56	0.44	0.13
	57		5.3	0.211	5.5	0.20	31.1	1.83	0.335	12.1	0.582	0.138				0.59	0.41	0.12
	47		4.5	0.179	4.7	0.17	24.1	1.95	0.327	11.0	0.527	0.124				0.62	0.38	0.10
	37		3.5	0.145	3.6	0.13	16.4	2.26	0.316	9.5	0.481	0.107				0.66	0.34	0.08
PKW5 L3 X3	67	26	7.4	0.248	7.7	0.30	51.2	1.31	0.337	12.9	0.641	0.150	3.00	1.00	1.56	0.56	0.44	0.14
	57		6.5	0.217	6.7	0.26	41.8	1.36	0.327	12.5	0.563	0.141				0.57	0.43	0.12
	47		5.6	0.184	5.8	0.22	33.2	1.42	0.318	10.8	0.537	0.123				0.61	0.39	0.10
	37		4.5	0.150	4.6	0.18	23.7	1.56	0.306	9.1	0.502	0.104				0.66	0.34	0.09
PKW5 L3 B3	67	26	7.1	0.250	7.4	0.29	48.3	1.39	0.334	13.0	0.636	0.151	3.00	1.00	1.56	0.55	0.45	0.14
	57		6.2	0.219	6.4	0.25	39.1	1.46	0.324	12.5	0.563	0.141				0.56	0.44	0.12
	47		5.4	0.185	5.6	0.21	31.5	1.49	0.316	11.0	0.527	0.124				0.61	0.39	0.10
	37		4.4	0.150	4.5	0.17	22.9	1.61	0.305	9.2	0.497	0.105				0.66	0.34	0.09
PKW5 L3 D3	67	26	6.7	0.253	7.0	0.27	44.5	1.50	0.330	13.0	0.636	0.151	3.00	1.00	1.56	0.54	0.46	0.14
	57		5.9	0.221	6.1	0.24	36.5	1.56	0.321	11.8	0.596	0.136				0.58	0.42	0.12
	47		5.1	0.187	5.3	0.20	29.0	1.62	0.313	11.1	0.523	0.125				0.60	0.40	0.11
	37		4	0.152	4.1	0.16	20.0	1.85	0.301	9.4	0.486	0.106				0.65	0.35	0.09
PKW5 L4 X4	67	24	7.8	0.260	8.1	0.34	55.6	1.21	0.321	12.7	0.651	0.149	2.78	1.00	1.50	0.54	0.46	0.15

Name of Model	Qa (lt/s)	P (cm)	h_1 (cm)	V_1 (m/s)	H_1 (cm)	H_1/P	Qt (lt/s)	C_d	E_1 (m)	h_2 (cm)	V_2 (m/s)	E_2 (m)	L/W	W_i/W_o	B/P	$\frac{(E_1-E_2)}{E_1}$	E_2/E_1	Fr
	57		7.2	0.226	7.5	0.31	48.7	1.17	0.315	12.5	0.563	0.141				0.55	0.45	0.13
	47		6.1	0.193	6.3	0.26	37.7	1.25	0.303	11.0	0.527	0.124				0.59	0.41	0.11
	37		5	0.158	5.1	0.21	27.8	1.33	0.291	9.5	0.481	0.107				0.63	0.37	0.09
PKW5 L4 B4	67	24	7.5	0.263	7.9	0.33	52.6	1.27	0.319	13.0	0.636	0.151	2.78	1.00	1.50	0.53	0.47	0.15
	57		7	0.227	7.3	0.30	46.8	1.22	0.313	12.5	0.563	0.141				0.55	0.45	0.13
	47		6	0.193	6.2	0.26	36.8	1.28	0.302	11.1	0.523	0.125				0.59	0.41	0.11
	37		4.9	0.158	5.0	0.21	27.0	1.37	0.290	9.7	0.471	0.108				0.63	0.37	0.09
PKW5 L4 D4	67	24	7.2	0.265	7.6	0.31	49.7	1.35	0.316	13.0	0.636	0.151	2.78	1.00	1.50	0.52	0.48	0.15
	57		6.8	0.228	7.1	0.29	44.9	1.27	0.311	12.8	0.550	0.143				0.54	0.46	0.13
	47		5.8	0.195	6.0	0.25	35.1	1.34	0.300	11.5	0.505	0.128				0.57	0.43	0.11
	37		4.7	0.159	4.8	0.20	25.4	1.46	0.288	9.5	0.481	0.107				0.63	0.37	0.09

RESUME

EDUCATION:

Bachelor: Graduation year, University, Faculty, Section

Master: Graduation year, University, Faculty, Department, Program

PROFESSIONAL EXPERIENCE AND REWARDS

PUBLICATIONS/PRESENTATIONS ON THE THESIS:

- Ganapuram S., Hamidov A., Demirel, M. C., Bozkurt E., Kındap U., Newton A., 2007. Erasmus Mundus Scholar's Perspective on Water And Coastal Management Education In Europe. *International Congress - River Basin Management,* March 22-24, 2007 Antalya, Turkey. (Presentation sample)
- Satoğlu, Ş.I., Durmuşoğlu, M. B., Ertay, T. A., 2010. A Mathematical Model And A Heuristic Approach For Design Of The Hybrid Manufacturing SystemsTo Facilitate One-Piece Flow, *International Journal of Production Research*, 48(17), 5195-5220. (Article sample)
- Chen, Z., 2013. Intelligent Digital Teaching and Learning All-In-One Machine, Has Projection Mechanism Whose Front End Is Connected with Supporting Arm, And Base Shell Provided With Panoramic Camera That Is Connected With Projector. Patent number: CN203102627-U (Patent student)

LIST OF PUBLICATIONS AND PATENTS:

PUBLICATIONS/PRESENTATIONS ON THE THESIS

Ganapuram S., Hamidov A., Demirel, M. C., Bozkurt E., Kındap U., and Newton A., 2007: Erasmus Mundus Scholar's Perspective on Water and Coastal Management Education In Europe. *International Congress - River Basin Management*, March 22-24, 2007 Antalya, Turkey.